Thesis/
Reports
Zeller,
K. F.

FOX

United States
Environmental Protection
Agency

Atmospheric Research and Exposure
Assessment Laboratory
Research Triangle Park NC 27711

Research and Development

November, 1988

INTERNAL REPORT

USFS PAWNEE DRY DEPOSITION RESEARCH SITE
(WESTERN CORE SITE)
FY-88 OPERATION: PROGRESS REPORT NO. 1

November 1988

USFS PAWNEE DRY DEPOSITION RESEARCH SITE (WESTERN CORE SITE) FY-88 OPERATION: PROGRESS REPORT NO. 1

by

Karl F. Zeller
USFS Rocky Mountain Forest
and Range Experiment Station
Fort Collins, Colorado 80526

Interagency Agreement DW 12933093-01-0

Project Officer

Kenneth T. Knapp
Methods Research and Development Division
Atmospheric Research and Exposure Assessment Laboratory
Research Triangle Park, North Carolina 27711

RMRS Library
USDA Forest Service
MAR 1 3 2006
240 W Prospect Rd
Fort Collins CO 80526

ATMOSPHERIC RESEARCH AND EXPOSURE ASSESSMENT LABORATORY
OFFICE OF RESEARCH AND DEVELOPMENT
U. S. ENVIRONMENTAL PROTECTION AGENCY
RESEARCH TRIANGLE PARK, NORTH CAROLINA 27711

NOTICE

The information in this document has been funded by the U. S. Forest Service and the U. S. Environmental Protection Agency under Interagency Agreement DW 12933093-01-0 with the U. S. Forest Service. Mention of trade names or commercial products does not constitute endorsement or recommendation for use.

PREFACE

The U. S. Forest Service (USFS) and the U. S. Environmental Protection Agency entered into an interagency agreement (IAG) in April 1988 to upgrade and continue operation of the USFS Pawnee Eddy Correlation Dry Deposition Research Site. Without the IAG, data collection operations and research at the site would have been discontinued.

This report covers USFS accomplishments, IAG requirements completed, and data capture from January 1988 through September 1988.

Dr. Douglas Fox manages the overall USFS acid deposition research program. Dr. William Massman, Dr. David Stocker (University of Denver), and Mr. Rick McKinney contributed to the analysis, preparation, and editing of data appearing in this report. Mr. Don Lukens is the Pawnee site technician responsible for daily site operations. Dr. Don Hazlett conducted leaf area index (LAI) measurements at the Pawnee site and prepared the LAI discussion herein.

Karl Zeller
Pawnee Site Project Manager
November 1988

CONTENTS

SECTION		PAGE
Preface		iii
Table of Figures		vi
1.0	Introduction	1
2.0	Pawnee Site Activities	2
2.1	Fast-Response Chemical Instrumentation	2
2.1.1	Ozone and Nitrogen Dioxide Monitors	2
2.1.2	Zero-Air System	2
2.2	Special Experiments	2
2.2.1	EPA/ASRL Eddy Accumulation Experiment	3
2.2.2	Constant Flux Layer	3
2.2.3	NOAA Aeronomy Laboratory Nitrogen Flux Experiment	3
2.2.4	Filter-Pack Measurements	3
2.2.5	Energy Balance and Water Stress	3
2.2.6	Leaf Area Index Measurements	4
2.3	Research Protocol and Quality Assurance	4
2.4	August 1988 Site Fire	4
3.0	Data Collection Procedure and Presentation of Data	4
3.1	Data Collection	4
3.2	Data Presentation	5
3.2.1	June 1988 Data Summaries	5
3.2.2	July 1988 Weekly Data	6
4.0	Appendices	
A.	Initial Results from the Pawnee Eddy Correlation System for Dry Acid Deposition Research	A1
B.	Research Protocol Methodology and Quality Assurance Plans for the USFS Pawnee Eddy Correlation Dry Deposition Research Site	B1

CONTENTS

SECTION		PAGE
C.	Leaf Area Development in Four Communities of the Colorado Steppe	C1
D.	Report on the Fire at the Pawnee Grasslands Field Site on August 13, 1988	D1
E.	June 1988 Data Listings	E1

LIST OF FIGURES

FIGURE		PAGE
1.	Diurnal maximum, mean, and minimum heat flux measured at the Pawnee site for June 1988	8
2.	Diurnal maximum, mean, and minimum Reynolds stress measured at the Pawnee site for June 1988	9
3.	Diurnal maximum, mean, and minimum ozone concentration measured at the Pawnee site for June 1988	10
4.	Diurnal maximum, mean, and minimum ozone flux (negative value indicates downward flux) measured at the Pawnee site for June 1988	11
5.	Diurnal maximum, mean, and minimum NO_2 concentration measured at the Pawnee site for June 1988	12
6.	Diurnal maximum, mean, and minimum NO_2 flux measured at the Pawnee site for June 1988	13
7.	Pawnee site temperature for the seven-day period beginning July 5, 1988 (Julian day 187)	14
8.	Pawnee site heat flux for the seven-day period beginning July 5, 1988 (Julian day 187)	15
9.	Pawnee site net radiation for the seven-day period beginning July 5, 1988 (Julian day 187)	16
10.	Pawnee site soil heat flux for the seven-day period beginning July 5, 1988 (Julian day 187)	17
11.	Pawnee site ozone concentration for the seven-day period beginning July 5, 1988 (Julian day 187)	18
12.	Pawnee site ozone flux for the seven-day period beginning July 5, 1988 (Julian day 187)	19
13.	Pawnee site nitrogen dioxide concentration for the seven-day period beginning July 5, 1988 (Julian day 187)	20
14.	Pawnee site nitrogen dioxide flux for the seven-day period beginning July 5, 1988 (Julian day 187)	21

LIST OF FIGURES

FIGURE		PAGE
15.	Pawnee site oxides of nitrogen concentration for the seven-day period beginning July 5, 1988 (Julian day 187)	22
16.	Pawnee site oxides of nitrogen flux for the seven-day period beginning July 5, 1988 (Julian day 187)	23
17.	Pawnee site wind speed for the seven-day period beginning July 5, 1988 (Julian day 187)	24
18.	Pawnee site momentum flux (Reynolds stress) for the seven-day period beginning July 5, 1988 (Julian day 187)	25
19.	Pawnee site vapor flux for the seven-day period beginning July 5, 1988 (Julian day 187)	26

TABLE

TABLE		PAGE
1.	1988 Pawnee Site Weekly Data Capture	7

1.0 INTRODUCTION

The dry deposition of sulfur compounds, nitrogen compounds, and ozone is the focus of several large research programs currently underway across the United States. To optimize the techniques for obtaining total deposition data that are used to study ecological effects on forested watersheds, the U. S. Forest Service (USFS) has established a research site for measuring dry deposition. The site, referred to herein as the Pawnee site, was started in July 1986 at the Central Plains Experimental Range adjacent to and west of the Pawnee National Grasslands, Colorado. The concept was to begin measurements over simple terrain, gain experience and understanding, then adapt the technology to more complex situations.

National Oceanographic and Atmospheric Administration (NOAA) dry deposition by inferential monitoring (DDIM) filter-pack measurements have been made at the Pawnee site since July 1986. A major goal of Interagency Agreement (IAG) DW 12933093-01-0 is to provide data from eddy correlation measurements of dry deposition concurrent with data from other methods for dry deposition determination. Such candidate methods for dry deposition measurement are the U. S. Environmental Protection Agency's National Dry Deposition Network (EPA/NDDN) and Atmospheric Research and Exposure Assessment Laboratory (AREAL) filter pack systems, the NOAA/DDIM filter pack, EPA's eddy accumulation system, and the NOAA Aeronomy Laboratory's box NO_x measurements.

Eddy correlation measurements at the USFS Pawnee site were first taken in December 1986 for a three-week period to initiate activities at the site and prove its operational capability. Measurements began in earnest in May 1987. Appendix A, "Initial Results from the Pawnee Eddy Correlation System for Dry Acid Deposition Research," contains a detailed report describing the mathematical procedures to reduce uncertainty and correct errors in eddy correlation system, the initial data results, and the fast-response chemical sensors. Measurements discussed in Appendix A and all data collection prior to mid-August 1987 were accomplished by using a R. M. Young UVW anemometer for micrometeorological wind measurements. All micrometeorological wind measurements collected after mid-August 1987 were made with an Applied Technologies, Inc., three-axis research-grade sonic anemometer.

Except for a four-week period commencing mid-August 1988, the Pawnee site has been in continuous operation since May 1987. Momentum flux and heat flux data are available for the overall period, even though the sensors required for eddy correlation measurements of chemical flux have not always been operational. This progress report covers the data collection period January 1988 through October 1988. This is essentially the period for which initial IAG funds were planned for and used.

The remainder of this report discusses site activities which include changes and upgrades, special experiments, the August 1988 fire, data collection including data capture and the presentation of some June and July 1988 data, and leaf area index (LAI) measurements made during the 1988 growing season.

2.0 PAWNEE SITE ACTIVITIES

This section constitutes a report on the physical changes and upgrades made to the Pawnee site. It also lists special studies that were either conducted or started, a presentation of the Pawnee research protocol methodology and quality assurance plans, and a discussion of the August 1988 instrument shelter fire. In addition to the physical changes to be discussed below, the USFS has assigned a full-time Pawnee site technician as of April 1987.

2.1 FAST-RESPONSE CHEMICAL INSTRUMENTATION

2.1.1 Ozone and NO_2 Monitors

Research-grade prototype chemiluminescence ambient air monitors (CAAMS) were purchased from the University of Denver for the fast-response sensing of ozone (CAAM1) and for the fast-response sensing of NO_2 (CAAM2). These instruments were installed at the Pawnee site during March 1988. Descriptions of these instruments and their response times can be found in Appendix A. The protocol for operating these instruments is given in Appendix B, "Research Protocol Methodology and Quality Assurance Plans for the USFS Pawnee Eddy Correlation Dry Deposition Research Site."

2.1.1 Zero-Air System

The sensitivity of the fast-response chemical instruments requires that they be frequently zeroed and calibrated. The automated zero-air system is an integral part of the USFS's ability to gather eddy correlation data during periods when the Pawnee site is unmanned.

The Pawnee site zero-air system was upgraded and automated during March and April 1988. Now, at the end of each sampling period, all chemical instruments are automatically zeroed prior to the next period of data collection. The results of the automatic zero readings, in addition to span data, are then monitored to determine significant changes in instrument sensitivity and response.

2.2 SPECIAL EXPERIMENTS

A number of experiments or projects associated with dry deposition research have been undertaken at the Pawnee site. These are briefly introduced below.

2.2.1 EPA/ASRL Eddy Accumulation Experiment

During a two-week period running from the end of May 1988 through early June 1988, the EPA Atmospheric Sciences and Research Laboratory collected HNO_3 vapor and water vapor flux data by using the EPA eddy accumulation system. EPA is currently working on the results from this effort. The USFS Pawnee site data for this effort is available.

2.2.2 Constant Flux Layer

An effort to answer basic micrometeorological questions relating to a constant flux layer within the surface layer has been initiated at the Pawnee site. The ability to simultaneously collect eddy correlation flux measurements at two levels, 2 m and 8 m, was added at the end of July 1988. There are no presentable results from this effort because the August 1988 fire destroyed the data from this experiment. Enough data was collected to test the physical setup, and this experiment will be run again in the summer of 1989.

2.2.3 NOAA Aeronomy Laboratory Nitrogen Flux Experiments

During June 1988, personnel from NOAA Aeronomy Laboratory set up their mobile laboratory adjacent to the USFS Pawnee site. Flux measurements of various nitrogen compounds were made. During that period, USFS eddy correlation data was collected for O_3, NO_2, and NO_x. The fast-response NO_x analyzer was provided by the University of Denver. The USFS is cooperating with the Aeronomy Laboratory in the analysis of the data. Intercomparisons between the two measurement programs are presently being conducted.

2.2.4 Filter-pack Measurements

NOAA DDIM filter-pack samples are routinely collected at the Pawnee site. One one occasion, an ASRL filter-pack was employed to compare with the NOAA filter-pack. Results from this effort await filter chemical analysis by the NOAA contract laboratory and the EPA filter analysis.

2.2.5 Energy Balance and Water Stress

To validate dry deposition measurements by studying the energy balance, the USFS added a fast-response krypton hygrometer to the eddy correlation system during late May 1988. Net radiation and soil heat flux instruments also have been added to the Pawnee site. The data from these data sensors, in addition to the evaporation data from the Colorado State University (CSU) weighing soil lysimeter located 50 m northwest of the Pawnee site, are being used to establish an energy balance. To evaluate water stress, a method to estimate daily soil moisture availability should be established.

2.2.6 Leaf Area Index Measurements

The USFS funded the CSU Range Science Department to provide LAI measurements during the 1988 growing season. LAI measurements were made at the Pawnee site, in addition to three other nearby sites with varying soil and vegetation types. Appendix C, "Leaf Area Index Development in Four Plant Communities of the Colorado Steppe" presents the draft results of this effort. There is a difference in response between cold season and warm season plants. In addition, water stress plays a role in LAI.

2.3 RESEARCH PROTOCOL AND QUALITY ASSURANCE

The IAG requires that the Pawnee site be upgraded to CORE standards as set by NOAA and EPA for the other CORE sites, and that it be operated under a quality assurance plan. With these two requirements in mind, the USFS has developed a research protocol methodology and quality assurance plans which specify how data collection is and will be conducted. Appendix B contains this document.

2.4 AUGUST 1988 SITE FIRE

The interior of the Pawnee site instrument shelter experienced a fire on August 13, 1988. The fire apparently started within the University of Denver fast-response NO_x analyzer (not part of IAG equipment purchase list.) Appendix D, "Report on the Fire at the Pawnee Grasslands Field Site on August 13, 1988," discusses the fire in greater detail. Chemical instrumentation and computer data collection equipment immediately underwent extensive repair and refurbishment. Eddy correlation measurements were resumed on September 10, 1988. Data loss from this incident extended from July 28 to September 9. Unfortunately, the data from the period July 28 to August 13 was stored on magnetic media at the Pawnee site and was mostly ruined. The USFS will be installing automatic fire protection in the near future.

3.0 DATA COLLECTION PROCEDURE AND PRESENTATION OF DATA

This section presents information on the data that were collected during the report period and the parameters derived from calculations. Selected data paramters for June 1988 and part of July 1988 are presented.

3.1 DATA COLLECTION

Data collection at the Pawnee site is a complex process. Data are collected and summarized in half-hour averaging periods. From 11 to 14 sensors provide input signals (here the three-axis sonic anemometer which has three input signals is counted as one sensor) to produce from 65 to

105 calculated output values per half-hour sampling period. Eddy correlation data are collected with a personal computer data acquisition system. The program used to collect and process the data has been adapted from a similar flux data collection program developed by personnel at the NOAA Atmospheric Turbulence and Diffusion Division. The eight-channel version is presented in Appendix B.

Data that do not pertain to eddy correlation are collected on a Campbell Scientific CR-21x data logger. These include soil heat flux, net radiation, temperature difference (delta T), and slow-response ozone concentrations.

When sampling with eight channels at 20 Hz, there are 288,000 data points to process into the 65 output values each half-hour. USFS eddy correlation data is archived in one-week blocks commencing 8:00 a.m. Mountain Standard Time (MST) each Tuesday. This archival approach has been adopted to coincide with National Atmospheric Deposition Program and existing filter-pack data collection protocols. An "x" in Table 1 lists selected data that are available from the Pawnee site. The data parameters listed are most important for dry deposition determination. Table 1 indicates that data capture from that week exceeds 50% for that specific parameter. The date column in Table 1 gives the month and Julian date for the beginning day of the data week. For instance, Jun 159 means data for the seven-day period beginning 08:00 MST June 7, 1988.

3.2 DATA PRESENTATION

Data from June and July 1988 has been chosen for display in this section to give an example of data quality and completeness. The data presented here has been calibrated and edited and are typical for this time of the year. Data collected during periods of equipment failure or that are invalid for various other reasons have been omitted. Unless otherwise noted, the data presented here have not been corrected or adjusted for sensor time response, temperature and moisture fluxes, sample volume averaging, or sonic anemometer shadowing. These corrections can sometimes be substantial and should be made before these flux values are used. Discussion of these corrections except for shadowing are given in Appendix A.

3.2.1 June 1988 Data Summaries

June 1988 data matrix tables for heat flux, Reynolds stress (momentum flux), average O_3 concentration, O_3 flux, average NO_2 concentration, and NO_2 flux are presented in Appendix D. The data are presented by half-hour average columns and by day rows; and minimum, mean, and maximum are allied for each day and each half-hour period. Figures 1 through 6 present the measured diurnal values for heat flux, Reynolds stress, O_3 concentration, O_3 flux, NO_2 concentration and NO_2 flux, respectively. The mean half-hour

ozone flux, (Figure 4) for instance, varies from -0.02 ppb*m/s at night to -0.20 ppb*m/s during the day. Once corrected for the phenomena listed above, the actual maximum average diurnal ozone flux could be as much as a factor of 2 greater.

3.2.2 July 1988 Weekly Data

The seven-day period beginning July 5, 1988, has been selected to present examples of time series plots of relevant Pawnee data. Figures 7 through 19 are plots of temperature, heat flux, net radiation, soil heat flux, O_3 concentration, O_3 flux, NO_2 concentration, NO_2 flux, NO_x concentration, NO_x flux, wind speed, momentum flux, and vapor flux. NO_2 and NO_x flux data in Figures 14 and 16 have been corrected for sensor time response, heat flux, volume averaging, and sonic anemometer shadowing.

The maximum nitrogen dioxide concentrations (Figure 13) are observed at night. These data are most likely caused by high-concentration-NO_2 air parcels wafting across the site. The maximum concentration observed at 01:00 MST occurs about 1 to 2 h after a wind shift to a northwest wind on June 8. A northwest wind is also observed at 02:30 to 03:00 on June 14 when another NO_2 maximum was recorded. In both cases the O_3 concentration was depleted, and the NO_2 and O_3 concentration variances were large. The Raw Hide power plant is approximately 60 km west-northwest of the Pawnee site, and Cheyenne is about 60 km north-northwest of the site; both are possible sources. A similar occurrence was observed at 07:00 on June 28 for both NO_2 and NO_x (Figure 15). These data points have been removed from the NO_2 flux data bases because large variances usually indicate that the steady-state conditions required for flux measurements by eddy correlation have been violated.

The maximum upward NO_2 fluxes (Figure 14) occur during the late afternoon. The maxima at 16:00 to 16:30 on June 9 followed a hailstorm and are possibly related to an increase in microbial activity following the storm. The maximum downward NO_2 flux occurred at 04:00 on June 30. Maximum downward values were also recorded for Reynolds stress, heat, O_3, and NO_x fluxes for that period.

TABLE 1

1988 PAWNEE SITE WEEKLY DATA CAPTURE

Each "x" indicates >50% data recovery.

Julian Date:	WS	WD	u'w'	Temp	w'T'	w'O3'	Avg O3	Vap. w'q'	Avg NO2	w'NO2'	Avg NOx	w'NOX'	Delta Temp	Net Rad	Soil HF
Jan 5															
Jan 12	x	x	x				x								
Jan 19	x	x	x				x								
Jan 26	x	x	x				x								
Feb 33	x	x	x				x								
Feb 40	x	x	x	x	x		x								
Feb 47	x	x	x	x	x		x								
Feb 54	x	x	x	x	x		x								
Mar 61	x	x	x	x	x		x		x	x					
Mar 68	x	x	x	x	x	x	x		x	x					
Mar 75	x	x	x	x	x		x		x	x					
Mar 82	x	x	x	x	x		x		x	x					
Apr 89	x	x	x	x	x	x	x		x	x					
Apr 96	x	x	x	x	x	x	x		x	x					
Apr 110	x	x	x	x	x	x	x		x	x			x		
Apr 117	x	x	x	x	x	x	x		x	x			x		
May 124	x	x	x	x	x	x	x		x	x					
May 131	x	x	x	x	x	x	x		x	x			x		
May 138	x	x	x	x	x	x	x		x	x			x		
May 145	x	x	x	x	x	x	x		x	x			x		
May 152	x	x	x	x	x	x	x	x	x	x			x		
Jun 159	x	x	x	x	x	x	x	x	x	x			x		
Jun 166	x	x	x	x	x	x	x	x	x	x			x		
Jun 173	x	x	x	x	x	x	x	x	x	x	x	x	x	x	x
Jun 180	x	x	x	x	x	x	x	x	x	x	x	x	x	x	x
Jul 187	x	x	x	x	x	x	x	x	x	x	x	x	x	x	x
Jul 194	x	x	x	x	x	x	x	x	x	x	x	x	x	x	x
Jul 201	x	x	x	x	x	x	x	x	x	x	x	x		x	x
Jul 208															
Aug 215															
Aug 222															
Aug 229					(PAWNEE SITE FIRE)										
Aug 236															
Aug 243															
Sep 250															
Sep 257	x	x	x	x	x	x	x	x						x	x
Sep 264	x	x	x	x	x	x	x	x						x	x
Sep 271	x	x	x	x	x	x	x	x						x	x
Oct 278	x	x	x	x	x	x	x	x						x	x
Oct 285	x	x	x	x	x	x	x	x						x	x
Oct 292	x	x	x	x	x	x	x	x						x	x
Oct 299	x	x	x	x	x	x	x	x					x	x	x

Legend for Column Headings:

- WS: Wind speed
- WD: Wind direction
- u'w': Reynold's Stress
- Temp: Ambient temperature
- w'T': Heat flux
- Avg. O3: Average ozone concentration
- w'O3': Ozone flux
- Vap w'q': Water vapor flux
- NO2: Average ambient nitrogen dioxide concentration
- w'NO2': NO2 flux
- NOx: Average ambient oxides of nitrogen
- w'NOx': NOx flux
- Delta Temp: Temperature difference (2-6 meters)
- Net Rad: Net Solar Radiation
- Soil HF: Soil Heat Flux

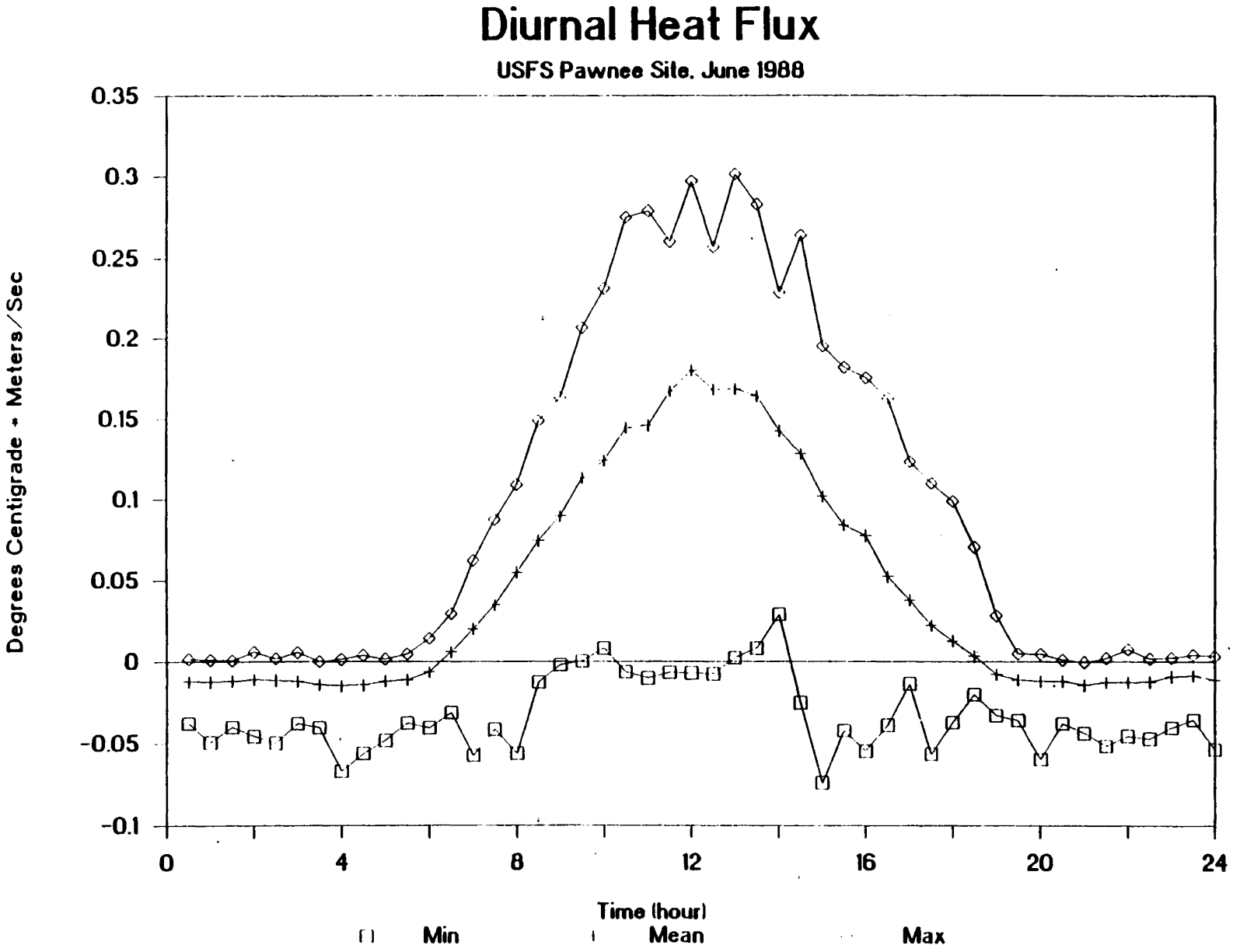

FIGURE 1: Diurnal maximum, mean, and minimum heat flux measured at the Pawnee Site for June, 1988.

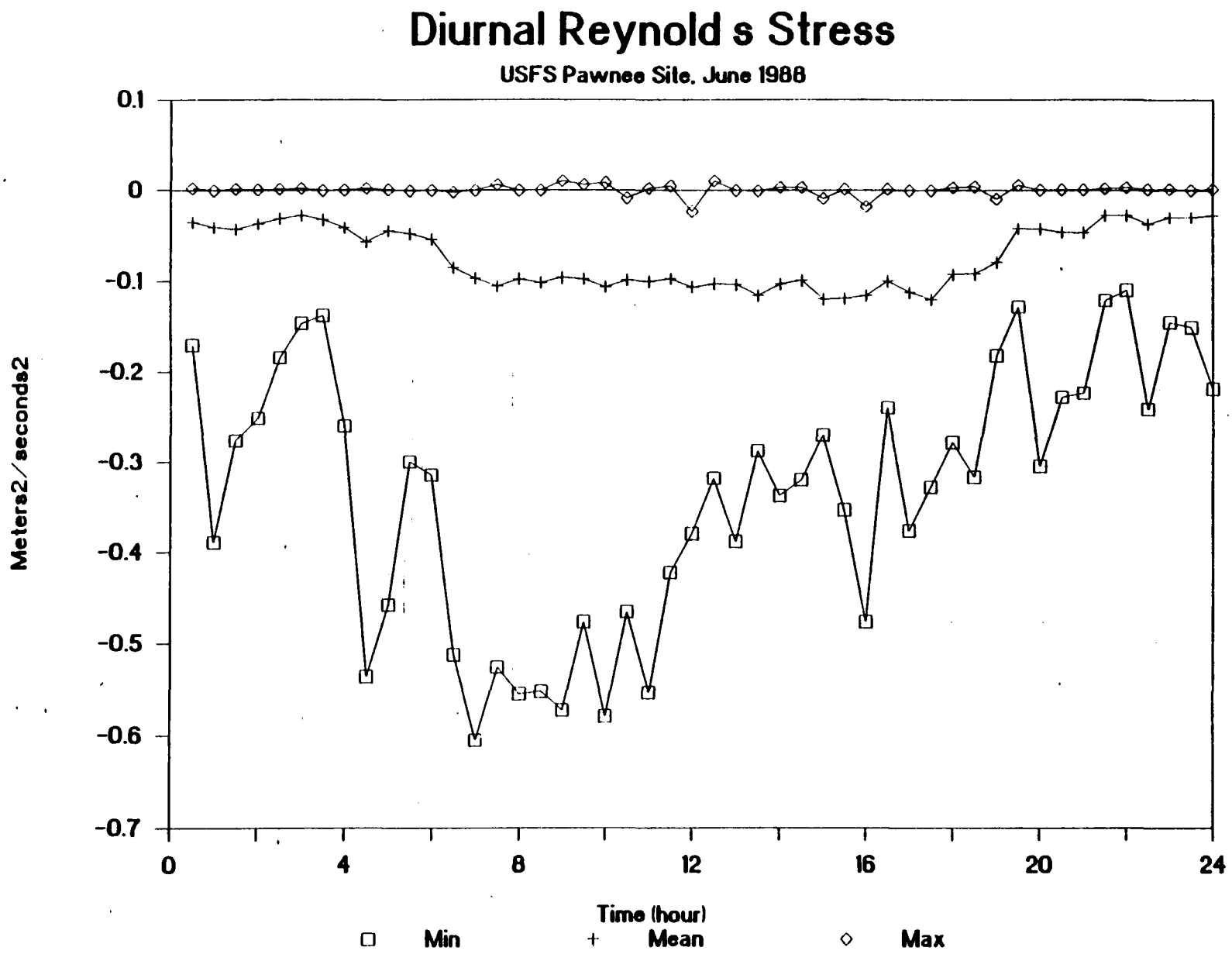

FIGURE 2: Diurnal maximum, mean, and minimum Reynolds Stress measured at the Pawnee Site for June, 1988.

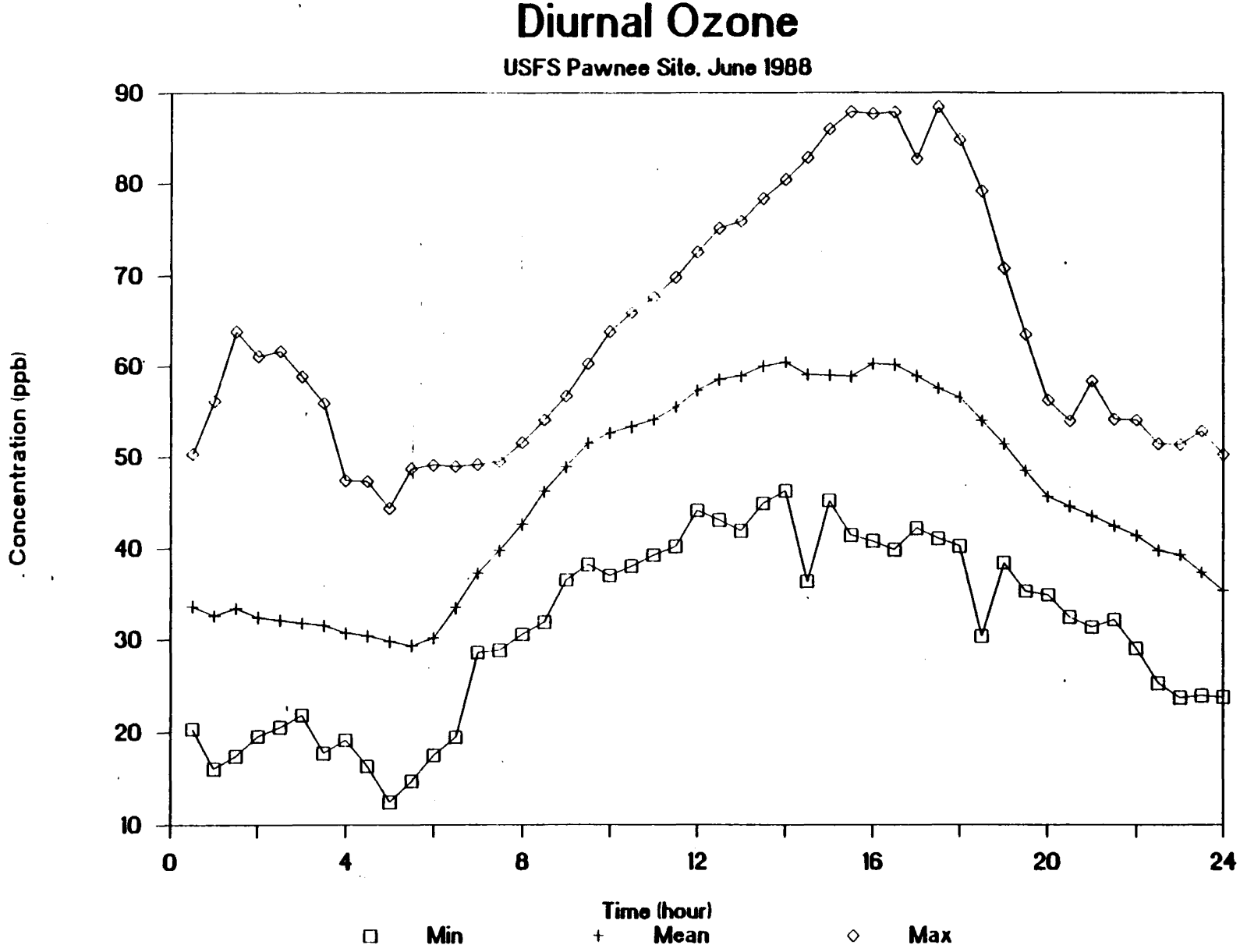

FIGURE 3: Diurnal maximum, mean, and minimum ozone concentration measured at the Pawnee Site for June, 1988.

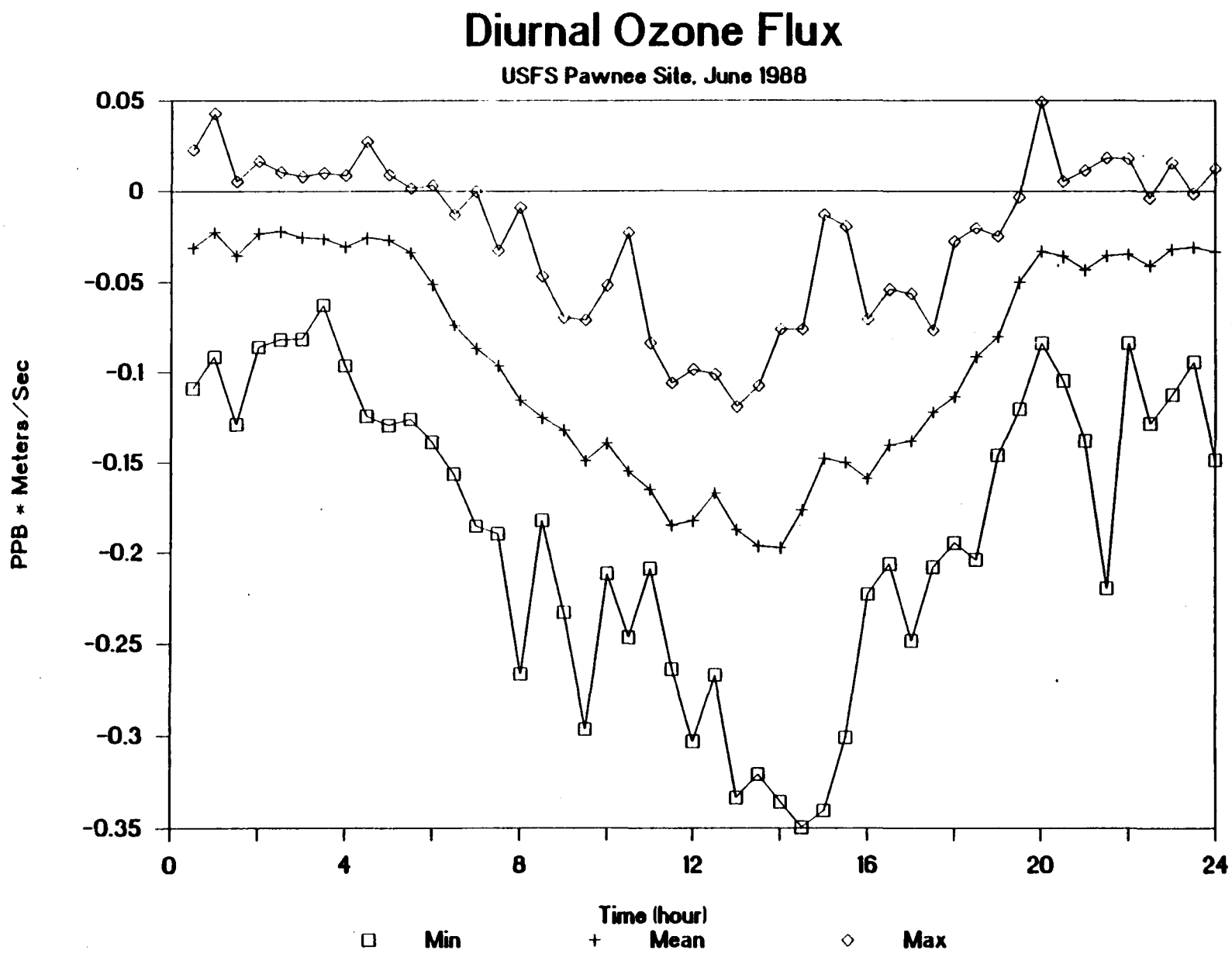

FIGURE 4: Diurnal maximum, mean, and minimum ozone flux (negative value indicates downward flux) measured at the Pawnee Site for June, 1988.

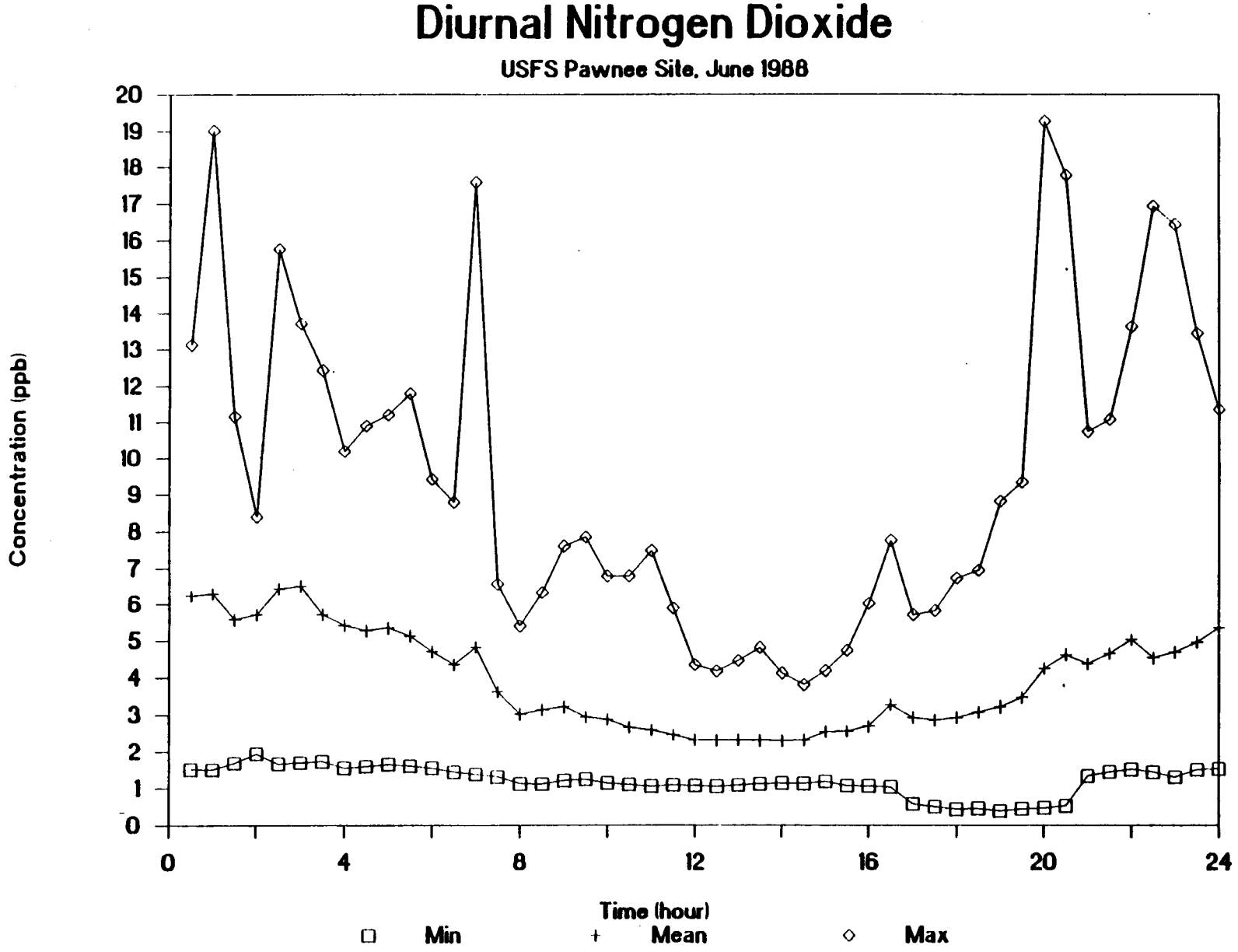

FIGURE 5: Diurnal maximum, mean, and minimum NO2 concentration measured at the Pawnee Site for June, 1988.

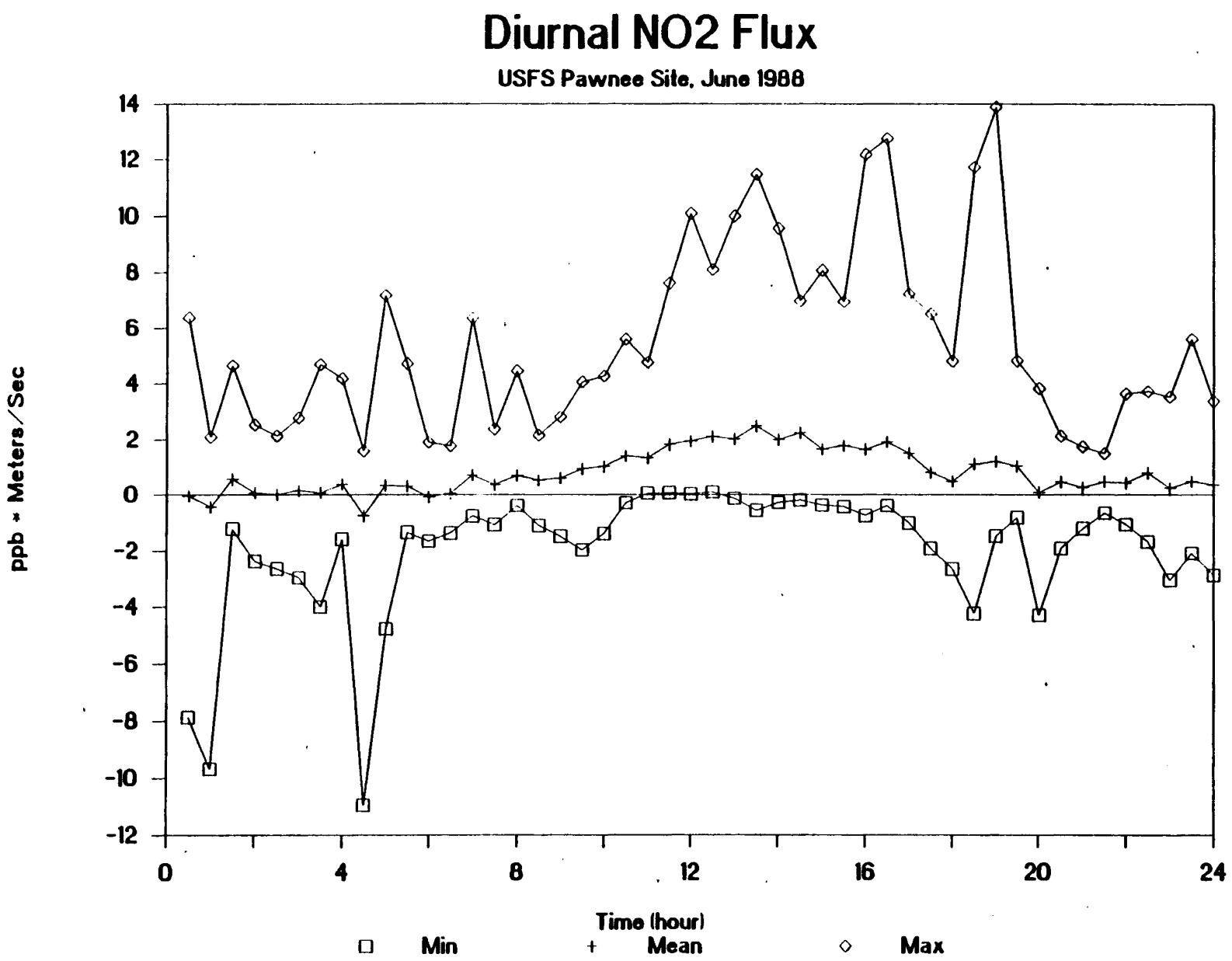

FIGURE 6: Diurnal maximum, mean, and minimum NO2 flux measured at the Pawnee Site for June, 1988.

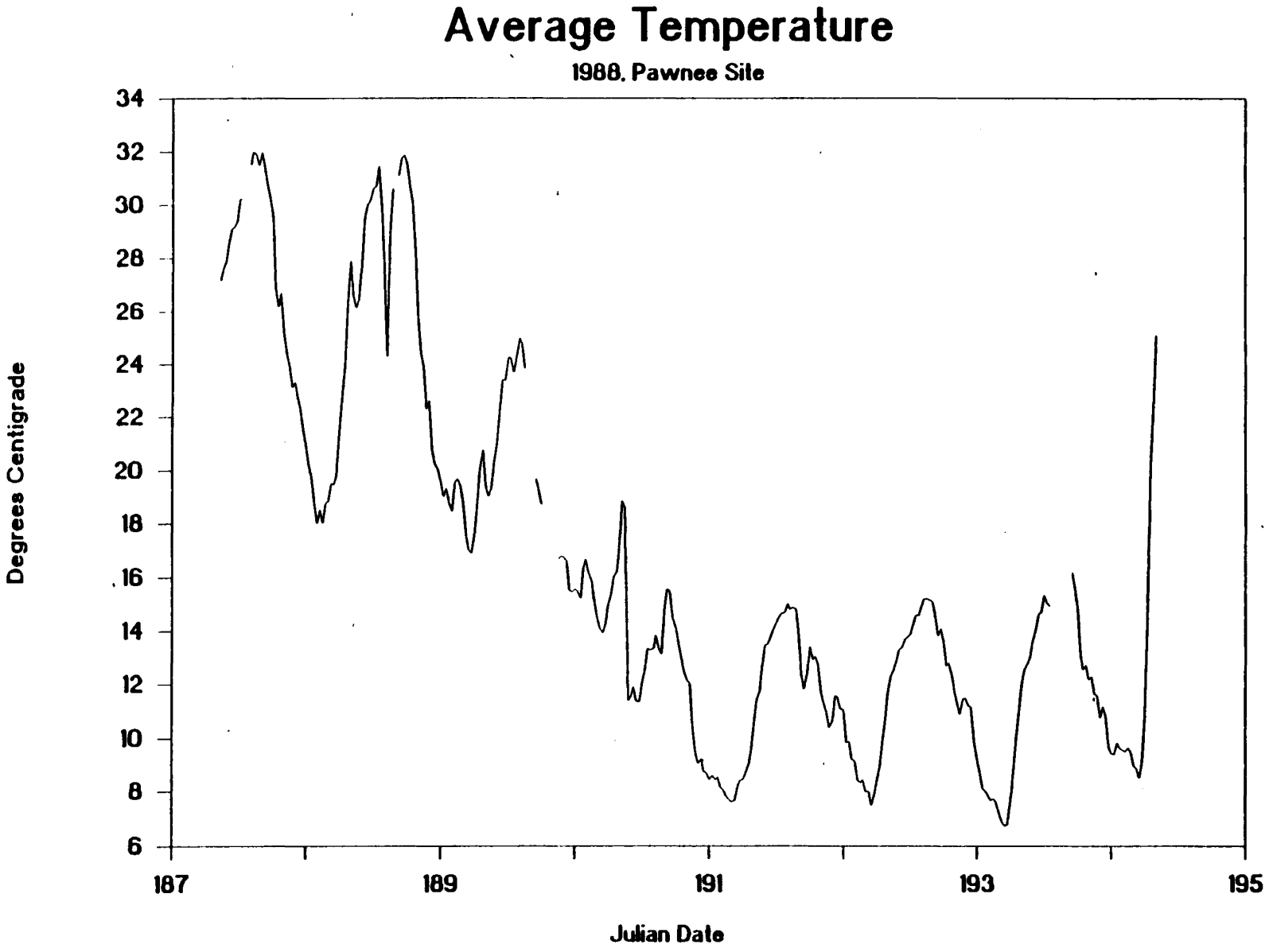

FIGURE 7: Pawnee Site Temperature for the 7 day period beginning July 5, 1988. (Julian day 187)

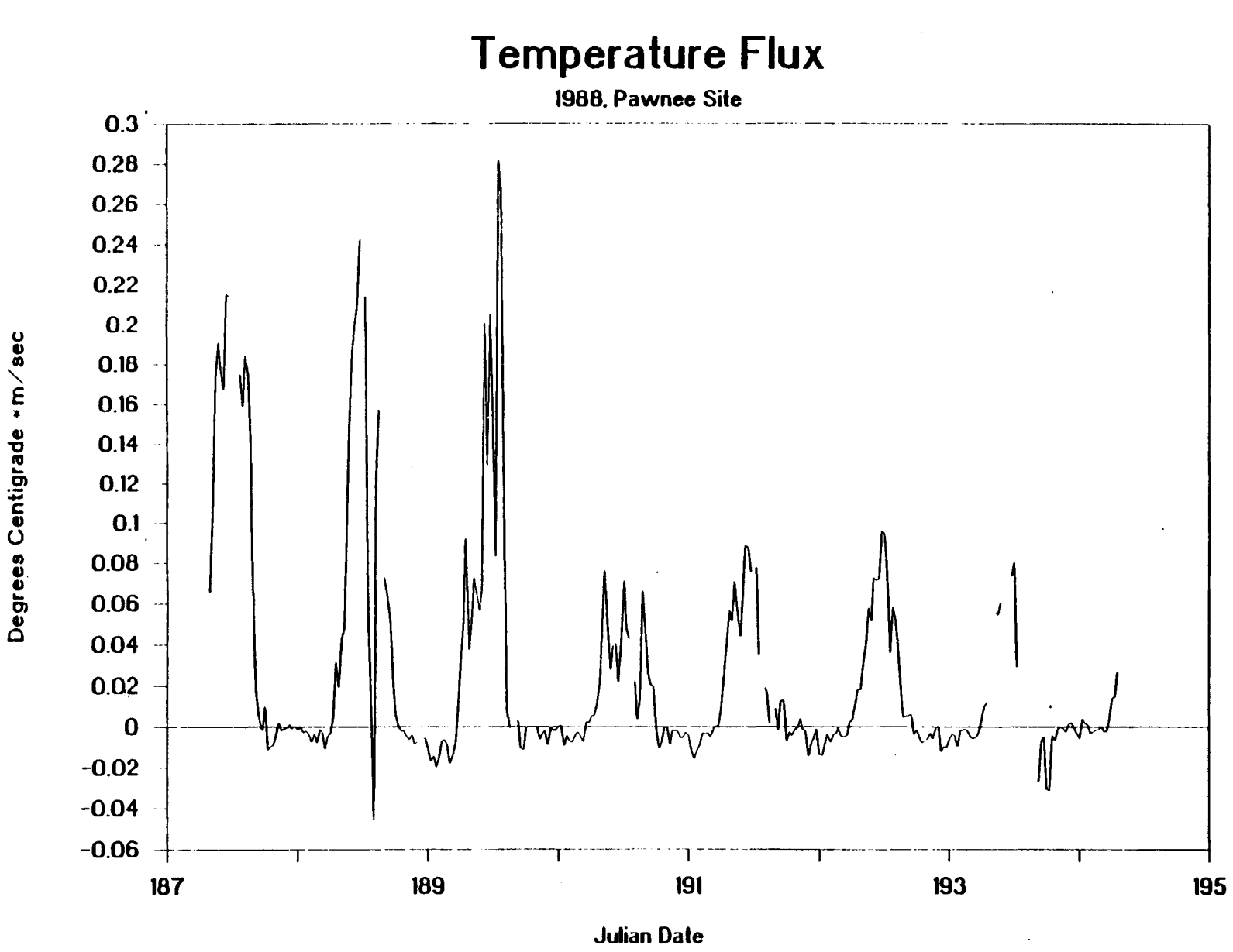

FIGURE 8: Pawnee Site Heat Flux for 7 day period beginning July 5, 1988. (Julian day 187)

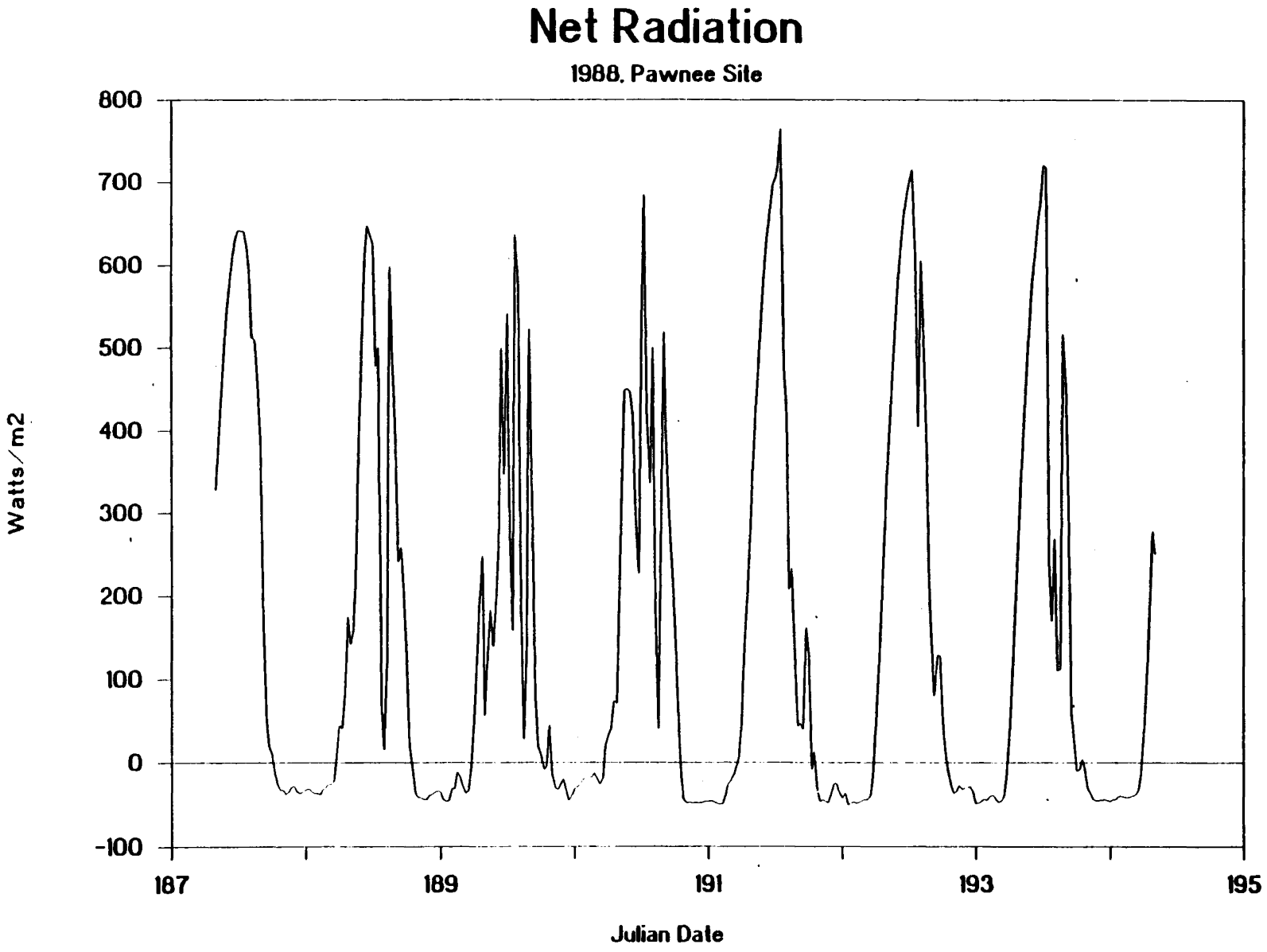

FIGURE 9: Pawnee Site Net Radiation for 7 day period beginning July 5, 1988. (Julian day 187)

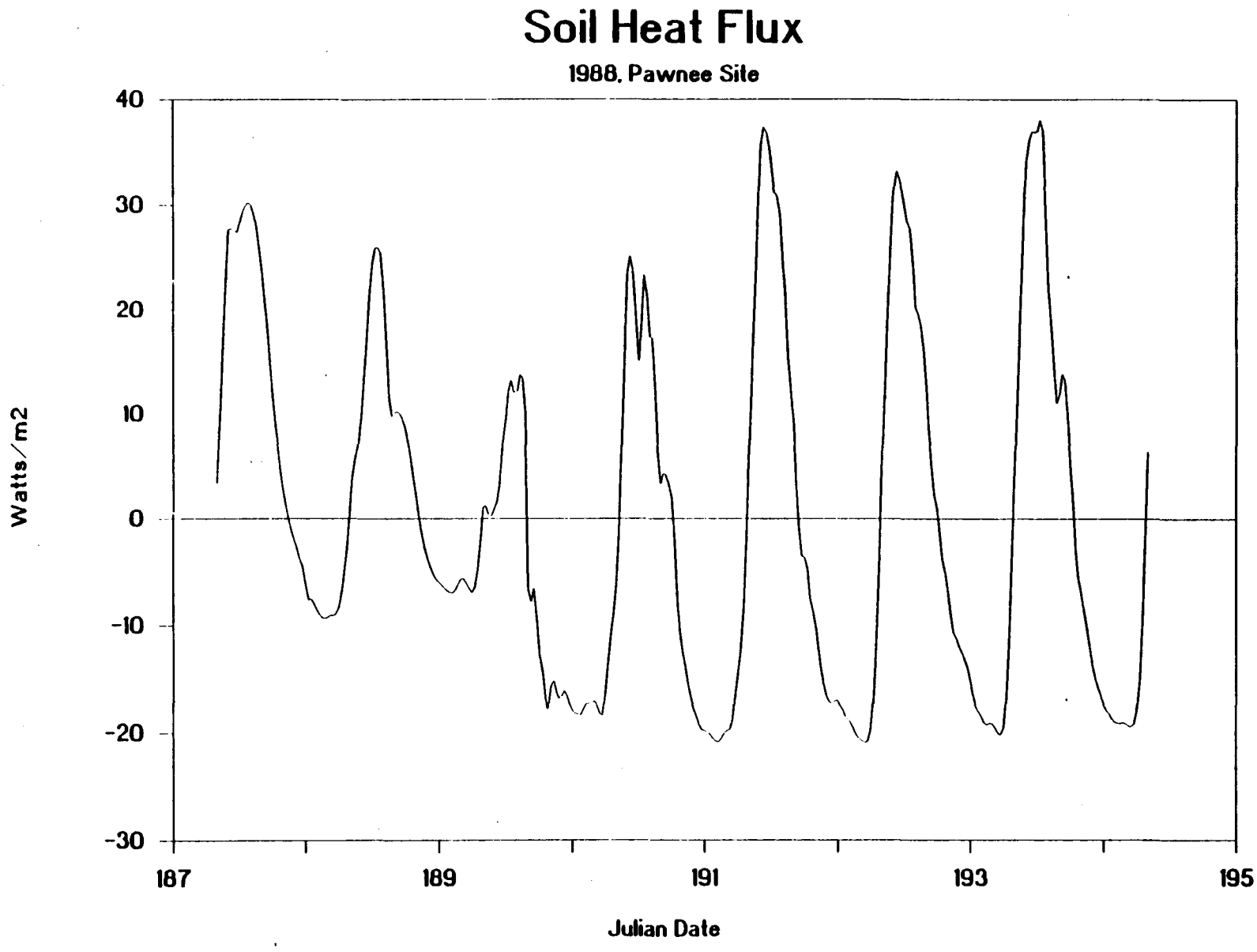

FIGURE 10: Pawnee Site Soil Heat Flux for 7 day period beginning July 5, 1988. (Julian day 187)

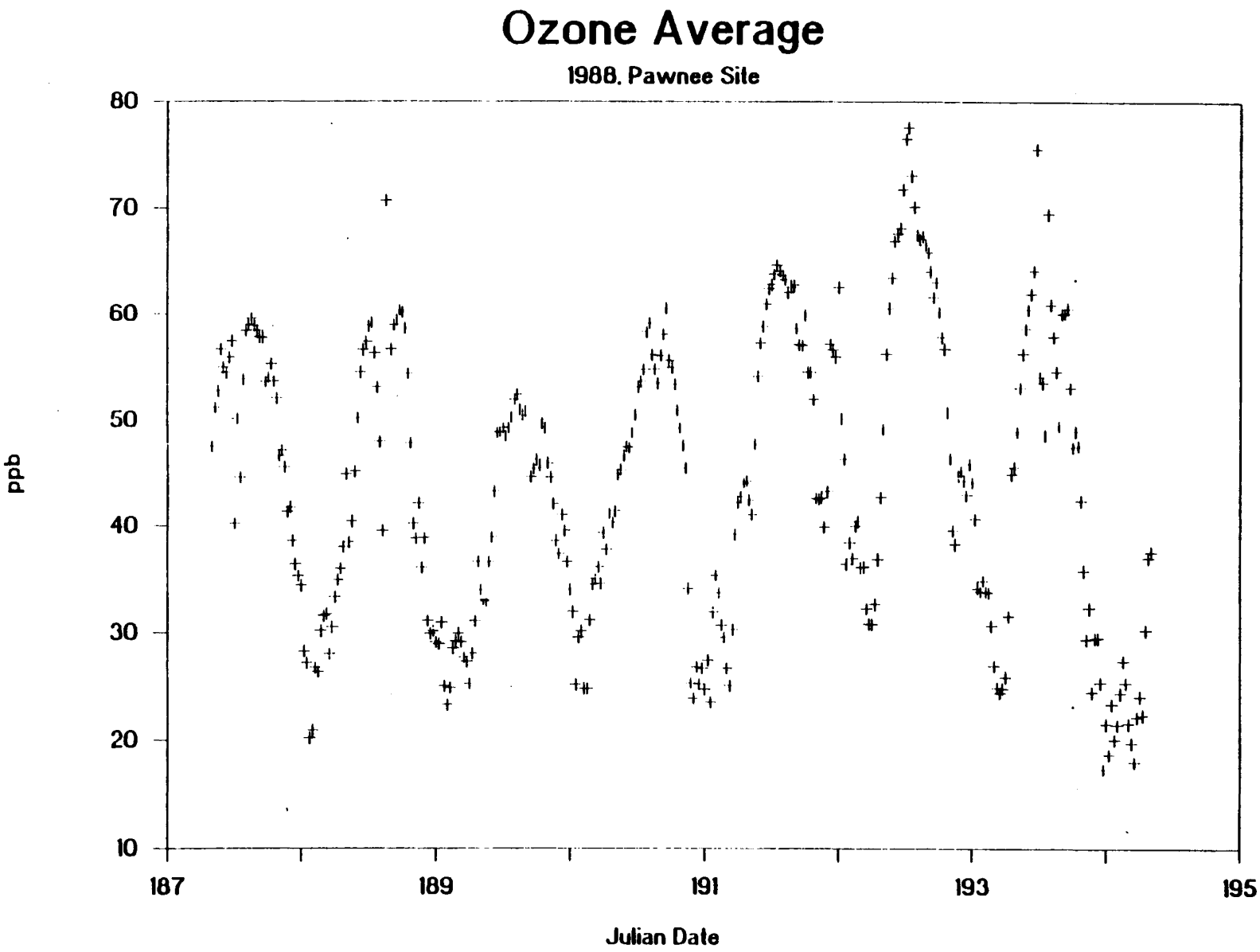

FIGURE 11: Pawnee Site Ozone Concentration for the 7 day period beginning July 5, 1988. (Julian day 187)

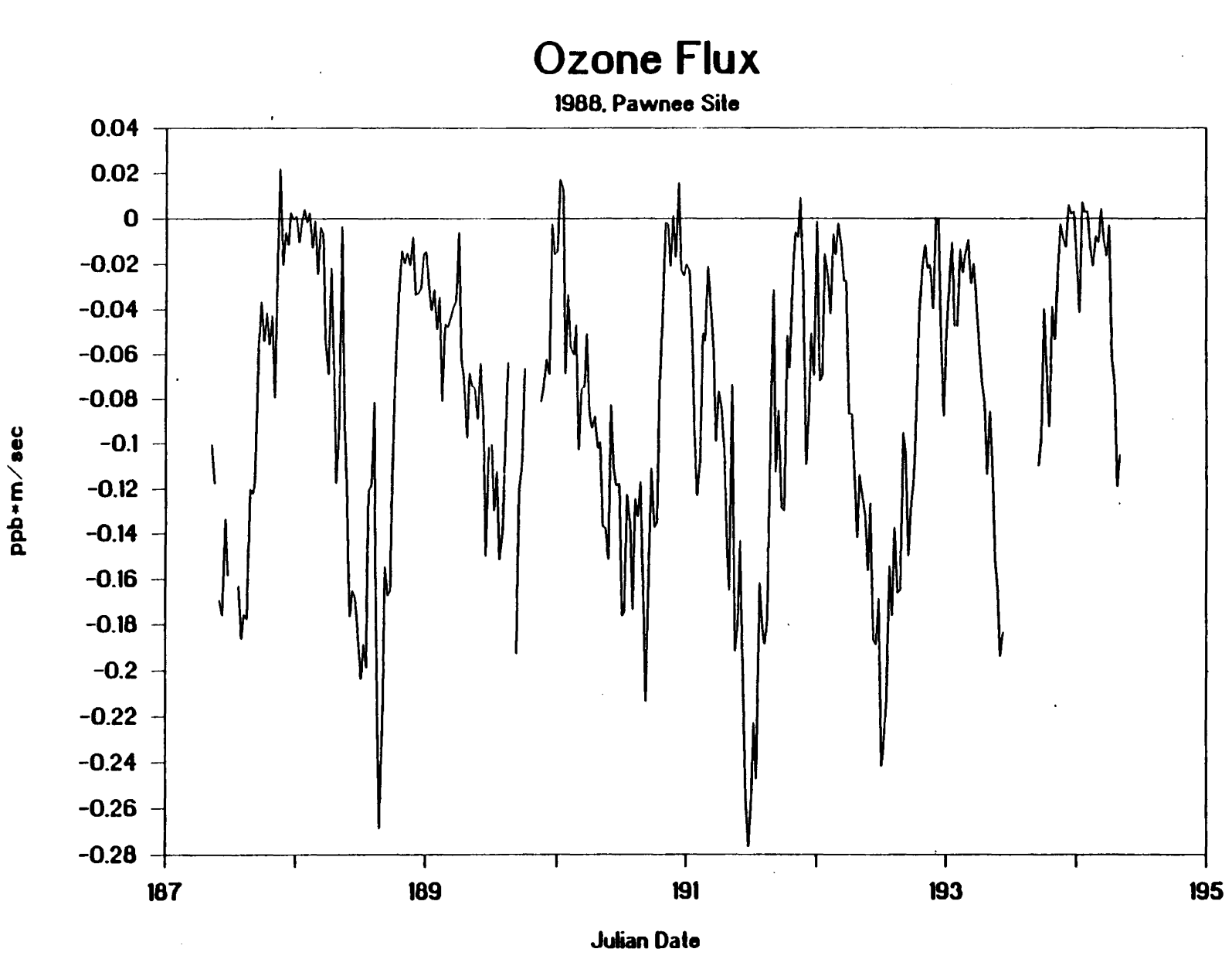

FIGURE 12: Pawnee Site Ozone Flux for the 7 day period beginning July 5, 1988. (Julian day 187)

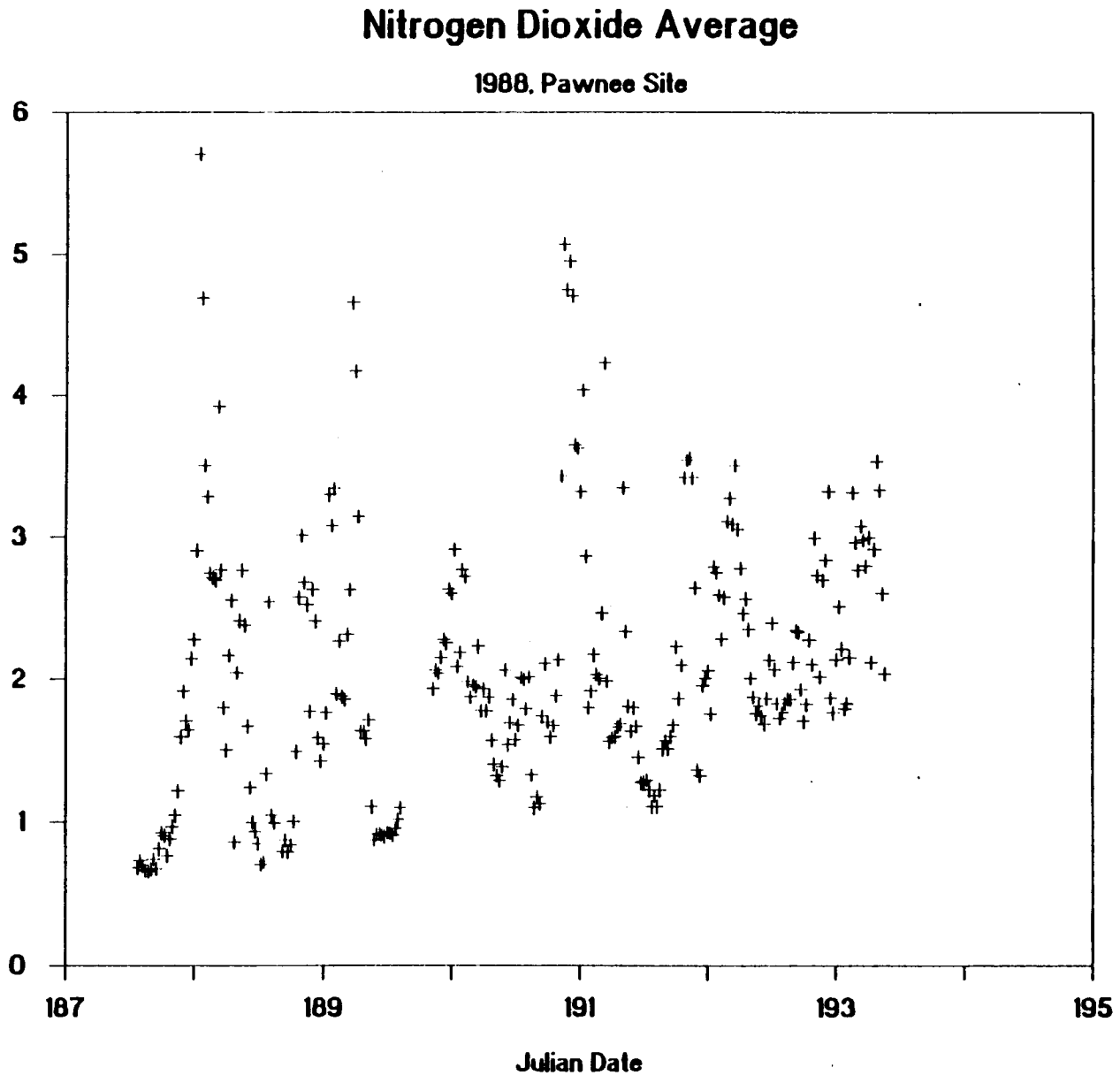

FIGURE 13: Pawnee Site Nitrogen Dioxide Concentration for the 7 day period beginning July 5, 1988. (Julian day 187)

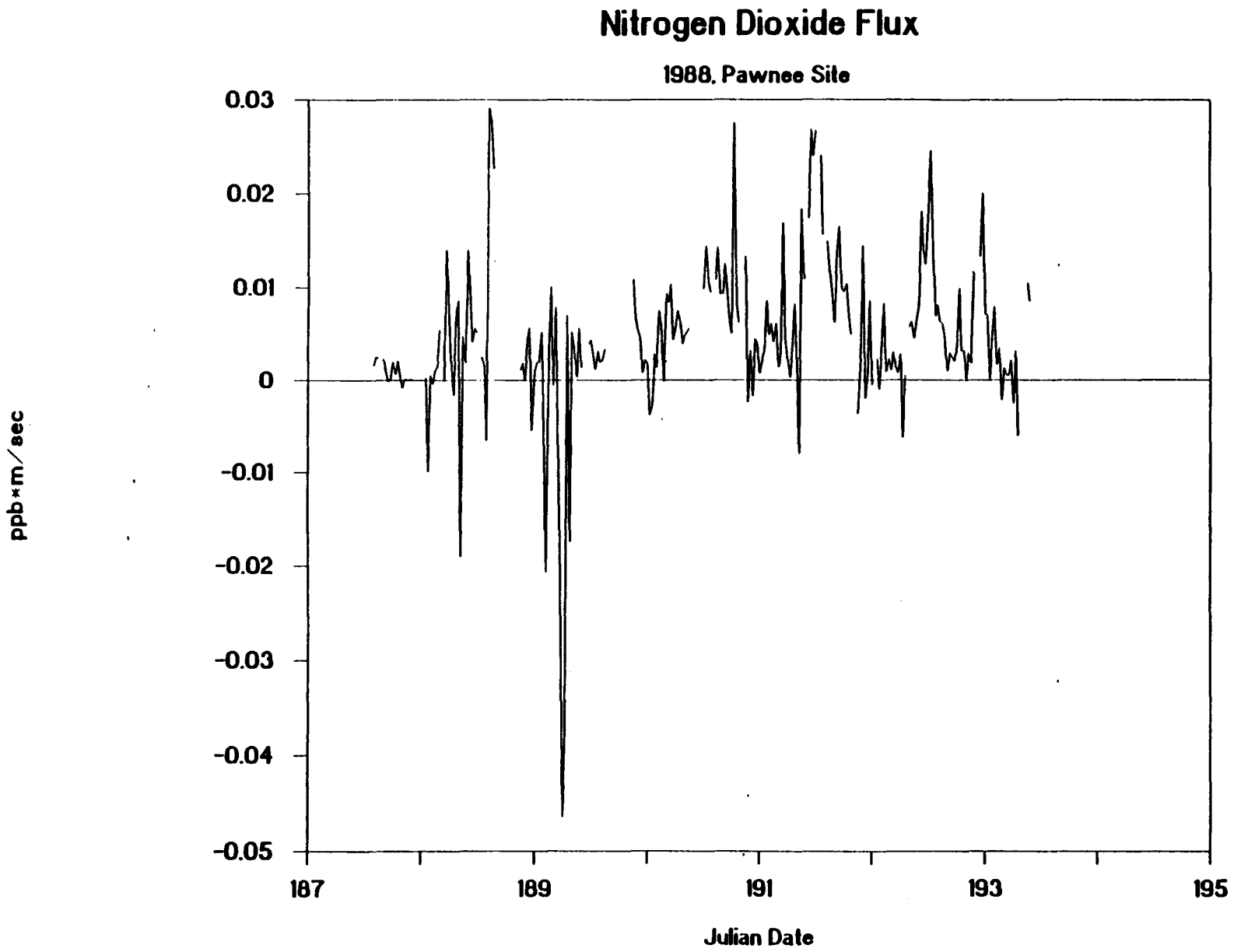

FIGURE 14: Pawnee Site Nitrogen Dioxide Flux for the 7 day period beginning July 5, 1988. (Julian day 187)

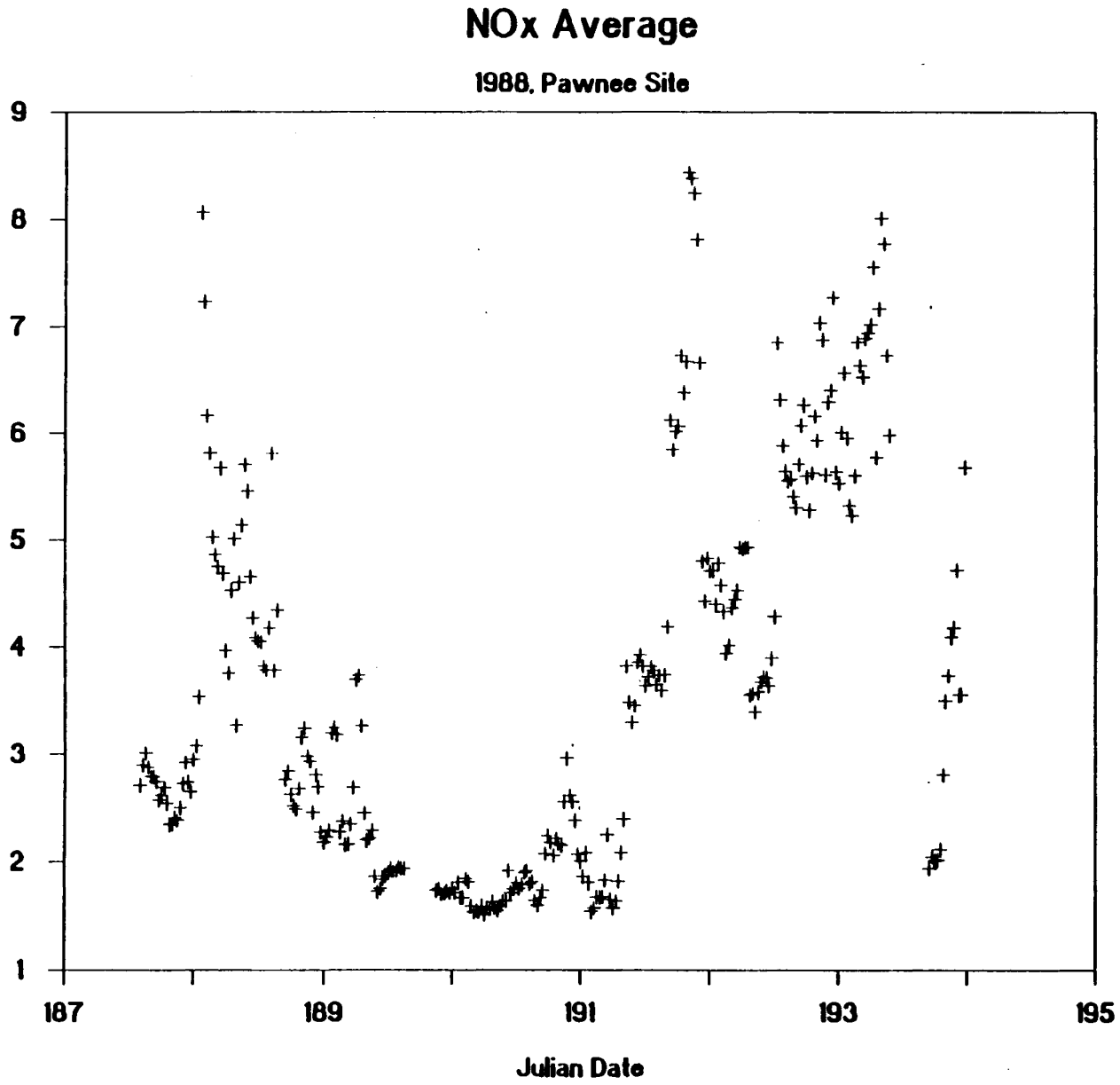

FIGURE 15: Pawnee Site Oxides of Nitrogen Concentration for the 7 day period beginning July 5, 1988. (Julian day 187)

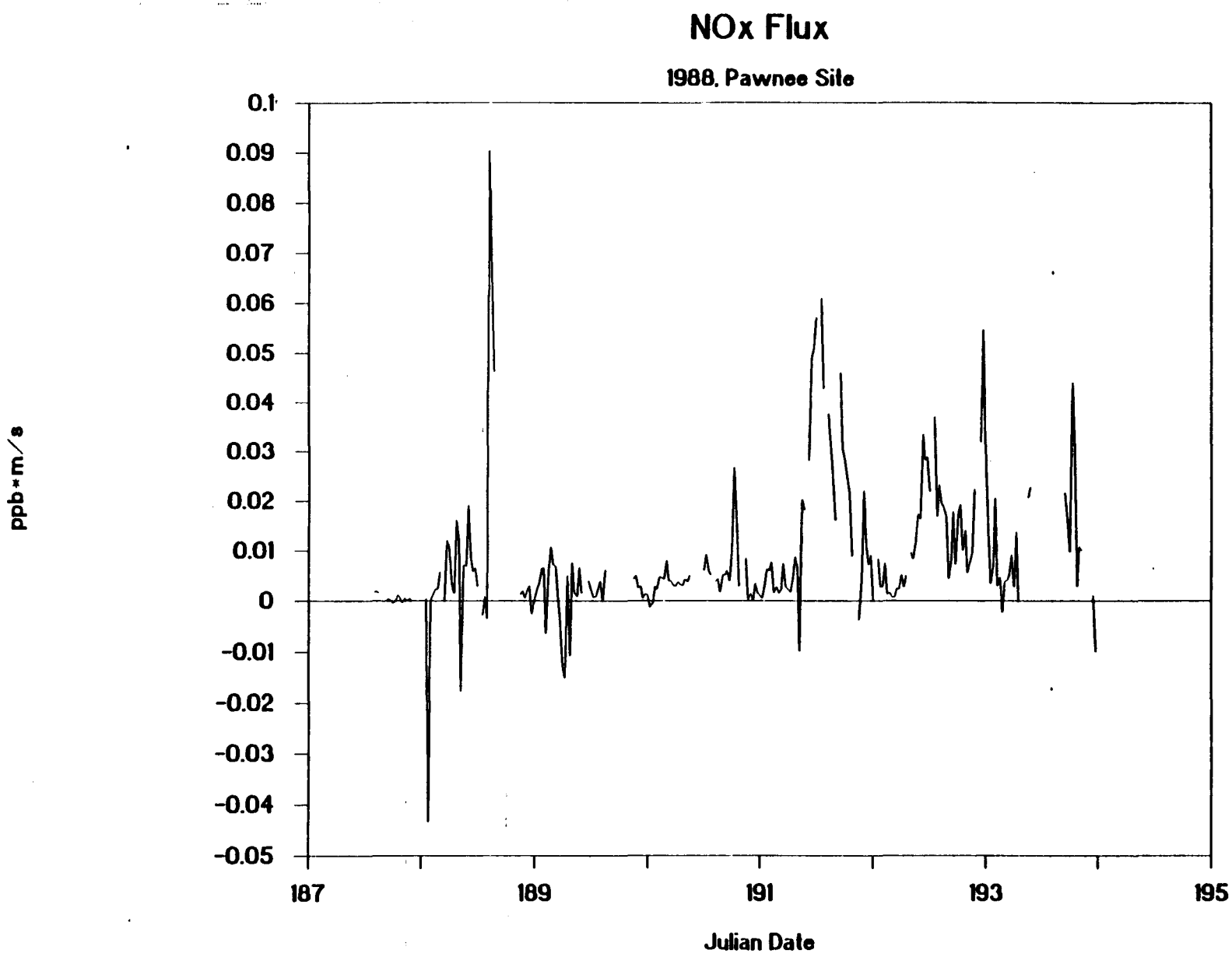

FIGURE 16: Pawnee Site Oxides of Nitrogen Flux for the 7 day period beginning July 5, 1988. (Julian day 187)

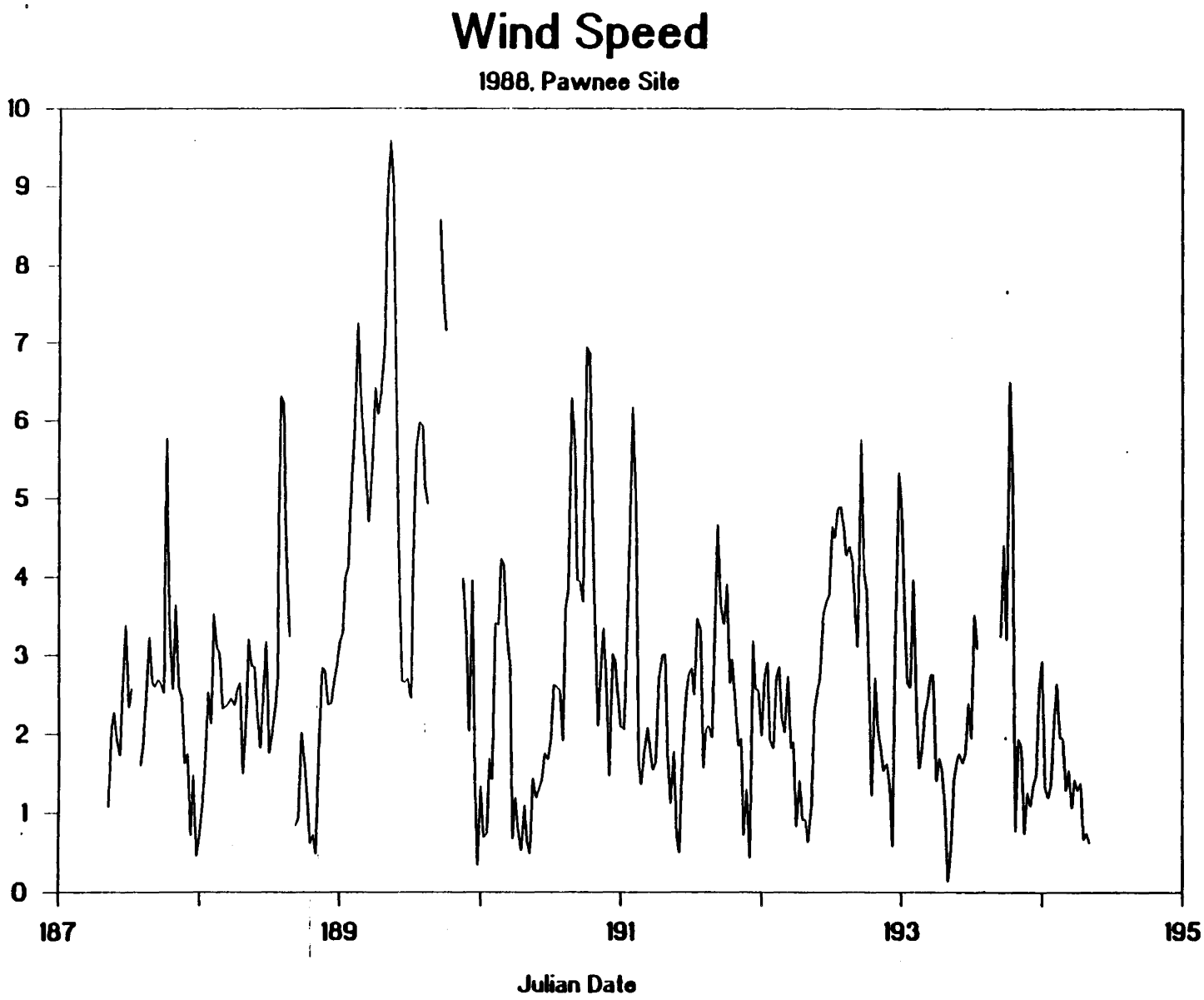

FIGURE 17: Pawnee Site Wind Speed for the 7 day period beginning July 5, 1988. (Julian day 187)

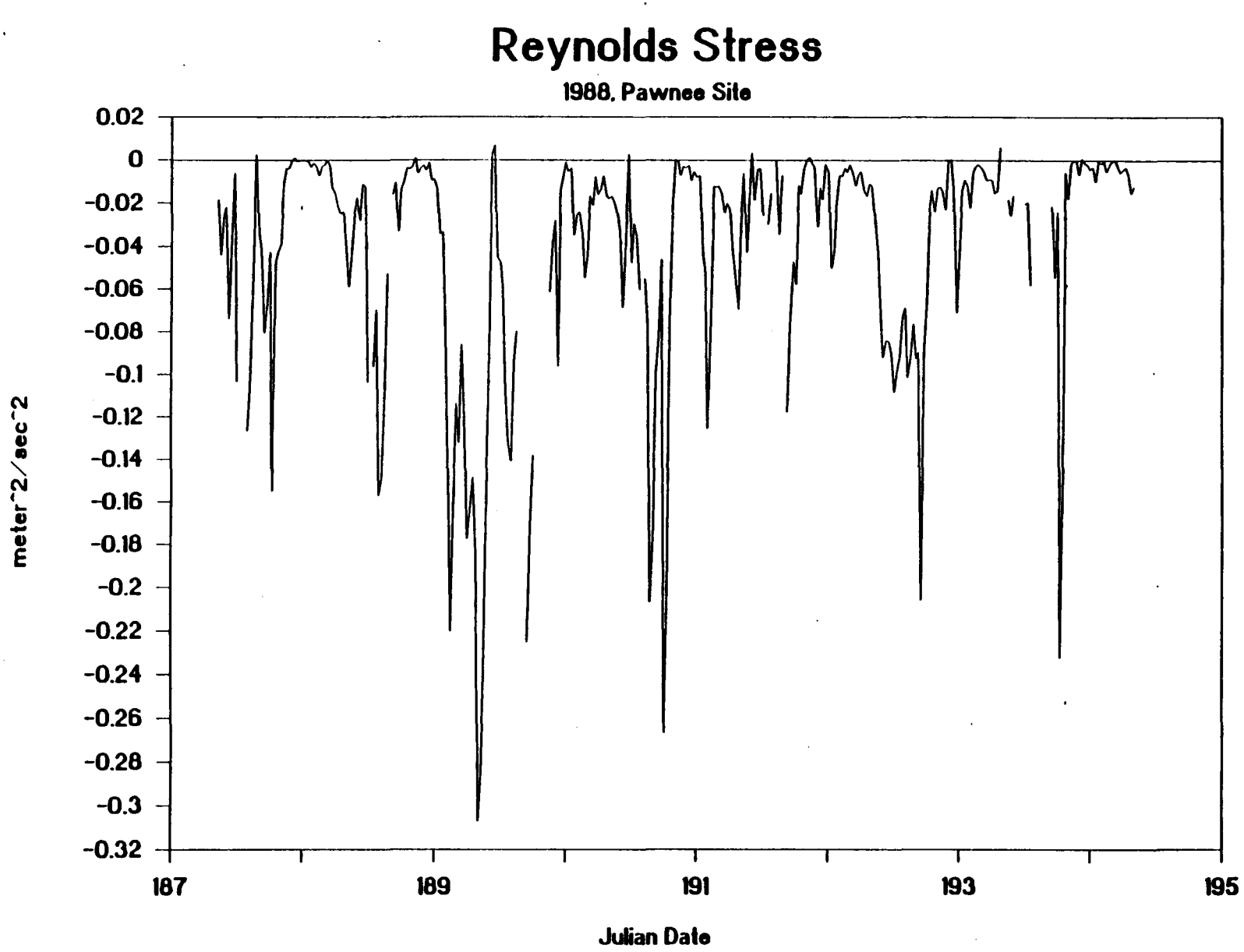

FIGURE 18: Pawnee Site Momentum Flux (Reynolds Stress) for the 7 day period beginning July 5, 1988. (Julian day 187)

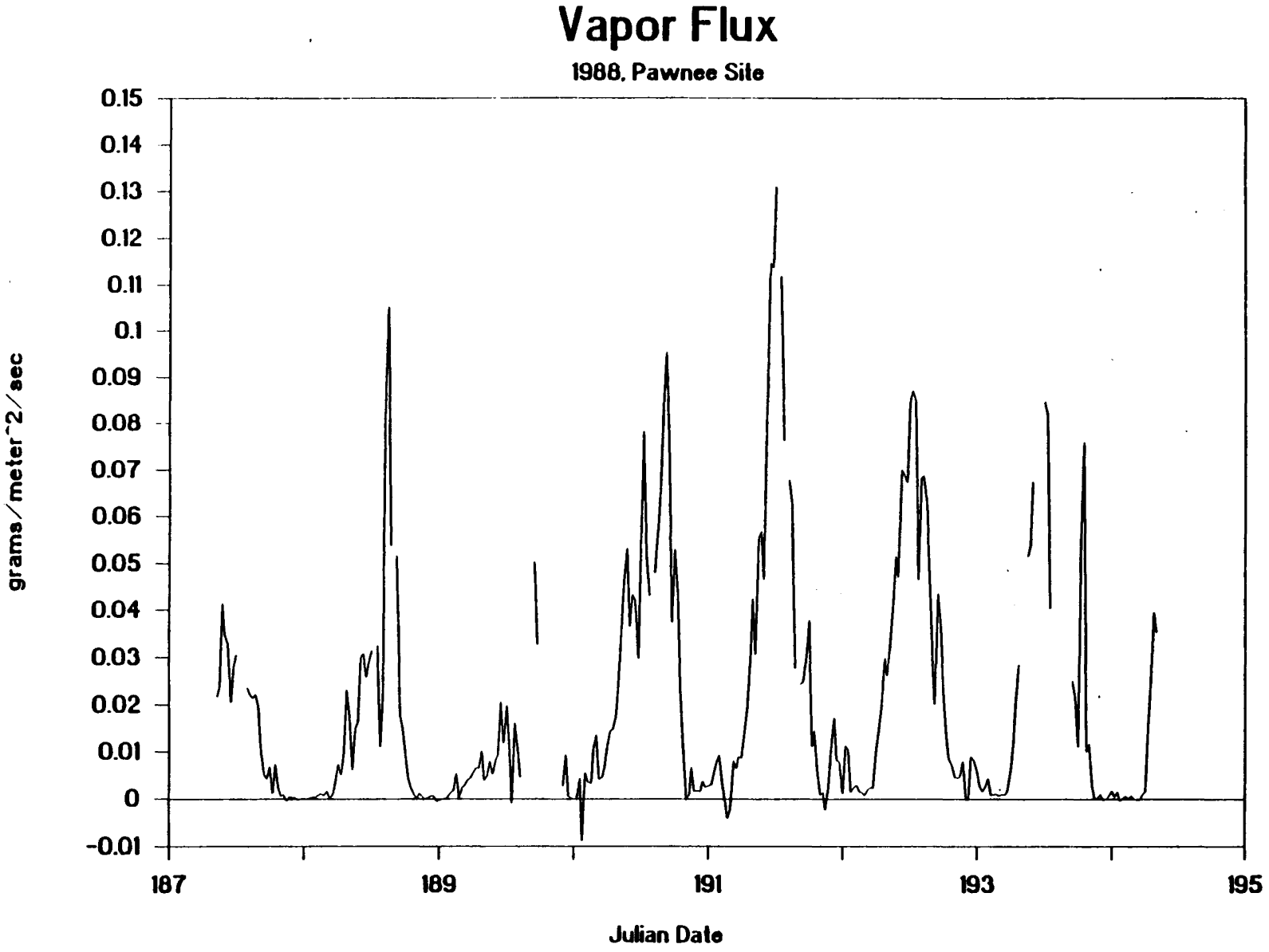

FIGURE 19: Pawnee Site Vapor Flux for the 7 day period beginning July 5, 1988. (Julian day 187)

Appendix A:

Initial Results from the Pawnee Eddy Correlation System for Dry Acid Deposition Research

Initial Results from the Pawnee Eddy Correlation System for Dry Acid Deposition Research

Karl Zeller

William Massman

David Stocker

Douglas G. Fox

Donald Stedman

Donald Hazlett

Research Paper RM-

Rocky Mountain Forest and

Range Experiment Station

Forest Service

U.S. Department of Agriculture

Abstract

The Pawnee Grassland Eddy Correlation Dry Deposition Project is described. Instrumentation, methods of analysis, and initial data and research findings are presented. Data from this eddy correlation system show agreement with (a) previous observations of deposition velocities for atmospheric ozone, NO_2, and NO_x; (b) micrometeorological theory; and (c) micrometeorological site characteristics.

ACKNOWLEDGMENTS

The authors are particularly indebted to B. B. Hicks, R. T. McMillan, J. D. Womack, and R. Martin of NOAA's ATDD for providing much of the on-line software for the analysis of the data and for sharing their time and experience with instrumentation with us. The authors also thank J. A. Businger, J. C. Wyngaard, D. R. Miller, B. B. Hicks, and R. T. McMillen for reviewing an initial version of this report.

USDA Forest Service

Research Paper RM-

MS on

diskette

Revision of 5/24/88

JP

Initial Results from the Pawnee Eddy Correlation System for Dry Acid Deposition Research

Karl Zeller, Meteorologist

Rocky Mountain Forest and Range Experiment Station[1]

William Massman, Meteorologist

Rocky Mountain Forest and Range Experiment Station[1]

David Stocker, Research Associate

Denver University[2]

Douglas G. Fox, Chief Meteorologist

Rocky Mountain Forest and Range Experiment Station[1]

Donald Stedman, Professor

Denver University[2]

Donald Hazlett, Research Associate

Natural Resource Ecology Laboratory[3]

[1]Headquarters is in Fort Collins, in cooperation with Colorado State University.

[2]Chemistry Department, Denver, Colorado.

[3]Colorado State University, Fort Collins, Colorado.

Contents

Page

MANAGEMENT IMPLICATIONS . . . . .

INTRODUCTION . . . . .

PAWNEE RESEARCH SITE DESCRIPTION . . . . .

EDDY CORRELATION SYSTEM ERRORS . . . . .

Flux Loss Corrections . . . . .

Variance Loss Corrections . . . . .

Additional Sources of Error . . . . .

DATA RESULTS AND ANALYSIS . . . . .

Site Roughness and Monin-Obukhov Similarity Theory . . . . .

Ozone . . . . .

NO_2 and NO_x . . . . .

SUMMARY . . . . .

LITERATURE CITED. . . . . .

APPENDIX A. Description of Fast Response Chemical Sensors . . . . .

APPENDIX B. Eddy Correlation System Response Characteristics . . . . .

APPENDIX C. Transfer Function for Volume Averaging . . . . .

APPENDIX D. Table of Symbols . . . . .

Initial Results from the Pawnee Eddy Correlation System for Dry Acid Deposition Research

Karl Zeller, William Massman, David Stocker, Douglas G. Fox, Donald Stedman, and Donald Hazlett

MANAGEMENT IMPLICATIONS

The deposition of sulphur (S) and nitrogen (N) compounds is the focus of a large research program being carried on currently throughout the United States. The objective of this research program is to determine what loadings of S and N, (in kilograms/hectare/year) will cause adverse ecological effects and to quantify these effects. Furthermore, research on forested ecosystems suggest that ozone, a pollutant photochemically generated from emissions of nitrogen oxides and hydrocarbons, must also be included with S and N in determining forest health.

Depending upon climate and the ambient atmospheric environment, S, N, and ozone may be deposited by either dry "processes" or by precipitation. This paper discusses only the dry deposition process.

At first glance measuring dry deposition might seem to be an easy task; for example, simply put out a bucket and measure what falls in when it is not raining. However, dry deposition measurements are not simple because the surfaces on which dry deposition occurs may themselves actively be removing the pollutant. Therefore, simple passive monitoring is not adequate for a full description of the dry deposition process. Some understanding of the nature of the underlying surface is also required.

The most accurate techniques for measuring dry deposition employ aerodynamic methods. Essentially these involve measuring how much pollution passes by a fixed level in the atmosphere. This procedure works best when the vegetation is uniform and the terrain is flat. The research reported on in this paper represents a test of the aerodynamic method known as eddy correlation under circumstances where it is expected to work well.

Eventually, we plan to use eddy correlation to make dry deposition measurements in typical alpine and subalpine ecosystems. These eddy correlation measurements will then be used to confirm simpler technologies for routine measurements of the levels of S, N, and ozone present and depositing to forested lands.

INTRODUCTION

Awareness that acid precipitation and dry deposition of acid gases and aerosols can have potentially significant impacts on the biota at the earth's surface has grown steadily in recent years (NAPAP 1987, Wetstone 1980). However, the processes by which pollutants are transported to and subsequently interact with the biota and the soils, and the influence that these pollutants can have upon the biota, remain largely unknown. In an effort to better understand these processes the USDA Forest Service, Rocky Mountain Forest and Range Experiment Station (USFS/RMFRES), Atmospheric Deposition Research Project, has undertaken a dry deposition monitoring program. This paper describes that program, outlines the data analysis methods used, and presents some initial results from our measurements.

This report specifically details efforts to implement the eddy correlation method of estimating the dry deposition fluxes of ozone, NO_2, and

NO_x. This micrometeorologically based method uses a direct measurement of the covariance between the fluctuating vertical velocity and the fluctuating concentration of the acid gas to determine the vertical flux (or rate of deposition per unit of surface area) of the pollutant to the underlying surface. The eddy correlation technique is not the only method available for estimating fluxes (Wesely and Hicks (1977) and Businger (1986) give reviews of this and other meteorological methods); but, it does have several advantages over the other approaches. It is the most fundamental of the different meteorological methods because it requires the fewest assumptions and, at present, is also the only method capable of providing a direct measure of the vertical flux of a quantity to or from the underlying surface. It is important to note that the eddy correlation flux data, although taken at a fixed point, can be considered to be the integration of the surface fluxes from some distance upstream. A disadvantage of the eddy correlation method is that it is the most demanding technically because dry deposition rates are particularly difficult to measure. For example, Sehmel (1984) lists fifty-one separate variables that can affect dry deposition rates.

The paper first gives the physical and biological description of our research site and an overview of the instrumentation used before addressing the errors associated with measurement systems in general and this system in particular. Then, initial results of the data analysis are presented. Also included are several appendixes that detail important aspects of our overall effort.

PAWNEE RESEARCH SITE DESCRIPTION

The Pawnee Project eddy correlation research site is 50 km northeast of Fort Collins, CO, at the Central Plains Experimental Range (CPER), a research area adjacent to and west of the Pawnee National Grasslands. The CPER is a 6,500-ha area of shortgrass prairie that is administered by the Agricultural Research Service of the USDA. Also located at the CPER is a long-term ecological research (LTER) shortgrass steppe research station (Halfpenny and Ingraham 1984). The LTER station is managed by Colorado State University (CSU) and is funded by the National Science Foundation. The exact CPER location of the eddy correlation research site is within a 6-ha grazing exclosure in Weld County (section 27, 1641 m elevation, latitude 40°28′23″ N. and longitude 104°45′15″ W.) (fig. 1). This exclosure was established in 1969 as an appropriate and "representative" site for meteorological instrumentation. The area is level, bordered on all sides by gently undulating plains, and is not near major ridges or bluffs that would seriously influence measurements.

Vegetation on the CPER is dominated by shortgrasses (64%), succulents (20%), and half-shrubs (8%). The immediate area surrounding the eddy correlation instrumentation is dominated by blue grama grass (Bouteloua gracilis), the major plant community type of the shortgrass steppe area in eastern Colorado (Lauenroth and Milchunas 1985). Blue grama, a warm season grass that exhibits the dicarboxylic acid biochemical pathway of CO_2 fixation, has an optimum photosynthetic temperature (when soil water is not limiting) of between 26°C and 33°C (Brown and Trlica 1974). Also present, but less common, are Bouteloua gracilis-Agropyron smithii (blue grama-western wheatgrass) plant communities. Western wheatgrass is a "cool season grass" (greatest growth during the spring and early summer) that is infrequent in the research vicinity. However, Stipa comata (needleandthread), also a cool

season grass, is common and nearly a codominant in the immediate vicinity of the Pawnee Project instrumentation tower. The most frequent forbs in the area are Opuntia polyacantha (pricklypear cactus), Gutierrezia sarothrae (snakeweed), and Artemisia frigida (fringed sage). Table 1 provides further details on species composition within the exclosure site.

The maximum total green leaf area index (LAI) attained from studies of various vegetation types at the CPER was 0.55 (Knight 1972). Peak LAI was reached about mid-June and from 60% to 80% of total LAI was blue grama. In 1971 the greatest LAI increment occurred between April 20 and June 15, with a steady decline after June 15. This seasonal pattern of total LAI production for steppe vegetation was similar to the pattern of total amounts of chlorophyll (Rauzi and Dobrenz 1970). Patterns similar to these can be expected for any year, but the rate, time, and amount of LAI or chlorophyll production for a given year will reflect different precipitation and vegetation patterns. For example, the LAI production in the vicinity of the Pawnee Project meteorological tower may have a bimodal peak because of the frequent needleandthread in addition to the dominant blue grama.

Standard meteorological data has been gathered by CSU within the 6-ha grazing exclosure for several years. In addition, the exclosure includes a 8-m^2 weighing soil lysimeter. Seventy percent of the 311 mm of mean annual precipitation occurs between April and September. This low rainfall, generally flat to gently rolling terrain, the absence of local air pollution sources, along with the long-term meteorological data records, make it a good site for attempting to measure dry deposition.

The exclosure site described above is also a pollutant deposition research facility hosting three separate acid deposition monitoring programs:

1. National Atmospheric Deposition Program/National Trends Network (NADP/NTN). Wet and dry deposition chemistry measurements are collected and analyzed at a central NADP laboratory in Champaign, IL. Data from this site (NADP site no. 06222) are available from March 1978 to present.

2. NOAA/ATDD Dry Deposition Inferential Monitoring (DDIM). This site is no. 11 of the NOAA/ATDD core dry deposition sites. Filter-pac chemical analyses of site samples collected during the same sampling period and frequency as the NADP/NTN wet chemistry samples are conducted by the USGS laboratory in Atlanta, GA. Dry deposition chemistry is coupled with micrometeorological data to infer dry acid species fluxes (Hicks et al. 1985). Dry deposition chemistry and associated meteorological data are available from July 1986 to present.

3. USFS/RMFRES, Atmospheric Deposition Research Project, Pawnee Eddy Correlation Acid Deposition Research Site. Ambient air concentrations and eddy flux measurements of NO_2, NO_x, ozone, heat, and momentum have been collected during two short-term data collection periods from mid-December 1986 through January 1987 and from mid-May 1987 through July 1987.

This last program is the subject of this paper.

Our eddy correlation system requires simultaneous measurements of the fluctuations in the vertical wind speed, heat, and chemical concentrations. These measurements are made at a rate between 10 and 20 Hz. Hence, both the wind sensor and chemical sensors must have relatively short response times (see appendixes A and B for a discussion of response times). Meeting these fast response time requirements requires very sensitive meteorological sensors and chemical analyzers. The chemical analyzers for this measurement program were provided by the University of Denver (Appendix A). These instruments are housed in an instrument shelter, and ambient air was brought to them using a

high-volume sample pump and a large-bore Teflon tube. A more detailed description of these sensors is given in appendix A and by Ray et al. (1986), Wendel et al. (1983), and Wesely et al. (1982). Table 2 lists the sensing instruments and analyzers integrated into the overall eddy correlation program.

During the two field periods, all eddy correlation measurements were made using a 3-axis Gill propeller anemometer for wind velocity and velocity fluctuations, and a fast response platinum resistance thermometer for temperature fluctuations. The Gill anemometer was corrected in real-time for non-cosine response (Massman and Zeller 1988). During one short test period in December 1986, a one-dimensional sonic heat flux sensor was used to compare heat fluxes acquired with the Gill anemometer and the fast response platinum resistance thermometer. We also plan to replace the Gill anemometer in future experiments with a 3-axis sonic anemometer.

Data collection and processing were accomplished using a personal computer interfaced with an analog-to-digital conversion board. Eight channels are available on the board for data acquisition and all eight channels (table 3) were sampled at ca. 14 Hz. Output measures include means, variances, covariances, and other micrometeorological parameters as listed in table 3. The software used for real-time data processing was adapted from McMillen's (1986) basic flux program for eddy correlation in nonsimple terrain. The compiled basic program is capable of running the entire eddy correlation measurement system unattended for several days. Tasks accomplished in real-time by this program include real-time data acquisition and processing, raw data storage if required, statistical summaries at the end of the assigned averaging period (usually 1/2 hour), instrumentation zero each

half hour to ensure accurate chemical measurements, and instrument span calibration each half hour (not yet physically implemented).

The physical layout of the eddy correlation site is shown in figure 1. The relative directional location of the instrument shelter site to instrument tower was based on meteorological data collected during 1972-75 which showed the 210° azumuth as one of the least likely wind directions (Peterson and Parton, undated). However, the analysis of one year of 10-m-height wind data at the Pawnee Project tower (fig. 2) clearly shows that during daylight hours southerly wind directions dominate over all others, quite unlike what was expected from the 1972-75 data set.

EDDY CORRELATION SYSTEM ERRORS

Our dry deposition eddy correlation system employs a variety of instruments and support equipment; still, no data system is without sources of error. For example, Businger (1986) reviews and comments on several recent attempts by various researchers to measure dry deposition of gases and particles. He notes that up to the present there has been no discipline among the various researchers to ensure that their data have all ingredients for an accurate determination of dry deposition, and he presents ten specific sources of error that he claims are found in most field programs:

1. Failure to account for the effect of heat and water vapor fluxes;
2. Sampling errors due to insufficient averaging time;
3. Inadequate sensor response characteristics;
4. Sensors separated by too great a distance;
5. Random noise not accounted for;

6. Errors inherent in the horizontal uniformity and steady-state assumptions due to entrainment, advection, and nonstationarity;

7. Errors due to wrong sampling height;

8. Inadequate fetch;

9. Errors related to deliquescences of particles;

10. Errors due to flow distortion around sampling probes and mounting structures.

In order to make routine measurements of dry deposition fluxes, it is necessary to examine these and other errors and, where possible, account for them in the resulting data. We begin by examining errors that can arise from sensor limitations in size and response, and instrument separation and mismatch.

Flux Loss Corrections

Methods similar to those of Moore (1986), as detailed in appendix B, were used to estimate the flux losses with the Gill propellers in the sensor array and then the data were corrected for these errors. The heat, momentum, and chemical flux losses for stable and unstable atmospheric conditions as a function of wind speed are given in figures 3, 4, and 5, respectively. The solid lines assume matched sensors and the dashed lines on these figures assume mismatched sensors (if no dashed line appears then sensor mismatch was not significant). By matched sensors we mean that the two separate types of instruments used to make the flux measurements have identical response characteristics and mismatched sensors means they do not. The separation distances used for these computations were 36.0 cm between the vertical Gill propeller and the temperature sensor, 63.0 cm between the vertical Gill

propeller and the horizontal Gill propellers, and 37.8 cm between the vertical Gill propeller and the mouth of the intake tube leading to the chemical sensors. For matched sensors, this system will underestimate the heat flux by at least 20% to 30% for unstable conditions and about 50% for stable conditions. Likewise, the momentum flux is underestimated between about 10% and 60%, depending upon wind speed and stability. These latter results are quite consistent with Horst's (1973b) estimates of the momentum flux loss that can be expected with Gill propellers. Finally, the ozone, NO_2, and NO_x flux losses are between 30% and 90%, again depending upon stability and wind speed. The NO_x flux loss is slightly higher than that of the other two sensors because of its slightly slower response time. These large flux losses result from the slow response times for both the Gill propeller and the chemical sensors.

The dotted lines on figures 3 and 5 give the estimates of the heat flux losses and the chemical flux losses caused by mismatching. For the heat flux, mismatching can increase the flux loss by another 8% for an unstable atmosphere and another 15% for a stable atmosphere. For the chemical fluxes, at low wind speeds the estimates of flux losses are also increased. For a stable atmosphere the flux loss is an additional 8% for the chemical fluxes and for an unstable atmosphere it is about another 5%. As figure 5 also shows, mismatching has little effect on the chemical fluxes at moderate wind speeds, because the vertical Gill propeller has a response time comparable to that of the chemical sensors. Furthermore, this figure also shows that as the wind speed increases, mismatching again begins to contribute additional errors because of the reduction of the response time of the vertical Gill propeller at high wind speeds relative to the response time of the chemical sensors. Similar comparisons were made for the momentum flux losses. However, the

response times of the horizontal and vertical Gill propellers were not different enough to introduce any significant mismatching errors.

In addition to the above errors associated with the Gill UVW, two other matters relating to its use for estimating turbulent fluxes and variances are relevant. The first involves the need to correct the turbulence data gathered with these instruments for their lack of a perfect cosine response. Massman and Zeller (1988) discuss this at length and provide an algorithm that can be used to make this correction in real-time. They show that without this correction, turbulent heat and momentum fluxes are underestimated by about 30%.

Unfortunately, the second problem cannot be fully corrected. Because these propellers tend to stall whenever the flow is greater than about 88° off axis, they will always underestimate turbulent fluxes. This is most serious with the vertical propeller, which senses a field that is always fluctuating through the propeller's stall region. This problem will be most severe whenever the horizontal velocity is significantly greater than the vertical velocity. Finkelstein et al. (1986) discuss in greater detail the limitations of these sensors for turbulence measurements.

Again, the methods outlined in appendix B were used to estimate the flux loss errors associated with using the 3-axis sonic anemometer in place of the Gill anemometer. For this case, the separation distances are 6.35 cm, 0.0 cm, and 30 cm between the center of the vertical sonic's acoustic path and the temperature sensor, the center of the acoustic path of the horizontal sonic, and the mouth of the intake tube to the chemical sensors, respectively. The solid curves and dashed curves of figures 6, 7, and 8 give the results of the computations for the flux losses for the sonic anemometer corresponding to figures 3, 4, and 5, respectively. In general,

the 3-axis sonic anemometer provides much better estimates of the fluxes of heat and momentum at all wind speeds and the fluxes of the three chemical species at low wind speeds than does the Gill anemometer. Figures 6 and 7 show that the sonic anemometer will probably underestimate heat and momentum fluxes by about 5% to 30%, and figure 8 shows that the fluxes associated with the three chemical species will be underestimated for wind speeds below about 7 m/s between 20% or 30% to 60%, depending upon stability. At wind speeds above 7 m/s, there is little improvement in the estimates of the fluxes of O_3, NO_2, and NO_x with the sonic anemometer over the Gill anemometer; this is largely a reflection of the nature of the chemical sensors and their characteristics and is quite independent of the nature of the vertical velocity sensor.

The dotted curves of figure 8 also show that the mismatching of these two types of sensors can introduce an additional 5% to 10% underestimation of the chemical fluxes, depending upon atmospheric stability and wind speed. A similar computation for the heat flux measurements showed that the mismatching errors associated with the temperature sensor and the vertical sonic anemometer were negligible.

It is also important to note that at higher wind speeds the mismatch between the sonic anemometer and the chemical sensors is actually worse than it is between the Gill propeller anemometer and these chemical sensors. Consequently, there is a greater loss of flux at higher wind speeds when using a sonic anemometer to measure the fluctuating component of the vertical velocity than when using a Gill propeller anemometer. For correcting our flux measurements, we assume the instruments are mismatched and use the dashed curves in figures 3, 5, and 8.

Although it is important to use the results from these figures to correct turbulence data obtained with the sonic anemometer, it is also important to correct the data for shadowing effects. Shadowing will cause the measured velocity component to be underestimated because of partial shadowing of the acoustic path by the tranducers. We plan to use the algorithm being developed by Conklin et al. (1988) for this correction to the 3-axis sonic anemometer.

In addition to comparing and correcting flux estimates derived with the Gill and sonic anemometers, other aspects of sensor performance were considered. One was the relative importance of the volume averaging effects that the intake tube of the chemical sensors can have upon the estimates of the flux loss. These volume averaging effects arise because measurements of concentration are not made at a point, but rather such measurements represent the average concentration of a finite volume of air that has been drawn into the chemical sensors through the Teflon tube. To assess these effects, estimates of the O_3, NO_2, and NO_x flux losses with and without the response function appropriate to volume averaging (appendix C) were needed for both types of anemometers. Volume averaging effects were shown to be negligible in both cases. Therefore, the major reason for the significant losses of O_3, NO_2, and NO_x fluxes (fig. 5 and 8) is largely the slow response times of these sensors.

Variance Loss Corrections

In addition to the flux loss correction, the variance loss for the sensors was also estimated. Appendix B gives the details of the computations used in the following discussion.

The variance loss estimate for temperature, vertical velocity (for both the Gill and sonic anemometers) and the chemical species are presented in figures 9-12. The conclusions that can be drawn from these figures are the same as with the flux loss estimates; namely, (1) that the sonic anemometer generally represents an improvement over the Gill propeller anemometer, and (2) that the slow response of the chemical sensors can cause significant losses to the variance measurements, especially for stable conditions. However, there is one important difference between these variance loss estimates and the preceding flux loss estimates. In many cases, the variance loss is explicitly dependent upon the stability parameter z/L, as discussed in more detail in appendix B. This is always true whenever the atmosphere is stable, and it is true for the vertical velocity variance for unstable conditions as well. For the flux loss estimate, on the other hand, it is sufficient to know only whether the atmosphere is stable or unstable (equivalent to knowing only the sign of z/L or the direction of the heat flux). Therefore, in order to correct for any loss of variance, we must first correct for any loss of heat and momentum flux using the estimates derived above; next we compute a value for z/L based on the heat and momentum fluxes; and then we make an estimate of variance loss for that value of z/L. Obviously, estimating the variance loss is considerably more complicated than for estimating flux losses.

Finally, an important caveat must be stated concerning all estimates of the flux or variance losses. There is some uncertainty in the atmospheric spectra and cospectra used for these computations (see Moore (1986) for further discussion). Although this uncertainty is not serious for small estimates of loss (less than about 30%), it can become more important at

higher estimates of loss, which can make the correction less reliable whenever the flux loss is large.

Additional Sources of Errors

In addition to the errors associated with instrument response, size, and siting geometry, outlined above, it is equally important to be aware of and account for other important measurement limitations and problems associated with the eddy correlation technique. For example, both heat and moisture fluxes can significantly influence flux measurements (Webb et al. 1980), as can digitization noise (Kristensen and Kirkegaard 1987), random uncorrelated noise (Lenschow and Kristensen 1985), flow distortion effects (Wyngaard 1988, Högström 1988), and site inadequacies such as insufficient fetch and lack of surface uniformity.

Corrections to dry deposition fluxes due to heat and moisture fluxes arise because of the atmospheric density variation associated primarily with the heat flux and secondarily with the moisture flux. For our site the humidity is low and much of the time evapotranspiration (moisture flux) is not large; therefore, we will use the following expression for correcting the measured fluxes of O_3 and NO_2:

$$F = F_m + (\bar{\rho}_c \overline{w'T'})/\bar{T} \qquad [1]$$

where F_m is the measured flux after the instrument corrections outlined in the previous section have been applied, $\bar{\rho}_c$ is the mean concentration of the constituent (O_3 or NO_2), $\bar{T}$ is the mean ambient temperature, and $\overline{w'T'}$ is the heat flux also measured after the instrument corrections have been applied.

Our experience has shown that the correction term $(\bar{\rho}_c \overline{w' T'})/\bar{T}$ in this equation is typically between 1% and 20% of the measured ozone flux and is frequently significantly higher for the measured NO_2 fluxes. The NO_x sensor, on the other hand, does not require this correction. Fundamentally this sensor measures the mixing ratio rather than a concentration as do the ozone and NO_2 sensors. For measurements of fluxes based upon mixing ratios, Webb et al. (1980) have shown that no correction need be applied.

In the case of variance measurements, digitization noise can also influence measurements (Kristensen and Kirkegaard 1987). Although a correction for this effect was included in our data analysis, usually it was negligible.

Uncorrelated noise (Lenschow and Kristensen 1985) can also impact flux measurements. This is particularly true whenever the instruments are event counters. Our chemical sensors measure a current rather than counting photons, and the concentrations being measured are sufficiently high that this type of uncorrelated noise error does not contribute significantly to our errors.

Flow distortion effects caused by sensor geometry and their positioning on towers can also influence observations significantly (Wyngaard 1988, Högström 1988). Our measurements are undoubtedly influenced to some extent by these effects; however, drawing air samples into the shelter with an intake tube minimizes the amount of equipment placed on the towers, which should considerably reduce flow distortion effects.

Finally, patchiness in the local vegetation cover and inadequate fetch can also interfere with flux measurements; but, these site limitations do not appear at present to have had any significant impact on our data. (We say this because, as will be shown in the next section, our data agree with

previously and independently made observations). However, eddy correlation measurements of moisture flux and independent measurements of the surface energy balance are planned and should provide more insight into how much site limitations (and flow distortion as well) can influence the data.

DATA RESULTS AND ANALYSIS

Sample results from our Pawnee program were used to assess the utility and performances of the different meteorological and chemical sensors. To examine normalized variances of temperature and vertical velocity and the correlation coefficient between temperature and vertical velocity, the Monin-Obukhov similarity theory was used. Similar computations were performed for the ozone, NO_2, and NO_x fluxes. Deposition velocities and surface resistances derived from our system at the Pawnee site were compared with similar measurements made at other sites for these three acid species.

For this analysis, we selected a 2-week period beginning on June 30, 1987, at 9:00 a.m. MST, which made available a set of more than 600 potentially useful data points (fluxes, variances, etc.) at half-hour intervals. As an example of these data, figures 13, 14 and 15 give the corrected heat, momentum, and ozone fluxes, respectively, for the week beginning with June 30. These data have not been smoothed or checked for bad data points (discussed below), and breaks in the curves occur whenever data were not recorded. However, not all these data are useful, and the following criteria were developed for limiting the analysis to the best data.

1. Data taken when the wind direction was between 150° and 225° were eliminated. This precluded any interference by the tower and the instrument shelter on the measurements

2. Data taken when the horizontal wind speed was less than about 1.9 m/s were also eliminated. This criterion was necessary to ensure that the anemometry would resolve the momentum flux adequately. The exact value of this cutoff wind speed was determined by trial and error and resulted from an analysis of the roughness length appropriate to our site, as is discussed more fully later.

3. All momentum flux measurements larger than -0.0025 m^2/s^2 were also eliminated. The purpose here was to remove all positive momentum fluxes and all small negative stresses that are below the instrumentation's ability to resolve. Contrary to expectations, the observed momentum flux is sometimes positive, possibly because of the brief and intense "bursts," which in the atmospheric boundary layer have been observed to reverse the sign of the momentum flux (Haugen et al. 1971). These positive momentum fluxes were removed because all computations involving Monin-Obukhov similarity theory and surface roughness lengths require negative Reynolds stress only.

4. All time series (temperature, velocities, chemical concentration, fluxes, etc.) were visually checked and all obviously noisy data points were removed. These data were usually in the form of individual spikes in the data and were simply unrealistic on physical grounds. (Examples of this type of data would include ambient temperature measurements that exceed the boiling point of water.)

5. For the analysis of the NO_2 and NO_x data, our criterion required that the observed NO_x concentration exceed the observed NO_2 concentration (otherwise the data from both sensors were eliminated). In a few instances, the observed NO_2 concentration did exceed the observed NO_x concentration. In some cases, this was due to low or nonexistent flow rates of the chemiluminescent reactant through the reaction chamber; in other cases,

however, this discrepancy was not fully understood but may have been due to problems in the calibration of these two sensors.

6. All data referring to the fast response chemical sensors taken during periods of calibration of the chemical instruments were eliminated. During a calibration period (usually twice weekly), the instruments were manually being adjusted and tested; hence the data recorded by the computer system during this time will not reflect ambient conditions. A calibration of these instruments typically requires between 30 and 60 minutes.

Employing these six criteria reduced the total number of acceptable data points from a potential of more than 600 to between 200 and 300, depending on what parameter was being analyzed.

Site Roughness and Monin-Obukhov Similarity Theory

Wind speed above a surface is influenced by the momentum flux, the surface roughness length, and the atmospheric stability. The relationship between these variables is defined as follows:

$$\bar{u} = \frac{u_*}{k}[\ln(z/z_o) - \psi_m(z/L)] \qquad [2]$$

where ψ_m is the atmospheric stability influence function for momentum, z_o is the surface roughness length, z is the instrument height (6 m), k is the von Karman constant, and u_* is the friction velocity defined as $(-\overline{u'w'})^{1/2}$ where $-\overline{u'w'}$ is the Reynolds stress.

The influence function, ψ_m, is generally expressed as follows (Paulson 1970, Businger et al. 1971):

$$\psi_m(z/L) = \begin{cases} 2\ \ln\left(\frac{1+x}{2}\right)+\ln\left(\frac{1+x^2}{2}\right)-\tan^{-1}x+\pi/2 & z/L\leq 0 \text{ (unstable, neutral)} \\ -5\ z/L & z/L>0 \text{ (stable)} \end{cases} \quad [3]$$

where $x = (1 - 16\ z/L)^{1/4}$.

Therefore, using our measurements of heat and momentum fluxes, wind speed, and temperature and employing the corrections outlined in the previous section, we could compute z_o with the above relationships. Figure 16 shows the computed values of roughness length plotted against wind speed for our data set for all wind speeds greater than 1.9 m/s. Except for one outlier ($z_o \approx 45$ cm, $\bar{u} \approx 3$ m/s), all roughness lengths are between about 0.5 and 30 cm. The reason 1.9 m/s was chosen as the lower cutoff speed for acceptable measurements is that all other outliers were associated with these lower wind speeds and not with wind direction. Therefore, it was concluded that our data system could not resolve momentum flux at wind speeds below about 1.9 m/s.

The average z_o computed from the data shown in figure 16 is 4.2 cm $\pm$ 5.0 cm, a value in good agreement with the 4 cm found by Korrell et al. (1982) for most wind directions at the Boulder (Colorado) Meteorological Tower which is located about 100 km southwest of our site in similar terrain with similar plant cover. However, our results, unlike theirs, did not show any correlation between z_o and wind direction, although with our 6-m measurement height our z_o values are probably influenced by local terrain features.

In addition to the large variability in our z_o values, it is also important to examine other effects that may lend further uncertainty to defining a z_o value for our site. Both the form chosen for ψ_m and any systematic underestimation of the momentum flux can cause z_o values to differ

significantly from those shown in figure 16. For example, the results presented by Carl et al. (1973) yield a different form for ψ_m appropriate to unstable atmospheric conditions; and, Högström (1988) found, when correcting [3] for flow distortion errors, that for unstable condition $x = (1-15.2\ z/L)^{1/4}$ and for stable conditions $\psi_m(z/L) = -4.8\ z/L$. These two corrections resulted in a better representation of $\psi_m(z/L)$ than [3]. The results of Carl et al. (1973) produce the following expression for unstable ψ_m:

$$\psi_m(z/L) = 3/2\ \ln\left(\frac{1+x+x^2}{3}\right) - \sqrt{3}\ \tan^{-1}\left(\frac{2x+1}{3}\right) + \pi/\sqrt{3} \qquad z/L \le 0 \qquad [4]$$

where $x = (1-15\ z/L)^{1/3}$.

Using [4] instead of [3] yields z_o values that are about 40% lower for unstable atmospheric conditions than those shown in figure 16, while Högström's formulation of [3] produced essentially negligible changes in the z_o values.

Likewise, systematic underestimation of the momentum flux can also impact our z_o computations. Such systematic errors can arise due to poor vertical alignment, degradation of the bearings in the Gill propeller, etc. We repeated our z_o computations assuming that the momentum stress was consistently underestimated by 25% and found that all z_o values were 50% higher than those shown in figure 16. Given these results and those concerning ψ_m and the variability in z_o in general, we take $z_o = 4$ cm for our site, but the uncertainty associated with this value is large. Finally, it should be noted that z_o should vary with time of year and the nature of the plant cover or snow cover. Therefore, our z_o value may be valid only for the present data set.

Monin-Obukhov similarity, in addition to providing some insight into the influence function, ψ_m, for our z_o correlations, also predicts the functional relationships between z/L and the normalized variances of vertical velocity, σ_w^2/u_*^2, and temperature, $(-z/L)\sigma_T^2 u_*^2/(\overline{w'T'})^2$. Because these two normalized variances are combinations of various quantities measured by our system, computing them with our data provides (1) a method to assess the quality or information content of our data set and (2) a means for checking the correction factors derived in the previous section.

Figure 17 is a plot of σ_w^2/u_*^2 vs. z/L as computed with our data and as expected from similarity theory (solid line = $1.7(1\text{-}3\ z/L)^{2/3}$, from Panofsky et al. (1977)). Although the individual data points obviously show significant variability, the data in some average sense appear to follow the expected curve. This suggests that the correction factors discussed in the previous section are realistic overall, but that they may be in error for individual points. This may arise in part from the assumption that the response length of the vertical Gill propeller is constant (appendix B); whereas, it is in fact a function of the wind velocity's angle of attack, which may vary from data point to data point. Some portion of the scatter shown in figure 17 is also probably due to errors in the measurement of the momentum flux. This is a particularly demanding measurement which is quite sensitive to even small errors in alignment and other effects. Finally, during stable atmospheric conditions ($z/L > 0$), these difficulties are further compounded because (1) the fluxes and variances will usually be much smaller in magnitude than for unstable atmospheric conditions, placing greater demands on the instrumentation, and (2) the correction factors become less certain for stable

conditions because the spectra and cospectra are themselves less well defined in stable conditions.

Figure 18 is a plot of $(-z/L)\sigma_T^2 u_*^2/(\overline{w'T'})^2$ vs. z/L as computed with our data and as expected from similarity theory (solid line = $0.92(-z/L)^{2/3}$, from Wyngaard et al. (1971). The agreement between our observations and similarity theory is better than in the previous figures and is actually surprisingly good except for a few points between z/L = 0 and z/L = -1.5. The reduction in scatter over the results in the previous figure may be due to the use of a relatively high-performance temperature sensor. Certainly fewer assumptions were involved in estimating variance and flux losses with this sensor than with the Gill propeller anemometer.

Figure 19 is a plot of the correlation coefficient, r_{wT} between temperature and vertical velocity vs. z/L. The correlation coefficient is defined as $\overline{w'T'}/(\sigma_w\sigma_T)$. This plot shows that in unstable conditions $r_{wT} \approx +0.55$, and for stable conditions $r_{wT} \approx -0.15$. However, the data possess a large amount of variability. For unstable conditions, our value of r_{wT} is in good agreement with Haugen et al. (1971). For stable conditions, however, Haugen et al. (1971) suggest that $r_{wT} \approx 0.3$. Again, this discrepancy could be the result of the many possible errors associated with these measurements during stable conditions.

Ozone

Up to now, we have simply assumed that ozone is transported and dispersed by atmospheric turbulence in a manner similar to temperature. However, comparing the normalized ozone variance $(-z/L)\sigma_{o_3}^2 u_*^2/(\overline{w'o_3'})^2$ against z/L,

provides an important consistency check of this similarity assumption. Figure 20 is the same as figure 18 except for a different range of z/L values and the use of the ozone data rather than the temperature data. Although there is somewhat more scatter and fewer data points in figure 20 than in figure 18, the results are still quite similar. There is nothing, therefore, in either of these figures to invalidate our assumptions of similarity between these two atmospheric scalars.

The correlation coefficient between ozone and the vertical velocity, r_{wo_3}, can also provide some information concerning the utility of the variance method of estimating the ozone flux (Businger 1986). From figure 21, which gives a plot of r_{wo_3} vs. z/L, r_{wo_3} can probably be approximated by a single value (-0.55) reasonably well. Although again these data show a lot of scatter, they are in good agreement with the r_{wT} for unstable conditions. However, for stable conditions all values between -0.1 and -0.6 seem to be about equally represented for r_{wo_3}. Thus, it is not possible to confirm or reject the usefulness of the variance method.

In addition to examining the ozone data using Monin-Obukhov similarity theory, we can also use this data to derive deposition velocities and surface resistances. The deposition velocity, v_d, is defined as the negative turbulent flux divided by the mean concentration; the surface resistance, r_s, is defined as follows:

$$r_s = \frac{1}{v_d} - \frac{1}{ku_*}[\ln(z/z_o) - \psi_c(z/L)] - \frac{2.63}{ku_*} \qquad [5]$$

where ψ_c is the influence function for ozone. Assuming that ψ_c is equal to the influence function for heat, we have (Paulson 1970):

$$\psi_c(z/L) = \begin{cases} 2\ln\left(\frac{1+x^2}{2}\right) & z/L \leq 0 \\ -5\ z/L & z/L > 0 \end{cases} \qquad [6]$$

where $x = (1-16\ z/L)^{1/4}$. From the definition of surface resistance, [5], we see that it is a residual and equal to the total resistance, $r_t = 1/v_d$, less the aerodynamic resistance, $([\ln(z/z_o) - \psi_c(z/L)]/ku_*)$, and the boundary layer resistance, $(2.63/ku_*)$. Further discussion of these latter two resistance terms can be found in Hicks et al. (1985).

Figures 22 and 23 give, respectively, the deposition velocities and the surface resistances for ozone as a function of the time of day for our data set. The mean deposition velocity for ozone is 0.43 cm/s and the range of our observed deposition velocities (about 0.1 cm/s to about 1.2 cm/s) are in good agreement with all other observations (e.g., Wesely et al. 1978; Sehmel 1980; Delaney et al. 1986). The surface resistance for ozone basically should reflect the behavior of the plant cover during the course of a diurnal cycle, which is roughly what figure 23 shows. Although there is a lot of scatter in these data, generally higher resistances are seen at night and lower resistance in the daylight hours, with a minimum resistance between 2 and about 4 s/cm between about 900 hours and 1600 hours and a maximum resistance between about 10 to 20 s/cm at other times during the day. This diurnal cycle of surface resistance as portrayed in the figure is in good agreement with the diurnal cycle of stomatal resistance for Bouteloua gracilis (Monson et al. 1986), the dominant plant in the area.

NO_2 and NO_x

The NO_2 and NO_x data were analyzed in a manner identical to that discussed above for ozone and, inasmuch as the results and conclusions apply equally to both NO_2 and NO_x, only the NO_2 sensor will be discussed. The results for the NO_2 sensor are summarized in the next four figures.

Figures 24 and 25 give the measured NO_2 concentration (in ppb/volume) and corrected NO_2 fluxes for the first week of our data set. Both the NO_2 concentrations and the NO_2 fluxes are highly variable. The positive NO_2 fluxes in figure 25 indicate that the surface itself may be a source for NO_2, as has in fact been observed (Slemr and Seiler 1984; Williams et al. 1987). Furthermore, the variability in the NO_2 source strength at the surface has also been observed to be extremely variable in both time and space. For example, Slemr and Seiler (1984) reported variation in source strength of over 100-fold. To further complicate the interpretation of our data, natural NO emitted from soils is oxidized in the presence of ozone and ultraviolet radiation to NO_2. When this occurs (which it certainly must at our site), Fitzjarrald and Lenschow (1983) and Lenschow and Delany (1987) have shown that the measured fluxes can be in error by significant amounts (about 30% at our measuring height of 6 m).

Figure 26 gives r_{wNO_2} as a function of z/L and figure 27 gives the deposition velocity for NO_2 as a function of the time of day. In the first of these two figures, there is no clear evidence of any correlation between the vertical velocity fluctuations and the NO_2 concentration fluctuations. The deposition velocities clearly reflect the variability in the NO_2 flux itself.

Although our results are inconclusive for NO_2, it should be noted that our observations are very similar to other observations of NO_2 and NO_x measurements (e.g., Delaney et al. 1986; Hicks et al. 1986). In general, until more is understood quantitatively about the role of generation and destruction of NO_x and NO_2 at the surface and within the soil, it will be difficult to make further progress on interpreting similar measurements. Furthermore, it will probably require some sort of a soil nitrogen cycle model coupled with a chemical and atmospheric transport model to fully interpret our results.

SUMMARY

Our efforts at measuring the dry deposition fluxes of ozone, NO_2, and NO_x employing the eddy correlation method have been outlined. Although this method is demanding and complex, at present it offers the only direct approach available for making these measurements and, therefore, we chose this technique over any other. Although an attempt was made to account for as many errors associated with this approach as possible, sources of errors undoubtedly remain. Nevertheless, the results of our initial analysis suggest that our eddy correlation system produces realistic and valid data that agree with many previous and independent meteorological and biological measurements.

Finally, it should be emphasized that this report is part of a continuing effort at the Pawnee Grasslands. More detailed analysis of the data gathered to date is planned, and the system will be expanded to include moisture flux measurements using eddy correlation methods. Furthermore, long-term comparisons of the eddy correlation fluxes of heat and moisture with other independently measured terms of the surface energy balance are also planned.

Hopefully, these and other future plans should further demonstrate the utility and validity of our system and the quality of our site.

LITERATURE CITED

Anderson, D.E.; Verma, S.B.; Clement, R.J. [and others]. 1986. Turbulence spectra of CO_2, water vapor, temperature and velocity over a deciduous forest. Boundary-Layer Meteorology. 38: 81-99.

Andreas, E.L. 1981. The effects of volume averaging on spectra measured with a Lyman-Alpha hygrometer. Journal of Applied Meteorology. 20: 467-475.

Brock, F.V.; Nicolaidis, C.E. 1985. Instructor's handbook on meteorological instrumentation. NCAR/TN-237+1A, National Center for Atmospheric Research, Boulder, CO.

Brown, L.F.; Trlica, M.A. 1974. Photosynthesis of two important grasses of the shortgrass prairie as affected by several ecological variables. IBP Technical Report No. 244. 190 p.

Burkhardt, M.R.; Maniga, N.I.; Stedman, D.H. [and others]. 1988. Gas chromatographic methods for measuring nitrogen dioxide and peroxyacetyl nitrate in air without compressed gas cylinders. Analytical Chemistry. 60: 816-819.

Busch, N.E.; Christensen, O.; Kristensen, L. [and others]. 1980. Cups, vanes, propellers, and laser anemometers. In: Dobson, F.; Hasse, L.; Davis, R., eds. Air-sea interaction, instruments and methods. New York, Plenum Press: 11-46.

Businger, J.A. 1986. Evaluating the accuracy with which dry deposition can be measured with current micrometeorological techniques. Journal of Climate & Applied Meteorology. 25: 1100-1124.

Businger, J.A.; Wyngaard, J.C.; Izumi, Y. [and others]. 1971. Flux profile relationship in the atmospheric surface layer. Journal of Atmospheric Science. 28: 181-189.

Carl, D.M.; Tarbell, T.C.; Panofsky, H.A. 1973. Profiles of wind and temperature from towers over homogeneous terrain. Journal of Atmospheric Science. 30: 788-794.

Conklin, P.S.; Knoerr, K.R.; Schneider, T.W. [and others]. 1988. A wind tunnel test of probe shadow effects on a sonic anemometer in two orientations. In: Eighth symposium on turbulence and diffusion. American Meteorological Society. Boston, MA.: 108-111.

Dahlquist, G.; Bjorck, A. 1974. Numerical methods. Englewood Cliffs, NJ: Prentice Hall. 573 p.

Delaney, A.C.; Fitzjarrald, D.R.; Lenschow, D.H. [and others]. 1986. Direct measurements of nitrogen oxides and ozone fluxes over grassland. Journal of Atmospheric Chemistry. 4: 429-444.

Dickerson, R.R.; Delany, A.C.; Wartburg, A.F. 1984. Further modification of a commercial NO_x detector for high sensitivity. Review of Scientific Instruments. 55: 1995-1998.

Drummond, J.W.; Voltz, A. 1982. Optimized chemiluminescence detector for tropospheric NO measurements. In: 2nd symposium on the composition of the non-urban troposphere. May 25-28. Williamsburg, VA., Cosponsored by American Meteorological Society; American Geophysical Union and National Aeronautics and Space Administration. Published by AMS, Boston, MA: 17-20.

Finkelstein, P.L.; Kaimal, O.C.; Gaynor, J.E. [and others]. 1986. Comparison of wind monitoring systems. Part I: In situ sensors. Journal of Atmospheric and Oceanic Technology. 3: 583-593.

Fitzjarrald, D.R.; Lenschow, D.H. 1983. Mean concentration and flux profiles for chemically reactive species in the atmospheric surface layer. Atmospheric Environment. 17: 2505-2512.

Fontijn, A.; Sabadell, A.J.; Ronco, R.J. 1970. Homogeneous chemiluminescent measurement of nitric oxide with ozone: implications for continuous selective monitoring of gaseous air pollutants. Analytical Chemistry. 42: 575-579.

Gurvich, A.S. 1962. The pulsation spectra of the vertical component of the wind velocity and their relations to the micrometeorological conditions. Izvestiya Atmospheric and Oceanic Physics 4: 101-136.

Halfpenny, J.C.; Ingraham, R.P., eds. 1984. Long-term ecological research in the United States: a network of research sites 1984. Available from: Forestry Sciences Lab., 3200 Jefferson Way, Corvallis, OR 97331.

Haugen, D.A.; Kaimal, J.C.; Bradley, E.F. 1971. An experimental study of Reynold's stress and heat flux in the atmospheric surface layer. Quarterly Journal of the Royal Meteorological Society. 97: 168-180.

Hicks, B.B. 1972. Propeller anemometers as sensors of atmospheric turbulence. Boundary-Layer Meteorology. 3: 214-228.

Hicks, B.B.; Baldocchi, D.D.; Hosker, R.P., Jr. [and others]. 1985. On the use of monitored air concentrations to infer dry deposition (1985). NOAA Tech. Memo ERL ARL-141 ATDD. Oak Ridge, TN: National Oceanic and Atmospheric Administration. 65 p.

Hicks, B.B.; Wesely, M.L.; Coulter, R.L. [and others]. 1986. An experimental study of sulfur and NO_x fluxes over grassland. Boundary-Layer Meteorology. 34: 103-121.

Högström, U. 1988. Non-dimensional wind and temperature profiles in the atmospheric surface layer: a re-evaluation. Boundary-Layer Meteorology. 42: 55-78.

Højstrup, J. 1981. A simple model for the adjustment of vertical velocity spectra in unstable conditions downstream of an abrupt change in roughness and heat flux. Boundary-Layer Meteorology. 21: 341-356.

Horst, T.J. 1973a. Spectral transfer functions for a three-component sonic anemometer. Journal of Applied Meteorology. 12: 1072-1075.

Horst, T.J. 1973b. Corrections for response errors in a three-component propeller anemometer. Journal of Applied Meteorology. 12: 716-725.

Kaimal, J.C. 1968. The effect of vertical line averaging on the spectra of temperature and heat-flux. Quarterly Journal of the Royal Meteorological Society. 94: 149-155.

Kaimal, J.C. 1975. Sensors and techniques for direct measurement of turbulent fluxes and profiles in the atmospheric surface layer. Atmospheric Technology. 7: 7-14.

Kaimal, J.C.; Wyngaard, J.C.; Haugen, D.A. 1968. Deriving power spectra from a three-component sonic anemometer. Journal of Applied Meteorology. 7: 827-837.

Kaimal, J.C.; Wyngaard, J.C.; Izumi, Y. [and others]. 1972. Spectral characteristics of surface layer turbulence. Quarterly Journal of the Royal Meteorological Society. 98: 563-589.

Knight, D.H. 1972. Leaf area dynamics of the Pawnee Grassland, 1970-1971. International Biophysical Program Technical Report No. 86. 28 p.

Korrell, A.; Panofsky, H.A.; Rossi, R.J. 1982. Wind profiles at the Boulder tower. Boundary-Layer Meteorology. 22: 295-312.

Kristensen, L.; Fitzjarrald, D.R. 1984. The effect of line averaging on scalar flux measurements with a sonic anemometer near the surface. Journal of Atmospheric and Oceanic Technology. 1: 138-146.

Kristensen, L.; Kirkegaard, P. 1987. Digitization noise in power spectra analysis. Journal of Atmospheric and Oceanic Technology. 4: 328-335.

Lauenroth, W.K.; Milchunas, D.G. 1985. The shortgrass steppe. Fort Collins, CO: Range Science Department and Natural Resource Ecology Laboratory, Colorado State University. 109 p.

Lenschow, D.H.; Delaney, A.C. 1987. An analytical formulation for NO and NO_2 flux profiles in the atmospheric surface layer. Journal of Atmospheric Chemistry. 5: 301-309.

Lenschow, D.H.; Kristensen, L. 1985. Uncorrelated noise in turbulence measurements. Journal of Atmospheric and Oceanic Technology. 2: 68-81.

Maeda, Y.; Aoki, K; Munenemori, M. 1980. Chemiluminesence methods for the determination of nitrogen dioxide. Analytical Chemistry. 52: 307-311.

Massman, W.J.; Zeller, K.F. 1988. Rapid method for correcting the non-cosine response errors of the gill propeller anemometer. Journal of Atmospheric and Oceanic Technology.

McMillen, R.T. 1986. A basic program for eddy correlation in non-simple terrain. NOAA Tech. Memo ERL ARL-147 ATDD. Oak Ridge, TN: National Oceanic and Atmospheric Administration. 32 p.

Monson, R.K.; Sackschewsky, M.R.; Williams, G.J. III. 1986. Field measurements of photosynthesis, water-use efficiency, and growth in Agropyron smithii (C_3) and Bouteloua gracilis (C_4) in the Colorado shortgrass steppe. Oecologia. 68: 400-409.

Moore, C.J. 1986. Frequency response corrections for eddy correlation systems. Boundary-Layer Meteorology. 37: 17-35.

National Acid Precipitation Assessment Program (NAPAP). 1987. Interim assessment: the causes and effects of acidic deposition. Volume 1. Executive Summary. 100 p.

Ohtaki, E. 1985. On the similarity in atmospheric fluctuations of carbon dioxide, water vapor, and temperature over vegetated fields. Boundary-Layer Meteorology. 32: 25-37.

Panofsky, H.A.; Tennekes, H.; Lenschow, D.H. [and others]. 1977. The characteristics of turbulent velocity components in the surface layer under corrective conditions. Boundary-Layer Meteorology. 11: 355-361.

Paulson, C.A. 1970. The mathematical representation of wind and temperature profiles in the unstable atmospheric surface layer. Journal of Applied Meteorology. 9: 857-861.

Peterson, T.C.; Parton, W.J. [n.d.] Behavior of winds: Pawnee Grasslands--1972-75. Available from: Natural Resource Ecology Lab, Colorado State University, Ft. Collins, CO 80523. [Unpublished.]

Press, W.H.; Flannery, B.P.; Teukolsky, S.A. [and others]. 1986. Numerical recipes. New York: Cambridge University Press. 818 p.

Rauzi, F.; Dobrenz, A.K. 1970. Seasonal variation of chlorophyll in western wheatgrass and blue grama. Journal of Range Management. 23: 372-373.

Ray, J.D.; Stedman, D.H.; Wendel, G.J. 1986. Fast chemiluminescent method for measurement of ambient ozone. Analytical Chemistry. 58: 598-600.

Redford, T.G. Jr.; Verma, S.B.; Rosenberg, N.J. 1980. Humidity fluctuations over a vegetated surface measured with a Lyman-Alpha hygrometer and a fine-wire thermocouple psychrometer. Journal of Applied Meteorology. 19: 860-867.

Sehmel, G.A. 1980. Particle and gas dry deposition: a review. Atmospheric Environment. 14: 983-1011.

Sehmel, G.A. 1984. Deposition and resuspension. In: US Dept. of Energy: Atmospheric science and power production. 533-583. Chapter 12. National Technical Information Service. Springfield, VA.

Silverman, B.A. 1968. The effect of spatial averaging on spectrum estimation. Journal of Applied Meteorology. 7: 168-172.

Slemr, F.; Seiler. W. 1984. Field measurements of NO and NO_2 emissions from fertilized and unfertilized soils. Journal of Atmospheric Chemistry. 2: 1-24.

Smith, S.D.; Anderson, R.J. 1984. Spectra of humidity, temperature, and wind over the sea at Sable Island, Nova Scotia. Journal of Geophysical Research. 89: 2029-2040.

Steffenson, D.M.; Stedman, D.H. 1974. Optimization of the operating parameters of chemiluminescent nitric oxide detectors. Analytical Chemistry. 46: 1074-1709.

Webb, E.K.; Pearman, G.I.; Leunig, R. 1980. Correction of flux measurements for density effects due to heat and vapor transfer. Quarterly Journal of the Royal Meteorological Society. 106: 85-100.

Wendel, G.J.; Stedman, D.H; Cantrell, C.A. [and others]. 1983. Luminol-based nitrogen dioxide detector. Analytical Chemistry. 55: 937-940.

Wesely, M.L.; Eastman, J.A.; Cook, D.R. [and others]. 1978. Daytime variations of ozone eddy fluxes to maize. Boundary-Layer Meteorology. 15: 361-373.

Wesely, M.L.; Eastman, J.A.; Stedman, D.H.; [and others]. 1982. An eddy-correlation measurement of NO_2 flux to vegetation and comparison to O_3 flux. Atmospheric Environment. 16: 815-820.

Wesely, M.L.; Hicks, B.B. 1977. Some factors that affect the deposition rates of sulfur dioxide and similar gases on vegetation. Journal of the American Pollution Control Association. 27: 1110-1116.

Wetstone, Gregory. 1980. Air pollution control laws in North America. Environmental Law Reporter, The Problem of Acid Rain and Snow. 10: 50,000-50,020.

Williams, E.J.; Parrish, D.D.; Fehsenfeld, F.C. 1987. Determination of nitrogen oxide emissions from soils: results from a grassland site in Colorado, United States. Journal of Geophysical Research. 92: 2173-2179.

Wyngaard, J.C. 1971. Spatial resolution of a resistance wire temperature sensor. Physics of Fluids. 14: 2052-2054.

Wyngaard, J.C. 1988. Flow distortion effects on scalar flux measurements in the surface layer: implications for sensor design. Boundary-Layer Meteorology. 42: 19-26.

Wyngaard, J.C.; Cote', O.R.; Izumi, Y. 1971. Local free convection, similarity, and the budgets of shear stress and heat flux. Journal of Atmospheric Science. 28: 1171-1182.

APPENDIX A. Description of Fast Response Chemical Sensors[1]

An earlier version of this research project was designed to measure the dry deposition of NO_2, NO_x (principally NO + NO_2 + peroxyacetyl nitrate [PAN]), ozone, and SO_x to grassland during winter and summer months. However, the SO_x sensor was not available during the field season because it was still undergoing further development in the laboratory to improve sensitivity and response time. This chemical analysis project included the installation, operation, and maintenance of the intake system, detectors, and the zero and calibration system.

The instruments were housed in the shelter, and air was brought from the tower to the shelter using a high-volume sample pump. The arrangement avoided introducing extraneous turbulence to the mean wind flow and kept the instruments in a temperature-controlled environment. The intake system consisted of a 26.5m-long, 5/8-inch-i.d. Teflon tube through which air was drawn at ca. 160 l/min using a high-volume air pump (Fuji ring compressor). The flow rate decreased with time (table A1). The chemical sensors sampled from the main air stream and returned their exhaust downstream of the sampling manifold to keep the pressure drop across the instruments to a minimum. The interference caused by adsorption/desorption was minimized by using large-bore Teflon tubing. Although the length of sample tube slowed the response of the chemical instruments and cut off some of the high-frequency flux data, the need for a complex temperature correction was eliminated by housing the instruments in a temperature-controlled shelter. Table A2 presents a summary of the chemical instruments and their specifications.

Chemiluminescent Ambient Air Monitors (CAAM)

The same instrument design was adapted to measure nitrogen dioxide (Wendel et al. 1983) and ozone (Ray et al. 1986) by changing the fluorescent reagent used. The sample flowed through a detection cell and over a filter pad wetted with the fluorescent reagent (see fig. A1). A blue-sensitive photomultiplier tube (PMT) monitored the light produced. The fluid and air exited at the bottom of the reaction cell and were separated by gravity in the catch reservoir. The fluid flow rate was 1 ml/min and the air flow rate was 10 l/min. The response of these instruments was pressure-dependent.

For the detection of nitrogen dioxide a basic solution of luminol (5-amino-2,3-dihydro-1,4-phthalazinedione) was used (Maeda et al. 1980). The solution was comprised of 0.05 M NaOH, 0.1 M Na_2SO_3, 2 x 10^{-4} M luminol, and 0.05% vol/vol t-butanol. The solution was used once and then discarded. Operating under these conditions, the sensitivity was ca. 0.2 μA/ppb (parts per billion volumetric mixing ratio) and the response was linear from 0.1 ppb (fig. A2). The response of the instrument did decay with time after a fresh solution was installed and the filter pad in the detection cell changed, probably because of degradation of the filter pad and aging of the solution. The solution was replaced approximately weekly and the instrument recalibrated (table A1 gives details of the calibration changes). When operated in the laboratory the instrument responded to a square wave pulse of NO_2 introduced to the intake of the instrument within 0.2 seconds. Under field conditions, the response to a square wave pulse of clean air introduced to the system at the tower was slower (0.7 s) because broadening of the sample occurred in the intake system (fig. A3). The detection limit was 0.14 ppb.

For the analysis of ozone the basic luminol solution was exchanged for a a solution of eosine-Y in ethylene glycol. The dye solution was recycled after each batch had passed through the instrument. The ozone detector was calibrated by comparing the output signal with that from a slow-response UV photometric ozone monitor (TECO model 49A). The sensitivity was 0.12 μA/ppb and the detection limit was <1 ppb in the field. In the laboratory the response of the instrument was 7 Hz, which decreased under field conditions to 1.4 Hz because of the broadening that occurred when sampling through the long intake tube, (fig. A4).

Total NO_x Analyzer

NO reacts with ozone forming electronically excited nitrogen dioxide. At reduced pressure the excited nitrogen dioxide decays to the ground state, emitting a photon;

$$NO + O_3 \longrightarrow NO_2^* + O_2$$

$$NO_2^* \longrightarrow NO_2 + h\nu \qquad (640\ nm)$$

The intensity of light produced is proportional to the concentration of NO, forming the basis for the total NO_x analyzer (Fontijn 1970).

The higher oxides of nitrogen were reduced to NO by passing the sample gas through a hot molybdenum converter at 400°C. The principle species reduced were NO_2 and PAN (Dickerson et al. 1984). Nitric acid is known to pass through the length of the sample tubes to reach the converter housed in the shelter, but it has been shown in the past to have a response time larger than 120 s. This slow response is presumed to arise from a "chromatographic" effect of HNO_3 sticking and releasing from the intake tubing. The response time for nitric acid is too slow to allow correlation with changes in vertical wind velocities to determine HNO_3 fluxes.

The reduced sample gas was mixed with excess ozone prior to entering the reaction chamber in front of a cooled red-sensitive photomultiplier tube (EMMI 9658). The walls of the reaction chamber were gold-plated to enhance reflectivity and provide an inert surface. Ozone was produced by passing 250 ml/min of O_2 through three parallel discharge tubes; a water bubbler in the ozone line decreases the background signal (Drummond and Voltz 1982). The analyzer is shown schematically in figure A5. The photomultiplier tube output was fed to a programmable electrometer (Keithley 18000-20).

The instrument was operated with a chamber vacuum of 5-10 torr and a sample flow rate of approximately 4 l/min. Under these conditions the instrument response was ca. 0.3 nA/ppb with background noise equivalent to a detection limit of ca. 0.07-0.2 ppb; however, at times the noise was greater than this. The sensitivity of the instrument was constant throughout each experimental period, as shown in table A1. The change in sensitivity between the two experimental periods was due to a fault in the electrometer. The instrument was less sensitive when ambient air was used for ozone generation, which was necessary when the oxygen cylinder had emptied. The response of the analyzer to NO_2 was linear until the signal to noise ratio approached unit (fig. A2). When operated in the laboratory, the instrument responded to a square wave pulse of 10 ppb of NO within 0.3 s (fig. A6). However, when operated in the field and sampling through the long intake tube, the instrument responsed somewhat more slowly at 0.9 s.

Experiments carried out by heating the intake gases to the analyzer while keeping the concentration of span gas constant showed no deviation in response; therefore, the response of the instrument was not pressure-dependent. This is consistent with the conclusions of Steffenson and Stedman (1974) provided constant-volume vacuum pumps are used.

Zero and Calibration Systems

The instruments used in this study are highly sensitive and consequently are susceptible to some baseline drift; thus, it is necessary to keep track of the response of these instruments to clean, unpolluted air.

"Zero air" was prepared by scrubbing ambient air using a series of traps. The first contained ferrous sulphate which reduced NO_2 to NO which was then removed by a second trap filled with Purafil. A third trap filled with activated charcoal removed ozone. A compressor was used to fill a 30-gallon tank to a pressure of 100 psi with zero air. At the end of each sampling period zero air was introduced at the inlet to the main sample line through 3/8-inch-i.d. black Teflon tubing. The flow of air to the tower intake, ca. 170 l/m, was sufficient to overvent the main sample flow at a constant flow rate for approximately 3 minutes.

The system was calibrated on a weekly basis. This was achieved by adding a known flow of span gas to the zero air supply while the zero air flow rate was still constant. The NO_x analyzer was calibrated using a span gas mixture of 10 ppm NO in N_2. The NO_2 CAAM instrument was calibrated using a 1000 ppm NO_2 in N_2 standard; the concentration of NO_2 reaching the instruments was checked against the NO_x analyzer.

Future Work

As soon as the SO_x analyzer is functioning in a reliable and predictable mode, field measurements of the flux of SO_x to prairie grassland and snow should be performed. Other chemical measurements of interest include the measurement of the flux of NO_y (NO_x + HNO_3) using a new intake system (currently under development) for the chemiluminescent NO_x analyzer used in this study. The NO_x analyzer in its present configuration is capable of

measuring the flux of NO, this along with the concentration of PAN should be measured to determine a nitrogen flux budget. The concentration of PAN should be determined using a chromatographic technique developed in these laboratories based on a luminol detector (Burkhardt et al. 1987).

Acknowledgements

The authors would like to thank Russ Nye and Jane Wilken for their help in preparing the instruments and installing them at the field site and the staff at the USDA Forest Service in Fort Collins.

APPENDIX B. Eddy Correlation System Response Characteristics

This appendix outlines the method we used to correct the flux measurements for sensor inadequacies such as slow response characteristics, spatial averaging effects, and sensor mismatching. The method is similar to Moore's (1986) in that it uses the frequency-dependent instrument response functions and the spectral and cospectral distribution functions associated with atmospheric turbulent variances and fluxes to derive the correction factors. It differs from Moore's (1986) method in that it employs chemical sensors, treats aliasing differently, and includes the effects of mismatched sensors.

Specifically, the correction, ΔF, of the true flux, F, of a quantity with specific density, q, is estimated as follows:

$$\frac{\Delta F}{F} = 1 - \frac{\int_o^\infty H_{wq}(n) C_{wq}(n) dn}{\int_o^\infty C_{wq}(n) dn} \qquad [A1]$$

where the true flux $F = \int_o^\infty C_{wq}(n)dn$, $\Delta F/F$ represents the percentage flux loss, and $H_{wq}(n)$ is the total system cospectral response function associated with the sensors for the vertical wind velocity, w, and the quantity, q. $H_{wq}(n)$ is the product of the separate response functions associated with the data logging system, sensor frequency response, sensor size, sensor separation, and sensor mismatch, and $C_{wq}(n)$ is the atmospheric cospectrum of w and q as a function of frequency, n.

The response functions appropriate to each of the various instruments and the data logging system are described.

Fast Response Chemical Sensors (O_3, NO_2, NO_x)

At present the fast response chemical sensors are housed in an air-conditioned shelter about 26.5 m south of the meteorological tower. The sampled air is brought rapidly into the shelter through a long Teflon tube, whose intake is positioned on the tower near the anemometers and temperature sensor. The response times of the sensors were determined in situ by a series of concentration step changes that involved alternately switching between passing ambient air and passing clean air (zero concentration) through the intake tube and into the sensors.

Figures B1-B3 give examples of the data gathered during one of the response time tests and table B1 gives the results of the tests. The tests were performed on three separate occasions and usually consisted of three or four positive and negative step changes. For a negative step change (decreasing from ambient to zero concentration), the data were fit with a decreasing exponential, $e^{-t/\tau-}$, and the best response time, $\tau-$, was found using a least squares minimization technique. (Here t represents time.) For a positive step change (increasing from zero to ambient concentration), the same method was employed except that the exponential, $e^{-t/\tau-}$, was replaced by $(1 - e^{-t/\tau+})$. Finally, only used data between 20% and 80% of maximum were used to fit the curves. The ozone sensor (fig. B1), which usually provides the least noisy signal, has a response time of about 0.7 s. Although its response time was independent of the magnitude of the step change, the ozone sensor does display some slight asymmetry in response to positive and negative step changes with the response time $\tau-$ being slightly shorter than $\tau+$. This asymmetry is also observed in the laboratory and is thought to be related to adsorption and desorption of ozone by the intake tube walls. The response time of 0.7 s is also slower (by a factor of about 2) than that observed in

the laboratory (Ray et al. 1986 and appendix A). Again, this is consistent with the adsorption and desorption processes, which will tend to lengthen the response time by adding ozone to the air stream as the concentration decreases to zero and by removing ozone from the air stream as the concentration increases to ambient. In addition, the mixing of gas samples and the resulting smearing of the high frequency changes in gas concentrations by the highly turbulent flows inside the Teflon tube (Reynolds number about 10^4) may also contribute to this lengthening of the response time of the chemical sensors over what has been observed in the laboratory.

The response times of the NO_2 and NO_x sensors (fig. B2 and B3, respectively) were more difficult to obtain because the sensors are noisier than the ozone sensor. For the NO_2 sensor the response time is 0.7 s and it is 0.9 s for the NO_x sensor. These response times were found by the same method as the ozone sensor except that there were fewer useful data sets with which to do the curve fitting. In the case of the NO_x sensor, a low pass RC analog filter with a 0.04-s time constant had to be incorporated to remove the high frequency noise in the signal. These two sensors, as does the ozone sensor, also display a slight asymetry in their response to positive and negative step changes, and a longer response time than observed in the laboratory (Wendel et al. 1983, Wesely et al. 1982). Again, as with ozone, adsorption, and desorption of these gases by the tube walls and the turbulent flows inside the tube are thought to be largely responsible for these differences. These last two figures also show another problem peculiar to these two sensors. In both cases, the NO_2 and NO_x concentrations increase above ambient just prior to the region where the concentrations begin to decrease to zero. The cause for this pulse of gas is unknown, but it may be

related to the valves that switch the clean air flow and the ambient air flow. For the response time tests this problem was not a consideration.

It is important to note that, in addition to the response times, these response time tests also give the lag or delay time required to move the air from the mouth of the intake tube to the sensors. The delay time is represented on figures B1-B3 as the time from input of clean air at the mouth of the intake tube ($t \approx 0$) to the time at which the concentration begins to decrease. These results show that the lag time was 2.0 s at a flow rate of 155 l/min. This direct method of determining the delay time was also independently verified from measurements of the flow rate and the length and cross-sectional area of the intake tube (inside diameter of intake tube = 5/8 inch). This independent estimate of the delay time was 2.1 s. For computing eddy correlation fluxes, the analog signals from these chemical sensors are shifted digitally in time by 2 s.

Finally, these response time tests also show that the zero concentration of these gases do not necessarily correspond to a zero voltage reading of the instruments. This bias in the data signal was intentional and was included in data calibration and reduction. Further details on the calibration of these chemical sensors is discussed in Appendix A.

With these response times, the response function that describes the dynamic frequency response of these chemical sensors is given as follows:

$$T_d(n) = 1/[1+(2\pi n\tau)^2] \qquad [B2]$$

Here we assume that these sensors are "first order systems" (Brock and Nicolaidis 1985).

In addition to the dynamic frequency response, another important question that needs to be addressed is that of spatial averaging effects caused by sampling a volume of air as it is drawn through the intake tube into the reaction chambers. This effect, which is likely to be important whenever the sampled volume of air is large and the sensor response is sufficiently fast, results from the fact that a measurement of concentration is not made at a point, but rather the measurements of concentration represent the average concentration within a finite volume of air that has been drawn into the sensor. These spatial averaging effects (in the form of line averaging rather than volume averaging) have been investigated for sonic anemometers (Silverman 1968, Kaimal et al. 1968, Horst 1973a), and for platinum wire thermometers (Kaimal 1968, Wyngaard 1971). They have also been investigated for the Lyman-Alpha Hygrometer by Andreas (1981) in the form of volume averaging over a right circular cylinder.

For our measurement system the response function associated with volume averaging (assuming a spherical volume) is given by the following equation, which is derived in Appendix C.

$$T_v(n) = \frac{10}{3\pi(k_1 R)^2} \int_o^\infty \int \frac{T_*(k_1 R, x_2, x_3)}{(1+x_2^2+x_3^2)^{11/6}} \, dx_2 \, dx_3 \qquad [B3]$$

where R is the radius of the sphere over which we are averaging and k_1 is the wave number in the direction of the mean horizontal wind and by Taylor's hypothesis, $k_1 = 2\pi n/\bar{u}$, where $\bar{u}$ is the mean horizontal wind speed. Here $T_*(k_1 R, x_2, x_3)$ is defined as:

$$T_*(k_1R,x_2,x_3)=\frac{9}{4x_3^2}\left[\int_o^{\pi/2}\sin 2\theta\,\sin(k_1Rx_3\cos\theta)\,J_o(k_1R\,(1+x_2^2)^{1/2}\,\sin\theta)\,d\theta\right]^2 \quad [B4]$$

where J_o is a Bessel function. Equations [B3] and [B4] were integrated numerically (see Appendix C and discussion below), and the results are given in figure B4, which is a plot of $T_v(k_1R)$. This figure and equation [B1] show that spatial averaging effects are important only when $T_v(k_1R)$ departs significantly from a value of unity, which occurs whenever $k_1R \gtrsim 1$ or, equivalently, whenever the physical dimensions of a turbulent atmospheric eddy are comparable to or smaller than the radius of the averaging volume. Because T_v is, in general, a function of wind speed, the importance of the volume averaging effects can only be assessed by evaluating the flux loss, equation [B1], as a function of wind speed with and without $T_v(n)$ as a component of $H_{wq}(n)$. This will be discussed below. It should also be noted that the spherical volume over which we are averaging becomes distorted by the wind speed; however, Taylor's hypothesis allows for this and thus k_1 becomes a function of the mean wind speed.

Finally, an estimate of the radius, R, is needed. A typical value of R can be estimated from measurements of the intake flow rate, Q, and the sampling frequency, n_s, as follows: $R = [3Q/(4\pi n_s)]^{1/3}$. This basically assumes that for any given period of time, Δt, the volume $Q\Delta t$ is divided into $n_s\Delta t$ spherical subvolumes for each of which we make a concentration measurement. Given typical flow rates of about 150-170 l/min and a sampling rate of 10-20 Hz, 4 cm is a reasonable estimate for the radius R. This value will be used in the next section for calculating flux loss estimates.

Gill UVW Anemometers

Like the chemical sensors, the 3-axis Gill propeller anemometer is also a first order system; hence, the response function associated with this instrument is also described by equation [B2]. However, the response time, τ, associated with the Gill propeller is not a constant as it is with the chemical sensors; rather, it is dependent largely upon the horizontal wind speed, u, and is given by $\tau = D/u$. The response length, D, has been determined from wind tunnel experiments to be a function of the attack angle of the wind. For a propeller measuring the horizontal wind speed, however, this effect is small, and D can be considered constant and equal to 1 m. For the vertical propeller, on the other hand, D is not necessarily constant but will increase from about 1 m to 2 m as the flow deviates from axial to about 80° off axis and will continue to increase to infinity at 90° off axis. Therefore, in general the response time of the Gill propellers varies constantly with the flow velocity. For the purposes of this work, the response time of the horizontal propellers is assumed to be 1 $m/\bar{u}$ and that of the vertical propeller 2.5 $m/\bar{u}$. Therefore, the response function for Gill propellers, which uses these latter two response times, is an approximation to the true response function. For more details on the subject of response characteristics of these sensors, see Hicks (1972) and Busch et al. (1980).

Sensor Mismatching

In addition to the errors in flux measurements caused by slow response times of individual sensors, mismatching of sensors used for flux measurements can introduce further errors. Mismatching errors are produced whenever sensors have different response characteristics. When this occurs, there is a relative phase shift in the time series gathered by the different sensors. If the relative phase shift is small, then the loss of correlation (or flux)

between the two time series is also small. However, as the relative phase shift increases, the two time series can become increasingly uncorrelated and, hence, the flux measurements may be seriously underestimated. In general, all sensors are somewhat mismatched unless they happen to have exactly the same response characteristics and, therefore, exactly the same response functions. However, mismatching is most serious when flux measurements are made with two first order sensors that have very different response times or when a slow response sensor is used in conjunction with a fast response sensor. In our case this corresponds to (1) the chemical flux measurements made using a Gill propeller during low or high wind speeds or at all wind speeds using a sonic anemometer and (2) the heat flux measurements made with the relatively slow responding vertical Gill propeller and the much faster responding temperature sensor.

The transfer function associated with mismatching is given simply as $T_m(n) = \cos(\varphi_1 - \varphi_2)$, where φ_1 and φ_2 are the phase shifts introduced into the measurements by sensor number 1 and number 2, respectively. For first order systems, the phase shift $\varphi = \tan^{-1}(2\pi n\tau)$, from which it follows that $\cos\varphi = 1/(1+(2\pi n\tau)^2)^{1/2}$ and $\sin\varphi = (2\pi n\tau)/(1+(2\pi n\tau)^2)^{1/2}$. Therefore, using these latter two relations and the definition of $T_m(n)$ it is straightforward to show that:

$$T_m(n) = \frac{1+(2\pi n)^2\tau_1\tau_2}{[(1+(2\pi n\tau_1)^2)(1+(2\pi n\tau_2)^2)]^{1/2}} \qquad [B5]$$

Again, this transfer function is appropriate to first order systems and is most significant whenever τ_1 is very different from τ_2.

Using the slower responding chemical sensors and the faster responding vertical sonic anemometer can also introduce mismatching errors in the O_3, NO_2, and NO_x flux measurements. For this case, we assume that [B5] is valid but that the response time for the sonic (e.g., τ_1) is zero, so the formulation of $T_m(n)$ simply reduces to $1/(1+(2\pi n\tau)^2)^{1/2}$, where τ is the response time of the chemical sensors. This approximation will produce a slight overestimation of the flux loss because the sonic anemometer does, in fact, produce a small phase shift in the spectra at higher wave numbers.

Sonic Anemometers

Unlike the chemical sensors or the Gill propellers, the sonic anemometer is not limited by a slow response time. Rather, its limitations are associated with line averaging effects (which is the one-dimensional equivalent to the volume averaging effects of the chemical sensors discussed earlier). The response function associated with line averaging of the vertical velocity is taken from Kaimal et al. (1968) and is given in the following equation:

$$T_{l_w}(n) = \frac{2\Gamma(4/3)}{\Gamma(1/2)\,\Gamma(5/6)\,(k_1 l_w)^2} \int_0^\infty \left[\frac{\sin^2(k_1 l_w x_3/2)}{(x_3/2)^2}\right] x \left[\frac{1}{(1+x_3^2)^{7/3}} + \frac{3/8}{(1+x_3^2)^{4/3}}\right] dx_3 \qquad [B6]$$

where l_w is the vertical sonic path (= 25 cm for our sonic), Γ is the Gamma function, and $k_1 = 2\pi n/\bar{u}$ as was discussed above. The expression given in [B6] has been adapted from Kaimal et al. (1968) to permit ease in computation.

The response function associated with line averaging of the horizontal velocity is dependent upon the instrument geometry and direction of the horizontal wind speed. For our sonic, which uses an orthogonal geometry in the horizontal plane, the following response function will be used to describe the effects of line averaging of the horizontal velocity:

$$T_{l_u}(n) = \frac{\sin^2(k_1 l_u/2)}{(k_1 l_u/2)^2} \qquad [B7]$$

where l_u is the horizontal sonic path (= l_w for our sonic). Figure B5 shows T_{l_w} and T_{l_u} as functions of $k_1 l$.

These two response functions assume that line averaging takes place over a single acoustic path; however, our sonic (and many others as well) actually employs two parallel acoustic paths. Horst (1973b) found that the effect of path separation was not significant in the vertical direction, and after a similar investigation, we found that for our sonic the path separation effects were negligible in the horizontal as well.

Temperature Sensor

For the platinum wire resistance thermometer that we are using, response functions for both line averaging effects and the response of a first order system will be included.

The response time of this thermometer is given by Kaimal (1968) as follows: $\tau = 0.039/(1+\sqrt{3u})$, where u is measured in meters per second. Again we are assuming that this sensor is a first order sensor and we use equation [B2] for describing the dynamic frequency response. The response function appropriate to line averaging (of a scalar quantity like temperature as

opposed to a vector quantity like the vertical velocity) was first developed by Gurvich (1962) and later extended by Silverman (1968). For ease of computation, their results have been adapted to give the following form:

$$T_1(n) = \frac{2\Gamma(4/3)}{\Gamma(1/2)\Gamma(5/6)(k_1 l)^2} \int_0^\infty \left[\frac{\sin^2(k_1 l x_3/2)}{(x_3/2)^2}\right]\left[\frac{1}{(1+x_3^2)^{4/3}}\right] dx_3 \qquad [B8]$$

where l is the length of the platinum wire (= 18 cm in our case). Figure B6 is a graph of T_1 as a function of $k_1 l$.

Sensor Separation

For a variety of practical reasons, sensors will always be separated from one another. Yet this separation will also cause an error in any flux measurement for which two separate quantities are being correlated. We follow Moore's (1986) suggestion that the following response function be used for describing both lateral and longitudinal separation effects:

$$T_s(n) = \frac{2^{1/6}}{\Gamma(5/6)} (k_1 s)^{5/6} K_{5/6}(k_1 s) \qquad [B9]$$

where s is the separation distance and $K_{5/6}$ is the modified Bessel function of the second kind. Figure B7 shows a plot of T_s as a function of $k_1 s$. As Moore (1986) cautions, however, [B9] is most applicable when the separation distances are not too great, and it may also lead to a slight overestimate of the flux loss.

Data Logging System

Incorporated into our data logging system is a filter that also must be taken into account. This filter is a high pass recursive filter that is

applied to all raw digitized sensor data to remove any linear or low frequency long-term trends from the data. These long-term trends can adversely affect the flux measurements (Kaimal 1975). The transfer function associated with this filter is approximated by Moore (1986) as follows:

$$T_R(n) = \frac{(2\pi n\tau_R)^2 a}{a+(2\pi n\tau_R)^2} \qquad [B10]$$

where $a = e^{-1/(\tau' n_s)}$ and $\tau' = 200$ s (for our filter), and $\tau_R = a/[(1-a)n_s]$.

Aliasing

Aliasing results from sampling at uniform intervals any continuous signal that contains energy at frequencies above the Nyquist frequency. The Nyquist frequency, which is defined as one-half the sampling frequency, will henceforth it will be denoted by n_o. As a result of aliasing, spectral energy at frequencies above the Nyquist frequency can be folded back into the spectra at frequencies below the Nyquist frequency at harmonics of the sampling frequency. For example, the effects of aliasing upon measurements of $C_{wq}(n)$ can be written as follows (Kaimal et al. 1968):

$$C^m_{wq}(n) = \begin{cases} H_{wq}(n)C_{wq}(n) + \sum_{j=1}^{\infty}\left[H_{wq}(jn_s-n)C_{wq}(jn_s-n)+H_{wq}(jn_s+n)C_{wq}(jn_s+n)\right] & 0\le n\le n_o \\ 0 & n>n_o \end{cases} \qquad [B11]$$

where $C^m_{wq}(n)$ is the measured cospectra of w and q. Here the effects of the sensor response functions and the filters associated with the data logging system are included as components of $H_{wq}(n)$. The summation term of [B11] is

the aliased portion of the measured cospectra. Although not specifically included in [B11], any spectra or cospectra can also be contaminated by aliased high frequency noise associated with the electronics, nearby power lines, or any other outside power source. For sensors with short response times (such as sonic anemometers), antialiasing filters should be used to minimize the aliasing of any naturally occurring frequencies and to eliminate any high frequency contamination of the analog signal from outside sources. These antialiasing filters are usually designed as Butterworth or other similar filters. For sensors with relatively long response times (such as our vertical Gill propellers and chemical sensors), it is unnecessary to use an antialiasing filter because they will naturally accomplish these goals.

To include the effects of aliasing of the naturally occurring frequencies upon the flux loss computation, it is sufficient for our purposes to confine the consequencies of aliasing to only the $(n-n_s)$ term of [B11]. Therefore, we can simply substitute the following expression for the integral given in the numerator of equation [B1]:

$$\int_o^{n_o} H_{wq}(n)C_{wq}(n)dn + \int_o^{n_o} H_{wq}(n_s-n)C_{wq}(n_s-n)dn$$

However, the above expression can be further simplified (by a change of variables) to the following:

$$\int_o^{n_s} H_{wq}(n)C_{wq}(n)dn$$

Therefore, equation [B1] can now be written in the following form:

$$\frac{\Delta F}{F} = 1 - \frac{\int_o^{n_s} H_{wq}(n) C_{wq}(n) dn}{\int_o^{\infty} C_{wq}(n) dn} \qquad [B12]$$

It is this last equation that was used to estimate the percentage flux loss from measurements taken with our system. The sampling frequency, n_s, of our system is about 14 Hz; this value will be used for all computations presented herein.

To include the influence of the antialiasing filter is quite simple with [B12] because in essence these filters are designed specifically to confine the effects of aliasing to only the $(n-n_s)$ term of [B11]. Therefore, all that needs to be done is to include as part of $H_{wq}(n)$ the spectral response function of a particular antialiasing filter. For example, a 2-pole Butterworth filter has a response function given as:

$$T_B(n) = 1/\left[1+\left(\frac{n}{n_o}\right)^4\right] \qquad [B13]$$

Other types of antialiasing filters are also easily included in the computations for the flux loss. However, before proceeding to the flux loss computation, we need to define the atmospheric cospectra, $C_{wq}(n)$, that will be used in [B12].

Atmospheric Cospectra

For the purposes of this work, the cospectra of momentum and sensible heat are the same for stable atmospheric conditions and are given by:

$$C_{uw}(n) = C_{wT}(n) = \frac{1}{1 + 2.34(z/\bar{u})^{2.1}n^{2.1}} \qquad [B14]$$

where z is the height of the sensors array above the zero plane displacement of the surface (z = 6 m for our site). This expression is taken from Kaimal et al. (1972), and although the normalization is not necessarily standard, for our purposes nothing more is needed. For unstable atmospheric conditions, the cospectra of momentum and sensible heat are different and given as follows:

$$C_{uw}(n) = \begin{cases} \dfrac{20.78}{[1+31(z/\bar{u})n]^{1.575}} & (z/\bar{u})n < 0.24 \\ \dfrac{12.66}{[1+9.6(z/\bar{u})n]^{2.4}} & (z/\bar{u})n \geq 0.24 \end{cases} \qquad [B15]$$

$$C_{wT}(n) = \begin{cases} \dfrac{12.92}{[1+26.7(z/\bar{u})n]^{1.375}} & (z/\bar{u})n < 0.54 \\ \dfrac{4.378}{[1+3.8(z/\bar{u})n]^{2.4}} & (z/\bar{u})n \geq 0.54 \end{cases} \qquad [B16]$$

These latter two equations were taken from Moore (1986).

For correcting the dry deposition fluxes of O_3, NO_2, and NO_x, we will assume that as atmospheric scalars, their cospectra are the same as that of temperature. There is some experimental evidence for the similarity between the spectra and cospectra of temperature and the spectra and cospectra of other scalars such as humidity and CO_2 (Redford et al. 1980, Smith and Anderson 1984, Ohtaki 1985, Anderson et al. 1986). However, no direct measurements of the spectra or cospectra of O_3, NO_2, or NO_x are available.

Atmospheric Spectra

With two simple modifications to [B12], the variance losses due to sensor limitations can be estimated in a manner completely analogous to that used for estimating the flux losses. First $H_{wq}(n)$ is replaced by the appropriate transfer function for a given instrument (i.e., H_w or H_c or H_T replaces H_{wq}) and, second, $C_{wq}(n)$ is replaced by the spectra appropriate to the quantity being measured.

For stable atmospheric conditions, the following variance spectra, taken from Moore (1986) will be used:

$$S_{qq}(n) = \frac{1}{1 + a_q[(z/\bar{u})n]^{5/3}} \qquad [B17]$$

where q refers to vertical velocity or temperature or any trace gas (O_3, NO_2 or NO_x). Again, the spectra associated with the trace gases is assumed to be the same as that associated with temperature. For q = vertical velocity, $a_q = 3.124[0.838+1.172(z/L)]^{-5/3}$, and for q = temperature, $a_q = 3.124[0.0961+0.644(z/L)^{3/5}]^{-5/3}$. Here z/L is the measure of atmospheric stability and is defined as $-kgz\overline{w'\theta'}/(u_*^3\bar{T})$ where L refers to the Monin-Obukhov length, k is the von Karman constant (= 0.41), g is the acceleration due to gravity (=9.8 m/sec^2), $\overline{w'\theta'} \approx 1.05\ \overline{w'T'}$ at our site with θ being the potential temperature, and u_* is the friction velocity ($u_* = (\overline{-u'w'})^{1/2}$). For stable conditions z/L is positive, and for unstable conditions z/L is negative. Neutral stability refers to z/L = 0.

For an unstable or neutral atmosphere ($z/L \leq 0$), the vertical velocity variance spectra is taken from Højstrup (1981) and the temperature variance spectra is taken from Kaimal et al. (1972).

$$S_{ww}(n) = \frac{1}{1+5.3[(z/u)n^{5/3}]} + \frac{16(-z/L)^{2/3}}{[1+17(z/u)n]^{5/3}} \qquad [B18]$$

$$S_{TT}(n) = \begin{cases} \dfrac{14.94}{[1+24(z/u)n]^{5/3}} & (z/u)n < 0.15 \\ \dfrac{6.827}{[1+12.5(z/u)n]^{5/3}} & (z/u)n \geq 0.15 \end{cases} \qquad [B19]$$

With all the above simplifying assumptions in mind, we applied these response functions and atmospheric cospectra to our eddy correlation system. For the vertical Gill propeller, $H_w(n) = T_d^w(n)T_R(n)$ where the w subscript and superscript refer to the vertical velocity sensor and $H_w(n)$ is the spectral response function for this instrument. Likewise, for the horizontal propellers, $H_u(n) = T_d^u(n)T_R(n)$; for the temperature sensor $H_T(n) = T_d^T(n)T_l^T(n)T_B(n)T_R(n)$, and finally for the chemical sensors $H_c(n) = T_d^c(n)T_R(n)T_v(n)$. For the vertical sonic $H_w(n) = T_{l_w}(n)T_B(n)T_R(n)$ and for the horizontal sonic $H_u(n) = T_{l_u}(n)T_B(n)T_R(n)$. Therefore, the total system response functions for heat and momentum and chemical fluxes are given, respectively, as follows:

$$\left.\begin{aligned} H_{wT}(n) &= \sqrt{H_w(n)H_T(n)}\; T_s^{wT}(n)\; T_m^{wT}(n) \\ H_{uw}(n) &= \sqrt{H_u(n)H_w(n)}\; T_s^{uw}(n)\; T_m^{uw}(n) \\ H_{wc}(n) &= \sqrt{H_w(n)H_c(n)}\; T_s^{wc}(n)\; T_m^{wc}(n) \end{aligned}\right\} \qquad [B20]$$

where the instrument separation and mismatching effects are denoted by $T_s(n)$

and $T_m(n)$, respectively, and the superscripts refer to that particular pair of instruments. It is important to note here that [B20] is an approximation. With [B20] we have "constructed" a response function. However, it is more appropriate to derive a response function for correcting the flux measurements similar to the way [B3], for example, was derived for correcting variance measurements; but, this more fundamental approach, except for the preliminary efforts of Kristensen and Fitzjarrald (1984), remains largely undeveloped both theoretically and observationally.

Computational Methods

Several different numerical methods were employed to evaluate equation [B12]. The denominator of this expression was evaluated analytically for the cospectra given by [B14], [B15], and [B16]. The numerator was evaluated numerically using the Romberg method of integration (Dahlquist and Bjorck 1974). The different transfer functions used for $H_{wq}(n)$ in [B20] were represented either directly by a specific analytical expression (e.g., [B2], [B5], [B10], and [B13]) or indirectly by a numerical table (e.g., [B3], [B6], [B7], [B8], and [B9]). The numerical tables were provided by a simple evaluation of a function (e.g., [B7] and [B9]), or by the numerical evaluation of an integral (e.g., [B3], [B6], and [B8]). As with [B20], these latter three integrals were also evaluated with the Romberg method of integration. Finally, the numerical evaluation of [B20] sometimes required interpolating between points of the numerical tables representing [B3] and [B6] through [B8]. This was done using a quartic polynomial interpolator.

APPENDIX C. Transfer Function for Volume Averaging

By using an intake tube to draw atmospheric samples into a reaction chamber, our chemical sensors average the turbulent fluctuations of O_3, NO_2, and NO_x over a spherical volume. Therefore, the spectral response of these sensors must degrade at higher wave numbers. This appendix provides a derivation of the response function associated with the volume averaging effects of the intake tube ($T_v(n)$ in equation [B3]), which can be used if necessary to correct the flux measurements for these effects. We begin by considering only spatial averaging effects; therefore, we will ignore other limitations of the sensors (such as a relatively long response time), which also influence the spectral response of these instruments.

From Andreas (1981) it is straightforward to show that the following relation holds between the measured constituent (O_3, NO_2, or NO_x) spectra, $\phi^m(\bar{k})$, and the true spectra, $\phi(\bar{k})$:

$$\phi^m(\vec{k}) = \frac{1}{\left(\frac{4}{3}\pi R^3\right)^2}\left[\int_{vol} e^{i\vec{k}\cdot\vec{s}}\,d\vec{s}\right]\left[\int_{vol} e^{-i\vec{k}\cdot\vec{s}'}\,d\vec{s}'\right]^* \phi(\vec{k}) \qquad [C1]$$

where $\vec{k}$ is the three-dimensional wave number and R is the radius of the volume over which we are averaging. In arriving at [C1] Andreas' (1981) results for a right circular cylinder have been modified to an expression appropriate to a sphere. We have chosen the same right-handed coordinate system as he did (x = direction of the mean horizontal wind; y = direction in the horizontal plane perpendicular to the x axis; z = vertical direction = alignment direction of the intake tube). However, as in his case, the choice of this particular coordinate system is immaterial.

From [C1] it is clear the integral, $I = \int_{vol} e^{i\vec{k}\cdot\vec{s}} d\vec{s}$, must be evaluated. In cylindrical coordinates the integral is given by the following expression:

$$I = \int_0^{2\pi} \int_0^{R} \int_{-(R^2-z^2)^{1/2}}^{+(R^2-z^2)^{1/2}} e^{ik_3 z} e^{ir(k_1\cos\theta + k_2\sin\theta)} \, d\theta r dr dz \qquad [C2]$$

where k_1, k_2, and k_3 are the 3 components of $\vec{k}$ along the x, y, and z axes. The integral over θ can be done explicitly (Andreas 1981) as can the integral over z (Silverman 1968, Wyngaard 1971), which yields:

$$I = 2\pi \int_0^{R} \frac{\sin((R^2-r^2)^{1/2} k_3)}{k_3/2} J_0(r(k_1^2+k_2^2)^{1/2}) r dr \qquad [C3]$$

where J_0 is a Bessel function.

Then changing variables from r to $\frac{r}{R} = \sin\theta$ yields:

$$I = \frac{2\pi R^3}{(k_3 R)} \int_0^{\pi/2} \sin 2\theta \, \sin(k_3 R\cos\theta) \, J_0(R\sin\theta(k_1^2+k_2^2)^{1/2} d\theta \qquad [C4]$$

Finally, using [C1] and [C4], we have

$$T'(\vec{k},R) = \frac{9}{4(k_3 R)^2} \left[\int_0^{\pi/2} \sin 2\theta \, \sin(k_3 R\cos\theta) \, J_0(R\sin\theta(k_1^2+k_2^2)^{1/2} d\theta\right]^2 \qquad [C5]$$

where $T'(\vec{k},R)$ is defined as $\phi^m(\vec{k})/\phi(\vec{k})$.

However, only the one-dimensional spectra is observable and the true and measured one-dimensional spectra (denoted by $\Psi(k_1)$ and $\Psi^m(k_1)$, respectively) are related to $\phi(k)$ as follows:

$$\Psi(k_1) = \int_{-\infty}^{\infty}\int \phi(\vec{k})\,dk_2\,dk_3 \qquad [C6]$$

$$\Psi^m(k_1) = \int_{-\infty}^{\infty}\int \phi^m(\vec{k})\,dk_2\,dk_3 = \int_{-\infty}^{\infty}\int T'(\vec{k},R)\,\phi(\vec{k})\,dk_2\,dk_3 \qquad [C7]$$

The transfer function we seek, $T_v(n)$ is defined as $\Psi^m(k_1)/\Psi(k_1)$. With this in mind, the integrals for $T_v(n)$ (viz., C5, C6, and C7) can be computed once is specified $\phi(\vec{k})$. Assuming local isotropic turbulence, the atmospheric variance spectra for a scalar quantity is given simply as $\phi(\vec{k}) = Ak^{-11/3}$ where A is a constant and k is the magnitude of $\vec{k}$. Therefore, $T_v(n)$ can be defined as follows:

$$T_v(n) = \frac{\int_{-\infty}^{\infty}\int k^{-11/3} T'(\vec{k},R)\,dk_2\,dk_3}{\int_{-\infty}^{\infty}\int k^{-11/3}\,dk_2\,dk_3} \qquad [C8]$$

The denominator can be evaluated analytically to give $6\pi/5\ k_1^{-5/3}$. With this last result [C8] and [C5] are equivalent to equations [B3] and [B4] of Appendix B and all that remains is to note that $x_2 = k_2/k_1$ and $x_3 = k_3/k_1$ and to change variables of integration appropriately.

The integrals given in [B3] and [B4] were evaluated numerically using the Romberg method of integration (Dahlquist and Bjorck 1974). The Bessel function J_o was also evaluated numerically using rational functions and rational polynomial approximations of J_o (Press et al. 1986). Finally, because evaluating $T_v(n)$ required evaluating a triple integral, some care in design and testing of the computer code was necessary in order to assure that figure B4 is a good representation of $T_v(n)$.

APPENDIX D. Table of Symbols

Symbol	Definition	Unit
c	pollutant concentration	kg/m^3 or ppb/v
$C_{wq}(n)$	atmospheric cospectrum of w and q as a function of n	
D	Gill propeller anemometer response length	m
F	corrected pollutant flux	$kg/m^2/s$ or (ppb/v)(m/s)
F_m	measured pollutant flux	$kg/m^2/s$ or (ppb/v)(m/s)
g	acceleration due to gravity	m/s^2
$H_{wq}(n)$	total cospectral response function for vertical wind w and quantity q as a function of frequency	
k	von Karman constant	
k_i	spectral wave number in ith direction	cycles/m
L	Monin-Obukov length	m
n	frequency	s^{-1}
q	specific density of an arbitrary measured quantity	
Q	flow rate	liters/min
r_s	surface resistance	s/m
r_t	total transfer resistance	s/m
r_{wc}	correlation coefficient between w and c	
R	radius	m

$S_{qq}(n)$	variance spectra for any quantity q as a function of n	
t	time	s
T	temperature	^{o}C
$T_B(n)$	response function for Butterworth filter	
$T_d(n)$	response function for dynamic frequency response	
$T_l(n)$	response function for line averaging	
$T_m(n)$	response function for mismatched sensors	
$T_R(n)$	response function for high-pass recursive filter	
$T_s(n)$	response function for sensor separation	
$T_v(n)$	response function for volume averaging	
u	horizontal wind speed	m/s
u_*	friction velocity	m/s
v_d	deposition velocity	cm/s
w	vertical wind speed	m/s
x_i	k_i/k_1, i=2,3	
z	vertical coordinate	
z/L	stability parameter: measurement height divided by Monin-Obukov length	
z_o	roughness length	cm
σ_T^2	temperature variance	$(^{o}K)^2$
σ_c^2	variance of c	$(ppb/v)^2$
σ_w^2	vertical velocity variance	$(m/s)^2$
θ	potential temperature	^{o}K

ρ_c	density of pollutant c	g/m^3
τ	sensor response time	s
φ	phase angle due to sensor mismatch	
ψ_c	universal stability influence function	

Zeller, Karl; Massman, William; Stocker, David; Fox, Douglas G.; Stedman, Donald; Hazlett, Donald. 1988. Initial results from the Pawnee eddy correlation system for dry acid deposition research. USDA Forest Service Paper RM-___, __ p. Rocky Mountain Forest and Range Experiment Station, Fort Collins, Colorado, 80526.

The Pawnee Grassland Eddy Correlation Dry Deposition Project is described. Instrumentation, methods of analysis, and initial data and research findings are presented. Data from this eddy correlation system show agreement with (a) previous observations of deposition velocities for atmospheric ozone, NO_2, and NO_x; (b) micrometeorological theory; and (c) micrometeorological site characteristics.

Keywords: Eddy correlation, dry deposition, Pawnee Grasslands, O_3, NO_2, NO_x, micrometeorology

Figure Captions

Figure 1.--Site location and vertical cross section of the instrument shelter, chemical instruments, and meteorological tower.

Figure 2.--Pawnee site: a, annual wind rose; b, daytime, growing season wind rose.

Figure 3.--Estimates of heat flux loss as a function of wind speed and atmospheric stability associated with using the Gill propeller anemometer for measurements of the vertical velocity fluctuations. Solid lines assume matched sensors, dashed lines assume mismatched sensors.

Figure 4.--Estimates of momentum flux loss as a function of wind speed and atmospheric stability associated with using 3-axis Gill propeller anemometer system for measuring the fluctuating velocity components.

Figure 5.--Estimates of chemical flux loss as a function of wind speed and atmospheric stability associated with using the Gill propeller anemometer for measuring the vertical velocity fluctuations. Solid lines assume matched sensors; dashed lines assume mismatched sensors.

Figure 6.--Same as figure 3 except for the use of a sonic anemometer rather than the Gill propeller anemometer.

Figure 7.--Same as figure 4 except for the use of the 3-axis sonic anemometer rather than the 3-axis Gill propeller anemometer.

Figure 8.--Same as figure 5 except for the use of the sonic anemometer rather than the Gill propeller anemometer.

Figure 9.--Estimates of temperature variance loss with the fast-response platinum wire resistance thermometer as a function of wind speed and atmospheric stability.

Figure 10.--Estimates of vertical velocity variance loss with the Gill propeller anemometer as a function of wind speed and atmospheric stability.

Figure 11.--Estimates of vertical velocity variance loss with a sonic anemometer as a function of wind speed and atmospheric stability.

Figure 12.--Estimates of variance loss from O_3, NO_2, and NO_x measurements as a function of wind speed and atmospheric stability.

Figure 13.--Corrected heat flux for week beginning June 30 (day 181).

Figure 14.--Corrected momentum flux for week beginning June 30 (day 181).

Figure 15.--Corrected ozone flux for week beginning June 30 (day 181).

Figure 16.--Roughness length vs. wind speed for the 2-week period June 30-July 14.

Figure 17.--Vertical velocity variance σ_w^2 normalized by u_*^2 vs. z/L. Observed data is given by ·, similarity theory prediction is given by the solid line.

Figure 18.--Normalized temperature variance vs. z/L for the 2-week period June 30-July 14. Observed data is given by ·; similarity theory prediction is given by the solid line.

Figure 19.--Correlation coefficient between the fluctuations of vertical velocity and temperature vs. z/L for the 2-week period June 30-July 14.

Figure 20.--Normalized ozone variance vs. z/L for the 2-week period June 30-July 14. Observed data is given by ·, similarity theory prediction is given by the solid line.

Figure 21.--Correlation coefficient between the fluctuations of vertical velocity and ozone concentration vs. z/L for the 2-week period June 30-July 14.

Figure 22.--Ozone deposition velocity as a function of time of day for the 2-week period June 30-July 14.

Figure 23.--Surface resistance to ozone uptake as a function of time of day for the 2-week period June 30-July 14.

Figure 24.--NO_2 concentration as a function of time during the 1-week period June 30-July 7.

Figure 25.--NO_2 flux as a function of time during the 1-week period June 30-July 7.

Figure 26.--Correlation coefficient between the fluctuations of vertical velocity and NO_2 concentration vs. z/L.

Figure 27.--NO_2 deposition velocity as a function of time of day for the 2-week period June 30-July 14.

Figure A1.--Schematic diagram of the Chemiluminescent Ambient Air Monitor, with an enlargement of the detection cell, which is machined from black Delrin; a glass window seals the cell.

Figure A2.--The response of the total nitrogen oxides detector and the nitrogen dioxide detector to low concentrations of nitrogen dioxide.

Figure A3.--Frequency response of the nitrogen dioxide detector: (a) to a square wave pulse of nitrogen dioxide in the laboratory and (b) to a square wave pulse of zero air introduced to the tower inlet in the field.

Figure A4.--Frequency response of the ozone detector: (a) to a square wave pulse of ozone in the laboratory and (b) to a square wave pulse of zero air introduced to the tower inlet in the field.

Figure A5.--Schematic diagram of the total oxides of nitrogen detector with a sectional view of the reaction chamber.

Figure A6.--Frequency response of the total NO_x analyzer: (a) to a square wave pulse of 10 ppb NO in the laboratory and (b) to a square wave pulse of zero air introduced to the tower inlet in the field.

Figure B1.--Response time tests for fast response ozone sensor, June 24, 1987.

Figure B2.--Response time tests for fast response NO_2 sensor, July 24, 1987.

Figure B3.--Response time tests for fast response NO_x sensor, July 24, 1987.

Figure B4.--Spectral transfer function, $T_v(k_1 R)$, associated with spherical volume averaging of the O_3, NO_2, and NO_x concentration fluctuation measurements. $k_1 = 2\pi n/\bar{u}$.

Figure B5.--Spectral transfer functions, $T_{l_w}(k_1 l_w)$ and $T_{l_u}(k_1 l_u)$, associated with line averaging of the vertical and horizontal wind velocity fluctuation measurements by the sonic anemometer.

Figure B6.--Spectral transfer function, $T_l(k_1 l)$, associated with line averaging of the temperature fluctuation measurements by the platinum wire thermometer.

Figure B7.--Spectral transfer function, $T_s(k_1 s)$, associated with the spatial separation of any two eddy correlation instruments.

Table 1.--Plant species in the immediate area of the NOAA/eddy correlation experimentation.[a]

Family	Species[b]
Cactacae	Opuntia polyacantha Haw.*
Chenopodiaceae	Chenopodium album L.
Chenopodiaceae	Kochia scoparia (L.) Schrad.
Commeliniaceae	Tradescantia occidentalis (Britt.) Smyth
Compositae	Artemisia frigida Willd.*
Compositae	Chrysothamnus nauseosus (Pall.) Britt.
Compositae	Cirsium undulatum (Nutt.) Spreng.
Compositae	Grindelia squarrosa (Pursh) Dunal
Compositae	Gutierrezia sarotharae (Pursh)* Britt. + Rusby
Compositae	Senecio tridenticulatus Rydb.
Compositae	Thelesperma filifolium (Hook.) A. Gray
Compositae	Tragopogon dubius Scop.
Convolvulaceae	Evolvulus nuttallianus R. + S.
Cruciferae	Lepidium densiflorum Schrad.
Cyperaceae	Carex eleocharis Bailey
Cyperaceae	Carex filifolia Nutt.
Graminae	Aristida longiseta Steud.*
Graminae	Bouteloua gracilis (H.B.K.) Steud.**
Graminae	Buchloe dactyloides (Nutt.) Engelm.
Graminae	Sporobolus cryptandrus (Torr.) Gray*
Graminae	Stipa comata Trin. + Rupr.*

Malvaveae	Sphaeralcea coccinea (Pursh) Rydb.*
Polygonaceae	Eriogonum effusum Nutt.

---

[a]Nomenclature taken from Flora of the Great Plains, 1986, T.M. Barkley et al. (editors), Great Plains Flora Association, University Press of Kansas, Lawrence, Kansas, 1392 p.

[b]Frequency of occurrence indicated as follows:

* Common in tower vicinity.

** Very abundant in tower vicinity.

All others occur infrequently.

Table 2.--Instrumentation used at Pawnee Acid Deposition Research Site for eddy correlation measurements.[a]

Instrument or model	Type	Parameter	Response time	Range
NO_x analyzer	chemiluminescence	NO_x	0.9 s	0.07 ppb - 1000 ppm
CAAM 2	chemiluminescence	NO_2	0.7 s	0.1-1000 ppb
CAAM 1	chemiluminescence	O_3	0.7 s	0.2-400 ppb
TECO 49	UV adsorption	O_3	2 min	1-500 ppb
R.M. Young UVW	Gill propeller anemometer	wind velocities	(b)	0.3-30 m/s
AIR, Inc.	platinum resistance	temperature	(b)	-50°-$+50^{\circ}$C
Atmos. Tech. Inc.	3-axis sonic	wind velocities	(b)	0-20 m/s
Campbell Scientific	vertical sonic (CA27T)	heat flux		$\pm 16^{\circ}$C/$\pm$4 m/s
AT&T 6300+	PC computer (80286)	data collection and processing	--	--
Data Translations, Inc.	DT2805 board	A/D conversion	--	--

[a]The use of trade and company names is for the benefit of the reader; such use does not constitute an official endorsement or approval of any service or product by the U.S. Department of Agriculture to the exclusion of others that may be suitable.

[b]See appendix B.

Table 3.--Data acquisition and measured parameters at Pawnee acid deposition research site.

Channel	Parameter	Output (every 1/2 hr)
1	w: vertical wind speed	$\bar{w}$, $\overline{w'^2}$
2	u: horizontal wind speed component	$\bar{u}$, $\overline{u'^2}$
3	v: horizontal wind speed component	$\bar{v}$, $\overline{v'^2}$
4	T: temperature	$\bar{T}$, $\overline{T'^2}$
5	O_3 (Teco 49): ozone	$\overline{O_3}$, $\overline{O_3'^2}$
6	O_3 (CAAM1): ozone	$\overline{O_3}$, $\overline{O_3'^2}$
7	NO_2 (CAAM2): nitrogen oxide	$\overline{NO_2}$, $\overline{NO_2'^2}$
8	NO_x (nitrogen oxide)	$\overline{NO_x}$, $\overline{NO_x'^2}$
*	Momentum flux	$\overline{w'u'}$, $\overline{w'v'}$
*	Heat flux	$\overline{w'T'}$
*	Ozone flux	$\overline{w'O_3'}$
*	NO_2 flux	$\overline{w'NO_2'}$
*	NO_x flux	$\overline{w'NO_x'}$
*	Horizontal wind speed	$(\bar{u}^2+\bar{v}^2)^{1/2}$
*	Wind direction	arctan(v/u)
*	Friction velocity	$(\overline{-w'u'})^{1/2}$
*	Drag coefficient	$(\overline{-w'u'})/\bar{u}^2$
*	Horizontal wind rotation angle	η
*	Vertical wind rotation angle	θ

*	Sample frequency	n_s
*	# of samples/sample period	N

*Derived from data recorded on first 8 channels.

Table A1.--Dates of calibration and field notes for the chemical sensors operated at the Pawnee Grasslands field site (Dec. 1, 1986 through Feb. 2, 1987 and May 1, 1987 through July 27, 1987).

Date	Julian date	Flow rate[a] (L/min)	Ozone[b,c] (ppb/V)	NO_2[c] (ppb/V)	NO_x[d] (ppb/V)
			Winter experiment		
11-Dec	345	178	Fresh	11.1[e]	3.13
17-Dec	351			3.2	2.78[f]
19-Dec	353		15:55		
22-Dec	356			2.53, 3.92[e]	
24-Dec	358		13:10		
29-Dec	363		Recycled		
31-Dec	365			e,g	
2-Jan	2		11:45		
7-Jan	7		Recycled		
8-Jan	8		h	2.13, 21.3[i]	2.77
12-Jan	12		Recycled		
16-Jan	16		Recycled		
20-Jan	20		Recycled	29.4	3.27
21-Jan	21			e	
24-Jan	24			e	
27-Jan	27	j	k	44.7	3.21

29-Jan	29		Recycled		
2-Feb	33	End of winter experiment.			

Summer experiment

13-May	133		Fresh	e	1
14-May	134	159		10.0	0.038
18-May	138		11:45	15.7[m], 12.1[e]	0.034
21-May	141		12:30	3.13[e,h,n,o]	0.034[p]
22-May	142			o	
23-May	143			2.1[e,n]	
24-May	144		refill (am)		
26-May	146			1.079[e,n,o,q]	
27-May	147			3.92	0.04
29-May	149		12:25		
1-Jun	152	158	r	7.41	
2-Jun	153		r		
5-Jun	156		9:05	1.56[e,m,n]	
8-Jun	159			s	t
9-Jun	160				u
10-Jun	161			4.39[e]	
11-Jun	162		8:46		
15-Jun	166		11:00		
16-Jun	167			7:83	0.083[p]
18-Jun	169		k	7:98	0.039

22-Jun	173		7:48		
23-Jun	174	158[v]		h,k	
24-Jun	175	164			
30-Jun	181	162	6:40[w]	8.98	0.048[p,x]
2-Jul	183			6.14	0.029
4-Jul	185			y	
6-Jul	187		7:48		0.031[p]
7-Jul	188			3.67[e,k]	
10-Jul	191			17.7, 2.71[h]	0.051
13-Jul	194		6:47		
15-Jul	196	z		6.33	0.038
16-Jul	197	aa			
20-Jul	201		11:30		
7-Jul	208	Site shutdown			

[a]Measured using a dry gas meter attached to the exhaust of the large sample pump, correcting for the flow through the NO_x analyzer that is not returned to the sample inlet.

[b]Wherever possible, the times when the dye solution was recycled is reported.

[c]The calibration factor is in units of ppb/V, the calibrated sensitivity in parts per billion mixing ratio per volt observed by the data acquisition system when the instrument is working with a full-scale deflection of 10 μA.

[d]10 nA full-scale deflection.

[e]Fresh solution.

[f]Converter heater repaired.

[g]Solution changed, but neither old nor new solutions calibrated.

[h]Change target pad.

[i]Changed full-scale deflection to 100 μA.

[j]Change zero air traps.

[k]Air pump replaced.

[l]Response of NO_x analyzer has changed by a factor of 100, which implies an electronic rather than a chemical fault is to blame. The response of the NO_x analyzer is also very noisy.

[m]Luminol flow stopped.

[n]No calibration of old solution.

[o]No luminol left.

[p]Oxygen tank empty.

[q]High calibration, signal may not have stabilized.

[r]TECO photometric ozone monitor recalibrated.

[s]No calibration possible as NO_x analyzer off line.

[t]Plugged frit in ozone line.

[u]Repair of ozone generator in Denver University laboratories.

[v]Change air filters in main sample line, system is off-line.

[w]Reservoir dry before refill.

[x]Plugged sample intake.

[y]Broken air pump.

[z]Zero air system self destructs, trap explodes.

Table A2.--Summary of the characteristics of the chemical sensors used during the field study.

Chemical measured	Instrument name	Sensitivity	Comments
Total NO_x	NO_x box	0.3 μA/ppb	Requires high-pressure O_2 cylinders for O_3 production; large vacuum pumps; cooled red-sensitive PMT; high power (240 v). Fast response <1 sec NO_x by catalytic reduction using Mo turnings at 400°C. Stable calibration.
NO_2	CAAM 2	0.2 μA/ppb	Uses a basic luminol solution which cannot be recycled. Each batch of reagent requires calibration. Sensitivity of solution decreases with time. Calibrate and check target pad weekly. Response time <1 sec. Portable low power required.
Ozone	Teco 49A	0.2mv/ppb	EPA standard. Slow response.
Ozone	CAAM 1	0.12 μA/ppb	Uses eosine-Y in ethylene glycol which can be recycled but some sensitivity is lost with use. Response time <1 sec. Calibrate using UV photometric instrument. period of unattended use limited by reservoir size. Target pad checked weekly. Portable low power required.

Table B1.--Optimal response times of fast response chemical sensors.[a]

Test Date	Sensor response time (seconds)		
	O_3 (CAAM1)	NO_2 (CAAM2)	NO_x
January 28, 1987			
τ^-	0.65	--	--
τ^-	0.66	--	--
τ^-	0.60	--	--
τ^+	1.02	--	--
τ^+	0.94	--	--
τ^+	1.07	--	--
June 3, 1987			
τ^-	0.62	0.72	--
τ^-	0.63	0.63	--
τ^-	0.64	0.48	--
τ^+	0.79	--	--
τ^+	0.83	--	--
τ^+	0.71	--	--
June 24, 1987			
τ^-	0.58	--	--
τ^-	0.66	--	--
τ^-	0.67	--	--
τ^-	0.56	--	0.95
τ^+	0.76	0.79	0.93
τ^+	0.87	0.63	0.84

τ^+	0.83	0.73	0.84
τ^+	0.84	0.65	0.79

[a] τ^- equals response time to step change from ambient to clear air and τ^+ equals response time to step change from clean air to ambient.

FOOTNOTES

[1]Taken from the Final Report to the USDA Forest Service, "Measurement of Dry Deposition of SO_x, NO_x, and NO_2 and O_3," September 1987, under USFS Contract No. 28-K6-384. Report was written by D.W. Stocker, D.H. Stedman, B.A. Watkins, and J.A. Armstrong of the University of Denver, Chemistry Department, Denver, CO 80208.

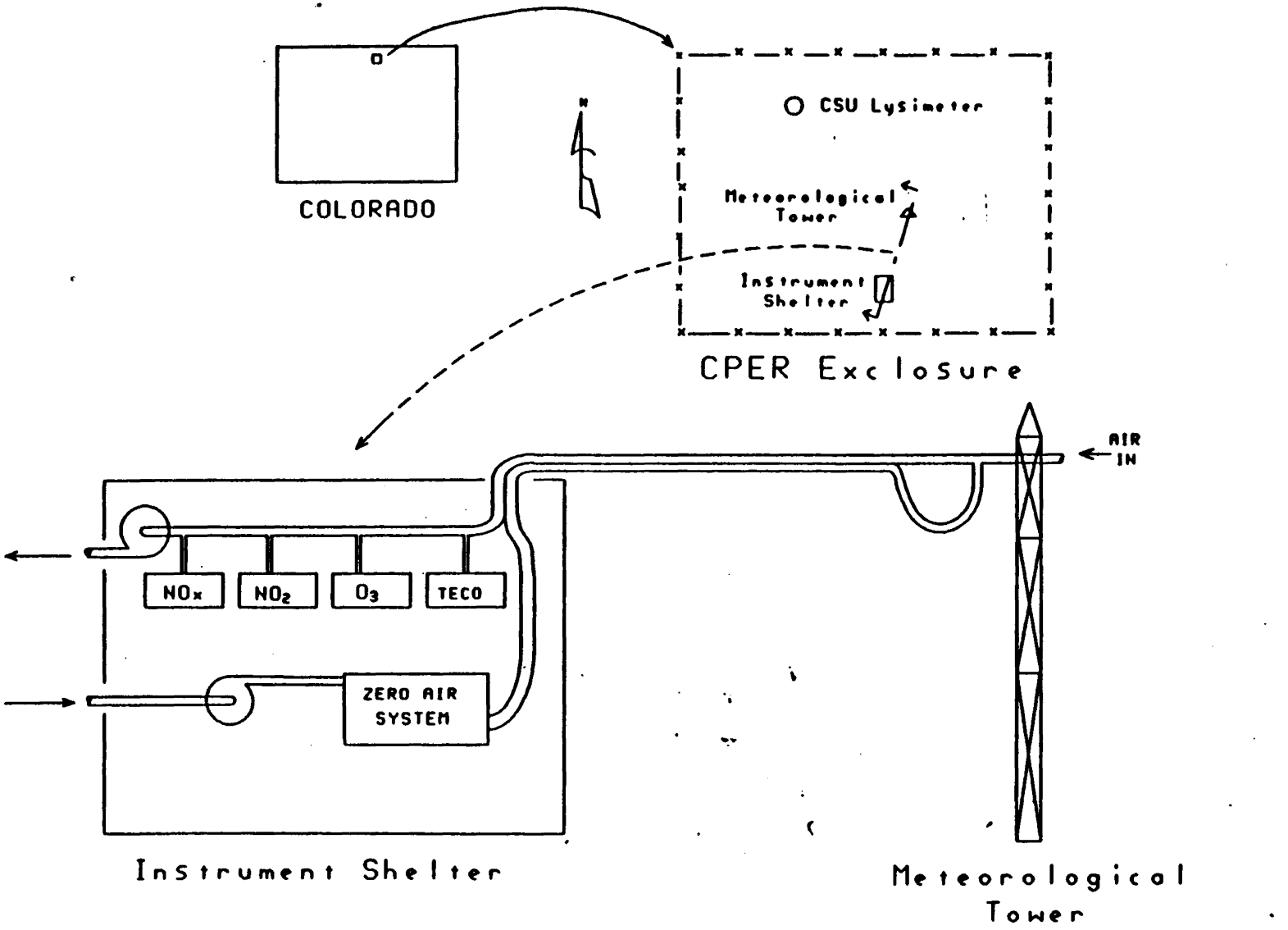
COLORADO
N
CSU Lysimeter
Meteorological Tower
Instrument Shelter
CPER Exclosure
AIR IN
NOx
NO2
O3
TECO
ZERO AIR SYSTEM
Instrument Shelter
Meteorological Tower

FIG. 1.

a.

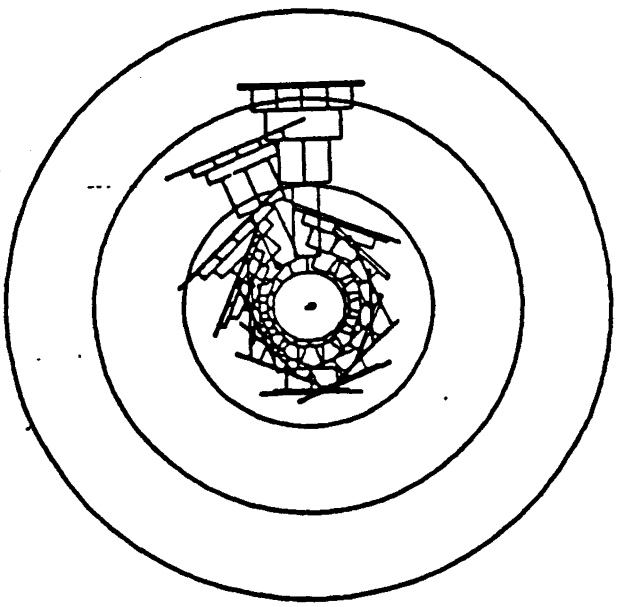

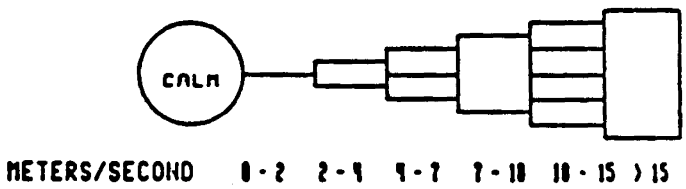

10% CIRCLES

JUL 86 - JUN 87

b.

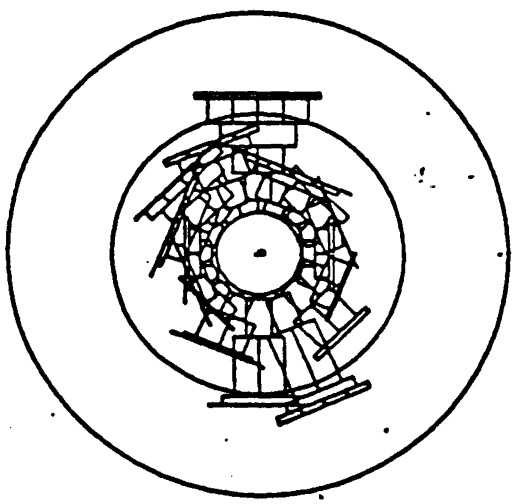

APR 87 - JUN 87

JUL 86 - SEP 86

(DAYLIGHT HOURS ONLY)

FIG. 2.

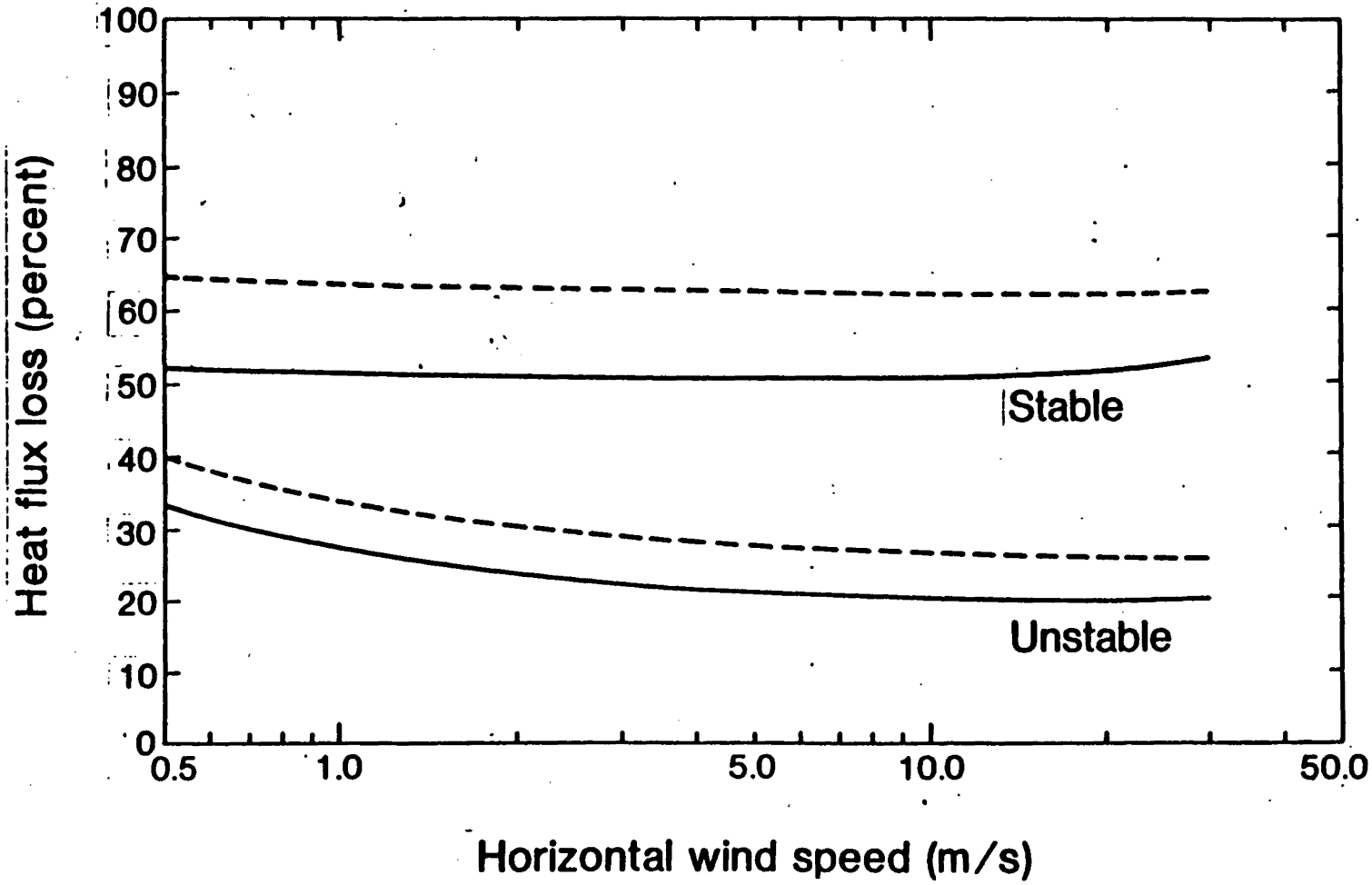
Heat flux loss (percent)
100
90
80
70
60
50
40
30
20
10
0
Stable
Unstable
0.5
1.0
5.0
10.0
50.0
Horizontal wind speed (m/s)

FIG. 3.

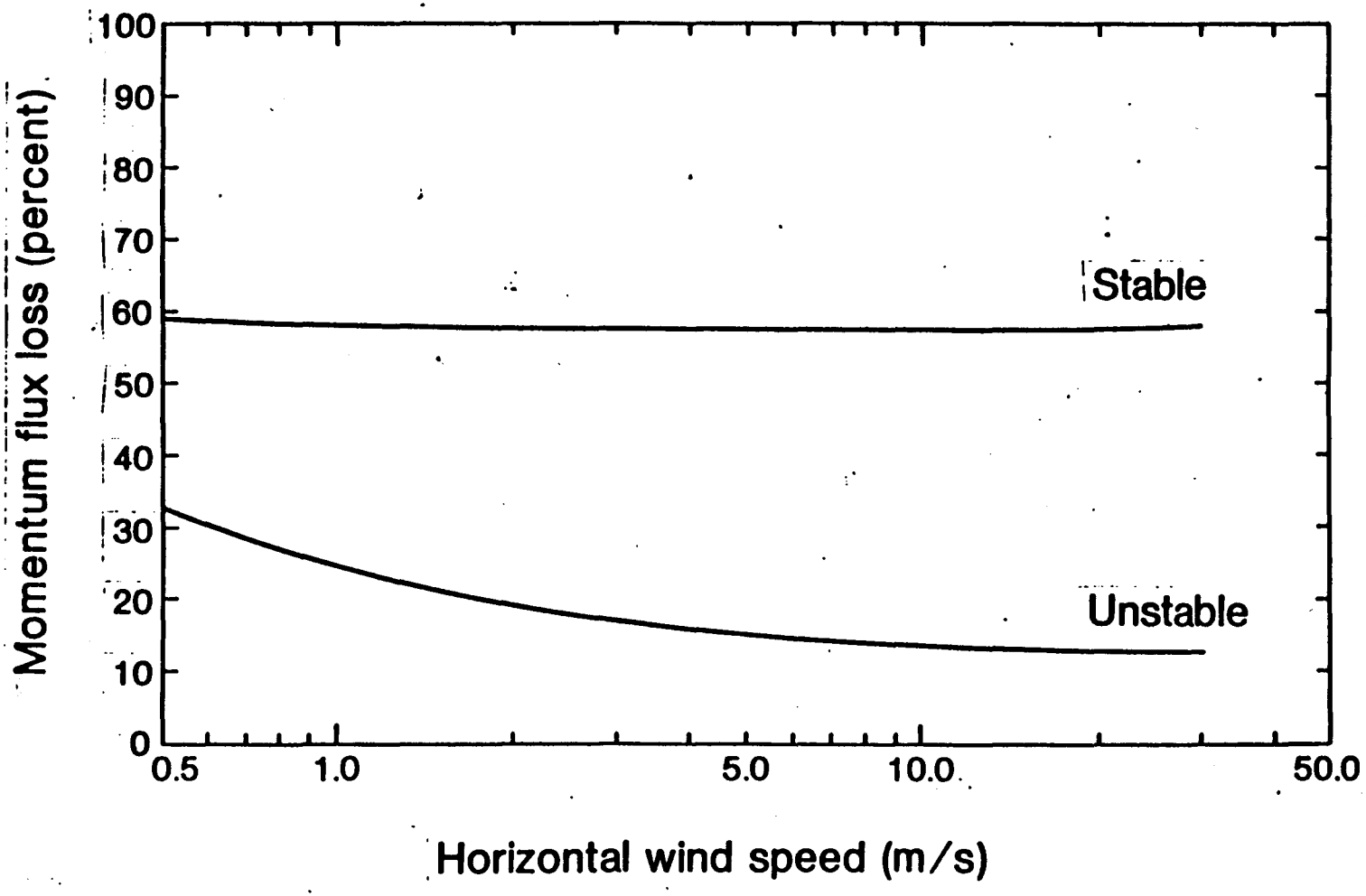
Momentum flux loss (percent)
100
90
80
70
60
50
40
30
20
10
0
Stable
Unstable
0.5
1.0
5.0
10.0
50.0
Horizontal wind speed (m/s)

FIG. 4.

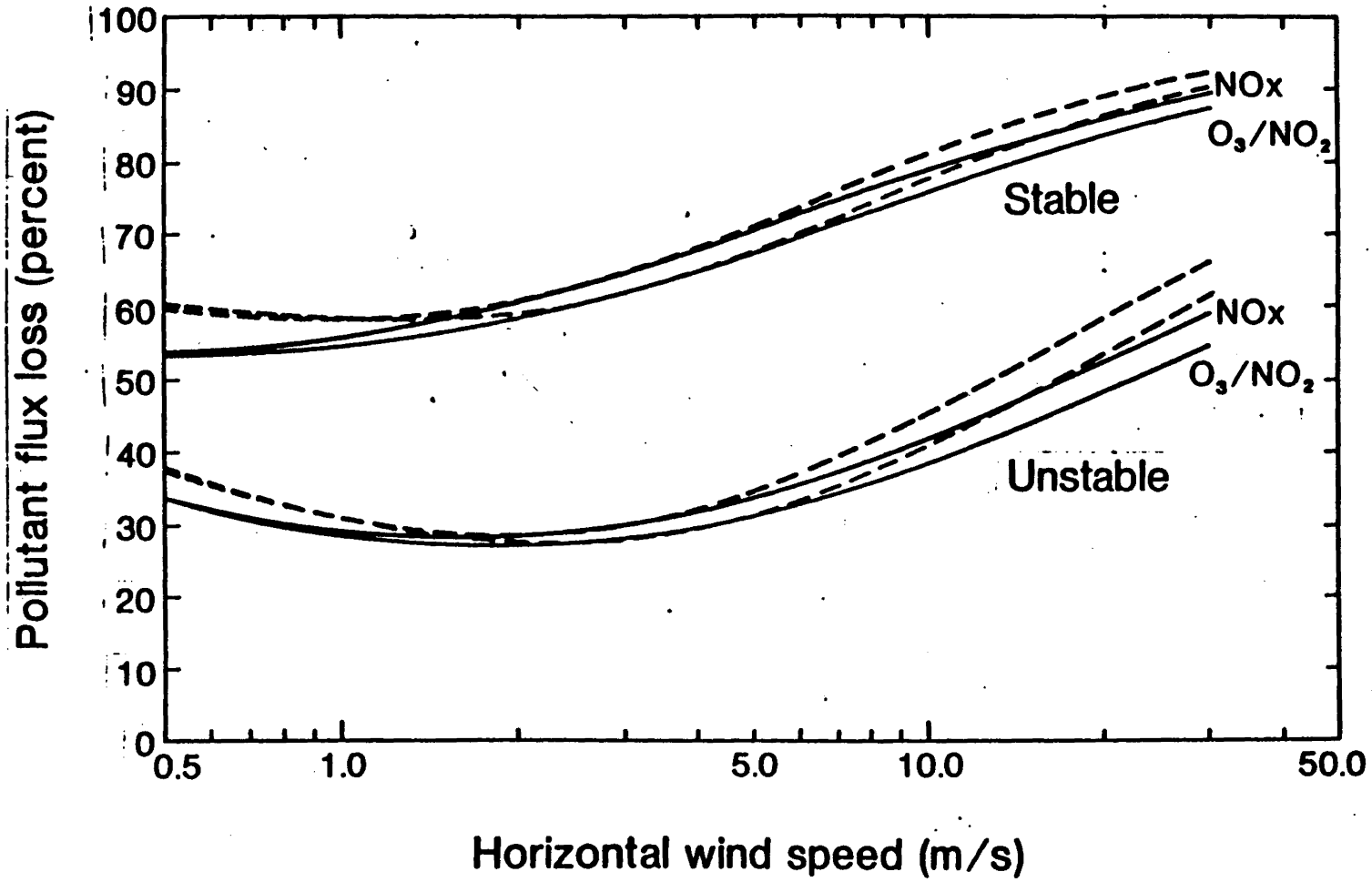
Pollutant flux loss (percent)
100
90
80
70
60
50
40
30
20
10
0
0.5
1.0
5.0
10.0
50.0
Horizontal wind speed (m/s)
NOx
O_3/NO_2
Stable
NOx
O_3/NO_2
Unstable

FIG. 5.

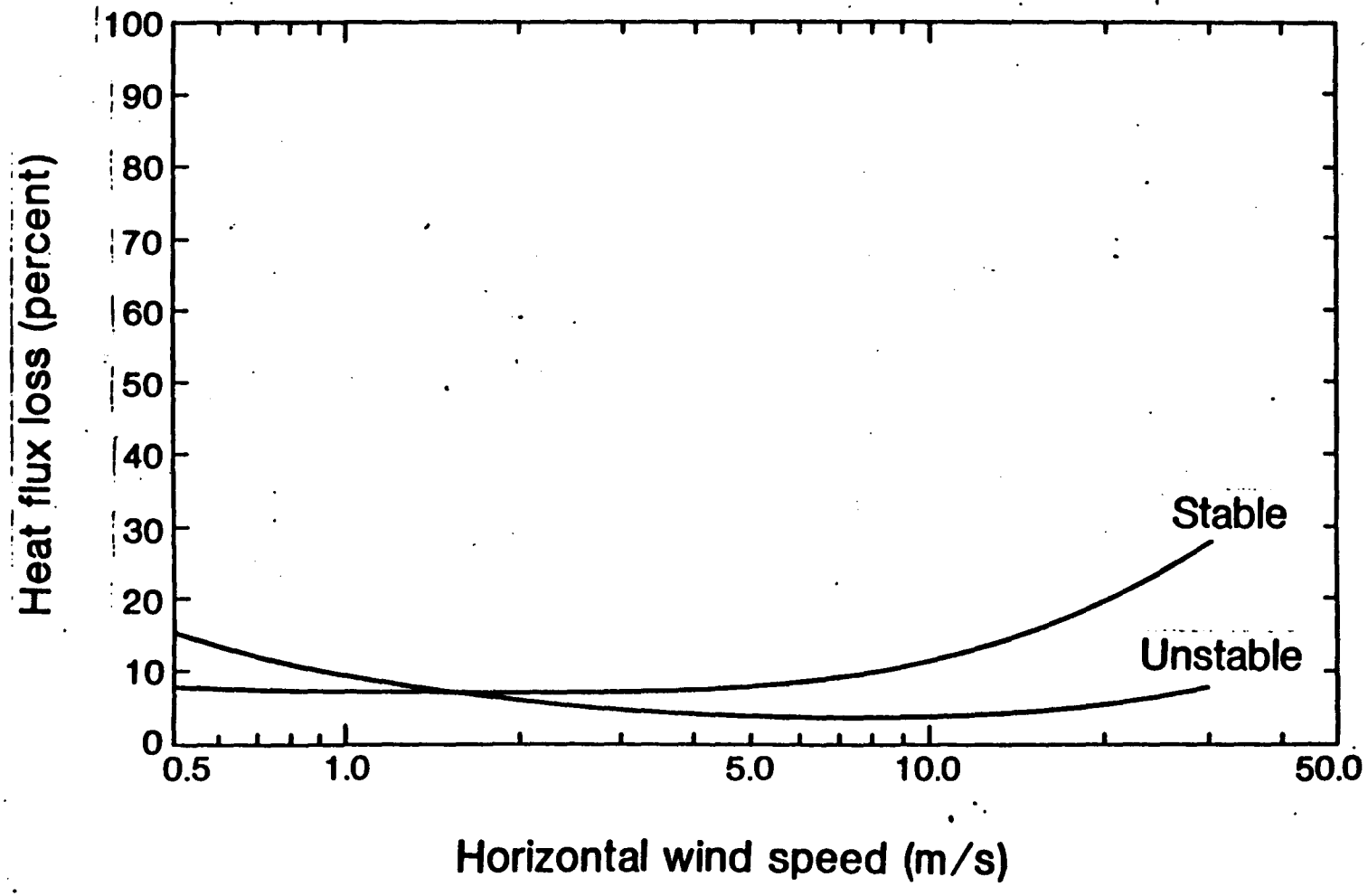
Heat flux loss (percent)
100
90
80
70
60
50
40
30
20
10
0
0.5
1.0
5.0
10.0
50.0
Stable
Unstable
Horizontal wind speed (m/s)

FIG. 5.

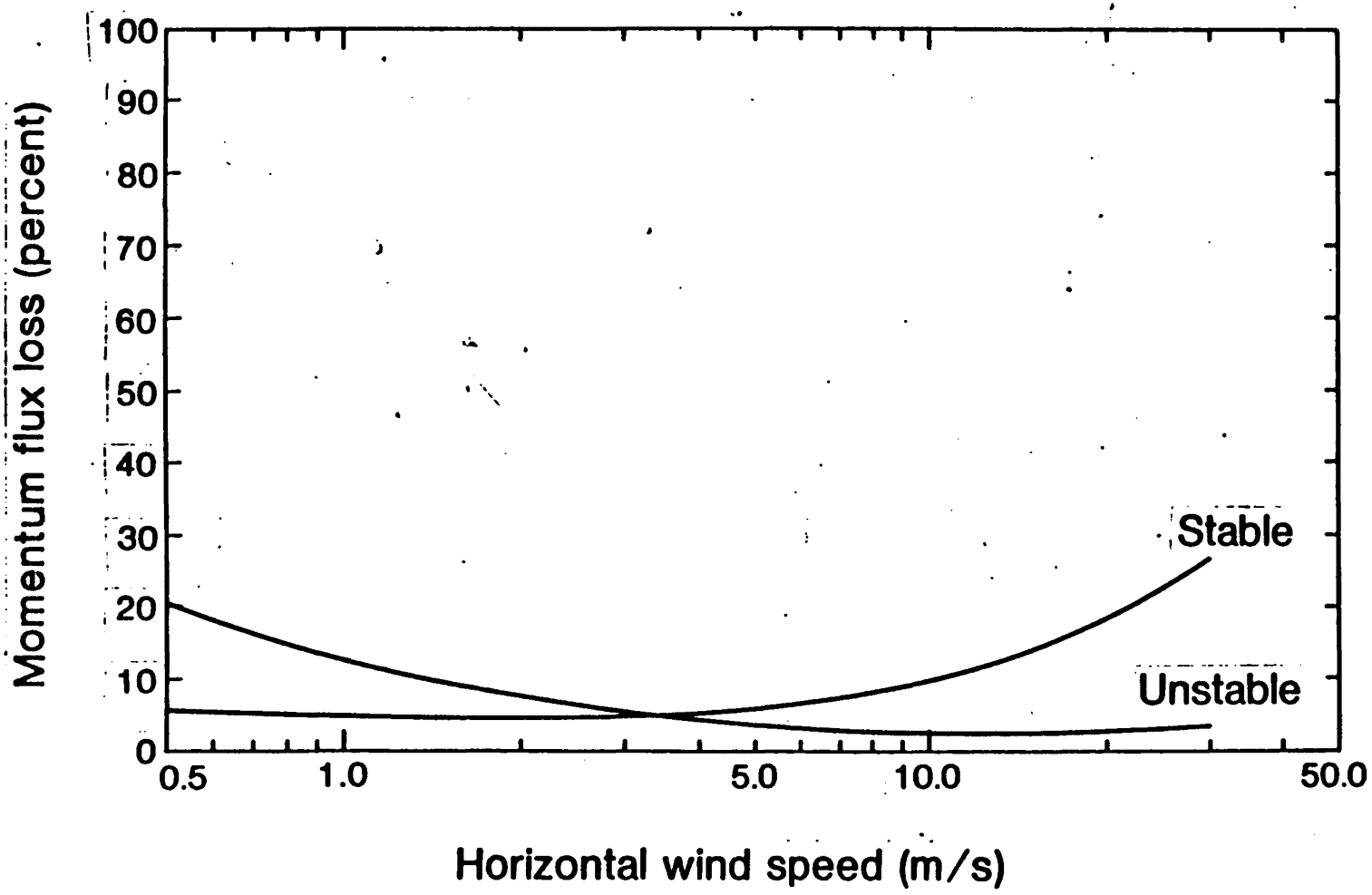
Momentum flux loss (percent)
100
90
80
70
60
50
40
30
20
10
0
0.5
1.0
5.0
10.0
50.0
Stable
Unstable
Horizontal wind speed (m/s)

FIG. 7.

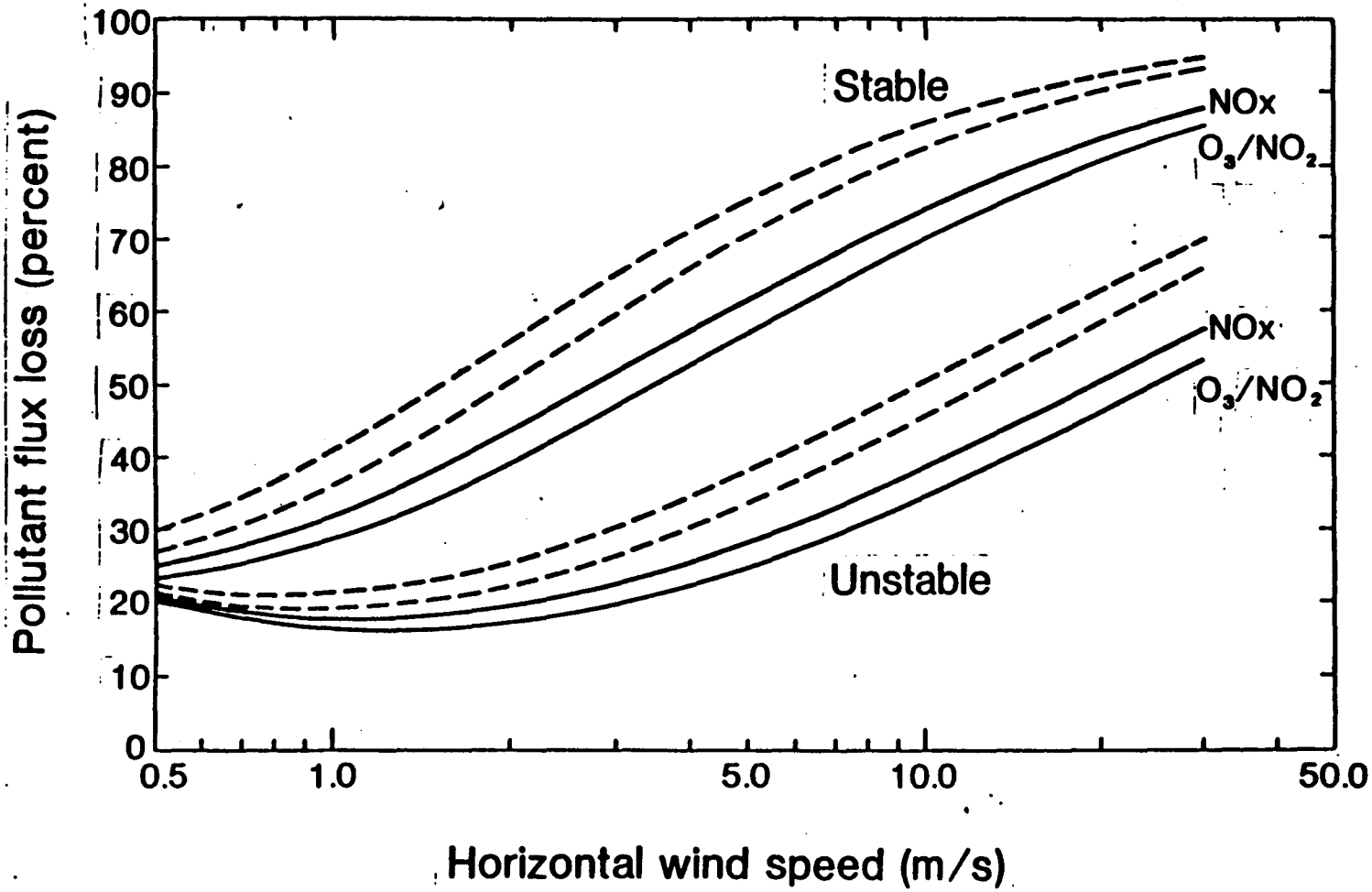
Pollutant flux loss (percent)
100
90
80
70
60
50
40
30
20
10
0
0.5
1.0
5.0
10.0
50.0
Horizontal wind speed (m/s)
Stable
NOx
O_3/NO_2
NOx
O_3/NO_2
Unstable

FIG. 8.

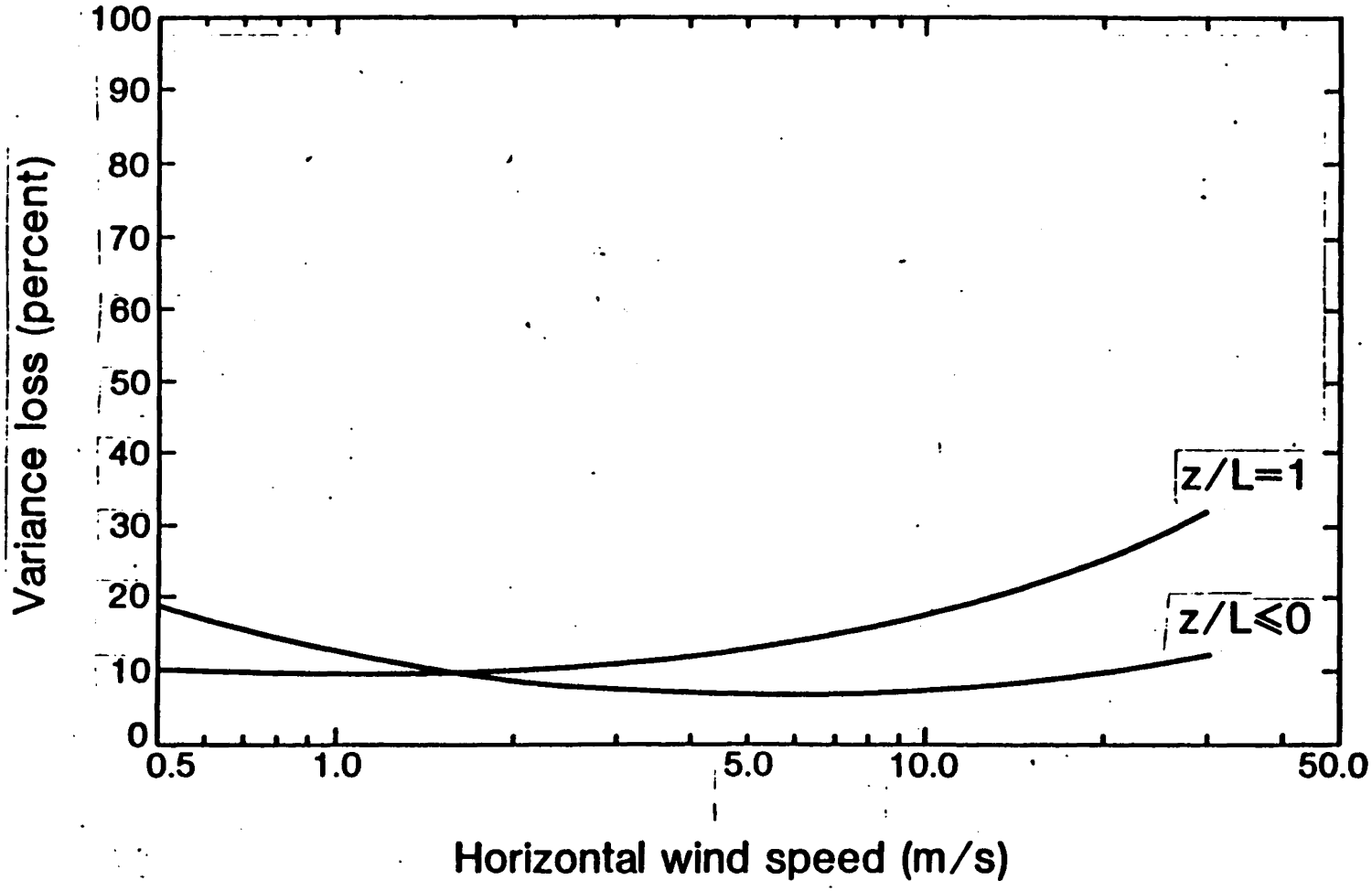
Variance loss (percent)
100
90
80
70
60
50
40
30
20
10
0
0.5
1.0
5.0
10.0
50.0
z/L=1
z/L≤0
Horizontal wind speed (m/s)

FIG. 9.

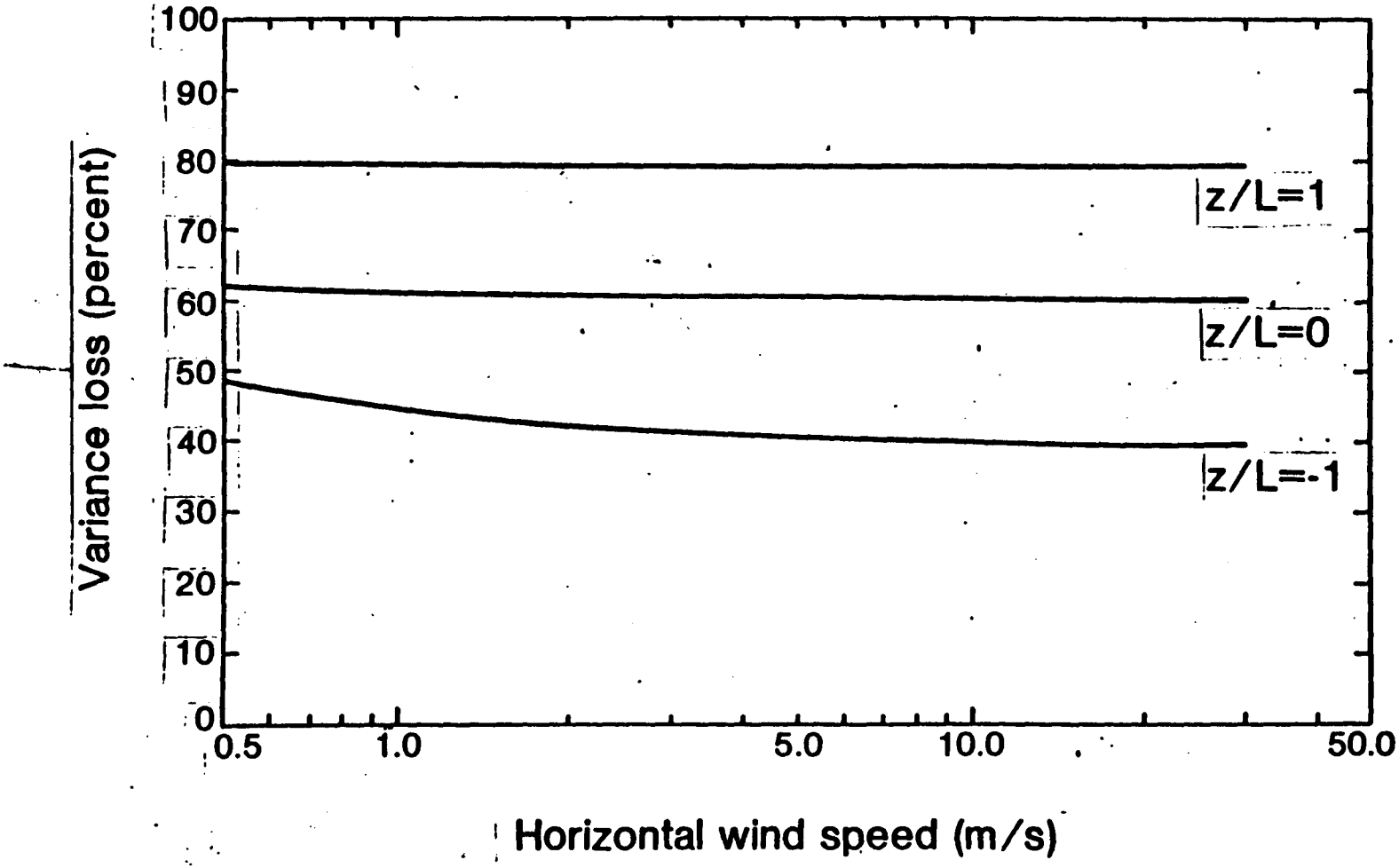
Variance loss (percent)
100
90
80
70
60
50
40
30
20
10
0
z/L=1
z/L=0
z/L=-1
0.5
1.0
5.0
10.0
50.0
Horizontal wind speed (m/s)

FIG. 10.

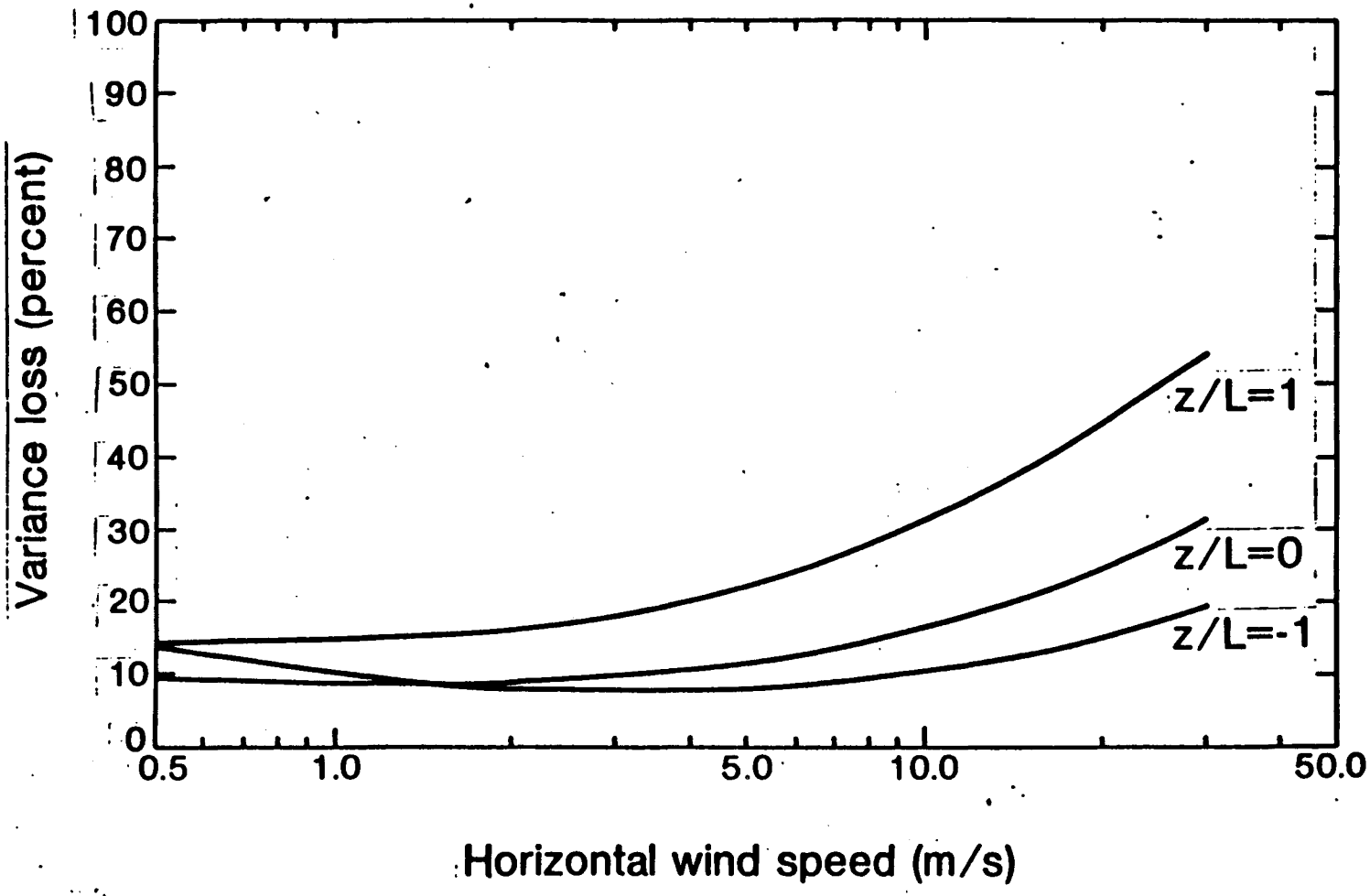
Variance loss (percent)
100
90
80
70
60
50
40
30
20
10
0
0.5
1.0
5.0
10.0
50.0
z/L=1
z/L=0
z/L=-1
Horizontal wind speed (m/s)

FIG. 11.

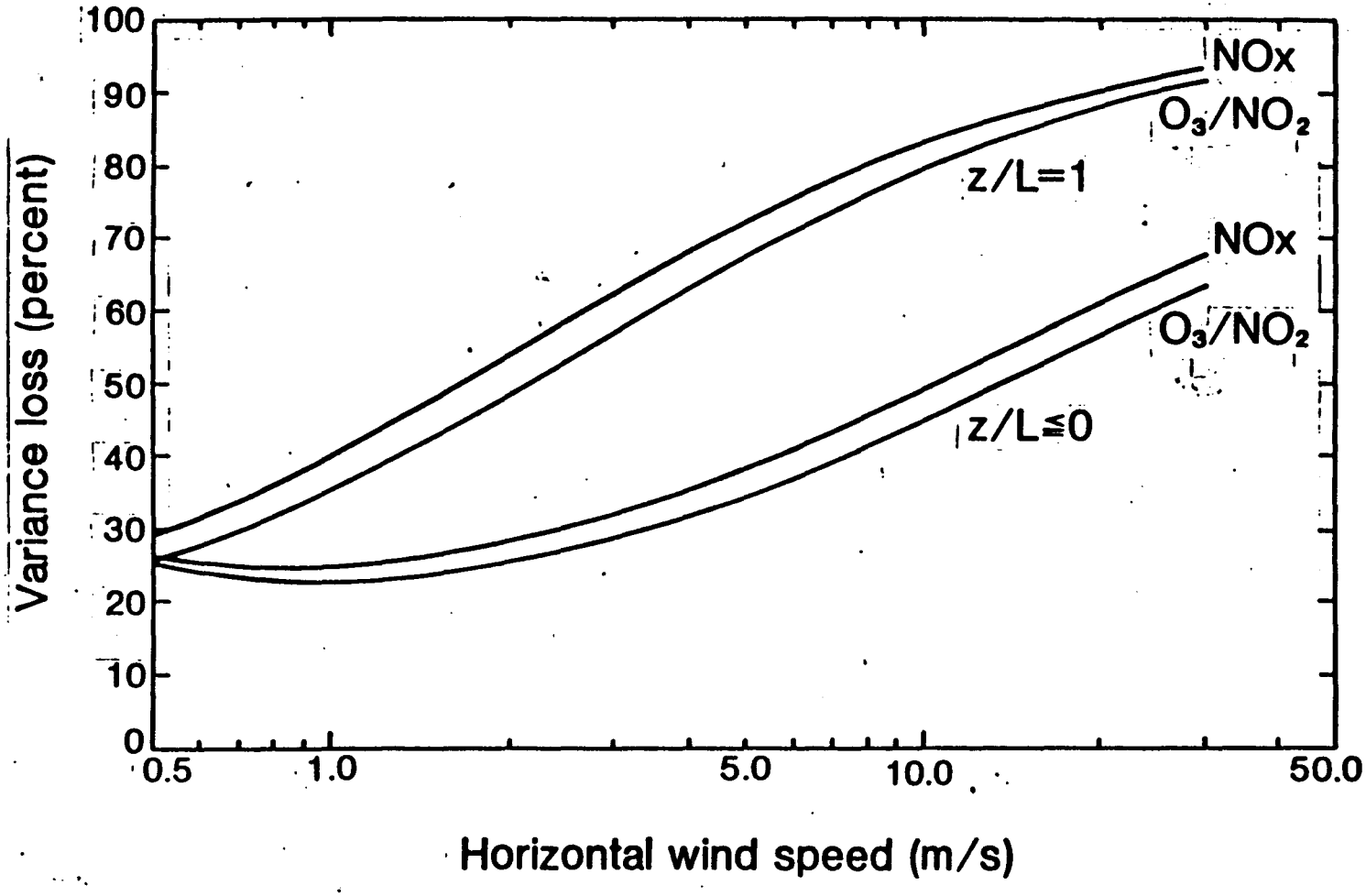
Variance loss (percent)
100
90
80
70
60
50
40
30
20
10
0
0.5
1.0
5.0
10.0
50.0
Horizontal wind speed (m/s)
NOx
O_3/NO_2
z/L=1
NOx
O_3/NO_2
z/L≤0

FIG. 12.

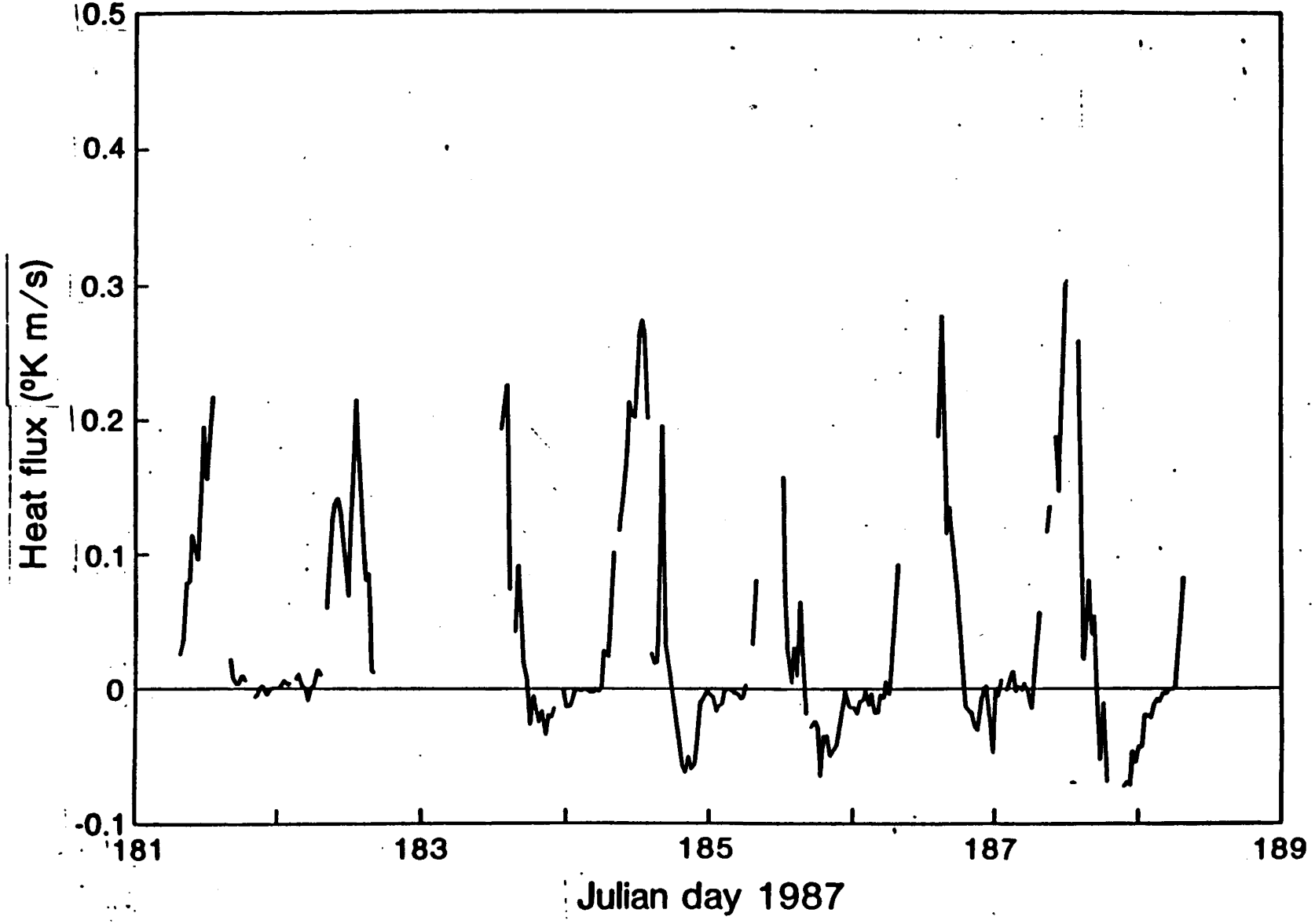
0.5
0.4
0.3
0.2
0.1
0
-0.1
Heat flux (°K m/s)
181
183
185
187
189
Julian day 1987

FIG. 13.

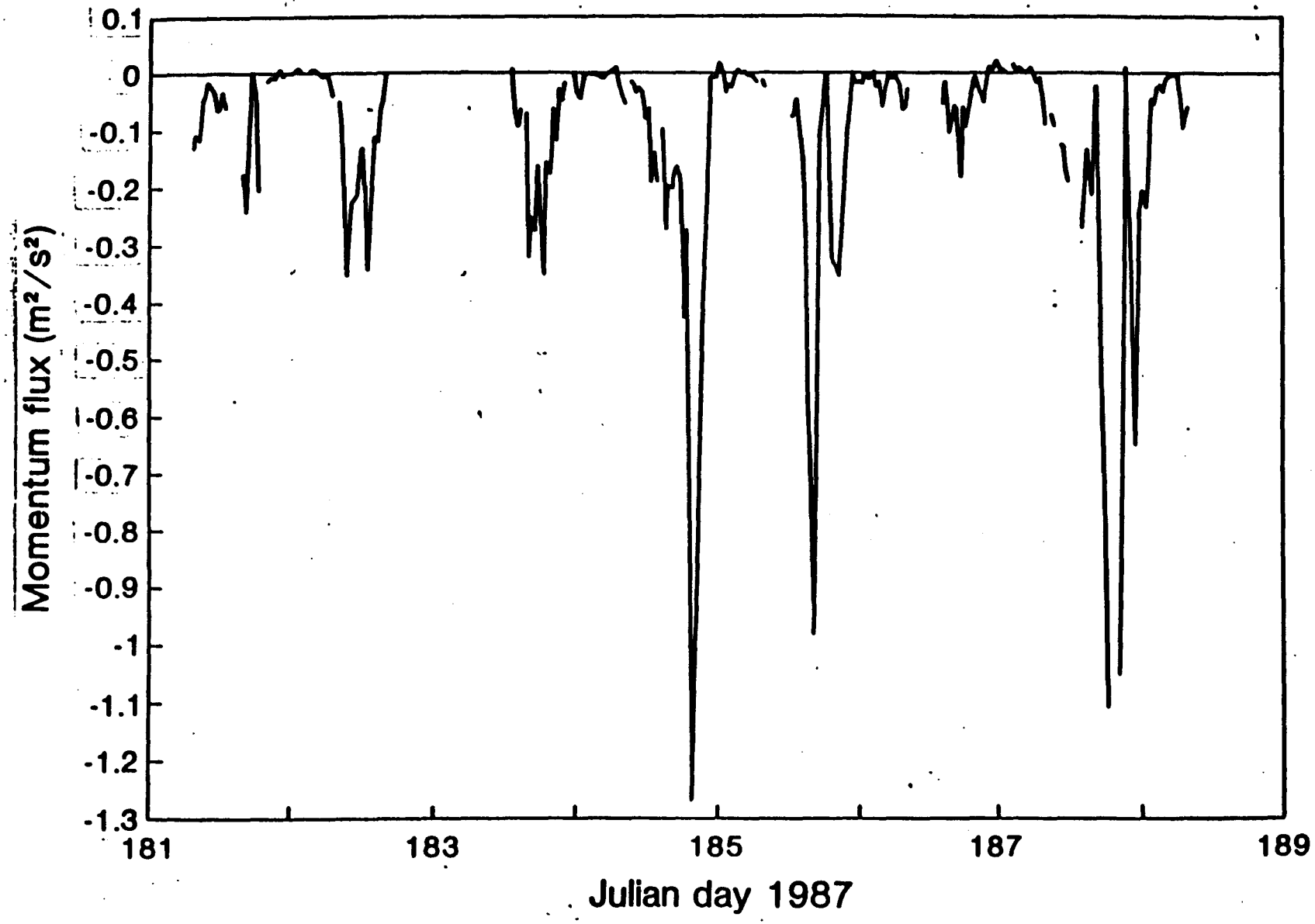
0.1
0
-0.1
-0.2
-0.3
-0.4
-0.5
-0.6
-0.7
-0.8
-0.9
-1
-1.1
-1.2
-1.3
Momentum flux (m²/s²)
181
183
185
187
189
Julian day 1987

FIG. 14.

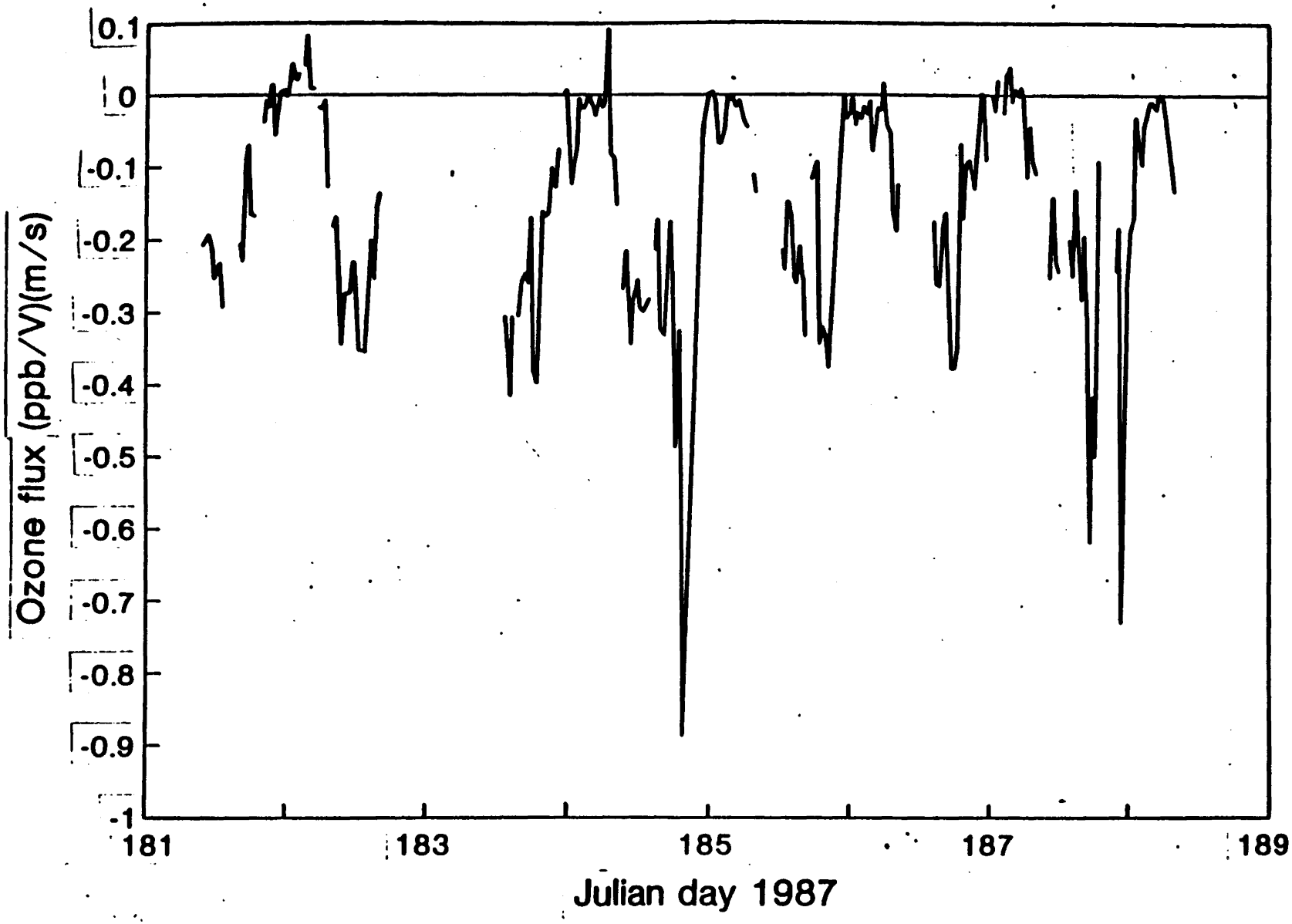
0.1
0
-0.1
-0.2
-0.3
-0.4
-0.5
-0.6
-0.7
-0.8
-0.9
-1
Ozone flux (ppb/V)(m/s)
181
183
185
187
189
Julian day 1987

FIG. 15.

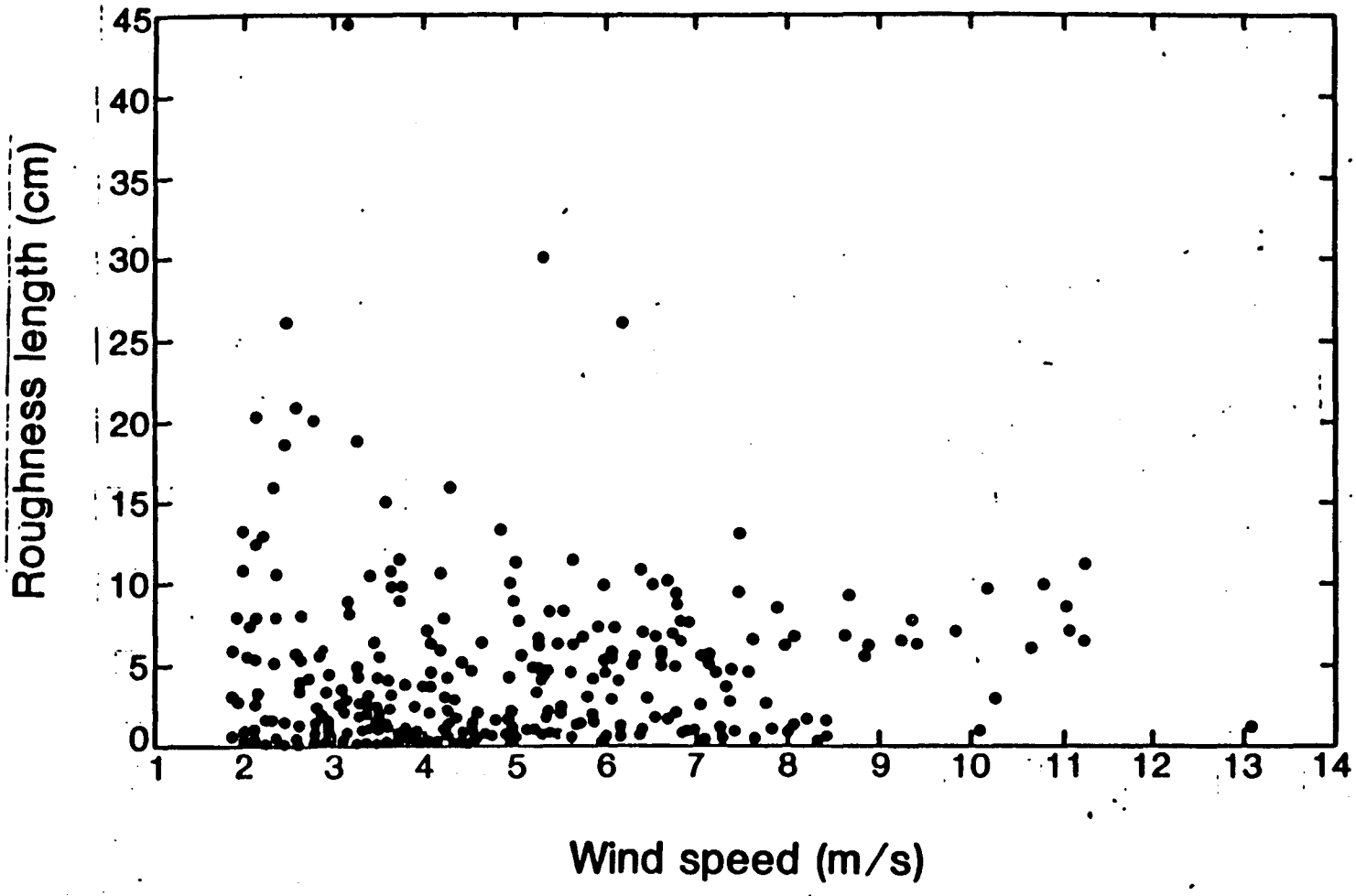
Roughness length (cm)
45
40
35
30
25
20
15
10
5
0
1
2
3
4
5
6
7
8
9
10
11
12
13
14
Wind speed (m/s)

FIG. 16.

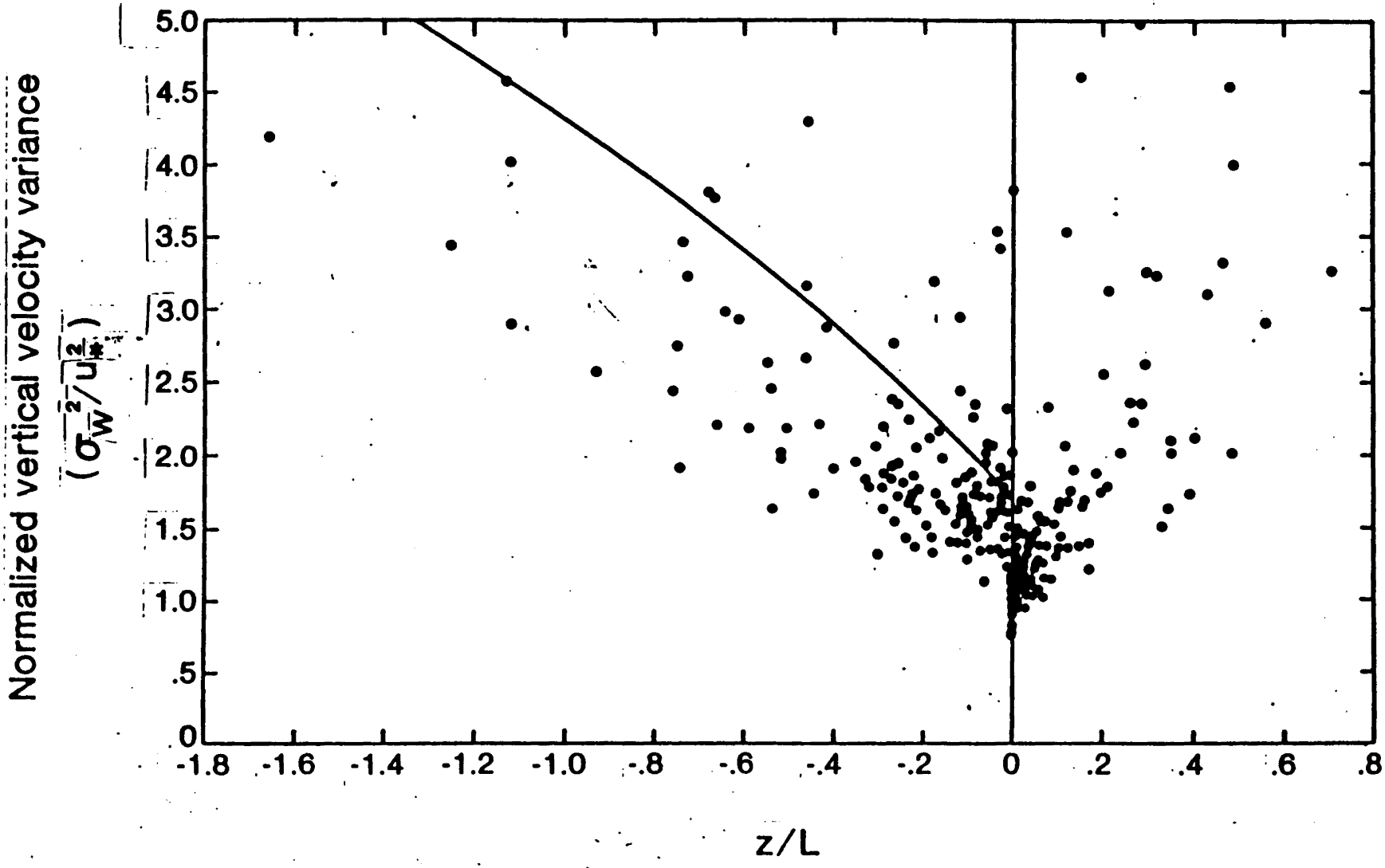
Normalized vertical velocity variance
$(\overline{\sigma_w^2}/\overline{u_*^2})$
5.0
4.5
4.0
3.5
3.0
2.5
2.0
1.5
1.0
.5
0
-1.8
-1.6
-1.4
-1.2
-1.0
-.8
-.6
-.4
-.2
0
.2
.4
.6
.8
z/L

FIG. 17.

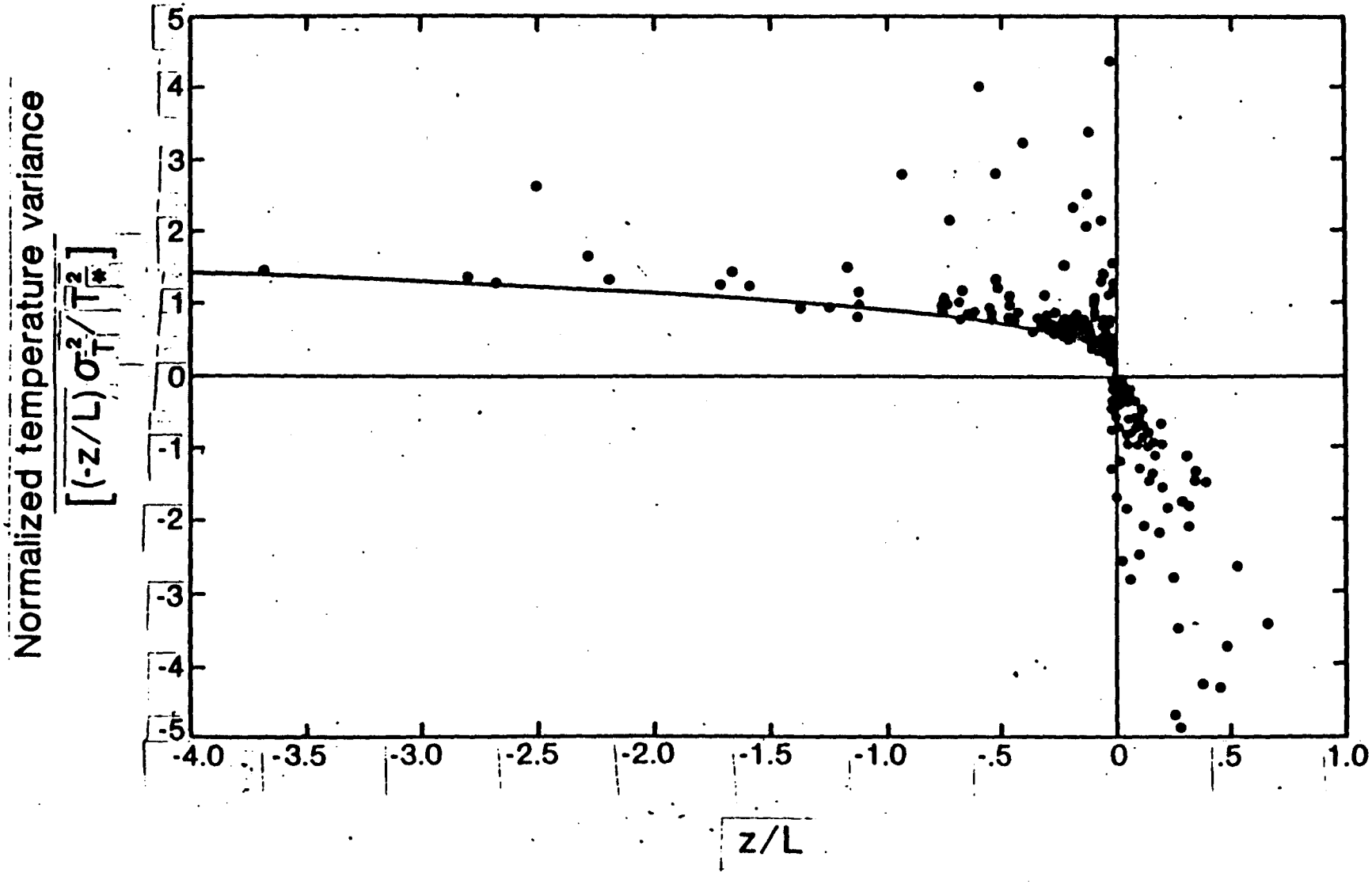
Normalized temperature variance
$\left[\overline{(-z/L)\,\sigma_T^2}/\overline{T_*^2}\right]$
5
4
3
2
1
0
-1
-2
-3
-4
-5
-4.0
-3.5
-3.0
-2.5
-2.0
-1.5
-1.0
-.5
0
.5
1.0
z/L

FIG. 18.

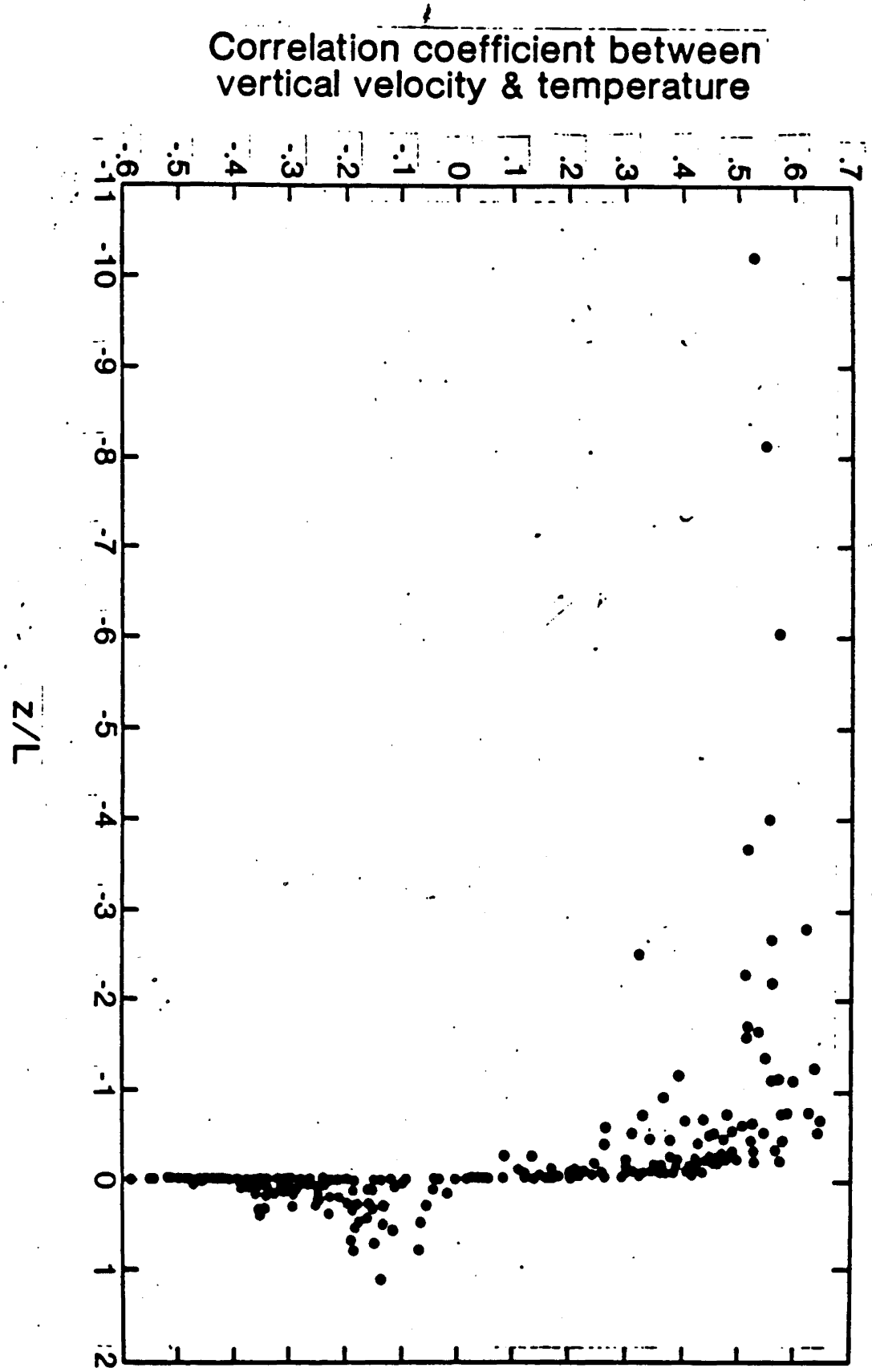
Correlation coefficient between
vertical velocity & temperature
-.6
-.5
-.4
-.3
-.2
-.1
0
.1
.2
.3
.4
.5
.6
.7
-11
-10
-9
-8
-7
-6
-5
-4
-3
-2
-1
0
1
2
z/L

FIG. 19.

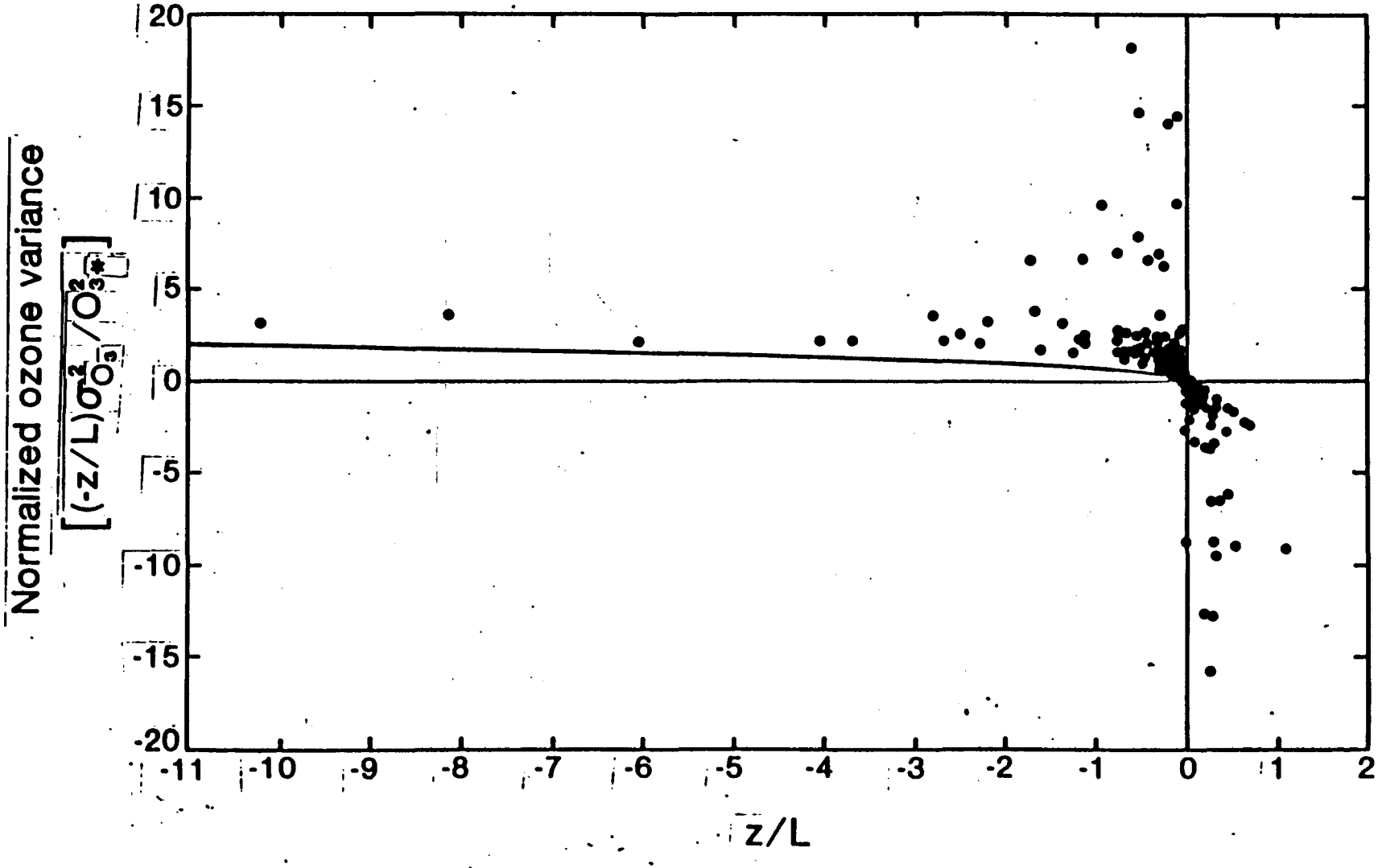
Normalized ozone variance
$[(-z/L)\sigma^2_{O_3}/O^2_{3*}]$
20
15
10
5
0
-5
-10
-15
-20
-11
-10
-9
-8
-7
-6
-5
-4
-3
-2
-1
0
1
2
z/L

FIG. 20.

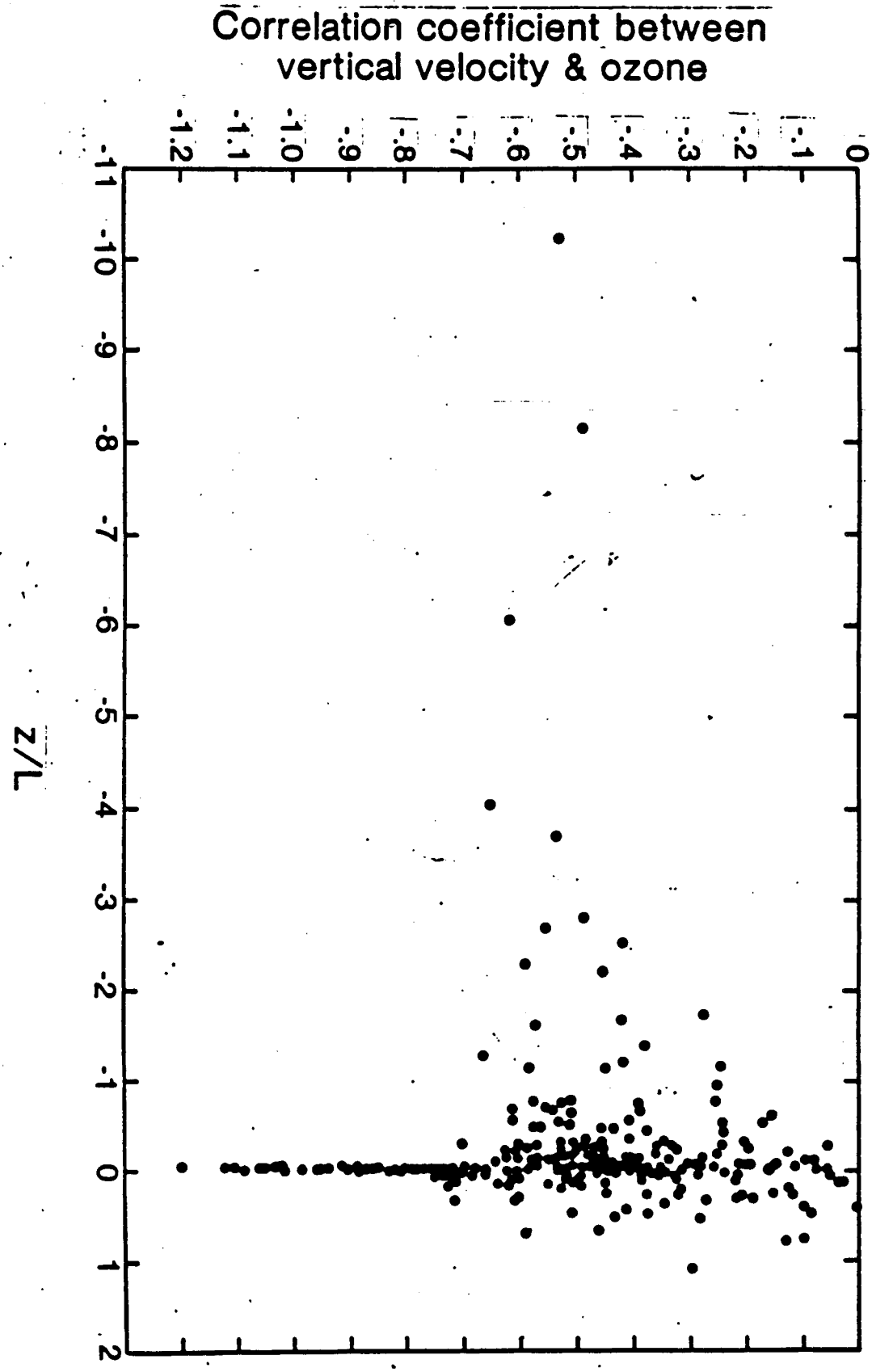
Correlation coefficient between
vertical velocity & ozone
-1.2
-1.1
-1.0
-.9
-.8
-.7
-.6
-.5
-.4
-.3
-.2
-.1
0
-11
-10
-9
-8
-7
-6
-5
-4
-3
-2
-1
0
1
2
z/L

FIG. 21.

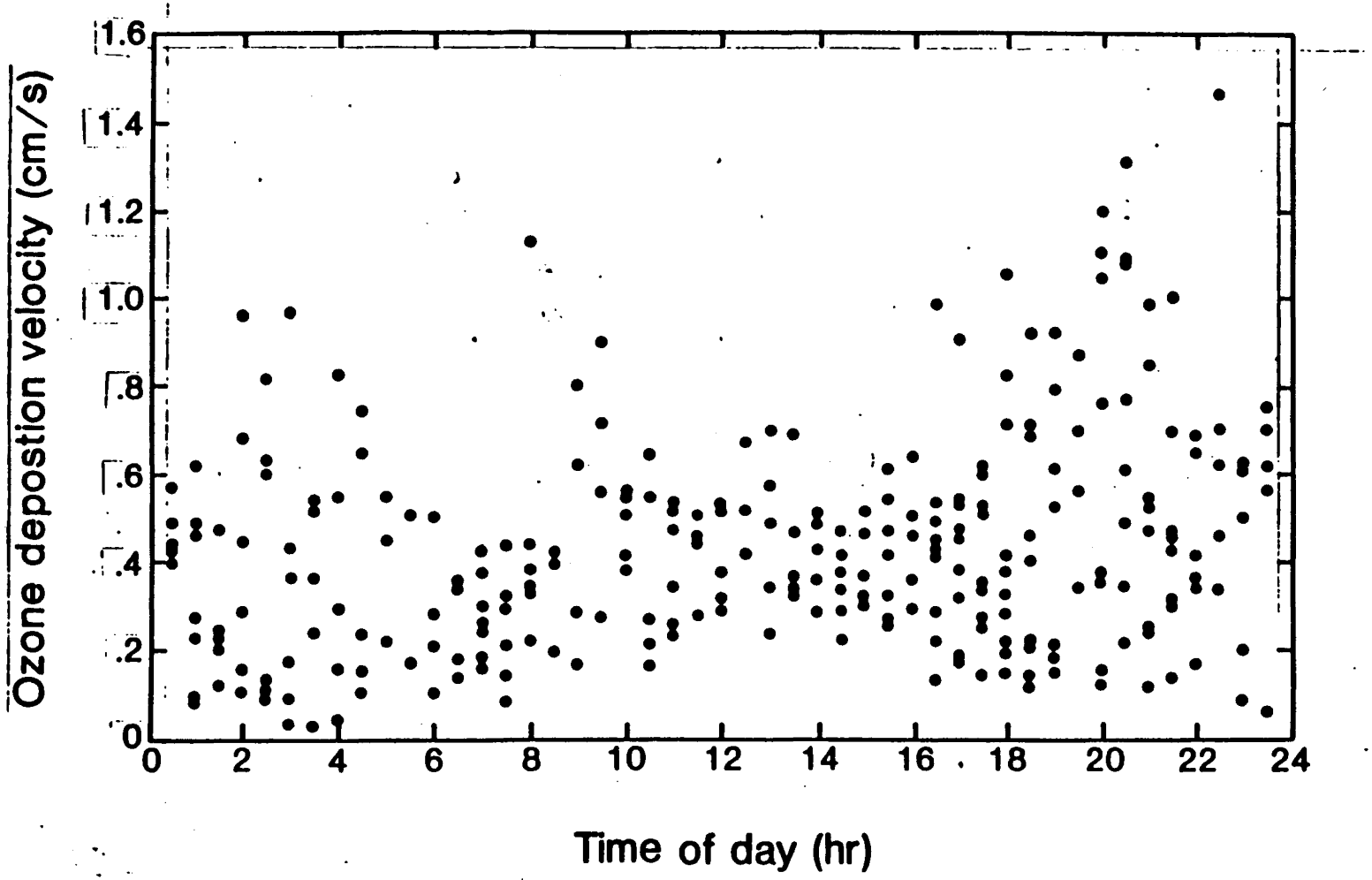
Ozone depostion velocity (cm/s)
1.6
1.4
1.2
1.0
.8
.6
.4
.2
0
0
2
4
6
8
10
12
14
16
18
20
22
24
Time of day (hr)

FIG. 22.

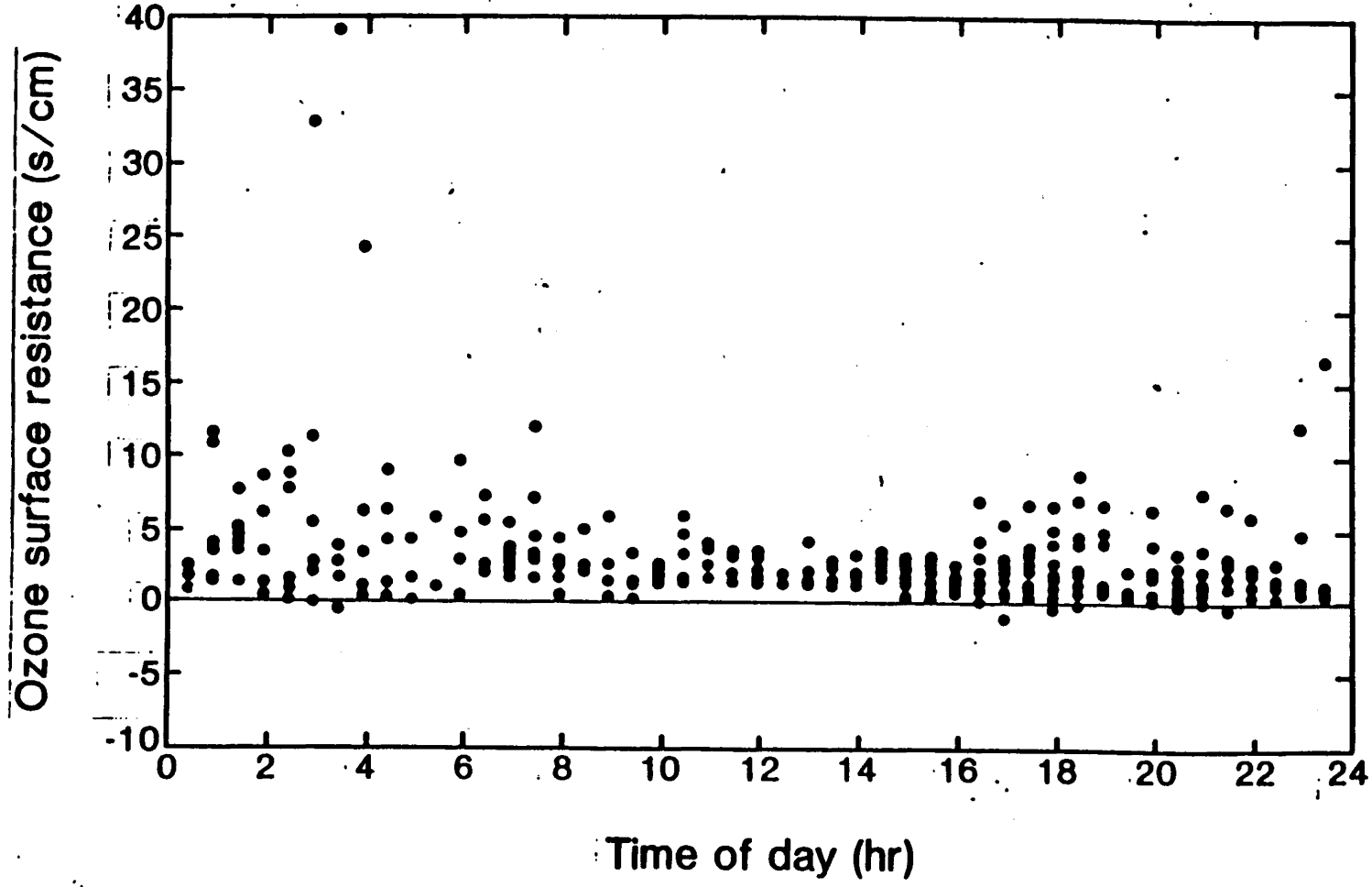
Ozone surface resistance (s/cm)
40
35
30
25
20
15
10
5
0
-5
-10
0
2
4
6
8
10
12
14
16
18
20
22
24
Time of day (hr)

FIG. 23.

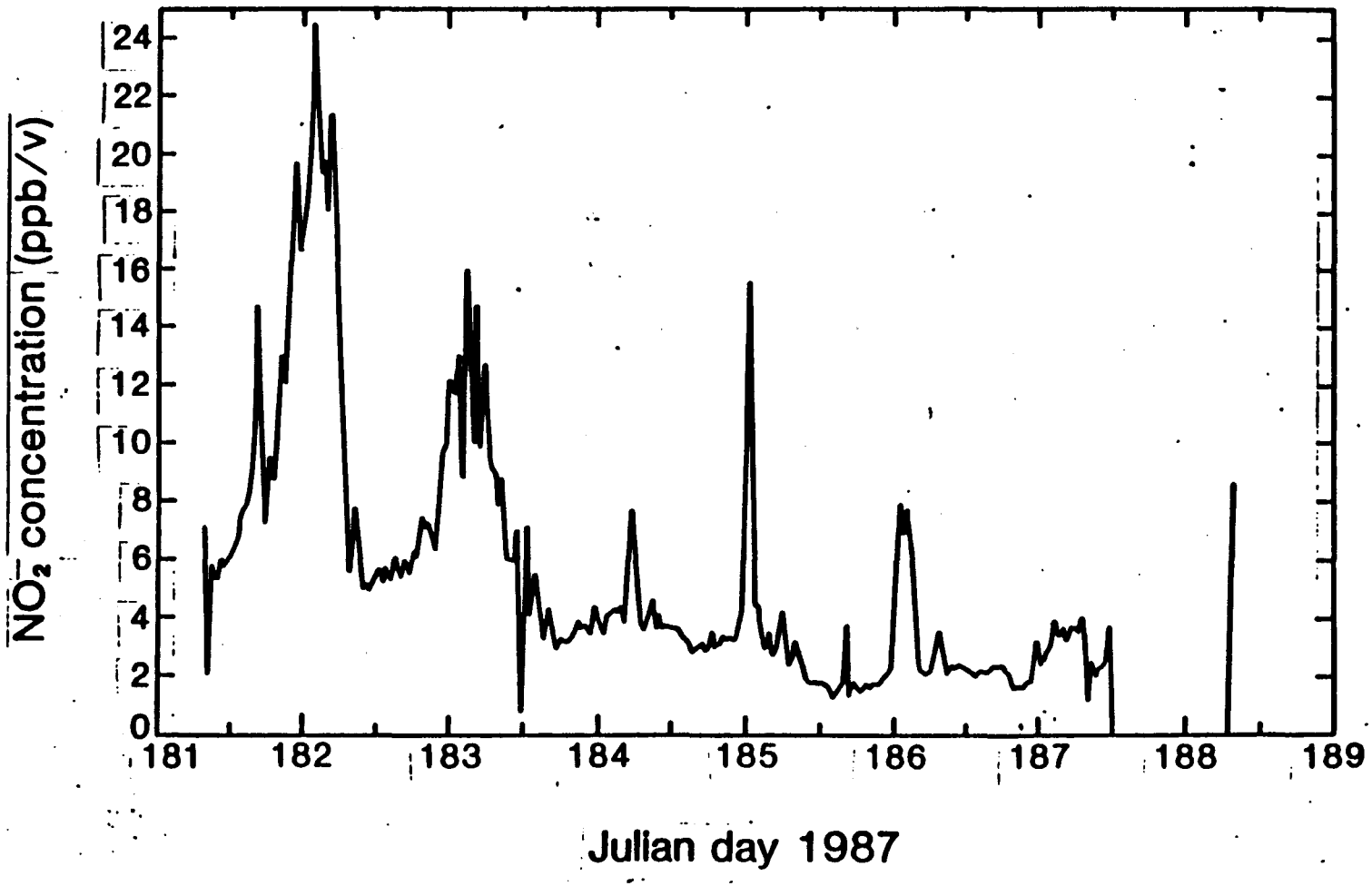
$\overline{NO_2^-}$ concentration (ppb/v)
0
2
4
6
8
10
12
14
16
18
20
22
24
181
182
183
184
185
186
187
188
189
Julian day 1987

FIG. 24.

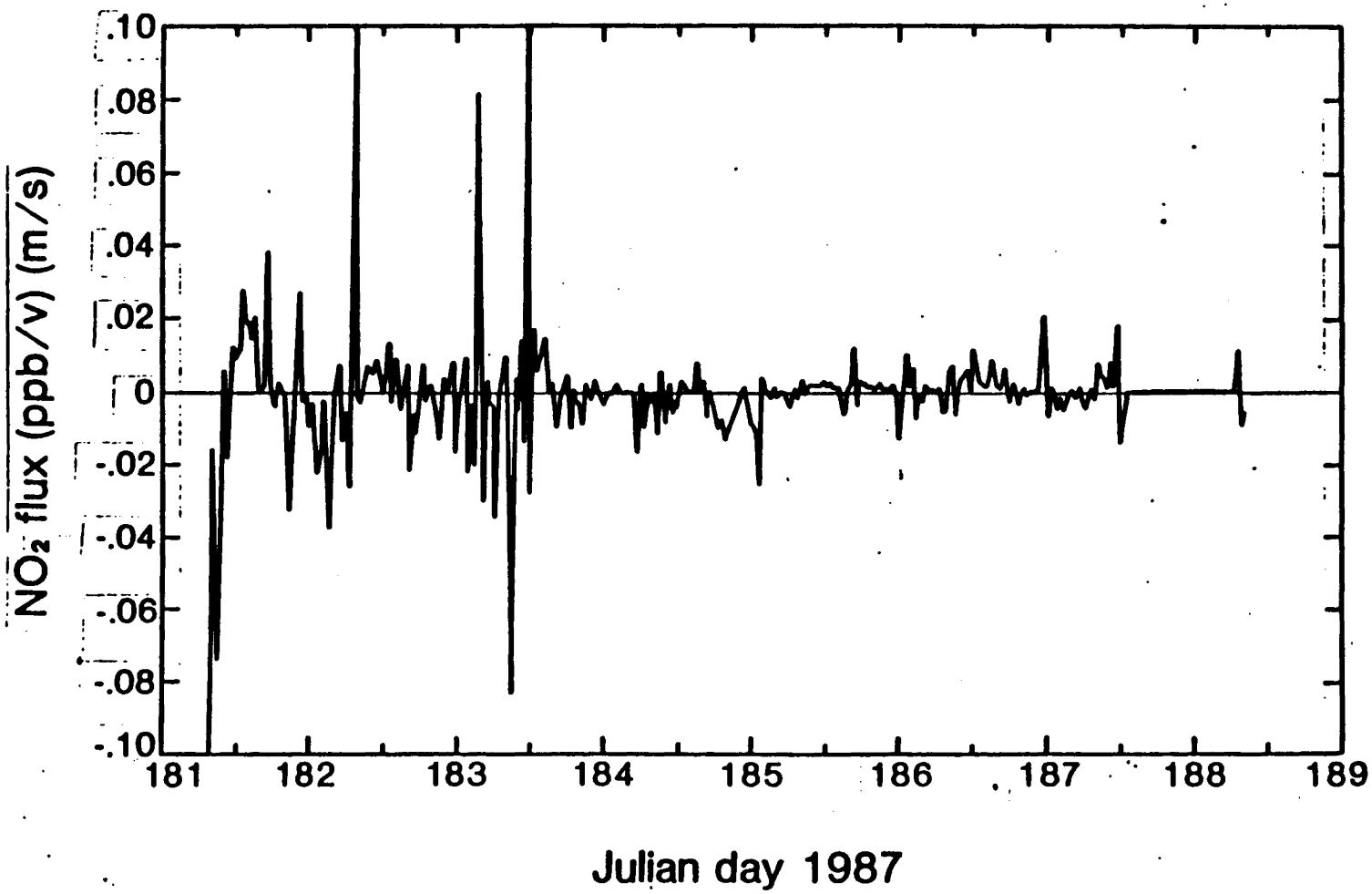
.10
.08
.06
.04
.02
0
-.02
-.04
-.06
-.08
-.10
$\overline{NO_2}$ flux (ppb/v) (m/s)
181
182
183
184
185
186
187
188
189
Julian day 1987

FIG. 25.

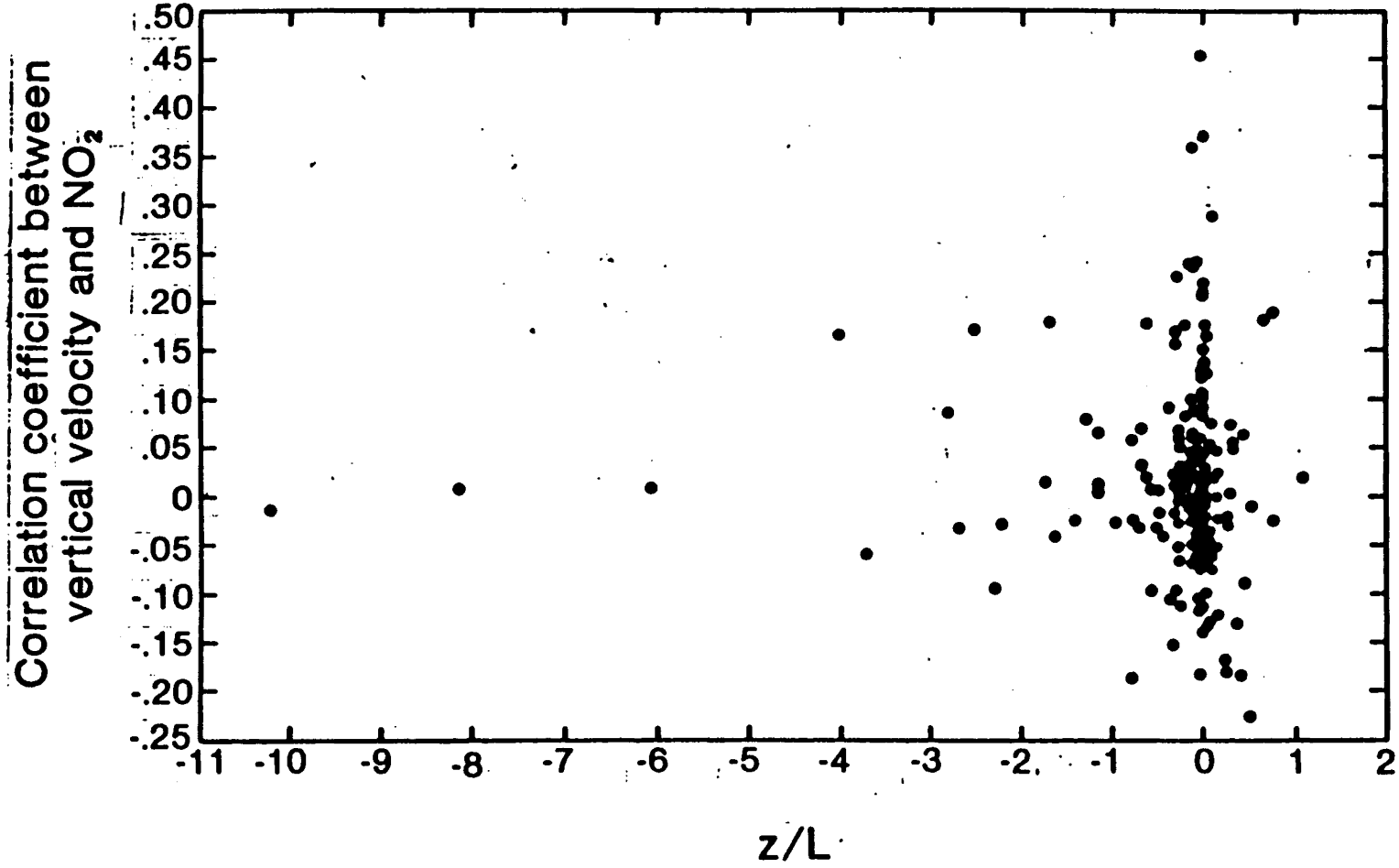
Correlation coefficient between vertical velocity and NO_2
.50
.45
.40
.35
.30
.25
.20
.15
.10
.05
0
-.05
-.10
-.15
-.20
-.25
-11
-10
-9
-8
-7
-6
-5
-4
-3
-2
-1
0
1
2
z/L

FIG. 26

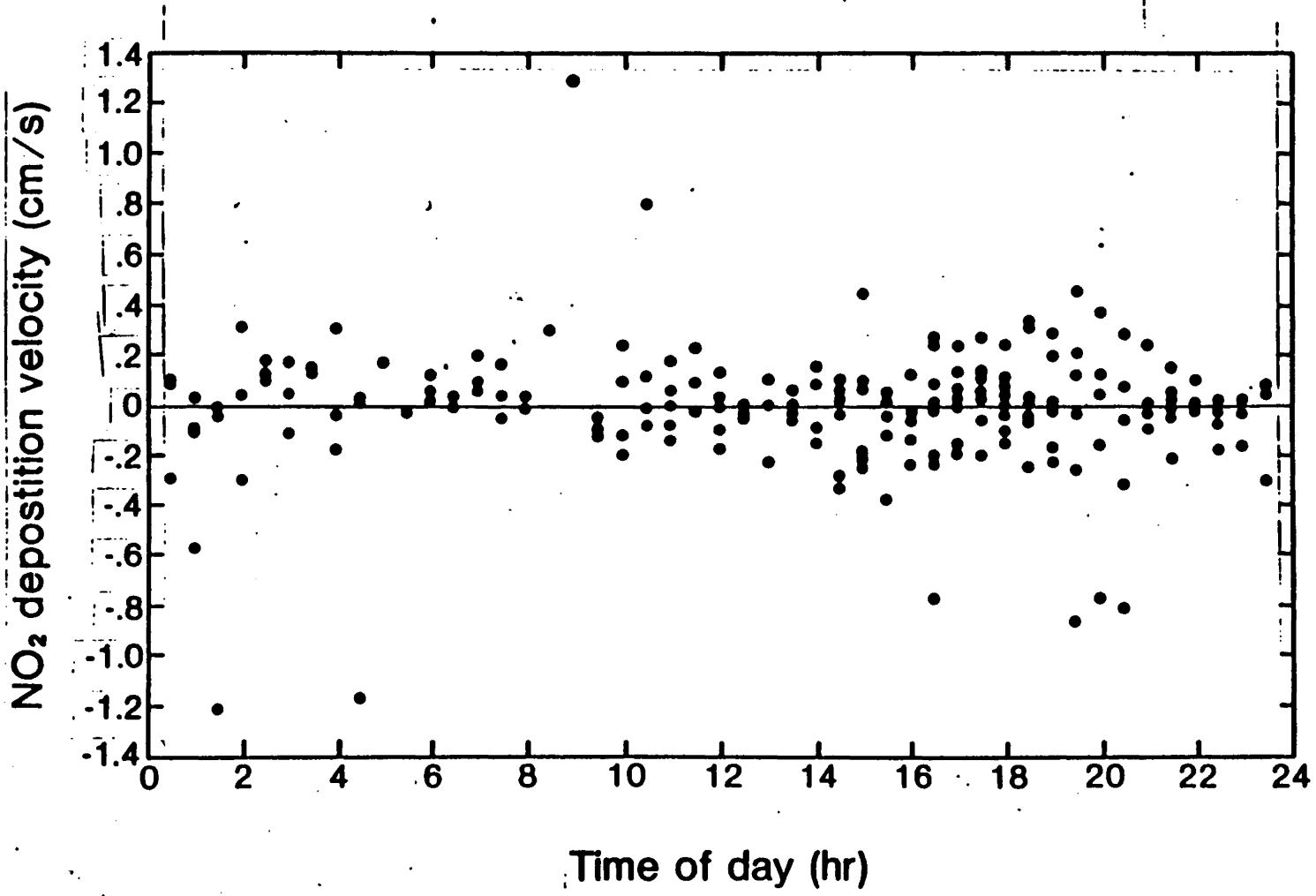
NO_2 deposition velocity (cm/s)
1.4
1.2
1.0
.8
.6
.4
.2
0
-.2
-.4
-.6
-.8
-1.0
-1.2
-1.4
0
2
4
6
8
10
12
14
16
18
20
22
24
Time of day (hr)

FIG. 27.

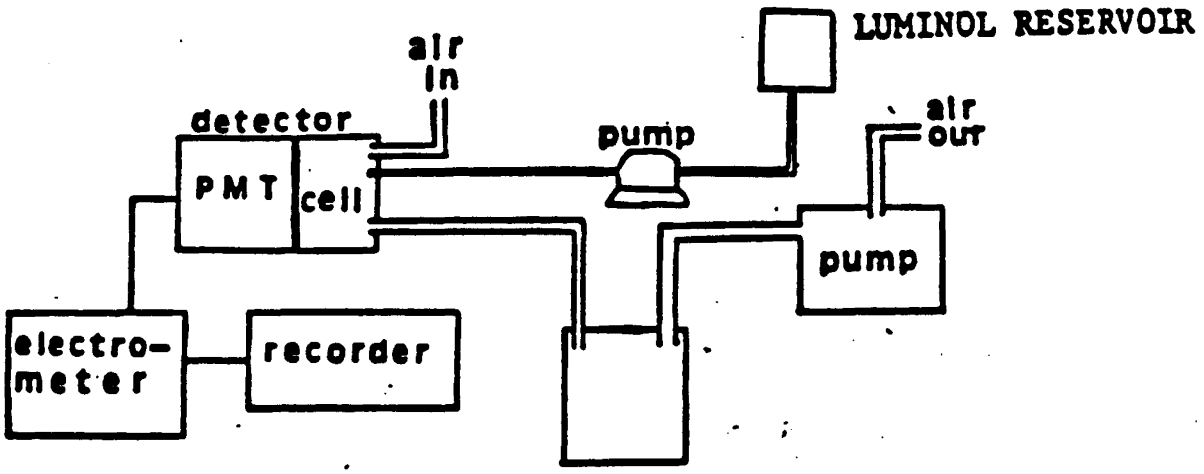

Detection cell design

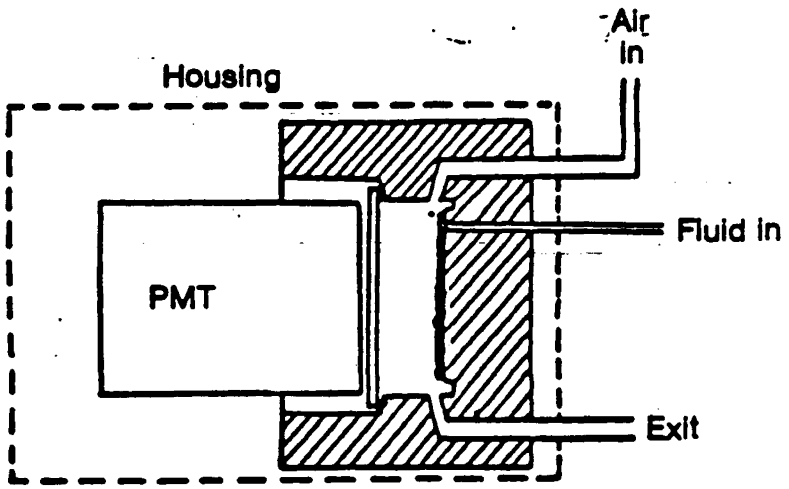

FIG. A1.

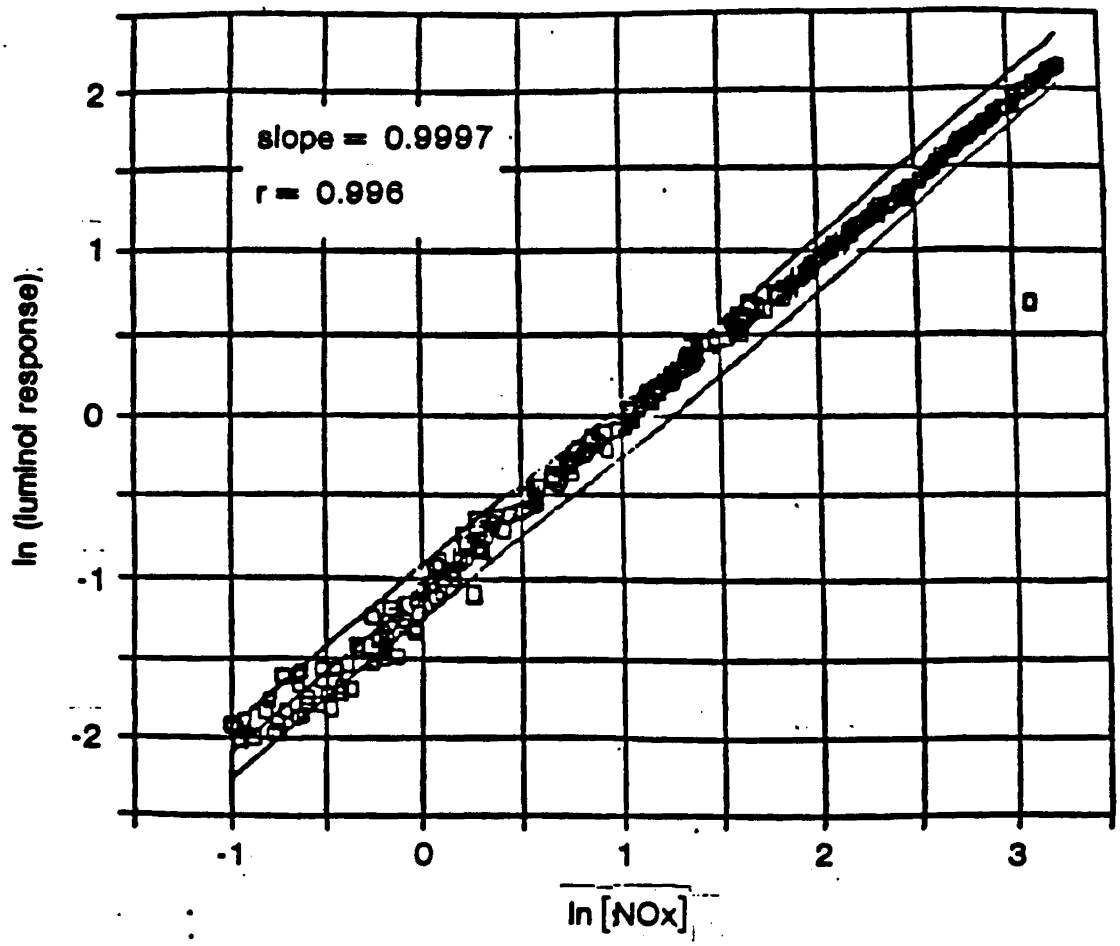
slope = 0.9997
r = 0.996
ln (luminol response)
ln [NOx]
2
1
0
-1
-2
-1
0
1
2
3

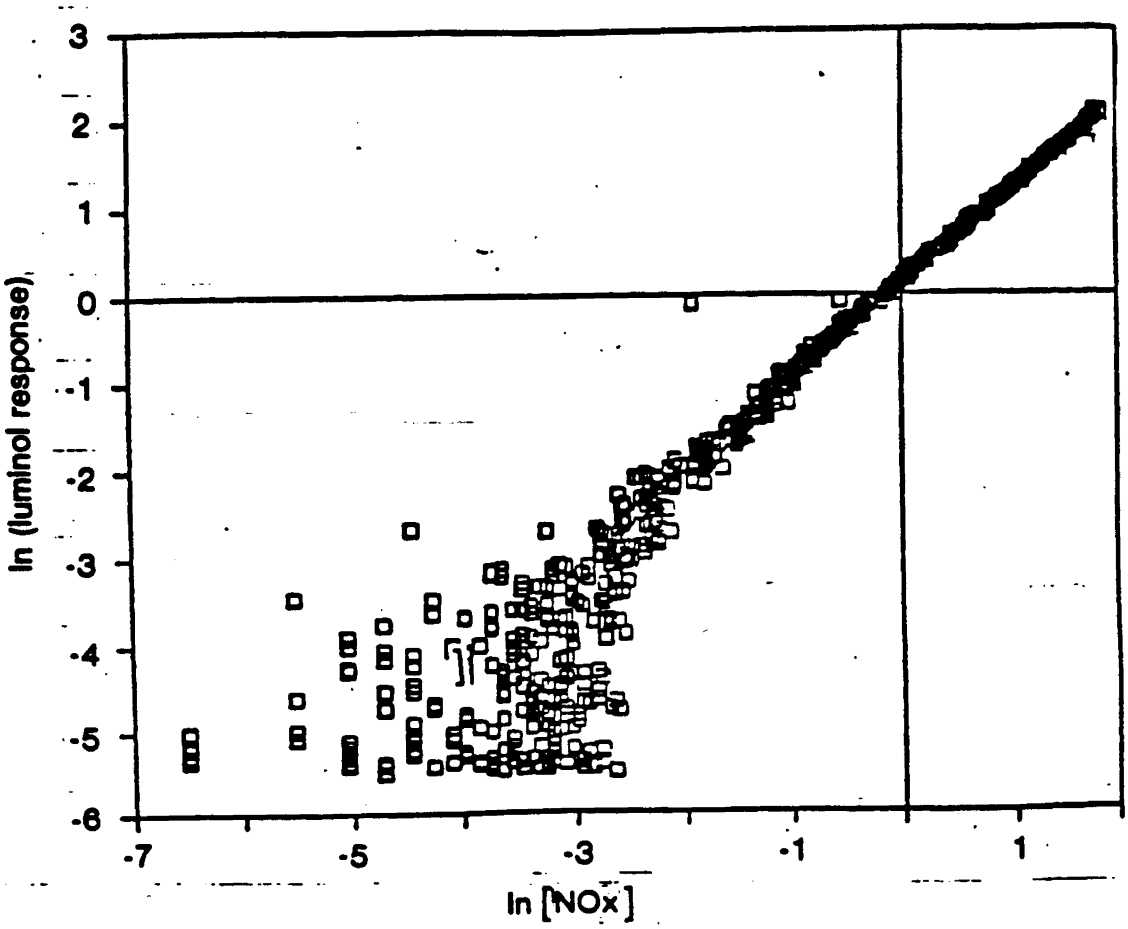
ln (luminol response)
ln [NOx]
3
2
1
0
-1
-2
-3
-4
-5
-6
-7
-5
-3
-1
1

FIG. A2.

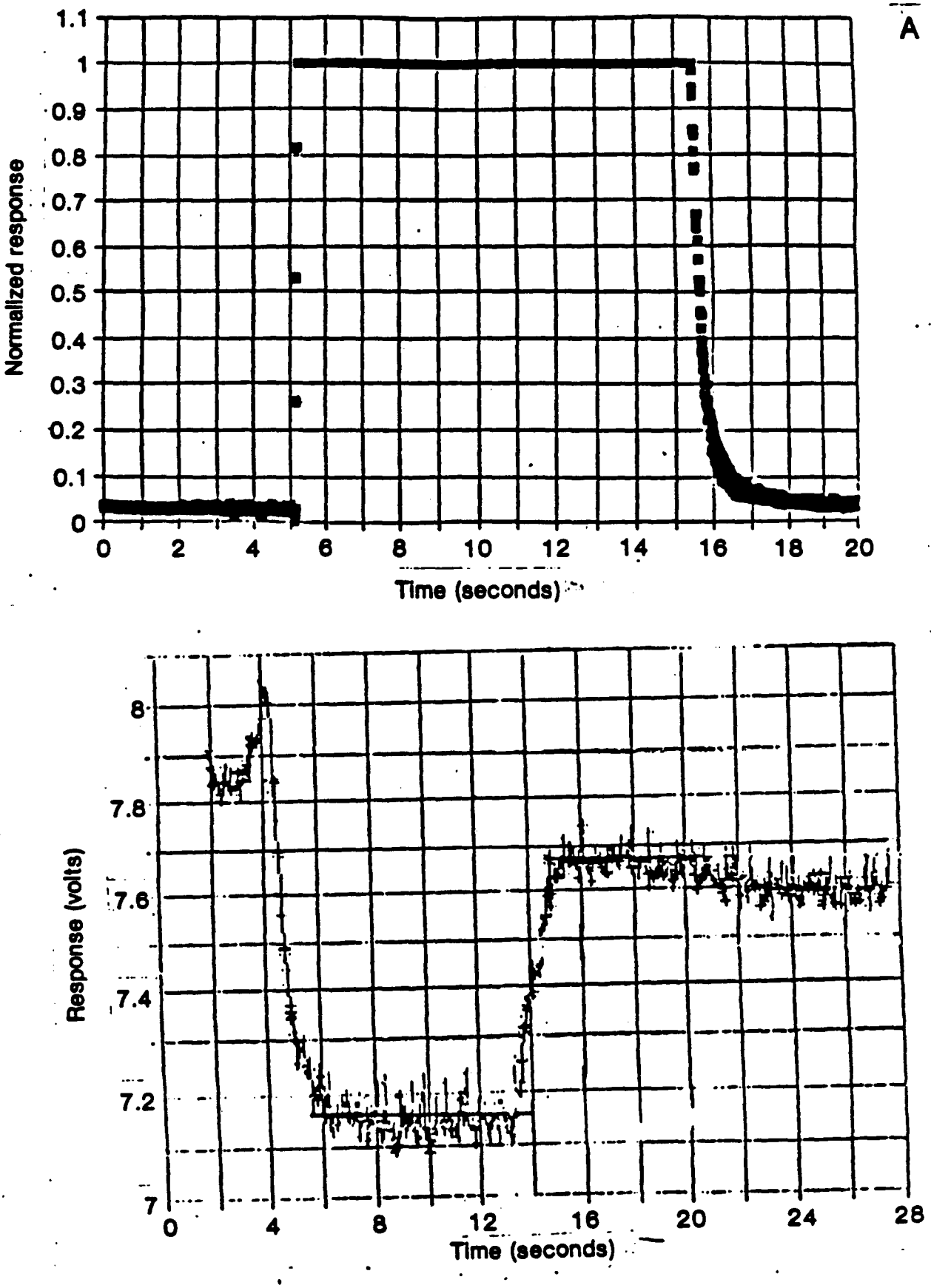
A
Normalized response
1.1
1
0.9
0.8
0.7
0.6
0.5
0.4
0.3
0.2
0.1
0
0 2 4 6 8 10 12 14 16 18 20
Time (seconds)
B
Response (volts)
8
7.8
7.6
7.4
7.2
7
0 4 8 12 16 20 24 28
Time (seconds)

FIG. A3.

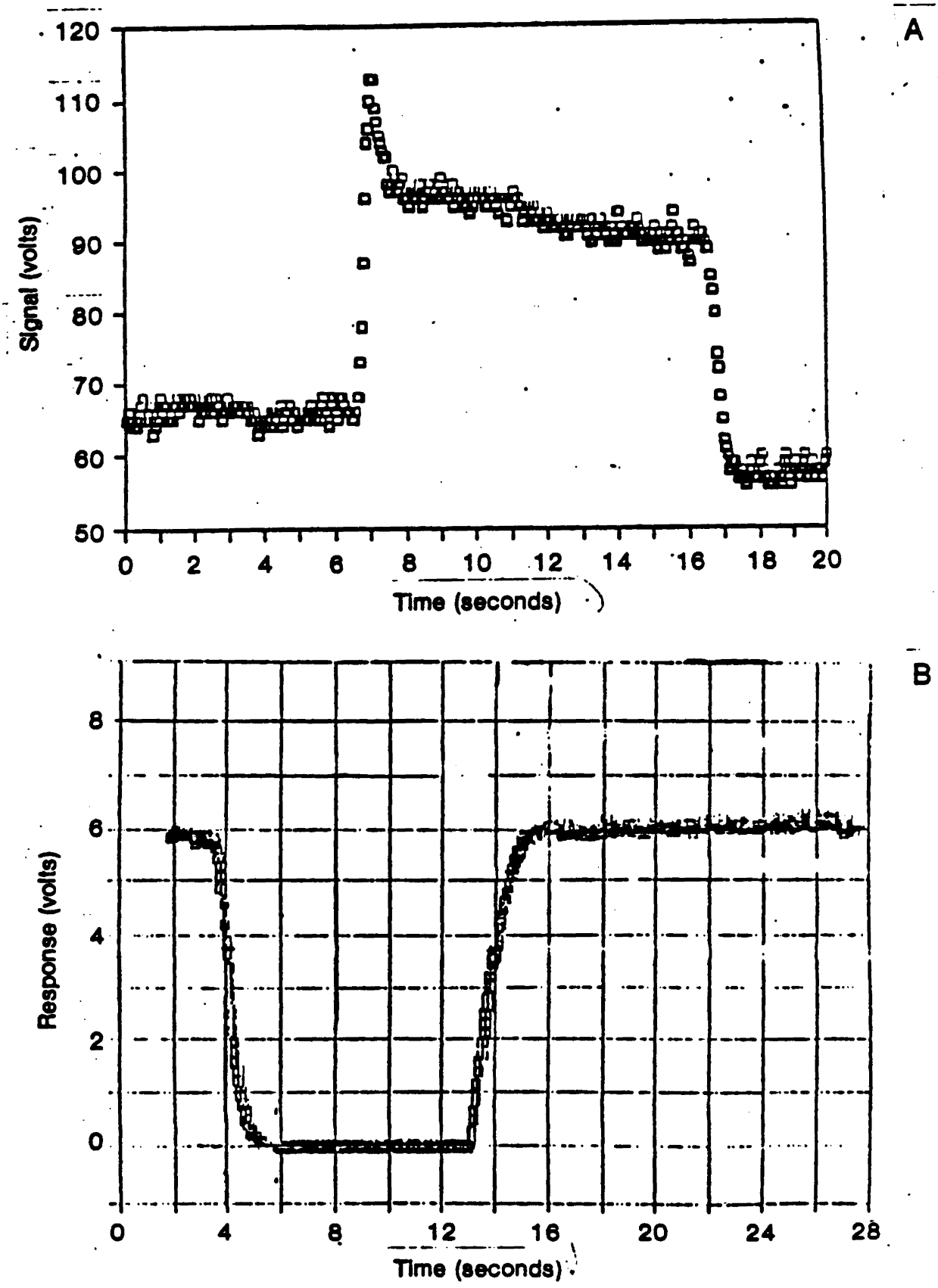
A
120
110
100
90
80
70
60
50
Signal (volts)
0
2
4
6
8
10
12
14
16
18
20
Time (seconds)
B
8
6
4
2
0
Response (volts)
0
4
8
12
16
20
24
28
Time (seconds)

FIG. A4.

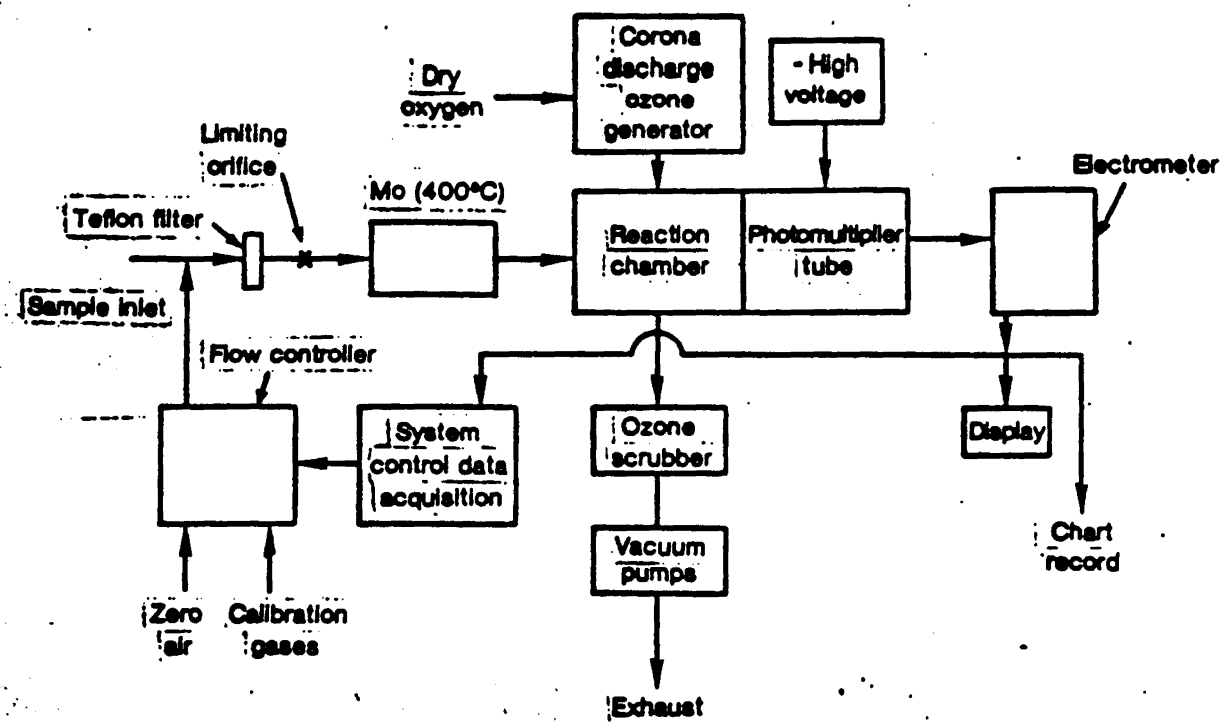
Dry oxygen
Corona discharge ozone generator
- High voltage
Limiting orifice
Mo (400°C)
Electrometer
Teflon filter
Reaction chamber
Photomultiplier tube
Sample inlet
Flow controller
System control data acquisition
Ozone scrubber
Display
Chart record
Vacuum pumps
Zero air
Calibration gases
Exhaust

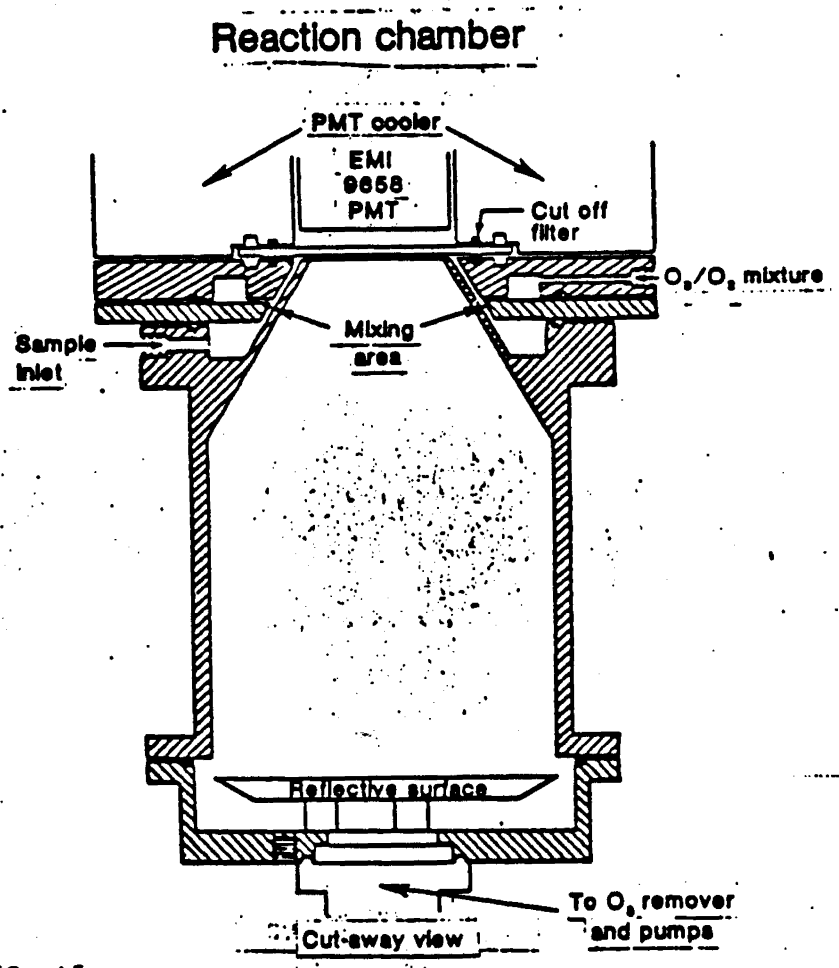
Reaction chamber
PMT cooler
EMI 9658 PMT
Cut off filter
O_3/O_2 mixture
Sample inlet
Mixing area
Reflective surface
To O_3 remover and pumps
Cut-away view

FIG. A5.

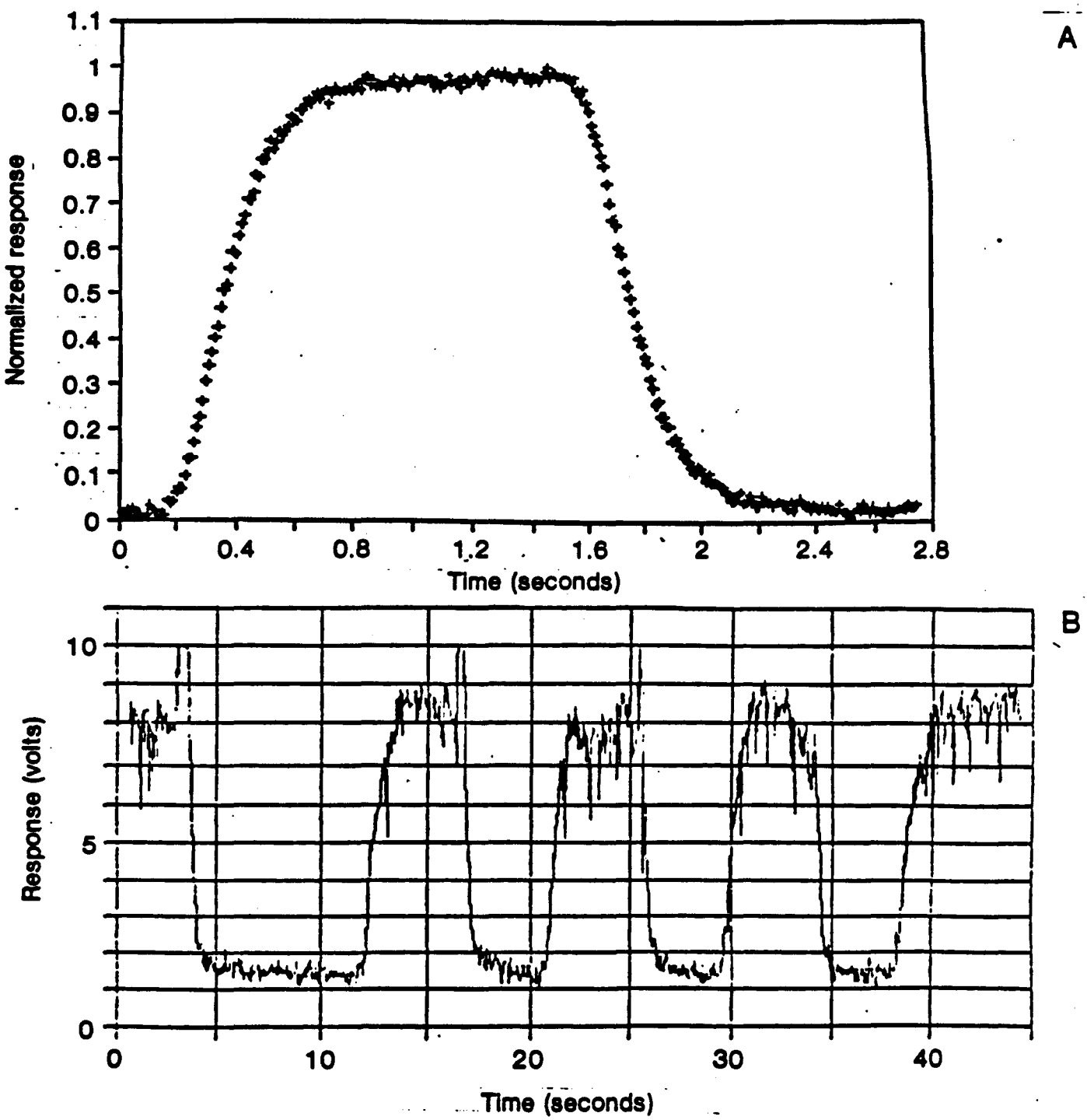
A
Normalized response
1.1
1
0.9
0.8
0.7
0.6
0.5
0.4
0.3
0.2
0.1
0
0
0.4
0.8
1.2
1.6
2
2.4
2.8
Time (seconds)
B
Response (volts)
10
5
0
0
10
20
30
40
Time (seconds)

FIG. A6.

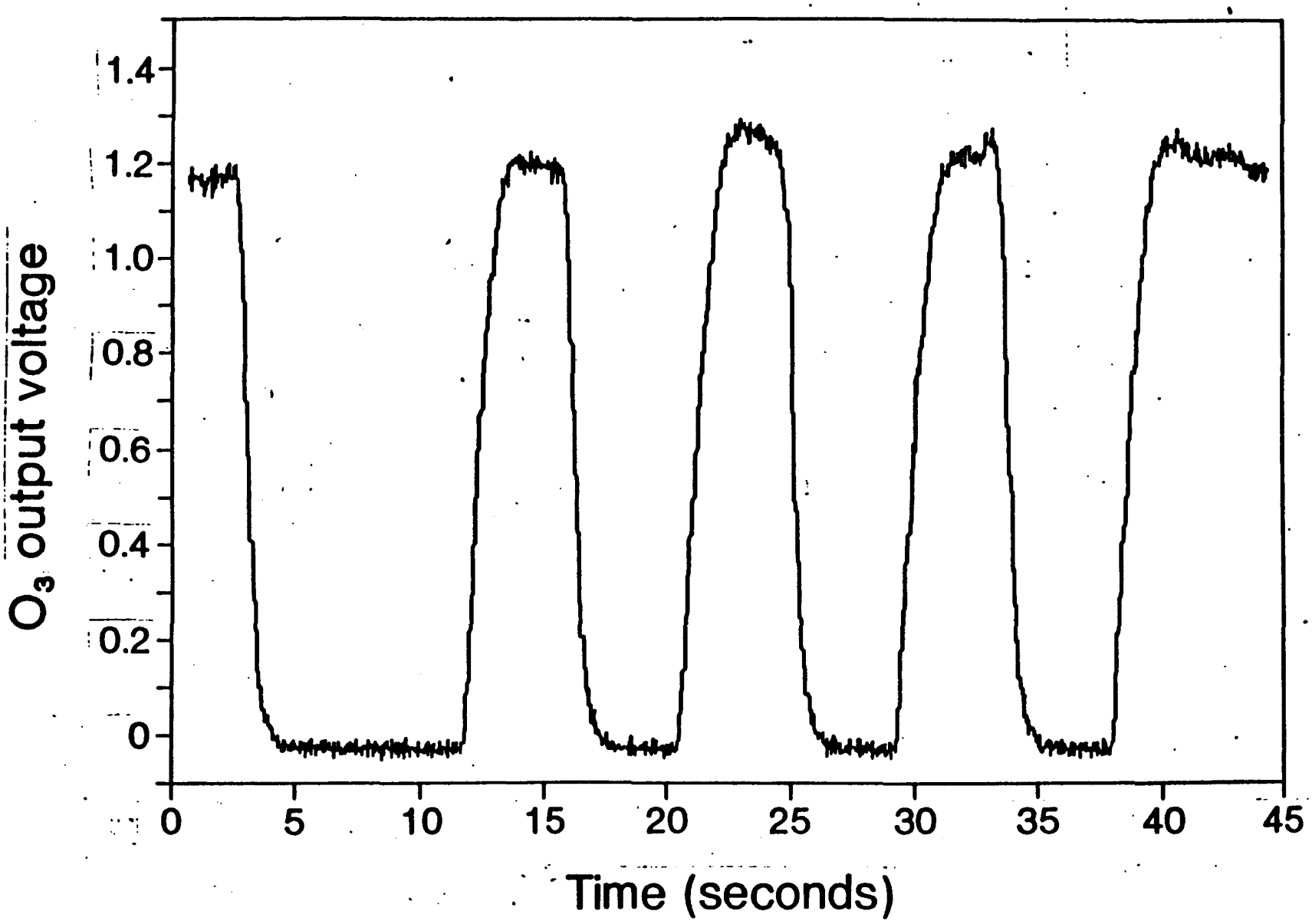
O_3 output voltage
1.4
1.2
1.0
0.8
0.6
0.4
0.2
0
0
5
10
15
20
25
30
35
40
45
Time (seconds)

FIG. B1.

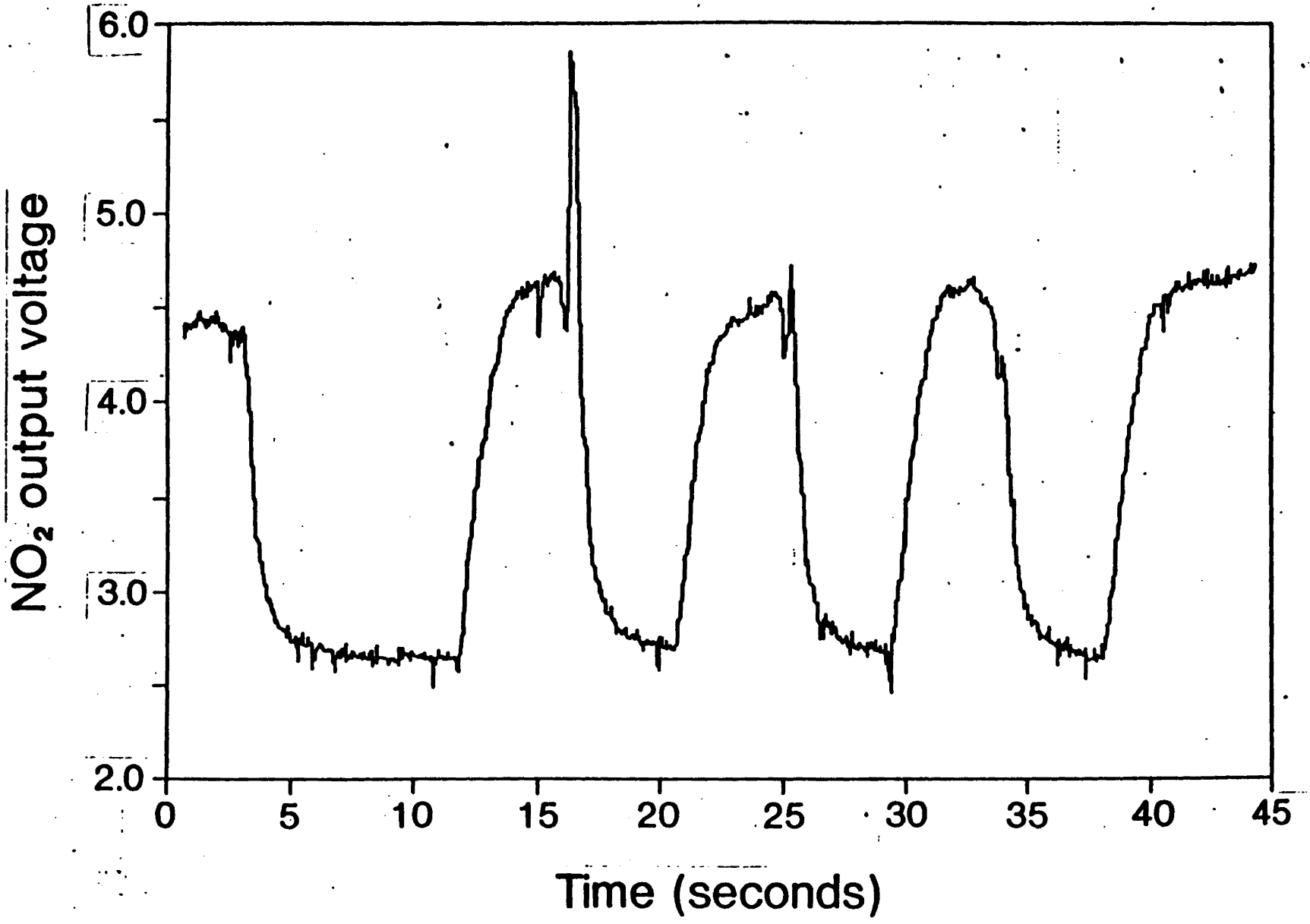
6.0
5.0
4.0
3.0
2.0
NO_2 output voltage
0
5
10
15
20
25
30
35
40
45
Time (seconds)

FIG. B2.

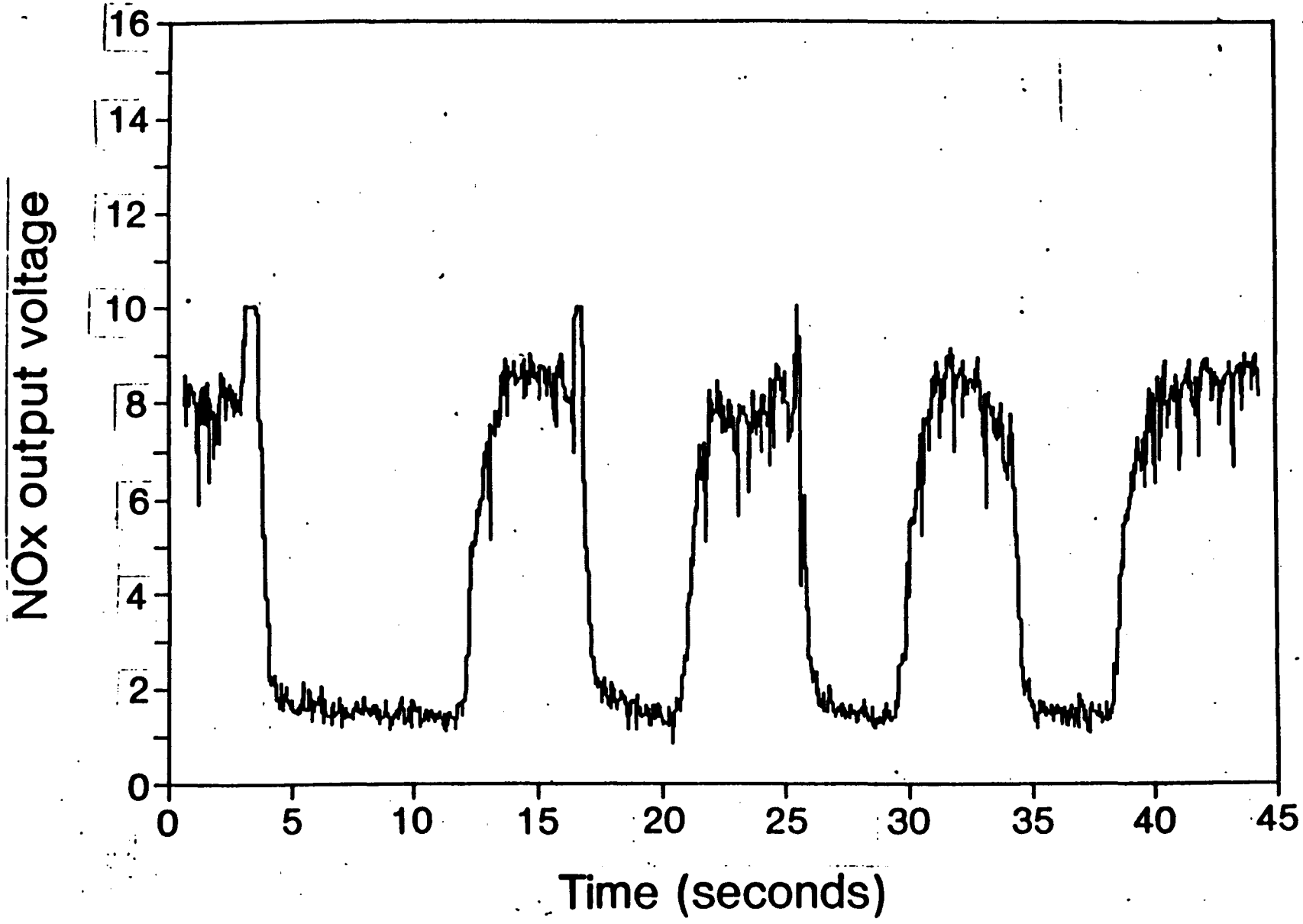
NOx output voltage
16
14
12
10
8
6
4
2
0
0
5
10
15
20
25
30
35
40
45
Time (seconds)

FIG. B3.

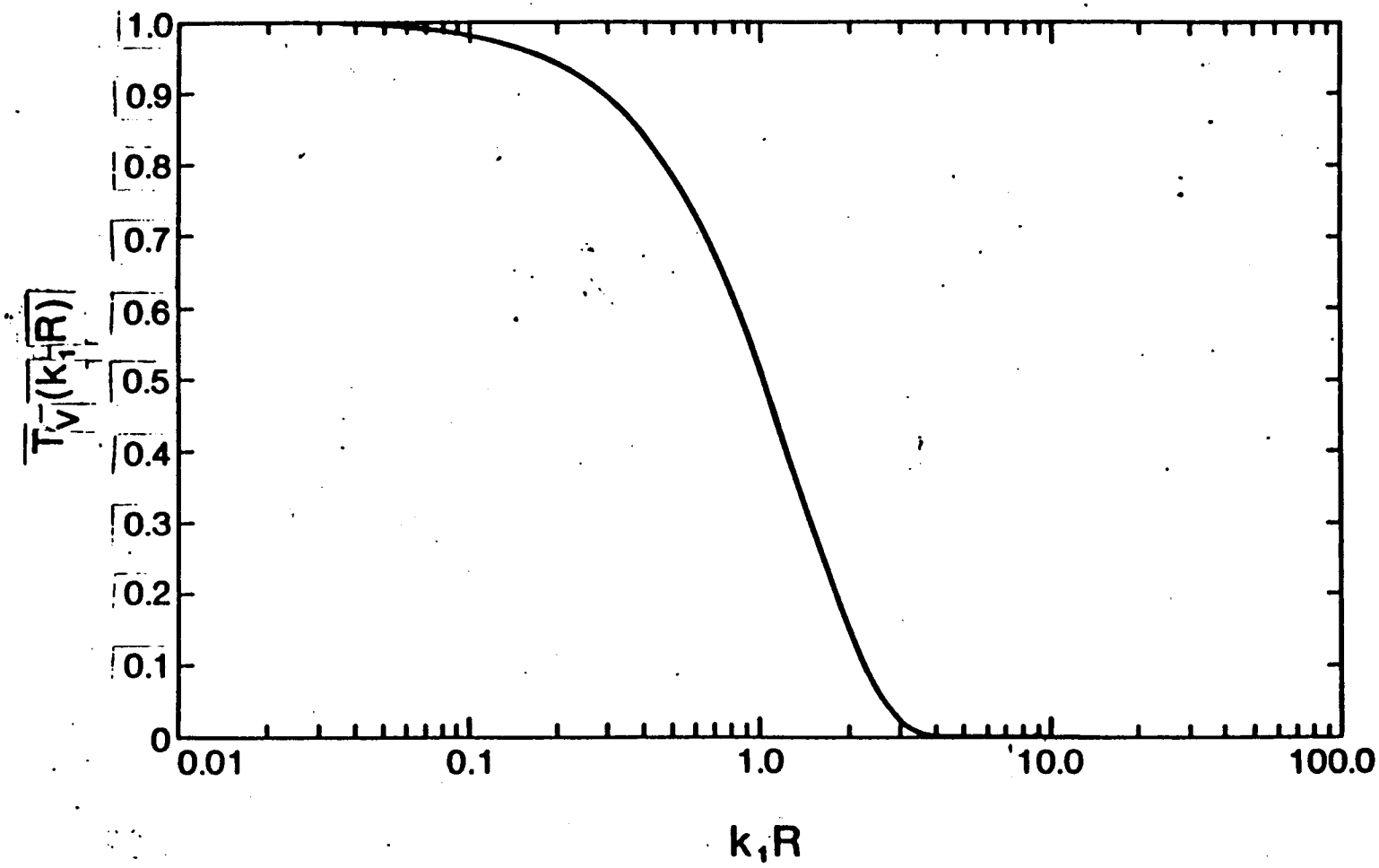
1.0
0.9
0.8
0.7
0.6
0.5
0.4
0.3
0.2
0.1
0
0.01
0.1
1.0
10.0
100.0
$\overline{T_{V_1}(k_1R)}$
k_1R

FIG. B4.

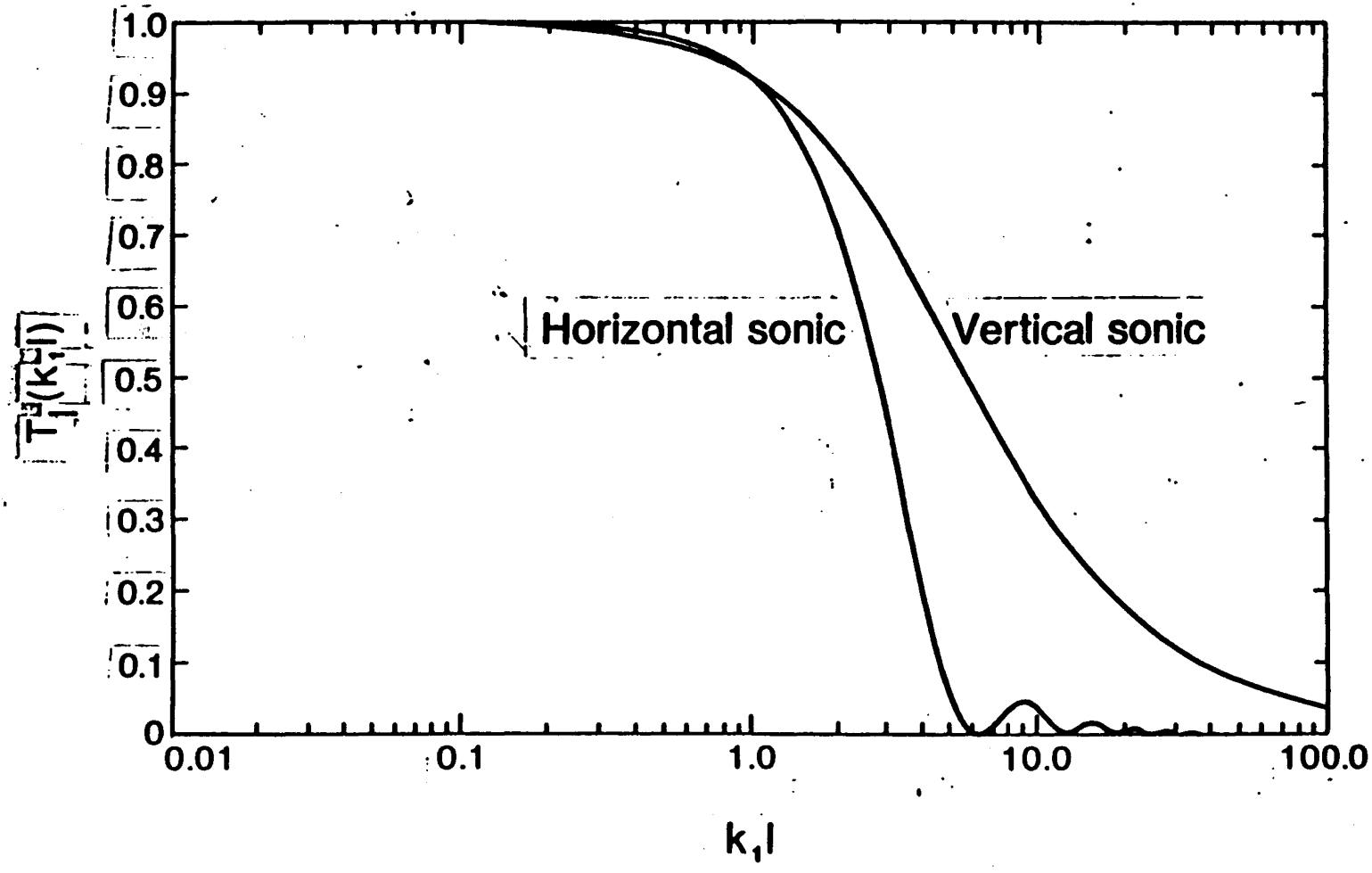
1.0
0.9
0.8
0.7
0.6
0.5
0.4
0.3
0.2
0.1
0
$|T_1^2(k_1 l)|$
Horizontal sonic
Vertical sonic
0.01
0.1
1.0
10.0
100.0
$k_1 l$

FIG. B5.

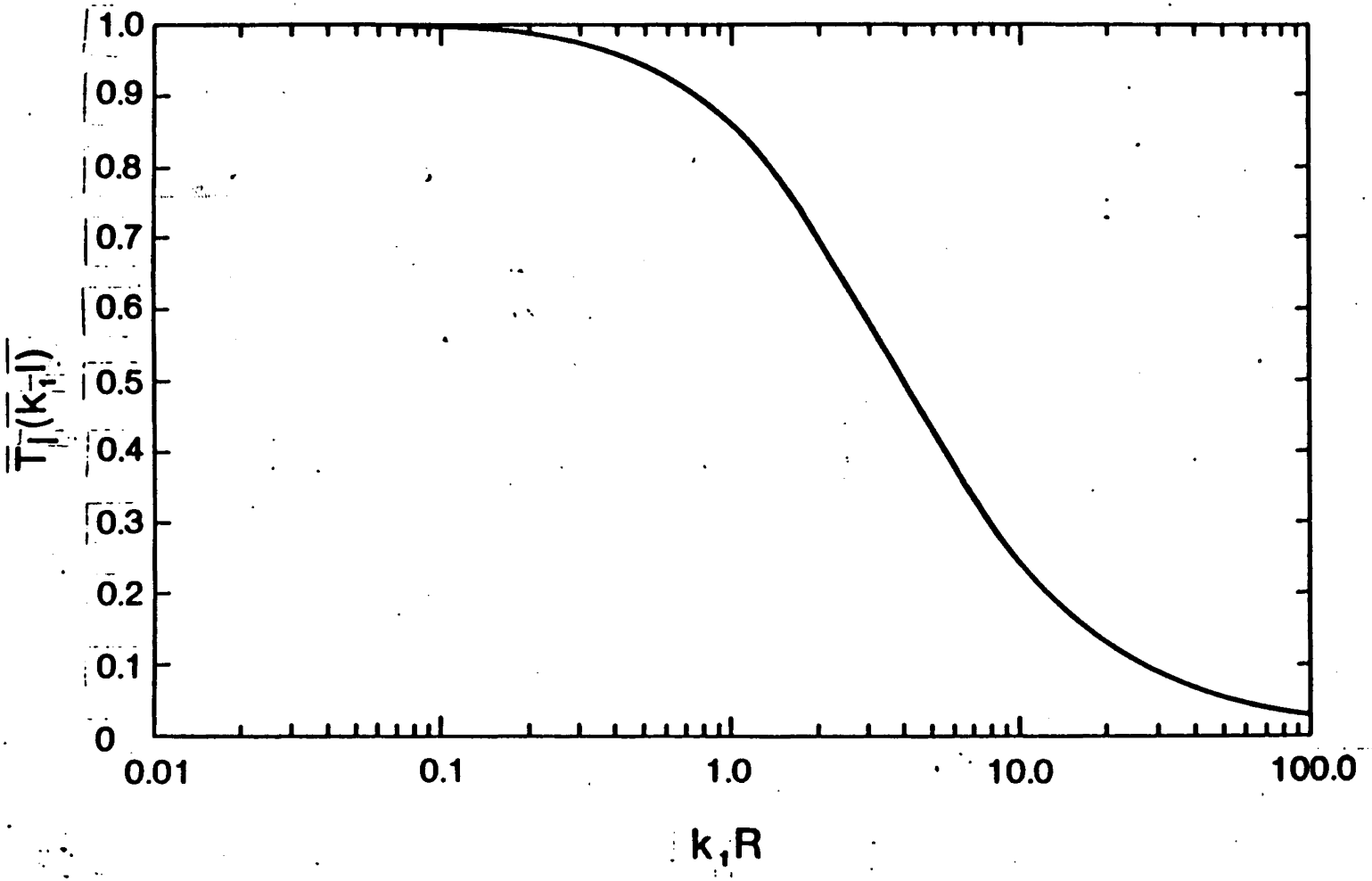
1.0
0.9
0.8
0.7
0.6
0.5
0.4
0.3
0.2
0.1
0
$\overline{T_J(k_1 l)}$
0.01
0.1
1.0
10.0
100.0
$k_1 R$

FIG. B6.

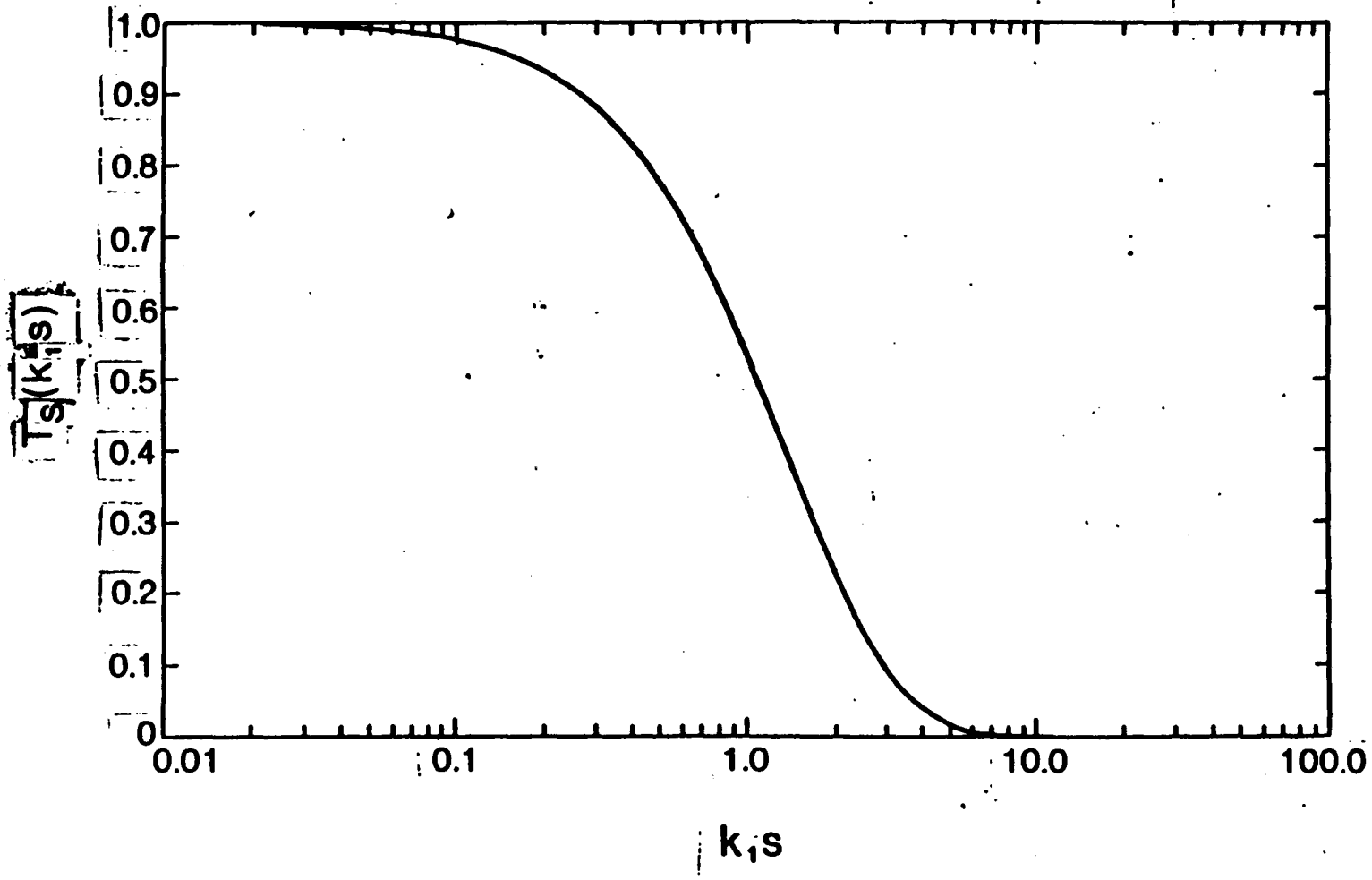

FIG. B7.

Appendix B:

Research Protocol Methodology and Quality Assurance Plans for the USFS Pawnee Eddy Correlation Dry Deposition Research Site

Research Protocol Methodology and Quality Assurance Plans for the USFS Pawnee Eddy Correlation Dry Deposition Research Site

Central Plains Experimental Range,
Pawnee Grasslands, Colorado.

USFS Rocky Mountain Forest and Range Experiment Station
240 W. Prospect
Fort Collins, CO 80526

Prepared by: D.W. Stocker
D.L. Lukens
20 November 1988

Table of Contents

Contents i

Foreword iv

1. Research Protocol Methodology

1.1. Intake System, Zero Air Supply and Calibration System 1.1 1

1.1.1. Principle of operation 1.1 1

1.1.2. Installation of the intake system 1.1 1

1.1.3. Operation and maintenance of the intake system 1.1 3

1.1.4. Zero-air production 1.1 3

1.1.5. Operation and maintenance of the zero-air system 1.1 4

1.1.6. The calibration system 1.1 4

1.1.7. Operation and maintenance of the calibration system 1.1 4

1.2. Fast Response Nitrogen Dioxide Monitor 1.2 1

1.2.1. Principle of Operation 1.2 1

1.2.2. Detection of NO_2 ..... 1.2 1

1.2.3. Installation of the NO_2 detector 1.2 2

1.2.4. Calibration and zero measurements 1.2 4

1.2.5. Operation and maintenance 1.2 6

1.3. Fast Response Ozone Monitor 1.3 1

1.3.1. Principle of operation 1.3 1

1.3.2. Detection of O_3 ..... 1.3 1

1.3.3. Installation of the O_3 detector 1.3 1

1.3.4. Calibration and zero measurements 1.3 3

1.3.5. Operation and maintenance 1.3 3

1.4. UV Photometric Ozone Analyser, TECO model 49A 1.4 1

1.4.1. Principle of operation 1.4 1

1.4.2. Installation of the UV photometric analyser 1.4 1

1.4.3. Calibration and zero measurements 1.4 1

1.4.4. Operation and maintenance 1.4 2

1.5. Data Collection and Reduction 1.5 1

1.5.1. Introduction 1.5 1

1.5.2. Installation 1.5 1

1.5.3. Operation and Maintenance 1.5 5

2. Quality Assurance Plan

2.1. Overview of Quality Assurance Procedures 2.1 1

2.1.1. Definitions 2.1 1

2.1.2. Responsibilities 2.1 2
2.1.3. Methods 2.1 2
2.1.4. Calibrations 2.1 3
2.1.5. Span Checks 2.1 3
2.1.6. Precision Checks 2.1 3
2.1.7. Systems Audit 2.1 3
2.2. Intake System 2.2 1
2.2.1. Quality Assurance Objective 2.2 1
2.2.2. Methodology 2.2 1
2.2.3. Quality Control 2.2 1
2.2.4. Data Validation 2.2 1
2.2.5. Preventative Maintenance 2.2 2
2.2.6. Corrective Actions 2.2 2
2.3. Zero-Air Supply 2.3 1
2.3.1 Quality Assurance Objective 2.3 1
2.3.2. Methodology 2.3 1
2.3.3. Quality Control 2.3 1
2.3.4. Data Validation 2.3 1
2.3.5 Preventative Maintenance 2.3 2
2.3.6. Corrective Actions 2.3 2
2.4 Calibration System 2.4 1
2.4.1. Quality Assurance Objective 2.4 1
2.4.2 Methodology 2.4 1
2.4.3. Quality Control 2.4 1
2.4.4. Data Validation 2.4 1
2.4.5. Preventative Maintenance 2.4 2
2.4.6. Corrective Actions 2.4-2
2.5. Quality Assurance Plan for Monitoring Nitrogen Dioxide 2.5 1
2.5.1. Quality Assurance Objective 2.5 1
2.5.2. Methodology 2.5 1
2.5.3. Calibrations 2.5 1
2.5.4. Quality Control 2.5 2
2.5.5. Data Validation 2.5 2
2.5.6. Preventative Maintenance 2.5 3
2.5.7. Corrective Actions 2.5 3
2.6. Quality Assurance Plan for Monitoring Ozone 2.6 1

2.6.1. Quality Assurance Objective 2.6 1
2.6.2. Methodology 2.6 1
2.6.3. Calibrations 2.6 2
2.6.4. Quality Control 2.6 3
2.6.5. Data Validation 2.6 3
2.6.6. Preventative Maintenance 2.6 4
2.6.7. Corrective Actions 2.6 4
2.7. Quality Assurance Plan for Meteological Data Collection 2.7 1
2.7.1. Quality Assurance Objective 2.7 1
2.7.2. Methodology 2.7 1
2.7.3. Calibrations 2.7 2
2.7.4. Quality Control 2.7 2
2.7.5. Data Validation 2.7 2
2.7.6. Preventative Maintenance 2.7 3
2.7.7. Corrective Actions 2.7 4
Appendix A
The Recrystallisation of Luminol
Appendix B
Data Collection Software
Appendix C
Quality Control Data Sheets
Appendix D
Front Range Ozone Monitoring Network Protocol

Foreword

The US Forest Service Rocky Mountain and Range Experiment Station acid deposition research project has established a dry deposition research site on the Central Plains Experimental Range, adjacent to and west of the Pawnee National Grasslands. Dry deposition fluxes are inferred from filter-pack measurements and are measured directly using the eddy correlation technique. Filter-pack measurements were started in June 1986 and eddy correlation experiments were first conducted in December 1986. A detailed site description and theoretical approach can be found in USFS/RMFRES Research Paper "Initial Results from the Pawnee Eddy Correlation System for Dry Acid Deposition Research" (Zeller et al., to be published in 1989).

This document and the procedures described herein are being developed to satisfy the special quality assurance requirements for conducting flux measurements by eddy correlation. On going monitoring is funded in part under EPA IA6 OW12933093-01-0.

1. Research Protocol Methodology.

1.1. Intake System, zero-air Supply and Calibration System.

D.W. Stocker
224 1179

1.1.1. Principle of operation. Owing to the highly sensitive nature of the fast response chemical instruments it is necessary to operate them in a temperature controlled instrument shelter. The shelter is set back from the tower which supports the meteorological sensors to avoid introducing anomalous turbulence to the air flows past the anemometer and ambient air intake system. The distance between the tower and shelter should be ca. 30m. to minimize the directional sector from which data must be discarded. Air is drawn from the tower to the instruments in the shelter as quickly as possible preserving the integrity of the samples i.e. the response frequency of the instruments and intake system should be at least 1 Hz. The instruments should be calibrated and zeroed through the entire intake system to accurately assess their performance. This is achieved by introducing zero-air and calibration span gases at the air inlet mounted on the tower.

1.1.2. Installation of the intake system. A continuous length of large bore Teflon tubing ($\frac{5}{8}$ inch i.d., $\frac{1}{16}$ inch wall) and a high volume pump (Fuji ring compressor) are used to continuously sample ambient air from the tower. The sample air intake mounted on the tower is at the same level as the 3-axis anemometer, about one foot away; close enough to measure the smaller eddies but far enough away so as not to disrupt the air flow past the anemometer. The possibilities of photochemical reaction occurring in the intake tube is reduced by shrouding it with black PVC irrigation pipe ($\frac{3}{4}$ inch i.d.). The air flow rate should be ca. 150-160 *l*/min, giving rise to a residence time in the intake system of ca. 2 seconds.

A filter is placed in the intake system down stream from the gas analysis instruments, between the manifold and pump to protect the pump from undue wear. This part of the installation can be checked for leaks by capping the inlet flow and attaching a flow meter to the exhaust of the pump. No flow will be observed if the system is leak tight. *Note* care is needed during this step as the pump relies on the pumped flow of air for cooling. The period of operation with the inlet capped should be kept to the

minimum to reduce the risk of damage to the pump, see manufacturers operating manual for further details. Any leaks found should be rectified.

The chemical instruments are connected to a manifold via $\frac{1}{4}$ inch Teflon tubing. The $\frac{1}{4}$ inch inlets are directed upstream, sampling from the middle of the flow in the large bore Teflon tube so that the gas samples reaching the instruments do not 'see' the manifold. The exhaust lines from the instruments are returned to the manifold downstream of the inlet ports, keeping the pressure drop across the instruments to a minimum, see Figure 1.1.1.

The manifold with connections to the instruments and the continuous

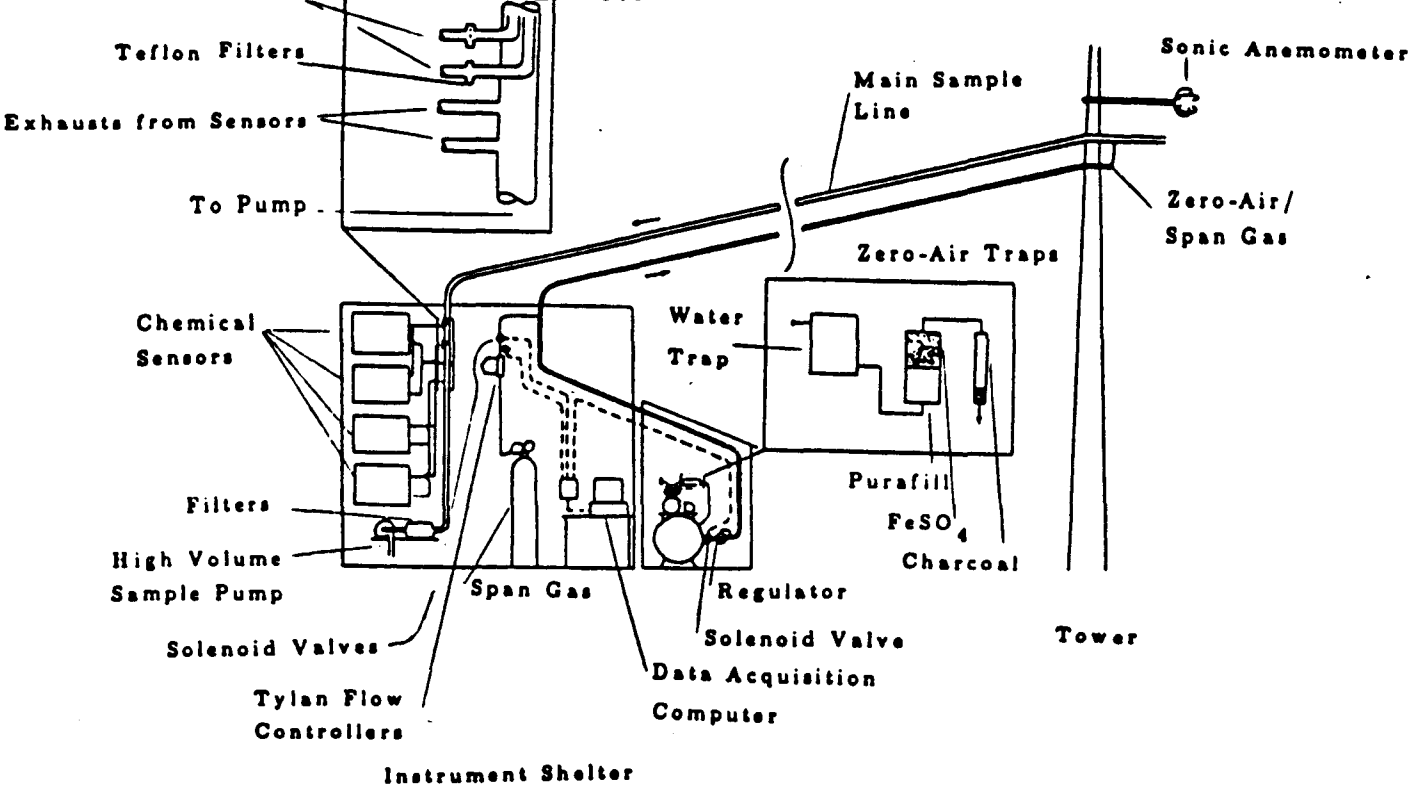

Figure 1.1.1. The intake zero-air and calibration system, showing details of the inlet manifold.

length of tubing to the tower can now be connected to the pump and filter. Once the chemical instruments have been installed (see Sections 1.2.3. and 1.3.3.) leaks around the manifold can be investigated by wafting a source of high concentration gas eg. NO_2 around the joints. Any leaks found need to be fixed.

The flowrate through the intake system is measured at the outlet of the ring compressor. Correction to the measured flow rate is made for heating of the air inside the pump. The flowrate is measured using a calibrated dry gas meter. In measuring the flows at least one revolution of the dial is required per reading, the flowrate reported being an average of at least ten readings. Except for the flow meter itself all plumbing parts necessary to attach the meter should remain in place during normal operation once the meter is removed.

1.1.3. Operation and maintenance of the intake system. Once installed the intake system should operate continuously. The flow through the system should be checked monthly and the residence time measured weekly (see Section 1.5.3.). The filters require replacement every six months, or whenever the flow through the intake system is low and the residence time exceeds three seconds. Care is needed to ensure that the filter holder is properly sealed when this is carried out.

1.1.4. Zero-air production. To ensure good quality data the response of the instruments and intake system to clean air, i.e. zero-air, is measured on a regular basis at the end of each sampling interval, every 30 minutes.

The zero-air is produced in an external shelter by passing ambient air through a series of scrubbers to fill a 30 gallon tank to 130 psi. The compressed air first passes through a refridgerated water trap (to prevent undue corrosion of the tanks), then traps containing ferrous sulphate (to convert nitrogen dioxide (NO_2) and peroxyacetyl nitrate (PAN, $CH_3COO_2NO_2$) to nitric oxide, (NO)), Purafill (to remove NO) and activated charcoal (to remove ozone and any residual nitrogen oxides, if the charcoal is brominated sulphur dioxide (SO_2) will also be removed). The series of traps is placed between the pump and the tank. The material used for construction of the zero-air lines up to the point of addition of the span gases is not critical, however, downstream of this point the zero-air lines should be of black-walled Teflon. The flow of zero-air is controlled by a solenoid valve at the exit of the tank which can be activated by the computer via a relay. The flow is regulated using a regulator also at the exit of the tank and a 55 cm length of $\frac{1}{4}$ o.d. Teflon inch tubing at the tower. The flow of air

through the zero-air line is measured with a calibrated dry gas meter on the tower, see Section 1.1.2. The zero-air/calibration line should join the main intake tube about 31 cm from the end of the intake tube to prevent entrainment of ambient air during periods of zeroing and calibration

1.1.5. Operation and maintenance of the zero-air system. The flow of zero-air must be greater than the flow of air through the intake tube. Setting the regulator on the tank to 40 psi will give a flow of zero-air of ca. 170 *l*/min. The flow rate should be checked monthly. The system should run continuously once installed. For automated zero response checks of the chemical instruments the "zero-air" solenoid valve should be under computer control.

The traps require replenishment periodically. The performance of the traps can be assessed by inspecting the stored data responses (zero-air offset values) of the instruments to zero-air stored on the computer. The response should normally be <10% of that to ambient air, unless ambient air is exceptionally clean. The spent ferrous sulphate and Purafill should be discarded, the charcoal can be reactivated by placing in an oven at 100°C. The air tanks should be drained of water weekly.

1.1.6. The calibration system. Span gases from high pressure cylinders can either be added to the zero-air flow or to the intake line upstream of the sampling manifold. All tubing should be $\frac{1}{8}$ inch o.d. Teflon with as little stainless steel as possible. Fittings can be drilled out so that tubing can be pushed all the way through, however, the stainless steel cylinder head and Tylan flow controller are unavoidable.

1.1.7. Operation and maintenance of the calibration system. The concentration of span gas can be calculated from the flowrates of zero-air and span gas. Check that the flow of zero-air is greater than the flow of air through the intake system. All periods of calibration must be clearly marked in the log book. The calibration of one instrument will effect the response of the others since all sample through a common intake line. Details of the calibration procedure for the fast response NO_2 analyser are given in Section 1.2.4; likewise the calibration procedures for the fast response ozone monitor are given in Section 1.3.4.

1.2. Fast Response Nitrogen Dioxide Monitor

D.W. Stocker
224 1179

1.2.1 Principle of operation. Nitrogen dioxide is monitored with a fast response Chemiluminescent Ambient Air Monitor (CAAM). The light produced by the reaction of nitrogen dioxide (NO_2) with the chemiluminescent reagent luminol is monitored. A solution of the chemiluminescent reagent wets a glass fiber pad at the back of the detection cell, air to be monitored flows through the cell over the wetted pad, see Figure 1.2.1. A blue sensitive photomultiplier tube (Hamamatsu R268) is used to detect the light produced, which is proportional to the concentration of reactive gas present. The photocurrent is converted to a 0-10V output signal which can be displayed on a chart recorder or computer.

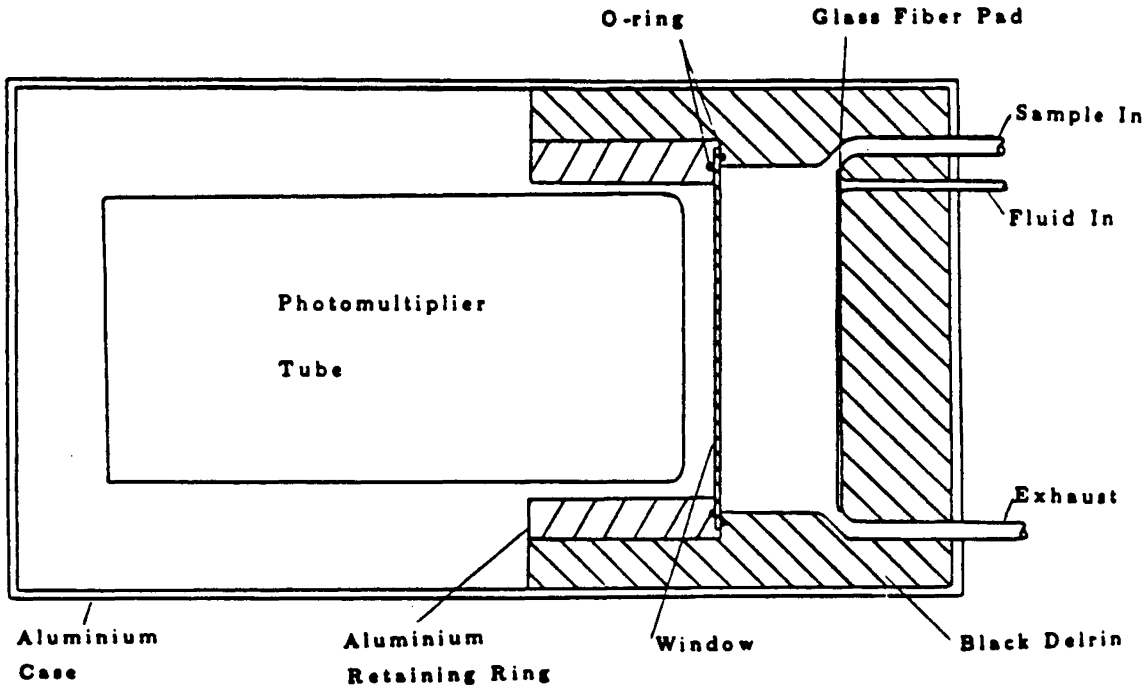

Figure 1.2.1. Design of the detection cell. The cell is machined out of black Delrin and aluminium. A glass window seals the cell. Both the cell and photomultiplier are housed in a light-tight aluminium casing.

1.2.2. Detection of NO_2. Nitrogen dioxide is monitored using a basic solution of luminol comprising;

2×10^{-4}M luminol (3-Aminophthalhydrazide)

0.05M NaOH

0.10M $NaSO_3$

0.05% v/v $(CH_3)_3COH$, t-Butyl alcohol

Luminol can be purchased from Pfaltz and Bauer, for better sensitivity the luminol needs to be recrystallised, see Appendix A for details. For field operation 10*l* of solution will last ca. 10 days. The solution is more stable when stored in a concentrated form and diluted as needed. The concentrate is prepared by dissolving;

0.354g luminol
20g NaOH
126g Na_2SO_3
5 m*l* $(CH_3)_3COH$

in 1*l* of deionized water. Dilute the concentrate with 9*l* of deionized water in the solution reservoir. The concentrated solution has a shelf life of about 3 months. Once diluted the luminol should be used immediately. It is not possible to reuse the luminol solution as it loses sensitivity.

1.2.3. Installation of the NO_2 detector. The CAAM should be mounted inside a temperature controlled shelter as close as possible to the manifold of the intake system. Connect a 24 VDC power supply to the Amphenol connection on the rear panel, see Figure 1.2.2, a 1.5 amp fuse is required. The photomultiplier tube high voltage and the voltage regulators for the pumps should already be set following laboratory trials. Refer to the operating manual if further adjustment is required.

The spent luminol solution and sample air exit together at the lower port on the front panel, and are separated by gravity in the catch bottle, see Figure 1.2.3. The catch bottle should have thick, rigid walls as the instruments are operating below ambient pressure. The separation and catch bottle should be connected between the ports marked "catch reservoir" and "return". The intake tube should be of Teflon and contain an ozone trap. Prepare an ozone trap by soaking 1g of glass wool in a solution comprising 2g of Crisco cooking oil in 20 ml of a suitable solvent eg. acetone or n-hexane. The trap should be dried overnight in a fumehood. The trap will remove >95% of the ambient ozone for at least two months.

Turn on the instrument main power on the front panel. The display will become active. Check that there are no light leaks by turning off the room lights and covering all windows. The output voltage of the instrument should remain constant. Rectify any light leaks before proceeding further. Turn on

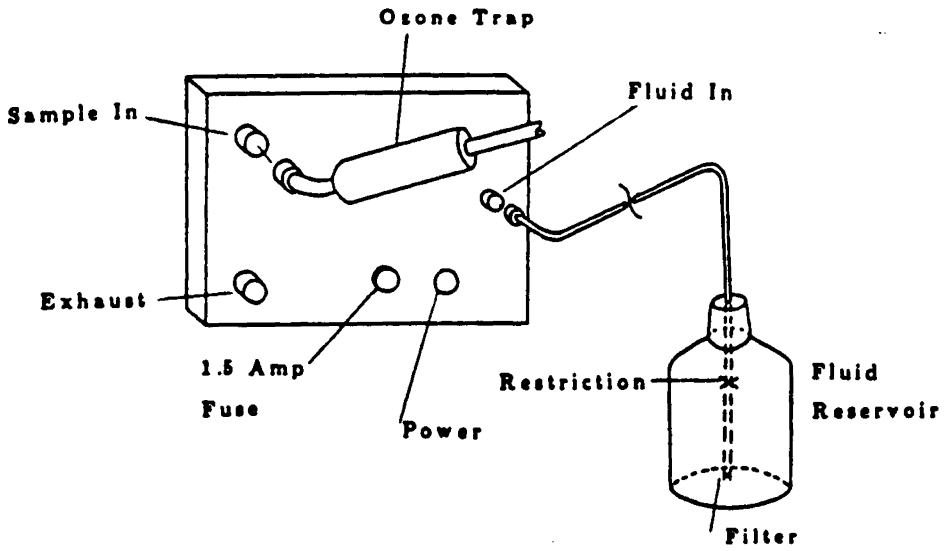

Figure 1.2.2. Diagram of the rear instrument panel and fluid line connections.

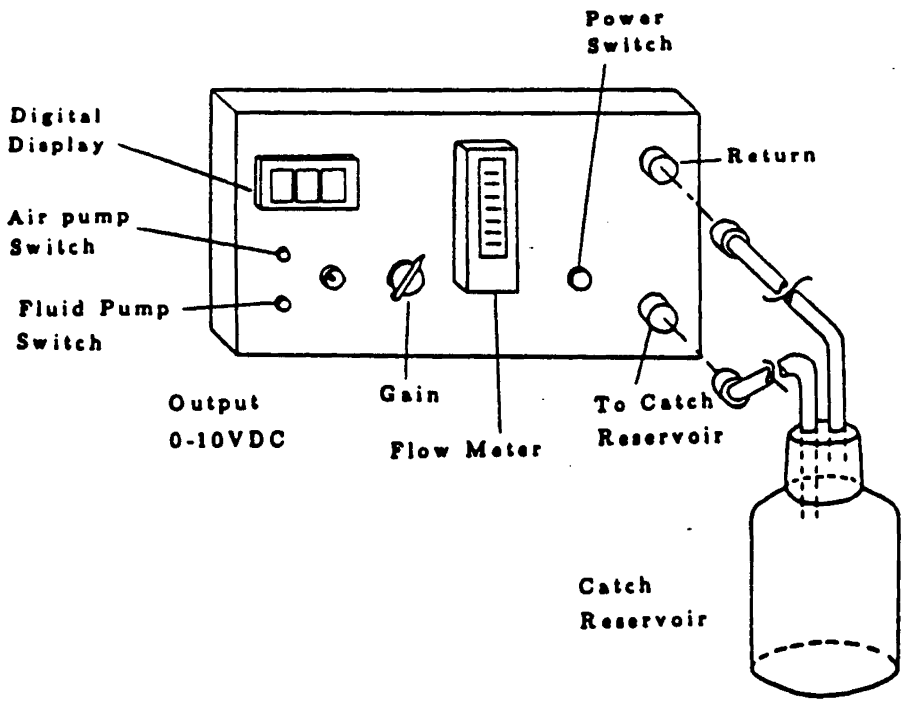

Figure 1.2.3. Diagram of the analyser front panel and catch bottle connections.

the air pump, the flow rate indicated by the flow meter on the front panel

should be 7-10 *l*/min. A leak check can be performed as a quick test of the integrity of the plumbing by capping the fluid and sample inlets to the instrument. Depending on the size of the catch reservoir 5-10 minutes may be required for the indicated flow to fall to zero. Any air leaks found must be rectified. Remove the caps if the instrument has no leaks, remove the "sample inlet" cap first. The sample inlet should now be connected to the intake manifold via a Teflon filter using a piece of $\frac{1}{4}$ inch o.d. Teflon tubing. The exhaust should also be attached to the intake system downstream of the inlet ports, see Figure 1.1.1. The type of tubing used for the exhaust is unimportant. Attaching the instrument to the intake system may increase the flowrate of gas through the instrument.

The solution reservoir should not be more than one foot below the level of the instrument[1]. Attach a piece of $\frac{1}{8}$ inch o.d. Teflon tubing from the reservoir to the port on the rear of the instrument, see Figure 1.2.2. Inside the lid of the reservoir is a length of $\frac{1}{8}$ inch o.d. tubing with a flow restricter and filter. The end of the tube should reach to the bottom of the reservoir. Turn on the fluid pump, the progress of the fluid front should be observable through the tubing. Eventually fluid will appear in the line connected to the port marked "catch reservoir" on the front panel. The fluid flow should be adjusted to ca. 0.5 ml/min using the flow restricter inside the fluid reservoir[2]. The fluid pump and lines may need priming using a syringe if dry.

Once fluid is observed in the "catch reservoir" line at least two hours should be allowed for stabilization of the instrument. Before any measurements are made the instrument response will need to be calibrated and the response to zero-air measured.

1.2.4. Calibration and zero measurements. A pulse of zero-air is sent to the tower mounted inlet of the intake system to measure the baseline

[1]This requirement is neccessary when using the gear pump. The reservoir may be placed on the floor (or where ever is convenient) if a peristaltic pump is used.

[2]The flow restricer will not be required when using a peristaltic pump. The fluid flow may stall if the instrument is disconnected from the intake system.

response of the instrument. The response of the instrument to zero-air is recorded at the beginning of each sampling period using a computer

The instrument is calibrated by adding NO_2 to the zero-air flow from a high pressure cylinder (ca. 100 ppm NO_2 in air). The concentration of NO_2 can be varied by altering the flow of NO_2 from the cylinder. The response of the instrument to five different [NO_2] in the range 2-20 ppb should be measured. This calibration procedure should be carried out quarterly. The response of these instruments has been shown to be linear for concentrations in the range 1-30 ppb following laboratory trials. A typical response is 0.2 μA/ppb.

Regular span checks should be made, at least once a week, by performing a single point calibration via the complete intake system. This measurement should be repeated until three consecutive calibration factors within 0.03 μA/ppb are obtained. The response of the instrument will decay as the luminol solution ages, a record of the decay can be obtained by performing standard additions. The apparatus used to perform these checks is currently under development. The objective is to carry out daily automated span checks by injecting 5-10 ppb of NO_2 into the intake line about 6 inches upstream of the manifold. The results of the standard additions can only be used to indicate the decay history of the luminol solution, they cannot be used as calibration factors as the combined response of the instrument and intake system has to be considered to calculate the calibration factors.

The flow of calibration gas is monitored and controlled using a calibrated Tylan mass flow controller. The flows of zero-air flow and of air through the intake system have been measured using a dry gas meter (see Section 1.1.4.). A multi-point calibration or a weekly span check is performed by first turning on the cylinder and opening the "calibrate" solenoid valve to flush the cylinder head and lines for about one hour if cylinder has not been used recently. The location of the solenoids is shown in Figure 1.1.1. While conditioning the cylinder head and calibration lines disable the auto-zero system by switching the "zero" solenoid to the "off" position. Once the lines have been flushed open the "zero" solenoid by switching solenoid to the "on" position. A stable reading should be obtained after about 3 minutes. Turn off the "calibrate" valve. The pressure on one side of the "calibrate" solenoid valve is relieved by opening the "dump"

valve for about 10 seconds to ensure that the "calibrate" valve fully closes. Allow about 30 seconds to obtain a zero reading, then close the "zero" valve and wait for the zero-air tank to refill (about 15 minutes) before repeating the measurement. When the calibration/span series is completed the "zero" and "calibrate" solenoid valves need to be switch back to computer control. Periods of manual calibration need to be clearly marked in the log book along with the results of the calibrations.

1.2.5. Operation and maintenance. Once Caam is installed and operating no further adjustment should be necessary. The following checks should be carried out every site visit, or at least weekly. The flowrate through the instrument should be at least 7 *l*/min as indicated by the flow meter on the front panel, and there should be a trickle of fluid in the "catch reservoir" line. Low air flow may indicate that the inlet line filter is dirty or that the air pump requires service. Replace the inlet filter if it is dirty. Check the voltage to the pump (24 VDC), the pump motor brushes, the fittings on the pump and the plumbing for blockages and leaks. Before turning the pump off or disconnecting any plumbing, the inlet tube should be removed from the rear of the instrument. Failure to do this will allow fluid to suck back into the inlet tubes. The open port of the inlet manifold should be plugged and the time during which the instrument is not in operation recorded in the log book as the response of other instruments may be affected. Check the level of fluid in the reservoir if there is no fluid flow, and for air leaks (fluid will not flow if the instrument is disconnected from the intake system or if there are leaks in the lines to and from the intake system), blockages in the fluid lines and air in the fluid pump. The pump may need priming.

There should be sufficient fluid in the reservoir to last until the next anticipated field visit. When replenishing the fluid reservoir, carry out a span check using the old solution as described in Section 1.2.4. Install a reservoir containing a fresh batch of luminol and recalibrate the response of the instrument. A calibration is performed by first disconnecting the Teflon intake tube at the rear of the instrument. Failure to do this will allow fluid to suck back into the inlet tubes as the top is removed from the catch bottle. Should fluid suck back, the lines can be

cleaned with deionized water. Cap the open port of the intake manifold. The time during which the instrument is not in operation should be recorded in the log book. Turn off the instrument main power. Remove the top of the catch reservoir. Prepare the fresh solution of luminol by adding the 1*l* of concentrated luminol to 9*l* of deionized water and mix well, this could be done before the old solution is calibrated to allow extra time for mixing. Once the old solution has been calibrated remove the top of the old reservoir, complete with the flow restricter and filter and place on the bottle containing the fresh luminol solution. Label the reservoir with the date and time that the solution was changed. Remove the top of the catch bottle and pour the spent luminol into the old reservoir. To reassemble the instrument, wipe the top of the catch bottle and stopper, replace the stopper and hold in place while the instrument is turned on. Cap the inlet to the instrument and check for leaks. Remove the cap if there are no leaks, inspect the inlet line filter (replace if dirty) and reattach the inlet line to the intake manifold. Allow two hours to flush the instrument before checking the span of the new solution. Neutralise the spent luminol solution with hydrochloric acid (HC*l*) before pouring down the drain.

The cell window may be dirty or the glass fibre pad may need replacement if the response of the instrument is low (<2 μA/ppb). Inspect the reaction cell by first disconnecting the inlet tube from the intake system and plugging the open port on the intake manifold. Then turn off the instrument and remove the power cord and signal leads. Disconnect the exhaust line and the fluid line to the reservoir from the rear of the instrument. Disconnect the lines to the catch bottle on the front of the instrument. It should now be possible to remove the instrument from the rack.

Remove the lid of the instrument. The reaction cell is housed in the aluminium cylinder lying across the rear of the instrument. Disconnect the air inlet line from the bulkhead fitting on the rear panel, the fluid line and the exhaust line at the union fittings. Disconnect the high voltage and signal BNC cables from the rear of the housing. Undo the strap holding the housing in place and gently lift out the housing. Before dismantling the housing find a black cloth to cover the photomutliplier tube once it has been removed.

Remove the screws from the side of the housing at the end with the electric connections to dismantle the cell. Push out the inner assembly, towards the cell end of the housing. Remove the bolts holding the stand-off legs alongside the photomultiplier tube. Carefully separate the photomultiplier tube from the cell. Cover the end of the photomultiplier immediately and put in a safe dark place. Unscrew the aluminium sleeve, *note* the sleeve is reverse threaded. The window can now be removed. Clean with deionized water and tissues. The glass fibre pad should be in good condition, i.e. it should be clean with no rips or tears. Replace the pad by prising out the retaining o-ring. Remove the old pad and clean the cell and o-rings with deionized water to remove any luminol deposits. Place a new pad in the cell (Whatman 934-AH, 3.2 cm diameter, catalogue N^{O} 1827 032), using the machined pipe fitting push the retaining o-ring in place. Care should be taken so as not to damage the pad at this stage. Assembly of the housing is the reverse of the steps to take it apart. Reinstall the instrument following the procedure in Section 1.2.3., checking for light leaks and leaks in the plumbing system.

1.3. Fast Response Ozone Monitor.

D.W. Stocker
224 1179

1.3.1. Principle of operation. Ozone is monitored with a fast response Chemiluminescent Ambient Air Monitor (CAAM). The basic design and operating principles are identical to that of the fast response NO_2 detector. Sample gas flows through a detection cell containing a pad wetted by a chemiluminescent dye, eosin-y. The light produced is detected by a photomultiplier tube, see Section 1.2.1. and Figure 1.2.1. for more details.

1.3.2. Detection of O_3. The chemiluminescent reagent used is a 1.4×10^{-3}M solution of eosin-y in a mixture comprising seven parts ethylene glycol and three parts water. 10^{-5}M copper nitrate ($Cu(NO_3)_2$) is also added to increase the sensitivity. Eosin-y can be obtained from Adrich Chemical C^o and used without further purification. The eosin-y solution can be recycled, although the response will deteriorate with use. The solution is recirculated batch-wise and is eventually replaced with fresh solution when the response is no longer acceptable.

8*l* of solution is sufficient to last ca. 10 days before recycling. The solution comprises;

5.6*l* ethylene glycol

2.4*l* water

8g eosin-y

1×10^{-2}g $Cu(NO_3)_2$, copper(II) nitrate.

Eosin-y is not very soluble, gentle heating may be necessary to get it to dissolve, however, the solution should not be boiled. The sensitivity of the solution decreases with use and will need replacement periodically, whenever the sensitivity is 80% of that when the solution was fresh.

1.3.3. Installation of the O_3 detector. Install the instrument in a rack and attach a piece of $\frac{1}{8}$ inch o.d. tubing from the reservoir to the peristaltic pump. Pour the eosin-y solution into the reservoir and check that the are no fluid leaks around the reservoir. Connect an $\frac{1}{8}$ inch o.d. tube from the peristaltic pump to the pulse dampener on the back of the instrument. The

pulse dampener is simply an inverted plastic bottle and should be level with the fluid inlet to the detection cell, see Figure 1.3.1. Attach the catch

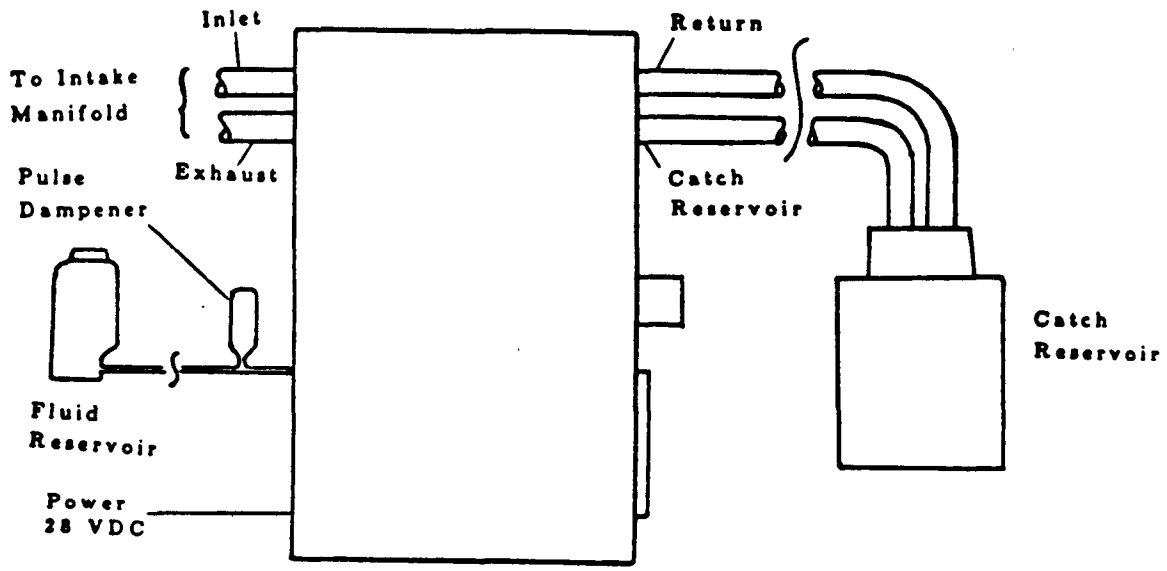

Figure 1.3.1. The installation of the fast response O_3 detector.

bottle to the outlets on the front of the instrument, see Section 1.2.3. and Figure 1.2.2. for more details. Attach a piece of $\frac{1}{4}$ inch black walled Teflon tubing to the inlet located on the rear instrument panel, see Figure 1.3.1. The tube should be sufficiently long to reach the inlet manifold.

The photomultiplier high voltage and voltage regulator for the air pump should have been set during laboratory trials. Refer to the operating manual if further adjustment is necessary. Connect a 24 VDC power supply to the rear of the instrument and turn on the main power switch on the front panel. Check for light leaks as for the fast response NO_2 detector, see Section 1.2.3. for further details. All light leaks must be rectified before proceeding.

Turn on the air pump, the flow indicated on the flow meter on the front panel should be 7-10 *l*/min. Plug the inlet and check for leaks in the plumbing, see Section 1.2.3. for further details. All leaks must be corrected before continuing. Turn on the fluid pump, the progress of the fluid front should be observable. Raise the reservoir above the level of the

instrument until the pump is primed and then lower again if the fluid flow stalls. Prime the pump by injecting dye solution into the fluid lines and pump if raising the reservoir fails to initiate the fluid flow. Fluid flow will eventually be evident in the "catch reservoir" line.

Attach the inlet line to the intake manifold via a Teflon filter. The exhaust should also be connected to the manifold downstream of the instrument's inlets, see Figure 1.1.1. Once the instrument has been connected to the intake system and a flow of eosin-y solution has been established through the detection cell allow 2 hours before checking the response of the instrument and making measurements.

1.3.4. Calibration and zero measurements. Send a pulse of zero-air to the tower mounted inlet of the intake system to zero the detector. Record the instrument's response to zero-air using a chart recorder.

The fast response ozone detector is calibrated by comparing the response of the detector with that of a U.V. photometric analyser (TECO model 49A) to ambient air. This is necessary because there are no suitable ozone sources available to permit a calibration by standard additions due to the large volumetric flows through the intake and zero-air lines. A typical response of the analyser is 0.4 μA/ppb. If possible a system will be developed to expose the instrument to a span concentration of O_3 (c.a. 80 ppb) during the automated daily span checks of the U.V. photometric analyser.

During normal operation the instrument is zeroed on a routine basis at the beginning of each sampling period. Calibration is continuous, comparing the average concentration observed by the U.V. photometric analyser with the average voltage output of the fast ozone analyser for the same period.

1.3.5. Operation and maintenance. These checks should be carried out every site visit, or at least weekly. The flowrate through the instrument should be at least 7 *l*/min as indicated by the flow meter on the front panel, and there should be a trickle of fluid in the "catch reservoir" line. Check the line filter if the air flow is low, replace if dirty. Check also the voltage to the pump (24 VDC), the pump motor brushes, the fittings on the pump and the plumbing for blockages. Before turning the pump off or

disconnecting any plumbing the inlet tube should be removed from the rear of the instrument. Failure to do this will allow fluid to suck back into the inlet tubes. The open port of the inlet manifold should be plugged and the time during which the instrument is not in operation recorded in the log book.

There should be sufficient fluid in the reservoir to last until the next anticipated field visit. The fluid should be recirculated if the fluid level is low and the sensitivity of the solution is still within the prescribed limits. This is carried out by first disconnecting the Teflon intake tube at the rear of the instrument. Failure to do this will allow fluid to suck back into the inlet tubes as the top is removed from the catch bottle. Should fluid suck back the lines can be cleaned with deionized water. Cap the open port of the intake manifold. The time during which the instrument is not in operation should be recorded in the log book. Turn off the instrument main power (and the power to the peristaltic pump if on an external switch). Remove the top of the catch reservoir. Pour the solution from the catch bottle into the reservoir if the dye is to be recirculated. Empty any remaining dye solution in the reservoir into the catch bottle if fresh dye is to be used. Fill the reservoir with the fresh solution and empty the catch bottle into the container used to carry the fresh solution to the field site. Label the reservoir with the date and time that the solution was replaced. Reassemble the instrument by wiping the top of the catch bottle and stopper, replacing the stopper and holding in place while the instrument is turned on. Cap the inlet to the instrument and check for leaks. Remove the cap if there are no leaks, inspect the line filter (replace if dirty) and reattach the inlet line to the intake manifold. Turn on the peristaltic pump and allow two hours to flush the instrument. Check the response of the instrument to a pulse of zero-air and ambient air, comparing with the response of the U.V. photometric analyser. The spent dye can be poured down the drain (it is essentially a solution of red ink in anti-freeze).

The detection cell window may be dirty or the glass fibre pad in the cell may need replacing if the response of the instrument is low and replacing the dye solution does not improve the response. See Section 1.2.5. for details of the procedure for dismantling the detection cell and replacing the pad.

1.4. U.V. Photometric Ozone Analyser, TECO model 49A.

D. Lukens
224 1343
D.W. Stocker
224 1179

1.4.1. Principle of operation. The extinction of light by ozone molecules at 254 nm in a cell filled with ambient air is compared with that in an identical cell filled with air from which ozone has been removed. The concentration of ozone (in ppb) is then calculated from Beers law, applying corrections for pressure and temperature. When operated under the conditions specified in the manfacturer's operating manual this analyser is accepted by the U.S. EPA as an equivalent method (EQOA-0880-047).

1.4.2. Installation of the U.V. photometric analyser. Install the instrument in the equipment rack. Connect a piece of Teflon tubing and a Teflon filter to the inlet and and turn on the instrument. The instrument will go through a warm-up routine. Follow the start-up procedures outlined in the operators manual.

Connect the inlet of the instrument to the intake manifold with Teflon tubing, via a Teflon filter. Plumb the exhaust to a port downstream of the instrument inlets. The ambient concentration should be in the range 20-100 ppb, more usually 40-60 ppb.

1.4.3. Calibration and zero measurements. The instrument will be calibrated using a transfer standard, TECO model 49PS. The transfer standard will be calibrated annually using either the ozone photometer at EPA Region VIII in Denver or another official EPA transfer standard.

The response of the instrument to zero-air will be measured at the beginning of each sample interval. An automated span check will be carried out daily at midnight, the apparatus necessary is currently under development.

A full calibration will be carried out quarterly. Calibration procedures outlined in the operators manual will be followed, as will quarterly performance checks.

1.4.4. Operation and maintenance. The following are to be carried out every site visit, or at least weekly; 1. Check that the air flow through the instrument is >1 *l*/min on each channel; 2. Check for sensible and consistent ozone readings when the sample is in channel A and Channel B; 3. Replace the inlet filter weekly. Refer to the operating manual for trouble-shooting procedures.

1.5. Data Collection and Reduction.

K.F. Zeller
224 1238
D.W. Stocker
224 1179

1.5.1. Introduction. Data will be collected and stored using a computer (AT&T 6300 or Compaq 386/20) with an A/D interface (12 bit Data Translations DT2805). The data will be processed continuously and summarised approximately every thirty minutes, the summarised data being stored on magnetic media. The data collection software will also control the automated zero checks (and span checks once implemented) by switching solenoid valves via relays. Data from auxillary slow response meteorological sensors (net radiometer, soil heat flux and delta temperature) will be processed and stored using a Campbell Scientific CR-21X data logger.

1.5.2. Installation. The computer, printer and A/D board should be installed according to the manufacturer's instructions. Set the clock in the computer to the current Mountain Standard Time (MST). An uninterruptable power supply should be used to power the computer, this will protect the computer during short power cuts as well as provide a measure of surge protection.

Mount the A/D junction board inside a metal box to shield the connections. The box and instrument racks should be connected to a good ground to eliminate spurious electronic noise on the data signals. Using shielded wire connect the signal outputs from the instruments to the A/D junction board. The anemometer should be connected to the first three ports, and the fast response Platinum wire thermometer to port 4. The Krypton hygrometer should be connected to port 6 and the NOx analyser (when used) to port 7. The channel numbers used from within the data collection routines, port numbers and instruments are summarised as;

Port 0	Channel 1	Anemometer w
Port 1	Channel 2	Anemometer u
Port 2	Channel 3	Anemometer v
Port 3	Channel 4	Thermometer
Port 6	Channel 7	Hygrometer
Port 7	Channel 8	NOx Analyser[3]

[3]The operation of the NOx analyser is not covered by this document.

The connections to the other ports are not critical, but should be known. Any unused ports should be grounded to reduce cross-talk between the channels.

The digital output bits of DIO port 2 are connected to the ports on the optical relay box as follows;

DIO Port 2	Bit 0	} NOx box range select[4]	
DIO Port 2	Bit 1		
DIO Port 2	Bit 2		
DIO Port 2	Bit 3	to Port 3	Zero-air On/Off
DIO Port 2	Bit 4	to Port 2	Zero-air level[5]
DIO Port 2	Bit 5	to Port 4	Intake level[6]

The data collection and reduction programme routines have been written using Basic. There are two versions of the programme in use, one to collect data from a single intake level (8 channels), the other from two intake levels (16 channels), "Duflux" and "Kzflux" respectively. Before running the programme make sure that it is configured for the current application, i.e. for a 12 bit Data Translations DT 2805 A/D board, with or without the NOx box[7], see Appendix B for a copy of the programme Duflux. A compiled version of the programme (Duflux.exe) should be in the current drive/directory. The programme name should be added to the "Autoexec.bat" file so that data collection will automatically restart after a power failure etc.

A series of data processing parameters have to be entered into the supporting initialisation data data table "Setup" (or "Kzset" for "Kzflux")before running the data collection software. This can be done using the *Notepad* in *Sidekick*. A copy of the data file is given in Appendix B. The

[4]These ports control the full scale range. The operation of the NOx analyser is not covered by this document.

[5]This port control the level to which the zero-air is sent, for use with kzflux and dual intakes.

[6]This port controls the level from which the CAAM instruments draw thier sample, for use with the programme kzflux and dual intakes.

[7]When the NOx analyser is used the subroutines selecting the full scale range should be active.

parameters are defined as;

- *Avg. time*: The number of minutes (less computational time) over which data will be collected and averaged.
- *Scan rate*: The maximun rate of data collection. (After the first sampling period this is set from within the programme).
- *# of channels*, *# of inst.* and *nprt*: These should all be 8.
- *Boom dir*: The angle by which the anemometer is mounted compared to True North.
- *Print?*: Set to 1 to obtain a hard copy of the output.
- *Disk for output*: Enter the letter of the drive to collect the data.
- *Raw Data?*: Set to 1 to collect unaveraged data. One hour of data from eight channels will require c.a. 720 kbytes of storage media.
- *Zlag*: The duration of the pulse of zero-air in minutes at the beginning of each sampling period.
- *Clag*: This parameter will be used to set the length of time required to span the instruments at the beginning of each sampling period.
- *Rlag*: The number of minutes allowed for the intake system and instruments to flush after the pulse of zero-air at the beginning of each sampling period.
- *Scrn. Scale*: The scaling factor for the visual screen output.
- *Instrument name*: A string enclosed in quotation marks identifying the instrument.
- *Lag time*: The response delay of the instrument, caused by the intake system. The lag time is determined for the fast response chemical instruments empirically, see below.
- *Calib. Coeff.*: Enter the manufacturer's calibration coefficient for the meteorological sensors and the U.V. photometric ozone analyser. Determine the calibration coefficients for the fast response chemical instruments by following the procedures outlined in Sections 1.1.7., 1.2.4. and 1.3.4.
- *Offset* : Enter the base line response of the instruments. This will either be determined at the beginning of each sampling period (for the fast response chemical instruments), or determined when the instruments are installed, calibrated, or as recommended by the manufacturer.
- *Status*: Set to 0 for each channel.

The response delay is determined by running the programme "Lgflux". This programme sends a series of square-wave pulses of zero-air to the tower mounted intake (at t=0, 11.3, 19.7 and 28.1 seconds) and records the response of the instruments. Make sure that the zero-air on/off solenoid is under computer control and type the name of the programme to run Lgflux. The first pulse lasts c.a. 8 seconds, the others c.a. 4 seconds. The programme writes the raw data to a file called "Lag". This file has to be renamed to include the extension ".prn". The renamed file is analysed using Lotus 123 or Symphony. The first eight columns of data will contain the data collected from the eight analogue input channels of the A/D board. The ninth column contains the time (seconds x 100). The lag time is found by converting the time to elapsed seconds and searching the relevant column of data until the response to the zero-air pulse is found. The lag time is the data entry in the same row of column 9. Figure 1.5.5. shows an example of the output from this programme.

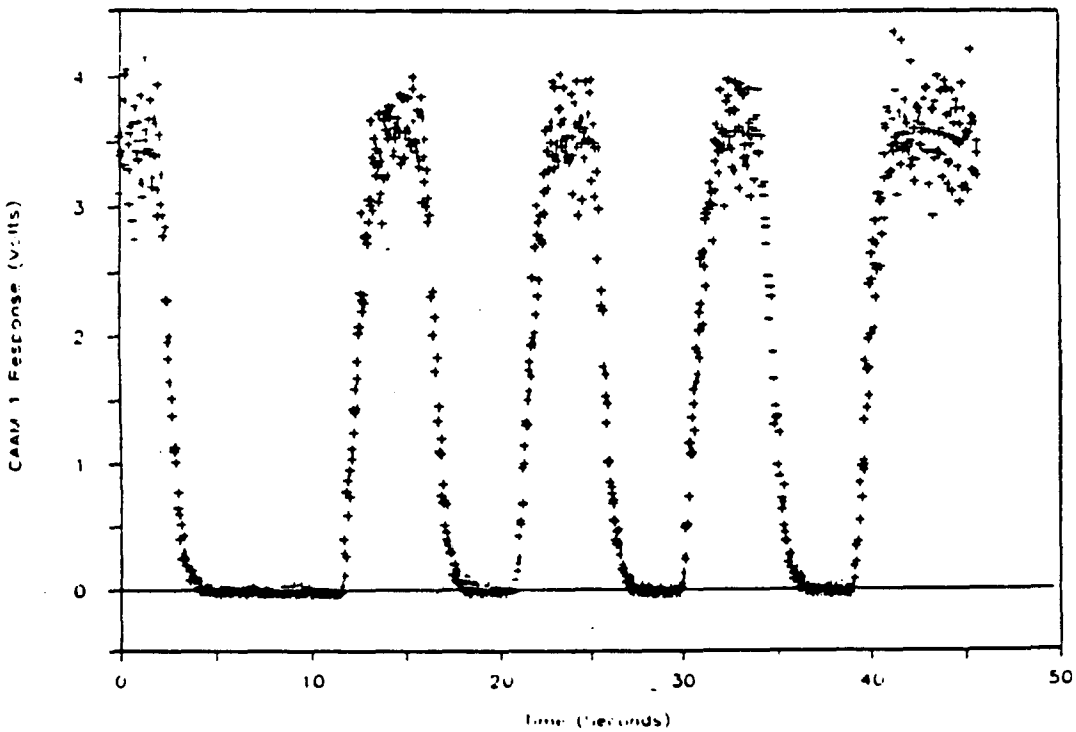

Figure 1.5.1. Determination of the response delay for CAAM 1, measuring O_3; A pulse of zero-air is sent to the tower at t=0, 11.3, 19.7 and 28.1 seconds. The response delay is 2.2 seconds.

The Campbell Scientific data logger should be installed following the manufacturer's instructions. A back-up battery pack and charger should be used to power the data logger. The processed data will be stored in an

internal memory of the data logger and copied to an external memory module; Campbell Scientific SM 64. The dip switches of the memory module should be set such that the baud rate is 1200 and the memory to fill and stop. The parity setting is not important. The module is initialised by setting right most switches on (up) and pushing the black bottom adjacent to the dip switches. After a couple of seconds the LED should light indicating that the memory is cleared and functional. When this operation is completed the switches must be turned off otherwise no data will be recorded on the storage module. The time and date of installation should be marked on the module as well as the starting memory location in the data logger (*7 on the data logger). To start data collection press *0 on the data logger. The time (MST) entered into the data logger should be the same as that in the data acquisition computer.

1.5.3. Operation and Maintenance. Initiate the programme by entering the programme name. Check that the voltages displayed across the top of the screen agree with the digital displays on the front of the instruments. The trace should show no sudden (non ambient related) deviations or spikes. The print out at the end of the sampling period should be reasonable. Check that the vertical and cross wind components are zero (w and v) and that the wind direction is reasonable. The values for the temperature sensor and chemical sensors should be within the specified ranges. The screen output should be turned off once the reasonableness of the output has been established. The screen is disabled by F6 and reactivated by F7. F2 will abort the programme and F3 will end the period and print the summarised values.

The data acquisition system should run uninterrupted once it as been set up. Each time the site is visited the data should be backed up onto a Bernoulli cartridge, without erasing the original. The Bernoulli box should be turned off when not in use. The amount of paper available to the printer should be sufficient to last until the next anticipated visit. Check the time (MST) displayed by the computer and data logger, reset if not correct. The response delay should be determined each week, as described in Section 1.5.3. and the new lag times entered in the setup data file along with any new calibration coefficients. Any changes made to the connections on the A/D junction board should also be entered in the setup data file and in the log book.

Once a week (Tuesday) the Bernoulli cartridge, Campbell Scientific storage module and the hard copy of the data will be returned to Fort Collins. To exchange the storage module simply unplug the connector from the old storage module and plug in the new one. To aid the recovery of data from the internal memory of the CR 21X, the date and time that the modules are exchanged should be marked on each module, as well as the current memory location of the data stored in the CR 21X; *7 will display the location.

A new Bernoulli cartridge and storage module will be left at the field site. An archival copy of the data, as collected, will be made on another Bernoulli cartridge and a Lotus 123/Symphony worksheet file containing one weeks worth of data (8:00 Tuesday to 7:30 Tuesday week inclusive) created. The data in this file will be subjected to intermediate data validation routines to alert the staff to possible measurement problems. This data will be processed further to include more vigorous validation routines outlined in Section 2. Thus three copies of each data file will be maintained: The original data file, unaltered as collected; the hard copy, also an original copy; and a calibrated, edited and validated data file.

2. Quality Assurance Plan

2.1. Overview of Quality Assurance Procedures. The following procedures will serve as a protocol for the collection of ambient nitrogen dioxide and ozone concentrations, and for the measurement of the fluxes of these pollutants at the USFS Pawnee Eddy Correlation Dry Deposition Research Site.

2.1.1. Definitions. The following terms will be used throughout the quality assurance document.

The *accuracy* is the extent to which a measurement or the average of several measurements recorded by a single analyser agree with the true value. The difference between the true and the measured values is defined as the error. An analyser is accurate if the error is less than the tolerance or control limit.

Calibrations are the relationships of an analyser with a recognized standard. A calibration should consist of comparisons using at least three concentrations and a zero for the chemical analysers.

A *fortnight* is two weeks.

Linearity is the maximum deviation between an actual instrument reading and the reading predicted by a straight line drawn between upper and lower calibration points.

1 ppb (part per billion) is one part per thousand million, i.e. 1 part in 10^9.

Performance Audits are an independant check of the data collection instrumentation and recording devices using standards and personnel different from those who normally operate the equipment.

The *precision* is a calculation upon population of related data points for the purpose of quantifying the degree of variability in the accuracy of the data.

Primary standards are methods, devices or materials to which all similar measurements are referenced. All calibration standards should be traceable to a primary standard maintained by the National Bureau of Standards.

Quality control procedures are designed to identify and rectify deviations from the optimum operating limits of the analysers. This is

achieved through a series of calibration span checks, zero response checks and log book maintenance.

Span checks are carried out to verify the analysers performance. A zero and a single calibration point are used, the results indicating a change in system performance.

Systems audits are regular systematic reviews of procedures, documentation and personnel that effect the collection, reduction and quality control of the data. The audits are typically performed annually by knowledgeable individuals independent of the routine operations.

Traceability refers to the written documentation supporting the accuracy relative to a primary standard.

A *transfer standard* (secondary standard) is a device, material or method which has been calibrated against a primary standard for comparison with a third device, material or method.

2.1.2. Responsibilities. The *field technician* will be responsible for the installation and maintenance of the monitoring and recording equipment. The routine quality control procedures are also the responsibility of the technician, including the precision and span checks, the multi-point calibrations and maintenance of the site log.

The *principle investigator* will oversee operations at the field site and review the calibration documents. The calculation of the precision statistics are the responsibility of the principle investigator as well as the validation, interpretation and reporting of the data. The principle investigator will review and update operational procedures and documentation as necessary.

2.1.3. Methods. The analysers will be installed and operated in a manner which is consistent with the manufacturer's recommendations and the procedures outlined in the Research Protocol Methodology in Section 1. Electrical and pneumatic connections will be of the minimum length and secured from abrasion and vibration. Signal wires will be shielded from spurious noise. Hazardous exhaust gases will be properly vented.

Calibration equipment will be maintained as required. Transfer standards will be certified and recertified as required. Primary standards will be periodically subjected to an inter-comparison

2.1.4. Calibrations. At least three concentrations and a zero are required to determine a calibration curve for an instrument. The span will be adjusted or recorded using the highest concentration. Other concentrations will be used to establish the linearity of response.

2.1.5. Span Checks. Level 1 span checks should be carried out fortnightly or weekly as appropriate, to augment the automated daily span checks (if available). The instruments will be subjected to a pulse of zero-air and a pulse of zero-air plus span gas through as much of the intake system as possible. The zero and span settings should not be altered during this procedure.

The results of the span and zero check will be recorded an the relevant data form and in the site log.

2.1.6. Precision Checks Precision checks should be carried out fortnightly or weekly as appropriate. The precision statistics will be calculated on a quarterly basis. The results of any precision check should be recorded on the relevant data form and in the site log.

2.1.7. Systems Audit. Upon request, the system will be audited by a group independent of the monitoring and flux measurement programme. The auditors will have free access to all notebooks, data sheets, and field site. They will review the day to day operation of the instruments and preventative maintenance procedures performed.

2.2. Intake System.

2.2.1. Quality Assurance Objective The intake system should not destroy the reactive gases being measured, nor should it impair the performance of the instruments. Air will be drawn from the tower to the instruments in the shelter with a residence time in the intake tube of no longer than 3.0 ± 0.1 seconds. The volumetric flowrate should be greater than 145 ± 2.0 /pm

The residence time will be measured weekly and the flowrate measured monthly.

2.2.2. Methodology. Air will be drawn from the tower to the instruments housed in the temperature controlled shelter (25±5)°C via a length of $\frac{5}{8}$ inch o.d. Teflon tubing. A high volume pump will be used to draw in the sample. The instruments will sample from a manifold constructed so that the gas samples are only ever drawn through Teflon tubes. The hot exhaust gases from the pumps will be vented outside.

2.2.3. Quality Control. The residence time (response lag of the instruments) will be measured on a weekly basis. This will be carried out following the procedure outlined in Section 1.5.3. The response lag will be entered into the setup data file for the eddy correlation data collection programme. The instrument response delay will be measured with an accuracy of 0.1s. The volumetric flow through the intake tube will be measured monthly following the procedure in Section 1.1.2. The speed of response of the instruments will be determined quarterly, by measuring the response to a pulse of zero-air.

If the delay is greater than 3.0 ± 0.1 seconds, or the flow less than 145 /pm, the filters will be changed and the pump inspected.

The results of the delay measurements and volumetric measurements will be recorded in the site log book and on the appropriate data sheets. Example quality control data sheets are in Appendix C.

2.2.4. Data Validation. All data collected when the flowrate through the tube is less than 145 /pm, or the residence time in the sample tube is greater than 3 seconds will be flagged and not included in the final data

analysis. The response time (τ) of the fast response instruments should be less than 1 second for eddy correlation studies. If the instruments have a response time greater than 1 second the data will be excluded from the flux database, but retained in the concentration monitoring database, provided all other quality assurance criteria are met.

The residence time of a sample in the intake tube should not vary greatly from week to week. If successive weekly sample delay measurements change by greater than 0.2 seconds or the response of the instruments varies by greater than 0.3 seconds over a six month period the data will be flagged for further investigation.

Data flagging will occur once the data has been returned to the data processing centre.

2.2.5 Preventative Maintenance. There will be at least one site visit per week. Routine preventative maintenance will include;

- A visual inspection of the sample intake tube and fittings, both inside the shelter and on the tower (if conditions permit). The operation of the pump and exhaust vent will also be subject to a visual inspection.
- Weekly determination of the sample residence time.
- Monthly determination of the flow rate through the intake tube.
- Maintenance of a log book and data sheets.

The intake line filters will be changed every six months, or whenever the flowrate or sample residence time are out of tolerance.

2.2.6. Corrective Actions. When ever the flow through the sample tube or the residence time of the sample in the intake tube exceed the prescribed criteria, the data collected for the purpose of eddy correlation flux measurements will not be included in the final database. The corresponding data points in the concentration monitoring database will be flagged as possibly being in error. These data points will be eliminated from the database if they cannot be verified.

All data removed from the database will be recorded in a log book.

2.3. Zero-Air Supply.

2.3.1 Quality Assurance Objective. The baseline response of the chemical instruments should be tracked to ensure the quality of the data. The response of the instruments to zero-air should be measured through as much of the intake system as possible.

2.3.2 Methodology. Zero-air is prepared by scrubbing ambient air of the trace gases to be measured, and stored in a tank for future use. The concentrations of the trace gas species in the zero-air stored in the tank should be less than 1 ppb.

Zero-air will be introduced to the intake system at the beginning of each sampling period. When a second intake level is being operated, zero-air will be introduced to the two systems sequentially. The same quality control and data validation criteria and procedures will be followed.

2.3.3. Quality Control. The response of each instrument to zero-air will be determined at the beginning of each sampling period, the results will be stored in the data files at the end of each period. The quality of the zero-air can be determined by inspecting the stored responses of the instruments to zero-air. The field site will visited at least once per week during which the zero-air system will be inspected. Specific checks include the pressure of zero-air stored in the tank (> 80 psi), pressure at the outlet during baseline response checks (42 psi) and the flowrate will be measured at the tower once per month (must be greater than the flow through the intake tube). The results of the checks and any maintenance performed will be entered in the log book and on the appropriate check sheets, see Appendix C for sample sheets.

2.3.4. Data Validation. The response of each instrument to zero-air will be recorded using the computer and A/D board at the beginning of each sampling period. The data will be collected and returned to the data management centre once a week. The data will be inspected, periods where the zero response is high (> 10% of the ambient response), or with an increasing zero response over a 12 hour period will be flagged as for further consideration

before inclusion in the final database. Data will also be flagged if the zero response of the instruments varies by greater than ± 1 ppb between successive determinations, or if the zero response increases by a factor of 2 between successive sampling periods.

The intake flow may not be overvented if the pressure inside the zero-air tank is less than 80 psi, but greater than 60 psi. In such cases the two flows should be measured, if this is not possible the data collected during these periods will be eliminated. Data eliminated if the pressure inside the tank is less than 60 psi as the intake flow will not be overvented. This will be determined from the record kept on the data sheets.

Data points removed from the database will be recorded in a log book along with the reason for removal of the data point.

2.3.5. Preventative Maintenance. There will be at least one visit to the field site per week. Routine preventative maintenance tasks to be carried out during these visits include;

- Visual inspection of the high pressure lines, fittings and electrical connections.
- A check of the pressure inside the zero-air tank and at the outlet during a zero run (80-130 psi and 42 psi respectively).
- A monthly determination of the flow rate.
- Renewal of the trap material every six months or sooner if indicated by elevated zero response of the instruments.
- Maintenance of the site log and completion of the relevant data sheet (see Appendix C).

2.3.6. Corrective Actions. Suspect data found during the data validation procedures will be removed from the database if its validity cannot be established. The data point removed will be recorded as well as the reason for its removal, the fault will be rectified in the field.

2.4. Calibration System

2.4.1. Quality Assurance Objective. The data quality relies upon frequent calibration and span checks. The calibration system adds a known concentration of span gas to the flow of zero-air, and is introduced to the instruments via as much of the intake system as possible. The concentration should be known to within ± 10% through the use of calibrated flow meters and referenced span gases.

2.4.2. Methodology. Span gas will be added to the flow of zero-air via a calibrated mass flow controller. The flow of zero-air will also be measured with a calibrated flow meter. The concentration of span gas added will be determined from the concentration of span gas in the tank and the flows of zero-air and span gas.

2.4.3. Quality Control. The span gases used should be traceable to an NBS standard. The flow meters should be calibrated to a primary standard prior to installation in the field, and recalibrated annually due to the corrosive nature of some of the span gases used. The spans of the instruments should not vary greatly, unless the instruments have been modified in any way, including chemiluminescent reagent changes. The span and calibration values recorded in the log book and on the data sheets will be evaluated every six months for reasonableness.

The field site will be visited at least once per week. During these visits the installation of the calibration equipment will be inspected, the data sheet completed (see Appendix C) and any preventative maintenance necessary will be performed. All actions will be recorded on the data sheet and in the log book.

2.4.4. Data Validation. Weekly or fortnightly span checks will be conducted for all the instruments, except for the fast response ozone monitors. For some of the instrumentation automated daily span checks will also be conducted. If it is not possible to complete the manual span checks the data will be flagged as being in possible error.

Successive spans should not vary greatly, e.g. changes of greater than

0.1 μA/ppb of NO_2 for the luminol based detector or span changes of greater than ± 6% for the U.V. photometric ozone analysers. All data found to meet or exceed these criteria will be flagged for further consideration. All data flagging will occur during the data processing stages.

2.4.5. Preventative Maintenance. The field site will be visited at least once per week. Routine preventative maintenance tasks to be carried out during these visits include;

- A visual inspection of the installation.
- Maintenance of good quality zero-air, see Section 2.3.5
- Calibration of flows as required.

All preventative maintenance tasks performed will be recorded in the site log and data sheets.

2.4.6. Corrective Actions. Questionable data values which are discovered during the data validation process will be investigated. All data that cannot be validated will be eliminated from the database.

2.5. Quality Assurance Plan for Monitoring Nitrogen Dioxide.

2.5.1 Quality Assurance Objective. Nitrogen dioxide concentrations will be collected with a precision (as a standard deviation) of less than 20% and an accuracy of ± 20% for values greater than 2 ppb. The goals may be revised and updated as experience is gained.

The precision will be checked weekly by introducing a known concentration of span gas to the instrument via the intake system. The accuracy will be determined whenever the operating conditions of the instrument are changed, eg, change of chemiluminescent reagent. A series of span gas concentrations will be introduced to the instrument, the linearity of the instrument and the accuracy (as a signed percent difference) can then be determined.

2.5.2. Methodology. The concentration of NO_2 will be monitored using a method based on the chemiluminescent reaction of NO_2 with a basic solution of luminol. The instrument will be housed in a temperature controlled environment, samples being brought to the analyser through an intake system described in Sections 1.1. and 2.2.

When possible a fast response ($NO+O_3$) chemiluminescence monitor will also be used to measure the concentration and flux of NOx and NO. The operation and quality control procedures for this instrument are not covered by the protocol set out in this document, but the data collected will be used to aid the development of the operating protocol and quality assurance procedures for the luminol based instrument.

2.5.3. Calibrations. The instrument will be calibrated after every chemiluminescent reagent change. The accuracy will be determined from these measurements. A series of five concentrations up to 80% of the upper range limit will be introduced to the instrument via as much of the intake system as possible. The response of the instrument should be linear, as demonstrated by laboratory trials for the range 1-30 pbb. The standard deviation of the slope of the linearity test will therefore give an indication of the error of measurement.

The response of the chemiluminescent reagent deteriorates as it ages.

Weekly span checks will track the change in response of the instrument. A plot of the response to the span gas versus time will give a time dependant calibration curve used to interpret the data during the final data analysis. The concentration of span gas should be in the range 5-10 ppb. The baseline response will also be measured.

The precision will also be determined weekly by measuring the response of the instrument at least four times, The precision will be calculated as;

$$\text{Precision} = \frac{\text{Calibrator Value - Instrument Average}}{\text{Calibrator Value}} \times 100$$

The precision reported will be the average of the four measurements (provided the solution lasts long enough to carry out these measurements).

An automated daily span check is currently under development. Span gas will be added to the intake system ca. 6 inches upstream of the inlet manifold. The results of these span checks will be used to track the response of the instrument as the chemiluminescent reagent ages. These checks cannot be used directly to interpret the output of the instrument as only a small portion of the intake tube is used.

2.5.4. Quality Control. The instrument zero will be checked at the beginning of each sampling interval. The span will be automatically checked daily if available. Manual span and precision checks will be conducted weekly and the accuracy determined every new batch of chemiluminescent reagent. The results will be recorded on the appropriate check sheet, see Appendix C, and in the site log.

The site will be visited at least once per week, during the visit the installation of the instrument will be inspected and the current operating conditions recorded on the appropriate data sheet. Any scheduled preventative maintenance will also be carried out during these site visits and recorded on the data sheets and in the site log.

2.5.5. Data Validation. The fast response NO_2 data will be collected using a personal computer and an A/D board at a rate of at least 10 Hz. The NO_2 concentration and flux will normally be recorded as half hour averages. The data will be retrieved once a week and returned to the data handling centre,

where the data will be validated. All data meeting or exceeding the following validation criteria will be flagged for further consideration before being included in the final data base;

- NO_2 concentration less than 0 ppb.
- NO_2 concentration greater than 100 ppb.
- Constant NO_2 concentration (± 1 ppb for more than 8 hours).
- NO_2 concentration greater than 20 ppb for 8 hours.
- NO_2 concentrations stored on the computer disagree with those recorded on the data sheets ($\Delta \geq 5$ ppb).

Data will also be eliminated if either the site log or data sheets indicate that it may be unreliable, eg. during the calibration of other chemical instruments or intake malfunction.

Data will be eliminated from the NO_2 data base if either the anemometers, chemical instruments or intake system are not functioning correctly as indicated in Sections 2.2. and 2.7. Data need not be removed from the concentration data base provided the chemical analyser and intake system are functioning correctly.

2.5.6. Preventative Maintenance. The field site will be visited at least once per week, the instrument installation will be inspected i.e. the plumbing, electrical wiring and fittings. The current operational parameters of the instrument will be recorded i.e. the flows and current output readings. Routine maintenance will be carried out as scheduled in Section 1.2.5. or whenever indicated by the span and zero checks. All preventative maintenance tasks performed will be recorded in the log book and the appropriate data sheets.

2.5.7. Corrective Actions. Any questionable data which cannot be validated will be removed from the database. The cause of the data removal will be recorded and remedied in the field.

2.6. Quality Assurance Plan for Monitoring Ozone.

2.6.1 Quality Assurance Objective. The ambient ozone concentration will be measured with a precision of 20% and an accuracy dependant on the ozone concentration;

Ozone Concentration	Accuracy
0 ppb	± 2 ppb
40-80 ppb	25%
>80 ppb	15%

using a U.V. photometric analyser. A fast response ozone analyser will be calibrated by comparing the voltage output with the concentration recorded by the photometric analyser at the end of each sampling period. The accuracy of the fast response instrument can thus be no better than the U.V. photometric analyser, the precision of the measurement by the fast response analyser will be ± 20%. The output from the fast response analyser will be used to measure the ozone flux by eddy correlation, the response time and delay should be ≤1s and ≤3s respectively. The zero response of both instruments will be recorded at the end of each sampling period. The precision will be checked once per fortnight and the accuracy once per quarter.

2.6.2. Methodology. Ozone will be measured using a U.V. photometric analyser (TECO 49A). The output from this instrument will be used to establish ambient ozone concentrations and to calibrate the output of a fast response analyser used to determine the ozone flux by eddy correlation. Both instruments will be housed in a temperature controlled shelter and draw samples from the intake system, described in Sections 1.1. and 2.2.

The operation of the U.V. photometric analyser is covered by the protocol for the Front Range Ozone Monitoring Network, see Appendix D. This protocol will be followed as closely as possible for The Pawnee Eddy Correlation Dry Deposition Research Project.

2.6.3. Calibrations The accuracy of the TECO 49A U.V. photometric analyser will be determined by introducing known concentrations of span gas (c.a. 80% of the upper range limit) to the inlet of the instrument via as much of the intake system as possible, using a transfer standard (TECO 49PS). The accuracy will be calculated quarterly from the percent difference between the concentration from the calibrator and the instrument response.

The influence of the intake system on the ozone concentrations will also be determined quarterly. This will be accomplished by comparing the response of the two U.V. photometric analysers, one sampling through the intake tube, the other drawing a sample from just outside the shelter (using the same inlet tubing and filters as when monitoring via the intake system). Over a one minute period the concentrations recorded by both instruments should be within ± 2 ppb of each other, with no systematic difference, i.e. one should not consistently read lower than the other. The test should then be repeated switching the rôles of the two analysers.

A system is currently under development to carry out an automated daily span check by generating a known concentration of ozone in zero-air using the internal ozonizer of the TECO 49A. The span gas will be introduced to the U.V. photometric analyser and fast response analyser through as much of the intake system as possible. The results will be recorded on the data logging devices. Once every two weeks a manual span check will be conducted to augment the automated span checks. The concentrations of ozone used for the span checks should be in the range 50-100 ppb, for the fast response analyser, and 400-500 ppb for the U.V. photometric analyser (this will be over range for the fast response analyser). The results of the manual span checks will be recorded on the appropriate form (see Appendix C) and in the log book for future comparison with the automated span checks. The zero response of the analysers will be recorded at the beginning of each sampling period by the data collecting devices.

After stabilising the instrument span values should be within 7% of the nominal value, and the zero response should not exceed the previous value by greater than ± 2 ppb for either instrument.

The precision will be determined once every two weeks by introducing a known concentration of ozone in the range 50-100 ppb to the inlets of both the U.V. photometric analyser and the fast response analyser, using as much

of the intake tubing as possible. The span concentration of ozone will be generated using the internal generator of the TECO 49A. The precision will be calculated quarterly, the final answer being the average of six values;

$$\text{Precision} = \frac{\text{Calibrator Value - Instrument Average}}{\text{Calibrator Value}} \times 100$$

No adjustments to the zero and span settings will be made during this process.

2.6.4. Quality Control. Once implemented the automated daily span checks will be logged by the computer or data logger and interpreted once every week at the data management centre. The automated zero response checks at the beginning of each sampling period will like-wise be interpreted weekly. The manual zero, span and precision checks will be recorded on the appropriate form and in the log book. The precision statistics will be calculated once per quarter. The instruments will be calibrated once per quarter, unless the results of the span or zero checks indicate a system malfunction.

The field site will be visited at least once per week. During each site visit a check sheet will be completed which will cover the current operating status of the instruments (see Appendix C for examples of the check sheets).

2.6.5. Data Validation. The fast response ozone data will be collected using a personal computer and A/D board at a rate of at least 10 Hz. The data from the U.V. photometric analyser will either be recorded by the computer or by a data logger. In both cases the ozone concentration (and flux) will be recorded as half hour averages. The data will be retrieved once per week and returned to the data management centre, where the data will be validated. Data validation routines will include; range testing, consistency checks, relationship tests and screening. All data meeting or exceeding the following validation criteria will be flagged for further consideration and examination;

- Ozone concentrations exceeding the limits 0 to 150 ppb
- Constant ozone concentration (± 1 ppb for more than 8 hours).
- Ozone concentration greater than 100 ppb for 8 hours.

- Ozone concentrations stored on the data logger disagree with those recorded on from the front panel meter during routine site visits. ($\Delta \geq 10$ ppb).

Data collected during periods when the instruments were being calibrated or spanned will be eliminated, as will data collected when the instruments are out of calibration as indicated by the routine span checks.

Data will be eliminated from the ozone flux database if the anemometers, chemical instruments or the intake system are not functioning correctly as indicated in Sections 2.2. and 2.7. Data need not be removed from the concentration database provided the chemical analysers and intake system are functioning correctly

2.6.6. Preventative Maintenance. The field site will be visited at least once per week, the instrument installation will be inspected, i.e. the plumbing, electrical wiring and fittings. The current operation of the instrument will be recorded, i.e. the flows and current output readings. Routine maintenance will be carried out as suggested by the manufacturer, including weekly inlet filter changes (as outlined in Sections 1.3.5. and 1.4.4.), and arising as a result of the routine span, zero and precision checks. All preventative maintenance tasks performed will be recorded in the log book and on the appropriate data sheets.

2.6.7. Corrective Actions. Any questionable data which cannot be validated will be removed from the database. The cause of the data removal will be recorded and remedied in the field.

2.7. Quality Assurance Plan for Meteorological Data Collection

2.7.1 Quality Assurance Objective. The baseline meteorological parameters to measured are: air temperature, wind speed, wind direction, net solar radiation, soil heat flux, vapour flux, heat flux, Reynolds stress and 3-axis turbulent eddies. The meteorological measurements will be used to compliment other research and monitoring efforts and to interpret and characterise atmospheric conditions during acid deposition events.

Because of the research orientation of the Pawnee site, the Quality Assurance Plan described herein is tentative and subject to revision as actual monitoring experience is gained. The quality assurance objectives are listed below;

Parameter	Method	Accuracy	Calibration Source
Wind speed Wind direction Reynolds stress	Atmospheric Tech. Inc 3-axis sonic anemometer		Sonic Chamber Alignment Calibrator
Net radiation Soil heat flux	Fritschen Q4		
Vapour Flux	Krypton crystal hygrometer		
Temperature Heat Flux Δ Temperature	AIR Inc. Pt resistance wire Thermocouple		
Data logger	AT&T 6300+ with DT 2805 Campbell CR-21X		

2.7.2. Methodology. Sensors for wind, temperature and water vapour will be mounted on the Pawnee dry deposition monitoring tower, at least 6m in height above the nearest vegetation. Data collection will be done in the adjacent instrument shelter. The net radiometer will be mounted c.a. 2m above the canopy on a frame distant from the tower so as not to introduce turbulence to steady-state the air flows nor to shadow the radiometer.

All sensors will be commercially available products of known quality and reputation. The methods of measurement are described in the respective manufacturer's manuals. The data loggers to be used are an AT&T 6300+ personal computer (or Compaq 386/20) and a Campbell Scientific 21X micro logger. Provisions for lightning protection, such as rods and spark gaps, will be incorporated into the meteorological package.

The meteorological data will be sampled automatically at at least 10 Hz for the fast response instruments and at 0.1 Hz for the slower instruments. The personal computer and data logger process the data in real time to form and subsequently store sequential 30 minute data arrays. Time and date tags are generated with each array.

2.7.3. Calibrations The meteorological instrumentation will be calibrated and zeroed upon installation in the field and the anemometers aligned. The calibration and zero measurements will be repeated quarterly, unless the results of the routine preventative maintenance checks indicate an out of tolerance condition. The instruments will also be calibrated after adjustments made or maintenance performed which could effect the performance of the instruments. The calibration factors for the sonic anemometers are a function of the ambient temperature and are therefore adjusted for temperature, using the ambient temperature measured by the platinum resistance thermometer for the previous sampling interval. The default temperature used calculate the calibration factor for the sonic anemomter, incase the temperature probe breaks, is 25°C.

The results of the calibration and zero measurements will be recorded in the site log.

2.7.4. Quality Control. The field site will be visited at least once per week, during which the status of the meteorological instruments will be examined. Regular calibration and zero checks will be conducted quarterly, or as deemed necessary following routine preventative maintenance tasks and data validation. The results of the calibration and zero checks will be entered into the log book.

2.7.5. Data Validation. Software routines in the personal computer and data logger will process the data and store the desired parameters and the associated errors once every 30 minutes.

The data review will include, when necessary, a discussion with the field technicians and data comparisons with adjacent monitoring stations located at the same field site, but operated by independant groups. The prevailing weather conditions in the region will also be taken into account.

The data validation measures will also include range testing, consistency checks and relationship testing. These measures are experimental and are subject to revision as further monitoring experience is gained. All data meeting or exceeding the following requirements will be flagged for further consideration and examination before inclusion in the final data base;

- Average wind speed less than 0 or greater than 20 ms^{-1}.
- Constant wind speed (± 1 ms^{-1}) for 4 hours.
- Mean wind direction less than 0^{o} or greater than 360^{o}.
- Constant wind direction ($\pm$ 10^{o}) for 4 hours.
- Average ambient temperature less than $-40^{o}C$ or greater than 50^{o}.
- Constant temperature ($\pm$ $1^{o}C$) for 4 hours.
- Heat flux less than -100 Wm^{-2} or greater than 500 Wm^{-2}.
- Constant heat flux ($\pm$ 1 Wm^{-2}) for 4 hours.
- Average net radiation less than -100 Wm^{-2} or greater than 900 Wm^{-2}.
- Constant net radiation ($\pm$ 20 Wm^{-2}) for 12 hours.
- Reynolds stress less than -9 m^2s^{-2} or greater than 0.1 m^2s^{-2}.
- Constant reynolds stress ($\pm$0.001 m^2s^{-2}) for more than 12 hours.
- Water vapour flux less than -100 Wm^{-2} or greater than 900 Wm^{-2}.
- Constant water vapour flux($\pm$ 10 Wm^{-2}) for 12 hours.

Data will be removed from the data base if the instruments were not operating under normal conditions, i.e. during periods of calibration or zero measurements, or during the maintenance of other instruments which could potentially interfere with the meteorological measurements (such as climbing the tower).

2.7.6. Preventative Maintenance. Site visits will be conducted at least once per week. Routine preventative maintenance tasks to be completed include a visual inspection of the tower, sensors, cabling and shelter. The operation of the data acquisition system will be inspected, as well as the wiring connections and time displayed by the data logging devices. The current sensor outputs will be examined for reasonableness and compared with the prevailing weather conditions. The hard copy of the data for previous sampling periods will be inspected for anomalous behaviour. See Section

2.7.5 for the out of tolerance conditions.

Scheduled refurbishment of the sensors will be carried out as per the manufacturer's operating instructions. All preventative maintenance tasks carried out will be recorded in the site log.

2.7.7. Corrective Actions. Any questionable data which cannot be validated will be removed from the database. The cause of the data removal will be recorded and remedied in the field.

Appendix A

The Recrystallisation of Luminol

Equipment and supplies

1 x 400 ml beaker
1 x mortar and pestle
buchner funnel and flask
filter papers
1 x aspirator
1 x ice bath
large watch glass
spatular

25g luminol
110 ml solution of 5% NaOH
ice
ether

Dissolve 25g of commercial luminol (Pfaltz and Bauer) in a solution of 5% NaOH (4.4:1 ratio of luminol:NaOH). Approximately $\frac{2}{3}$ of the luminol goes into solution in about 3 minutes. The solubility of luminol can be speeded up by using a mortar and pestle to break up the crystals. The solution should *not* be heated.

Filter into a flask (ca. 20 minutes). The filtrate is a dark green/brown. Filter as quickly as possible and immediately put filtrate on ice to recrystallise for about an hour, with scratching. There will be no crystallisation for quite a while, then within three minutes may have 95% crystals with 5% water. The crystals are light yellow/brown, and the liquid dark green/brown.

In a fumehood filter the crystals as soon as they are formed under suction until damp. Wash the crystals three times with ether, breaking up the crystals between washes. The final product should be off-white. The luminol may need to be recrystallised three times before the required purity is met.

Dry the crystals in a fumehood for several days.

```
10 ' ************************************************************************
30 ' *                              FLUX                                    *
40 ' *          A GENERAL PURPOSE EDDY-CORRELATION PROGRAM                  *
50  '*                                                                      *
60  '*                       ROBERT T. MCMILLEN                             *
70  '*          ATMOSPHERIC TURBULENCE AND DIFFUSION DIVISION               *
80  '*                    AIR RESOURCES LABORATORY                          *
90  '*         NATIONAL OCEANIC AND ATMOSPHERIC ADMINISTRATION              *
100 '*                       POST OFFICE BOX "E"                            *
110 '*                    OAK RIDGE, TENNESSEE 37830                        *
120 '*                                                                      *
130 '*           dt2805 dio for univ of Den  added Nov 86 :kz               *
140 '************************************************************************
150 '
160 ' Changing A/D from READ-A/D-IMMEDIATE to READ-A/D.        07-22-86 wrm
170 ' Speeded up A/D routines                                  07-10-86 wrm
180 ' Adding routines for Data Translation system              04-11-86 wrm
190 ' Added MACHINE%, NBITS, Error trapping. PreBasic format.  04-03-86 wrm
200 ' Modified for 12-bit                                      04-02-86 wrm
210 ' modified for dt2805 dio for univ of denver equip         10-29-86 kz
220 ' output filename.DAT modified (gosub 8000) for 123 use    May 87 kz
230 ' rapid response cosine correction (Massman's) 8100/575    May 87 kz
231 ' sonic LH coordinate correction at line 1595              Oct 28,87 kz
232 ' sonic cal updated to last period avg temp                Apr 12,88 kz
233 ' Butterworth filter added sub 8300 call line 576          Jul 17,88 kz
234 ' Krypton hygrometer lines 655 & 3775 caution on ?,avg     May 27,88 kz
235 ' Cross inlet zero added zxq to setup, jxzero, and sub6180Jul 17,88 kz
236 ' NOx Molly on/off added 771-replaced sub6800 never used   Jul 18,88 kz
237 ' ************************************************************************
238 WIDTH LPRINT 254
239     DEFINT I-P
240     DIM X(16), XA(16), XA1(16), XC(16), WX(16), X2(16), XP(16), VD(16)
245     DIM NLAG(16), LAG(16), Z(16), DEPVEL(16), YOLD(16)
250     DIM dat(8, 200), LAB$(16), ZCH(16), XAT(16), ISTAT(16)
255     DIM D(10, 10), CHAN(16), C(5000)
260     DIM WXX(16, 3), W(16, 3), WXX2(16), cal(16), XSCAL(16), xoff(16)
270     DIM XRAN$(16), X$(16)
280     DIM LOW(16), HIGH(16), datx(8,5)      'kz: datx for bw filter
281     DIM instmode(3), tvsum(8), fsd(8, 3)      'kz: ud parameter
290 '
300 ' The following function is a replacement for BASIC's STR$.
310 ' FNST$ converts from numeric to string without the leading space
320 ' STR$ includes for values >= 0.
330 '
340     DEF FNST$ (F) = RIGHT$(STR$(F), LEN(STR$(F)) + (F >= 0))
350     CR$ = CHR$(13)                  ' Carriage return.
360     ESC$ = CHR$(27)                 ' Escape character.
370 '
400     GOSUB 2740  ' Initialize files - includes read setup.
410     GOSUB 820   ' Initialize A/D.
411     GOSUB 6180  ' kz:zero inst. & establish xoff(i)
412     GOSUB 6610  ' kz:ambient air; nox run scale; adj xoff(nox) &cal: NOx, Temp
420     GOSUB 4620  ' Initialize timer.
430     GOSUB 3200  ' Initialize running means.
```

Appendix B

Data Collection Software

The following is a copy of the Basic programme to collect flux data. The version will read data from eight channels of a 12 bit Data Translations DT2805 A/D board. Routines are included to measure the base line response of the instruments at the beginning of each sampling period. An example of the "Setup" data file is also included.

```
890 '                           Flag bits.
900     CMD.WAIT% = 4                   '
910     WRITE.WAIT% = 2                 '
920     READ.WAIT% = 5                  '
930 '                           Command opcodes.
940     RESET.CMD% = 0
950     CLEAR.CMD% = 1
960     READ.ERROR.CMD% = 2
970     SET.CLOCK.CMD% = 3
971     csout = &H5                     ' kz: set dio for output
972     cdioout = &H7                   ' kz: dio output
973     dioport = 0                     ' kz: use all 16 channels for dio
980     TEST.CMD% = 11
990     READ.AD.I.CMD% = 12
1000    SET.AD.CMD% = 13
1010    READ.AD.CMD% = 14
1020    STOP.CMD% = 15
1030 '                          Stop and clear DT2805.
1040    OUT CMD.REG%, STOP.CMD%                         ' STOP A/D board.
1050    DUMMY% = INP(DATA.REG%)                         ' Read dummy value.
1060    value = CLEAR.CMD%:   GOSUB 1640                ' CLEAR A/D board.
1070    GOSUB 1170
1080    GOSUB 1100
1090    RETURN
1100 ' Set.period
1110    PERIOD! = INT(400000! / (HZ * NCH))
1120    IF PERIOD! < 2 THEN PERIOD! = 2
1130    IF PERIOD! > 65535! THEN PERIOD! = 65535!
1140    value = SET.CLOCK.CMD%: GOSUB 1640              ' Set internal
1150    value = PERIOD!:        GOSUB 1680              ' clock period.
1160    RETURN
1170 ' Set.AtoD
1180    GAIN.CODE% = 0
1190    START.CHANNEL% = 0
1200    END.CHANNEL% = NCH - 1
1210    NCONV% = NCH
1220    value = SET.AD.CMD%:  GOSUB 1640                ' Set A/D command:
1230    value = GAIN.CODE%:   GOSUB 1740                '    gain,
1240    value = START.CHANNEL%: GOSUB 1740              '    start channel,
1250    value = END.CHANNEL%: GOSUB 1740                '    end channel,
1260    value = NCONV%:       GOSUB 1680                '    # of conversions.
1261    value = csout:        GOSUB 1640                ' kz: set dio for output
1262    value = dioport:      GOSUB 1740                ' kz: first 8 dio chnls
1265    GOSUB 1900                                      ' kz: check error
1270    RETURN
1280 '                      ***************  A/D ROUTINE ***************
1290 '                              Data Translation DT2805
1300 ' AtoD
1310    XLP0 = XLP0 + 1
1320    CALL GETTIME(H%, M%, s%, T%)                    ' Read time via asm.
1330    HRS = H%                                        ' Change time values
1340    MIN = M%                                        '   to single precision
1350    SEC = s%                                        '   for later
1360    THS = T%                                        '   calculations.
```

```
440 '
450 '                    ***** BEGIN OUTER LOOP ****
460 ' Outer.loop
470     GOSUB 2030              ' Initialize graphics
480     GOSUB 4320              ' Initialize variables for loop
490 '
500 '                                                  BEGIN INNER LOOP
510 ' Inner.loop
515 if xnlp=0 then gosub 4600:STSEC = JULIAN*86400! + HRS*3600 + MIN*60 +SEC
520    KEY(2) STOP: KEY(6) STOP: KEY(7) STOP: KEY(3) STOP 'Disable print;end
530    XNPTR = XNPTR + 1                               ' Main pointer.
540 '     XPTR= XNPTR MOD XMLAG                        ' old Circular pointer.
550   xptr = CINT((XNPTR / XMLAG -INT(XNPTR/XMLAG)) * XMLAG)' Circular pointer.
570     GOSUB 1300                                    ' Take data.
575 '   gosub 8100                                    ' kz: Massman's uvw cos cor
576     gosub 8300                                    ' kz: Butterworth filter
580     IF iplt = 0 THEN GOSUB 2270                   ' Plot data. kz:iplt condition
590     IF XNPTR <= MAXLAG THEN 510
600     FOR j = 1 TO NINST
610        N = ((xptr - NLAG(j) + MLAG2) MOD XMLAG)     ' Pointer for channel.
620        X(j) = dat(j, N)                             ' Raw data.
630        XA(j) = X(j) * ALPHA + XA(j) * ALPHA1        ' Running mean.
640        XP(j) = X(j) - XA(j)                         ' Fluctuating component.
650     NEXT j
655  xp(7)=(x(7)-xa(7))/xa(7)   'vapor correction
660     FOR j = 1 TO NINST
670        XA1(j) = XA1(j) + X(j)                       ' Arithmetic average.
680        X2(j) = X2(j) + XP(j) * XP(j)                ' Variance term.
690        WXX2(j) = WXX2(j) + XP(j) * XP(j) * XP(1) * XP(1)' Error term.
700        FOR ij = 1 TO 3
710           WXX(j, ij) = WXX(j, ij) + XP(j) * XP(ij)  ' Covariance term.
720        NEXT ij
730     NEXT j
735  to3=to3+xp(4)*xp(5):qo3=qo3+xp(7)*xp(5)          'kz: additnl covar terms
740     KEY(2) ON: KEY(6) ON: KEY(7) ON: KEY(3) ON     'kz:3,6&7 added
745     XNLP = XNLP + 1
750     IF (SEC <> 0) OR (MIN MOD ATIM <> 0) THEN 520  ' Avg. period
760 '
770     GOSUB 3380                              ' Call output routine.
771     if mxq=1 then gosub 6800                ' kz: NOx to NO molly flush
772     GOSUB 6180                              ' kz: zero for new xoff(i)s
773     GOSUB 6610                              ' kz: ambient air flush
775     mctr = mctr+1                           ' kz: NO/NOx switch
780     GOTO 460                                ' Return to loop.
790 '
800 '                   ****************  A/D INITIALIZATION ***************
810 '                                  Data Translation DT2805
820 ' Init.AtoD
830 '
840 '                              Addresses & registers.
850     BASE.ADDR% = &H2EC                  ' factory address
860     CMD.REG% = BASE.ADDR% + 1           ' Command register.
870     STATUS.REG% = BASE.ADDR% + 1        ' Status register.
880     DATA.REG% = BASE.ADDR%              ' Data register (data in &  data out).
```

```
1900 ' Check.error
1910    WAIT STATUS.REG%, CMD.WAIT%
1920    STATUS = INP(STATUS.REG%)
1930    IF STATUS < 128 THEN RETURN
1940 '  IF NOT (STATUS AND &H80) THEN RETURN
1950    OUT CMD.REG%, STOP.CMD%
1960    DUMMY% = INP(DATA.REG%)
1970    value = READ.ERROR.CMD%: GOSUB 1640
1980    GOSUB 1850:   ERROR1% = value
1990    GOSUB 1850:   ERROR2% = value
2000    err.msg$ = "Fatal board error. STATUS=" + FNST$(STATUS) + " E1=" +
        FNST$(ERROR1%) + " E2=" + FNST$(ERROR2%)
2010    GOTO 6100
2020 '                          *********** GRAPHICS INITILIZATION ***********
2030 ' Init.graphics
2040    IF NCH = 0 THEN RETURN
2050    SCREEN 0, 0, 0
2060    FOR i1 = 1 TO NCH + 1
2070       Z(i1) = (180 / NCH) * (i1 - 1 / 2) + 20
2080    NEXT i1
2090    SCREEN 2, , 0, 0: CLS
2100    GET (100, 0)-(107, 199), C    'define screen layout:C
2110    GOSUB 2140
2120    RETURN
2130 '                          *********** ININTIALIZE SCREEN **************
2140 ' Init.screen
2150    IF NCH = 0 THEN RETURN
2160    XOLD = 0
2170    PUT (0, 0), C, PSET
2180    X = 0
2190    FOR i1 = 1 TO NCH
2200       LINE (550, Z(i1))-(600, Z(i1))
2210       IN = Z(i1) * (25 / 200)
2220       LOCATE IN, 78
2230       PRINT MID$(LAB$(i1), 1, 2);
2240    NEXT i1
2250    RETURN
2260 '                          ***************** PLOT DATA ****************
2270 ' Plot.data
2280    IF NCH = 0 THEN RETURN
2290    X = X + 1
2300    IF X MOD 8 = 0 THEN PUT (X, 0), C, PSET
2310    IF X MOD 10 = 0 THEN LOCATE 25, 1: PRINT HRS; MIN; SEC; XNLP;: LOCATE 1,
        :1: FOR i1 = 1 TO NPRT: PRINT USING " ###.###"; dat(i1, xptr); : NEXT i1
        'used for digital screen display of data
2320    FOR i1 = 1 TO NCH
2330       YN = -(dat(ZCH(i1), xptr) - XA(ZCH(i1))) * XSCAL(i1) + Z(i1)
2340       LINE (XOLD, YOLD(i1))-(X, YN)                ' Plot data.
2350       YOLD(i1) = YN                                ' Save point.
2360    NEXT i1
2370    XOLD = X
2380    IF X > 630 THEN GOSUB 2140
2390    RETURN
2400    END
```

```
1370    IF IRAW = 0 THEN GOTO 1420
1380    HRMIN = HRS * 100 + MIN
1390    SECTH = SEC * 100 + THS
1400    LSET HRMIN$ = MKI$(HRMIN)
1410    LSET SECTH$ = MKI$(SECTH)
1420 ' Read.loop
1430                            ' Read data from A/D.
1440    WAIT STATUS.REG%, CMD.WAIT%                     ' Wait until ready.
1450    OUT CMD.REG%, READ.AD.CMD%                      ' Send READ A/D cmd.
1460    FOR JKL = 1 TO NINST
1470       WAIT STATUS.REG%, READ.WAIT%                 ' Wait for READY &
1480                                                    '    DATA OUT READY.
1490       LOW(JKL) = INP(DATA.REG%)                    ' Read Low byte.
1500       WAIT STATUS.REG%, READ.WAIT%                 ' Wait for READY &
1510                                                    '    DATA OUT READY.
1520       HIGH(JKL) = INP(DATA.REG%)                   ' Read High byte.
1530    NEXT JKL
1540    FOR JKL = 1 TO NINST
1550       value = HIGH(JKL) * 256 + LOW(JKL)           ' Convert to 16 bit.
1560       IF value > 32767 THEN value = value - 65536! ' Correct sign.
1570       dat(JKL, xptr) = value / 204.8 - 10          ' Data Translation ONLY.
1580       IF IRAW = 1 THEN LSET XRAN$(JKL) = MKI$(value)' Write raw data.
1590    NEXT JKL
1595       dat(3, xptr) = -dat(3, xptr)           'sonic LH correction for v
1600    GOSUB 1900
1610    IF (IRAW = 1) AND (ical = 0) THEN PUT #3  'use to store raw data:ical=0
1620    RETURN                                          '     = run mode
1630 '
1640 ' Send.cmd          VALUE contains command byte.
1650    WAIT STATUS.REG%, CMD.WAIT%
1660    OUT CMD.REG%, value
1670    RETURN
1680 ' Send.data                VALUE contains 2 byte argument.
1690    HI.BYTE = INT(value / 256)                      ' MSB.
1700    LO.BYTE = value - HI.BYTE * 256                 ' LSB.
1710    value = LO.BYTE: GOSUB 1740                     ' Send LSB.
1720    value = HI.BYTE: GOSUB 1740                     ' Send MSB.
1730    RETURN
1740 ' Send.byte                VALUE contains 1 byte argument.
1750    IF value > 255 THEN 1680                        '# > 1 byte.
1760    WAIT STATUS.REG%, WRITE.WAIT%, WRITE.WAIT%      ' Wait for READY.
1770    OUT DATA.REG%, value                            ' Send byte.
1780    RETURN
1790 ' Receive.data             Returns data in VALUE.
1800    GOSUB 1850: LO.BYTE = value             ' Read LSB.
1810    GOSUB 1850: HI.BYTE = value             ' Read MSB.
1820    value = HI.BYTE * 256 + LO.BYTE                 ' Convert to 16 bit.
1830    IF value > 32767 THEN value = value - 65536!    ' Correct sign.
1840    RETURN
1850 ' Receive.byte             Returns byte in VALUE.
1860    WAIT STATUS.REG%, READ.WAIT%                    ' Wait for READY &
1870                                                    '    DATA OUT READY.
1880    value = INP(DATA.REG%)                          ' Read byte.
1890    RETURN
```

```
3030    IGAIN = 1
3040 '  DIVISOR=3276.8                      ' Divisor for 16 bit calibration.
3050 '  IF NBITS=12 THEN DIVISOR=204.8      ' Divisor for 12 bit calibration.
3060 '  XFACTOR=1/(IGAIN*DIVISOR)           ' Compute calibration.
3070    PI# = 3.1415927#
3080    radtdeg = 360 / (2 * PI#)
3090 '
3100    FOR I = 1 TO NPRT
3110       NLAG(I) = HZ * LAG(I)
3120       IF NLAG(I) > XMLAG THEN NLAG(I) = XMLAG
3130       IF NLAG(I) > MAXLAG THEN MAXLAG = NLAG(I)
3140    NEXT I
3150    FOR I = 1 TO NCH
3160       ZCH(I) = I
3161        FOR ij = 0 TO 2                 ' kz: initial fsd array
3162        fsd(I, ij) = 1!                 ' kz:       "
3163        NEXT ij                         ' kz:       "
3170    NEXT I
3171    instmode(0) = 3: fsd(8, 0) = 1E-09    ' kz: initial zero scale
3172    instmode(1) = 4: fsd(8, 1) = 1E-08    ' kz: initial cal  scale
3173    instmode(2) = 4: fsd(8, 2) = 1E-08    ' kz: initial run  scale
3174    jzero = 8: jxzero = 16: jmrun = 0     ' kz: operation modes dio
3175    mctr = 0                              ' kz: initial NOx molly set
3176    xal4 = 15                             ' kz: initial Temp for sonic cal
3180    RETURN
3190 '                          *************** INITIALIZE R. MEANS *********
3200 ' Init.means
3210    GOSUB 2030
3220    xptr = 1
3230    NLP1 = 600                          'kz changed to get more time
3240    FOR I = 1 TO NLP1
3250       ALPHA = 1 / I
3260       ALPHA1 = 1 - ALPHA
3270       GOSUB 1300
3280       FOR j = 1 TO NINST
3290          XA(j) = XA(j) * ALPHA1 + dat(j, 1) * ALPHA
3300       NEXT j
3310       GOSUB 2270
3320    NEXT I
3330    FOR I = 1 TO NINST
3340       PRINT "avg"; I; XA(I)
3350    NEXT I
3360    RETURN
3370 '                          ************** OUTPUT MODULE ***************
3380 ' Output
3390  IF IPRT = 1 THEN LPRINT CHR$(27) + "C" + CHR$(22);'formlength to 22 lns
3400  SCREEN 0, 0, 0
3410  OFFLIN$ = "*****************************************************************"
3420  NINTERVALS = NINTERVALS + 1
3430    IF MIN = 60 THEN MIN = 0: HRS = HRS + 1
3450    IF HRS = 24 THEN HRS = 0: day = day + 1: JULIAN = JULIAN + 1: lsthr = 0
3455    IF HRS = 0 AND lsthr = 23 THEN day = day + 1: JULIAN = JULIAN + 1
3460    SEC1 = JULIAN * 86400! + HRS * 3600 + MIN * 60 + SEC + THS / 100
3465    TIM$ = RIGHT$(STR$(HRS), 2) + ":" + RIGHT$(STR$(MIN), 2) + ":" +
        RIGHT$(STR$(SEC), 2)
```

```
2410 '                          ********** CLOSE AND END ***************
2420 ' Close.end         ' key F2 subroutine
2430    PRINT "Closing and ending"
2440    CLOSE
2450    END
2455 iplt = 1: RETURN  'screen on/off
2456 iplt = 0: RETURN  '    "
2460 '                          ********** ERROR ROUTINE ****************
2470 ' Error
2480    SOUND 100, 1
2481    ecount = ecount + 1
2482    IF ecount > 50 THEN GOTO 2540
2490    OPEN "ERROR.LOG" FOR APPEND AS #2
2500    'PRINT ERR, ERL
2510    PRINT #2, ERR, ERL, TIME$, DATE$, XSEC          'kz:xsec added
2520    PRINT #2, XOLD, YOLD(I), Y, YN, I, Ninst, il,j,ij
2530    CLOSE #2
2540    IF ERR = 24 OR ERR = 25 THEN IPRT = 0'24:device timeout; 25:device fault
2545    ecount = 0
2550    RESUME 770                                      'kz:770 replaced NEXT
2560 '
2730 '                          ************ INITIALIZATION ROUTINE *********
2740 ' Init.files
2750    CLS
2760    KEY OFF
2770    KEY(2) ON
2780    ON KEY(2) GOSUB 2420    'stop and end
2781    ON KEY(6) GOSUB 2455    'screen display on
2782    ON KEY(7) GOSUB 2456    '   "       "    off
2783    ON KEY(3) GOSUB 3380    'output routine
2790    TIMCONST = 200          'Set time constant for digital filter.
2800    GOSUB 5480              'Read setup file.
2810    IF IPRT = 1 THEN LPRINT ESC$ + "C" + CHR$(22); 'Set frmlngth to 22 lines
2820    MON = VAL(MID$(DATE$, 1, 2))
2830    day = VAL(MID$(DATE$, 4, 2))
2840    YER = VAL(MID$(DATE$, 7, 4))
2850    JULIAN = INT(30.57 * MON) + day - 30    ' Calculate Julian date.
2860    IF MON > 2 THEN JULIAN = JULIAN - 2
2870    IF YER / 4 = INT(YER / 4) AND MON > 2 THEN JULIAN = JULIAN + 1
2880    PRINT "JULIAN DATE IS "; JULIAN
2890    DSNAME$ = "F" + MID$(DATE$, 9, 2) + FNST$(JULIAN) + MID$(TIME$, 1, 2)
2900    dsname1$ = DSK$ + ":" + DSNAME$ + ".DAT"
2910    DSNAME2$ = DSK$ + ":OUTPUT.SAV"
2920    PRINT "DATASET NAME IS "; dsname1$
2930    OPEN dsname1$ FOR APPEND AS #1
2940    CLOSE #1
2950    OPEN DSNAME2$ FOR APPEND AS #2
2960    CLOSE #2
2970    IF IRAW = 1 THEN GOSUB 4180
2980    GOSUB 5670
2990    ITIM = 100 / HZ
3000    RMEAN = 1
3010    XMLAG = 200
3020    MLAG2 = XMLAG * 5
```

```
3910 '                          ********** PRINT SUBROUTINE ************
3920 ' Print
3930    PRINT #1, TIT0$; "  "; dsname1$
3940    PRINT #1, "Rotation angles: Theta(rad) Eta(rad) Beta(Deg)"
3950    PRINT #1, USING "                ###.###  ###.###  ###.###"; theta, eta,
        beta
3960    PRINT #1, TIT$
3970    FOR I = 1 TO NINST
3980       IF ISTAT(I) = 1 THEN PRINT OFF$: PRINT #1, OFF$: GOTO 4000
3990       PRINT #1, USING IMAGE$; LAB$(I), XA1(I), XAT(I), WXX(I, 1), X2(I),
           DEPVEL(I), WXX2(I), cal(I), xoff(I)
4000 ' Pr.next.i
4010    NEXT I
4020    PRINT #1, "Rey. Str.    U-bar      U*       Cd       Corr.Coef.
        Wind Dir.    T'03'     q'03' (03volts!)"
4030    PRINT #1, USING IMAGE2$; R, U, U2, C8, C9, WNDDIR, to3, qo3:
4040    PRINT #1, "WXX MATRIX"
4050    FOR j = 1 TO 3
4060       PRINT #1, j;
4070       FOR I = 1 TO 8
4080          PRINT #1, USING "##.##### "; WXX(I, j);
4090       NEXT I
4100       PRINT #1, ""
4110    NEXT j
4111    PRINT #1, "fsd NOx settings: zero   span   run  jmrun   sonic cal at:";
        XA14;" deg C"'kz
4112    PRINT #1, "                "; fsd(8, 0); fsd(8, 1); fsd(8, 2);jmrun 'kz
4113    PRINT #1, " "
4120    RETURN
4130 '                          ************* SETUP RAW DATA **************
4140 ' Raw.check
4150    IF IRAW = 0 THEN RETURN
4160    CLOSE #3
4170 '                          ***** RAW DATA SETUP INITIAL ENTRY POINT *****
4180 ' Init.raw
4190    DSNAM$ = "F" + MID$(DATE$, 4, 2) + MID$(TIME$, 1, 2) + MID$(TIME$, 4, 2) +
        ".RAW"
4200    N = INSTR(1, DSNAM$, " ")
4210    IF N <> 0 THEN DSNAM$ = MID$(DSNAM$, 1, N - 1) + MID$(DSNAM$, N + 1,
        LEN(DSNAM$) - N)
4220    DSNAME3$ = DSK$ + ":" + DSNAM$
4230    OPEN "R", #3, DSNAME3$, 22              ' Only for raw data: rand acc file
4240    FIELD #3, 2 AS HRMIN$, 2 AS SECTH$ ' alloc space in rand buffer
4250    OFFSET = 4
4260    FOR I = 1 TO 8
4270       FIELD #3, OFFSET AS DUMMY$, 2 AS XRAN$(I)
4280       OFFSET = OFFSET + 2
4290    NEXT I
4300    RETURN
4310 '                          ********** LOOP INITIALIZATION *************
4320 ' Init.loop
4330    GOSUB 4140
4335    ical = 0                  ' kz: indicates mode: 0=run; 1= zero or cal
4340    MAXLAG = 0
```

```
3470    XSEC = SEC1 - STSEC
3475    if xsec=0 then goto 400        'restart data collection
3480    HZ = XNLP / XSEC
3485    lsthr = HRS
3490    OPEN DSNAME2$ FOR APPEND AS #2                'output.sav
3500    PRINT #2, "DATA ";
3510    PRINT #2, TIM$; DATE$; HZ; XNLP; ALPHA; ISYSTAT;
3520    FOR I = 1 TO NINST
3530       XA1(I) = XA1(I) / XNLP                     'arith. avg.
3540       WXX2(I) = WXX2(I) / XNLP                   'error term
3550       X2(I) = X2(I) / XNLP                       'variance
3560       PRINT #2, XA1(I); XA(I); X2(I); WXX2(I); ISTAT(I);
3570       FOR j = 1 TO 3
3580          WXX(I, j) = WXX(I, j) / XNLP
3590          PRINT #2, WXX(I, j);
3600       NEXT j
3610    NEXT I
3615     to3=to3/XNLP: qo3=qo3/XNLP                  'kz: additional covar
3620    PRINT #2, "": CLOSE #2
3630    WNDDIR = ATN(XA1(3) / XA1(2)) * radtdeg
3640    IF XA1(2) < 0 THEN WNDDIR = WNDDIR + 180
3650    WNDDIR = BOOMAZIM - WNDDIR + 45        'kz: remove 45 deg for Gill uvw
3660    WNDDIR = (WNDDIR + 360) MOD 360
3670    GOSUB 4810     '   covariance rotation
3680    FOR I = 1 TO NINST
3690       XAT(I) = XA1(I)                            'keep volts @ xat
3700       XA1(I) = cal(I) * (XA1(I) - xoff(I))
3710       WXX2(I) = cal(1) ^ 2 * cal(I) ^ 2 * WXX2(I)
3720       X2(I) = cal(I) ^ 2 * X2(I)
3730       FOR j = 1 TO 3
3740          WXX(I, j) = cal(I) * cal(j) * WXX(I, j)
3750       NEXT j
3760       IF I > 3 AND XA1(I) <> 0 THEN DEPVEL(I) = WXX(I, 1) / XA1(I)
3770    NEXT I
3774    if xat(7)<0 or xat(7)=0 then xat(7)=0.00000000001
3775    xa1(7)=(log(xat(7)*1000)-log(1800))*cal(7)     'KH20 cal
3776    to3=to3*cal(4)*cal(5): qo3=qo3*cal(7)*cal(5)
3780    R = WXX(1, 2): U = XA1(2): V = 0
3790    U2 = ABS(R) ^ .5
3800    C8 = (U2 / U) ^ 2
3810    C9 = R / (X2(2) ^ 2 + X2(3) ^ 2) ^ .5
3820    TIT0$ = TIM$ + "  " + DATE$
3830    TIT0$ = TIT0$ + "  freq. = " + MID$(STR$(HZ), 1, 6) + "  # of scans = " +
        STR$(XNLP)
3840    IMAGE$ = "\        \ ###.####  ###.####   ###.######    ###.####
        ##.####  ##.######  ###.### ###.###"
3850    IMAGE2$ = "###.###    ####.##   ####.###   ##.#####   ##.#####    #####.#
        ##.#####  ##.#####"
3860    TIT$ = "Quantity     Average   Raw Avg.   Covariance    Variance    Vd
        Error      cal      xoff"
3870    OPEN dsname1$ FOR APPEND AS #1: GOSUB 8000: CLOSE #1
3880 'OPEN "O",#1,"SCRN:":GOSUB 3920 :CLOSE #1
3890    IF IPRT = 1 THEN OPEN "O", #1, "LPT1:": GOSUB 3920: CLOSE #1
3900    RETURN
```

```
4950    X2(2) = WXXB(2, 2)
4960    WXXB(3, 3) = WXX(3, 3) * CE ^ 2 + WXX(2, 2) * SE ^ 2 - 2 * WXX(2, 3) * CE
         * SE
4970    X2(3) = WXXB(3, 3)
4980    WXXB(1, 1) = WXX(1, 1) * CT ^ 2 + WXX(2, 2) * ST ^ 2 * CE ^ 2 + WXX(3, 3)
        * ST ^ 2 * SE ^ 2 + 2 * WXX(1, 2) * CT * ST * CE + 2 * WXX(1, 3) * CT *
        ST * SE + 2 * WXX(2, 3) * ST ^ 2 * CE * SE
4990    X2(1) = WXXB(1, 1)
5000    WXXB(1, 2) = WXX(1, 2) * CE * (CT ^ 2 - ST ^ 2) - 2 * WXX(2, 3) * CT * ST
        * SE * CE + WXX(1, 3) * SE * (CT ^ 2 - ST ^ 2) - WXX(2, 2) * CT * ST *
        CE ^ 2 - WXX(3, 3) * CT * ST * SE ^ 2 + WXX(1, 1) * CT * ST
5010    WXXB(2, 1) = WXXB(1, 2)
5020    WXXB(2, 3) = WXX(2, 3) * CT * (CE ^ 2 - SE ^ 2) + WXX(1, 3) * ST * CE -
        WXX(1, 2) * ST * SE - WXX(2, 2) * CT * CE * SE + WXX(3, 3) * CT * CE * SE
5030    WXXB(3, 2) = WXXB(2, 3)
5040    WXXB(1, 3) = WXX(1, 3) * CT * CE - WXX(1, 2) * CT * SE - WXX(2, 3) * ST *
        (CE ^ 2 - SE ^ 2) + WXX(2, 2) * ST * CE * SE - WXX(3, 3) * ST * CE * SE
5050    WXXB(3, 1) = WXXB(1, 3)
5060    FOR j = 4 TO 8
5070       WXXB(j, 2) = WXX(j, 2) * CT * CE + WXX(j, 3) * CT * SE + WXX(j, 1) * ST
5080       WXXB(j, 3) = WXX(j, 3) * CE - WXX(j, 2) * SE
5090       WXXB(j, 1) = WXX(j, 1) * CT - WXX(j, 2) * ST * SE - WXX(j, 3) * ST * SE
5100    NEXT j
5110    FOR I = 1 TO 8
5120       FOR j = 1 TO 3                    ' SIN(BETA)
5130          WXX(I, j) = WXXB(I, j)
5140       NEXT j
5150    NEXT I
5160    XA1(1) = WB
5170    XA1(2) = UB
5180    XA1(3) = VB
5190 'RETURN
5200 '                    ********** COORDINATE ROTATION - 3RD ROTATION *******
5210    K! = WXXB(1, 3) / (WXXB(3, 3) - WXXB(1, 1))
5220    CB = 1                             ' COS(BETA)
5230    SB = 0                             ' SIN(BETA)
5240 ' Rotate.3
5250    OSB! = SB: OCB! = CB
5260    SB = (-CB + (CB ^ 2 + 8 * K! ^ 2) ^ .5) / (4 * K!)
5270    CB = (1 - SB ^ 2) ^ .5
5280    IF ABS(OSB! - SB) > .00001 OR ABS(OCB! - CB) > .00001 THEN GOTO 5240
5290 'IF IPRT=1 THEN LPRINT "SB";SB;"CB";CB;"beta";ATN(SB/CB)*RADTDEG
5295 beta = ATN(SB / CB) * radtdeg'kz added
5300    WXX(3, 3) = WXXB(3, 3) * CB ^ 2 + 2 * WXXB(1, 3) * CB * SB + WXXB(1, 1) *
        SB ^ 2
5310    WXX(1, 1) = WXXB(1, 1) * CB ^ 2 - 2 * WXXB(1, 3) * CB * SB + WXXB(3, 3) *
        SB ^ 2
5320    WXX(1, 2) = WXXB(1, 2) * CB - WXXB(2, 3) * SB
5330    WXX(2, 1) = WXX(1, 2)
5340    WXX(2, 3) = WXXB(2, 3) * CB + WXXB(1, 2) * SB
5350    WXX(3, 2) = WXX(2, 3)
5360    WXX(1, 3) = WXXB(1, 3) * (CB ^ 2 - SB ^ 2) + WXXB(1, 1) * CB * SB -
        WXXB(3, 3) * CB * SB
5370    WXX(3, 1) = WXX(1, 3)
```

```
4350    FOR I = 1 TO NINST
4360       NLAG(I) = HZ * LAG(I)
4370       IF NLAG(I) > MAXLAG THEN MAXLAG = NLAG(I)
4380    NEXT I
4390    FOR I = 1 TO NINST
4400       NLAG(I) = MAXLAG - NLAG(I)
4410    NEXT I
4420    ALPHA = 1 / (TIMCONST * HZ)
4430    ALPHA1 = 1 - ALPHA
4440    ON ERROR GOTO 2470
4450    XNLP = 0
4460    ISYSTAT = 0
4470    FOR I = 1 TO NINST
4480       XA1(I) = 0
4490       WX(I) = 0
4500       WXX2(I) = 0
4510       X2(I) = 0
4520       FOR j = 1 TO 3
4530          WXX(I, j) = 0
4540       NEXT j
4550    NEXT I
4560    XNLP = 0:to3=0:qo3=0
4570    XNPTR = 0
4575    lsthr = HRS
4580    STSEC = JULIAN * 86400! + HRS * 3600 + MIN * 60 + SEC + THS / 100
4590    RETURN
4600 '                          ********** INITIALIZE TIMER ****************
4610 '                                  Data Translation DT2805
4620 ' Init.timer
4630    DEF FNRCONV (X) = X + 6 * INT(X / 10)
4640    DEF FNCONV% (X) = X - 6 * INT(X / 16)
4650    T$ = TIME$
4660    HRS = VAL(MID$(T$, 1, 2))
4670    MIN = VAL(MID$(T$, 4, 2))
4680    SEC = VAL(MID$(T$, 7, 2))
4690    RETURN
4790 '                          ****** COORDINATE ROTATION - TWO ANGLE    ****
4800 '
4810 ' Rotate
4820    DIM WXXB(8, 8), WXXC(8, 8)
4830    WS = (XA1(2) ^ 2 + XA1(3) ^ 2) ^ .5
4840    TW = (XA1(1) ^ 2 + XA1(2) ^ 2 + XA1(3) ^ 2) ^ .5
4850    eta = ATN(XA1(3) / XA1(2))     'horizontal  rad
4860    theta = (XA1(1) / WS)          'vertical rad.
4870    CE = XA1(2) / WS          'COS(ETA)
4880    SE = XA1(3) / WS          'SIN(ETA)
4890    CT = WS / TW              'COS(THETA)
4900    ST = XA1(1) / TW          'SIN(THETA)
4910    UB = XA1(2) * CT * CE + XA1(3) * CT * SE + XA1(1) * ST
4920    VB = XA1(3) * CE - XA1(2) * SE
4930    WB = XA1(1) * CT - XA1(2) * ST * CE - XA1(3) * ST * SE
4940    WXXB(2, 2) = WXX(2, 2) * CT ^ 2 * CE ^ 2 + WXX(3, 3) * CT ^ 2 * SE ^ 2 +
        WXX(1, 1) * ST ^ 2 + 2 * WXX(2, 3) * CT ^ 2 * CE * SE + 2 * WXX(1, 2) * CT
        * ST * CE + 2 * WXX(1, 3) * CT * ST * SE
```

```
6141  OPEN "error.log" FOR APPEND AS #2
6142  PRINT #2, err.msg$, TIME$, DATE$, ERR, ERL
6143  CLOSE #2
6150  SOUND 440, 10
6160  SOUND 32767, 10000
6164  goto 10                                              'trial reroute
6165  STOP
6170  END
6180  '******************** ZERO START ************************************ :kz
6181  GOSUB 1900
6182  value = cdioout: GOSUB 1640                          'kz: send dio cmd
6183  value = dioport: GOSUB 1740                          'kz: send dio port #
6184  value = instmode(0) + jzero+jmrun: GOSUB 1740        'kz: send instruction
6190  PRINT "zero instruments": aidlet = zlag: GOSUB 6540 '6540-get time
6200  idscale = 0: ntl = 0: ical = 1                       'ical stops *.raw save
6210  mode = jzero ':gosub 6380:ntl=0                      'set scale for nox zero
6215  PRINT "determine xoff's - idscale="; idscale
6220  FOR I = 5 TO 8 STEP 1
6221   tvsum(I) = 0
6222  NEXT I
6223  FOR I = 0 TO 200
6224    GOSUB 1430
6225     FOR j = 5 TO 8 STEP 1
6226      tvsum(j) = dat(j, xptr) + tvsum(j)
6227     NEXT j
6228    ntl = ntl + 1
6229  NEXT I
6230  FOR I = 5 TO 8
6231   xoff(I) = tvsum(I) / ntl: PRINT "xoff"; I; "=  "; xoff(I)
6232  NEXT I
6235  'inst=8:gosub 6700          'kz:only used for NOx box - range select
6240  if zxq=0 then goto 6360      'kz: is second inlet level used?
6241  GOSUB 1900
6242  value = cdioout: GOSUB 1640                          'kz: send dio cmd
6243  value = dioport: GOSUB 1740                          'kz: send dio port #
6244  value = instmode(idscale) +jzero+ jxzero+jmrun: GOSUB 1740
6245  PRINT "cross zero instruments": aidlet = zlag: GOSUB 6540 '6540-get time
6246  ntl = 0: ical = 1: tsum=0
6247  PRINT "determine xoff(CAAM2)"
6248   FOR I = 0 TO 200
6249    GOSUB 1430
6250     tsum = dat(6, xptr) + tsum
6251     ntl = ntl + 1
6252   NEXT I
6253   xoff(6) = tsum / ntl: PRINT "xoff(6) = "; xoff(6)
6360  RETURN
6370  '******************** SET SCALE FOR NOX ************************** : kz
6380  tvsum(8) = 0: ntl = 0: ical = 1
6390  FOR I = 0 TO 200
6400   GOSUB 1430
6410   tvsum(8) = dat(8, xptr) + tvsum(8)
6420   ntl = ntl + 1
6430  NEXT I
6431  testvolt8 = tvsum(8) / ntl
```

```
5380    WXX(2, 2) = WXXB(2, 2)
5390    FOR j = 4 TO 8
5400       WXX(j, 2) = WXXB(j, 2)
5410       WXX(j, 3) = WXXB(j, 3) * CB + WXXB(j, 1) * SB
5420       WXX(j, 1) = WXXB(j, 1) * CB - WXXB(j, 3) * SB
5430    NEXT j
5440    RETURN
5450 '
5460 '                          ********** END COORDINATE ROTATION **********
5470 ' ************ READ SETUP FILE *****************
5480 ' Read.setup
5490    DSSET$ = "SETUP"
5500    ON ERROR GOTO 5630
5510    OPEN "I", #1, DSSET$
5520    ON ERROR GOTO 0
5530    LINE INPUT #1, A$
5540    INPUT #1, ATIM, HZ, NCH, NINST, NPRT, BOOMAZIM
5550    LINE INPUT #1, A$
5560    INPUT #1, IPRT, DSK$, IRAW, zlag,xmolag,rlag, zxq,mxq
5570    LINE INPUT #1, A$
5580    FOR I = 1 TO NPRT
5590       INPUT #1, XSCAL(I), LAB$(I), LAG(I), cal(I), xoff(I), ISTAT(I)
5600    NEXT I
5610    CLOSE #1
5615    cal8 = cal(8)                  'kz: used when cal not in operation
5620    RETURN
5630 ' Missing.setup
5640    err.msg$ = "The setup file is not on the default disk."
5650    GOTO 6100
5660 '                ********** WRITE SETUP FILE **********
5670 ' Write.setup
5680    OPEN "I", #1, DSSET$
5690    OPEN DSNAME2$ FOR APPEND AS #2
5700    PRINT #2, "SETUP  ";
5705    IF ical = 1 THEN GOTO 5760     'ie don't print to printer - line 6696
5710    FOR I = 1 TO 13                'print to printer
5720       LINE INPUT #1, A$
5730       IF IPRT = 1 THEN LPRINT A$
5740    NEXT I
5750    IF IPRT = 1 THEN LPRINT dsname1$
5760    PRINT #2, ATIM; HZ; NCH; NINST; NPRT; BOOMAZIM; IPRT; DSK$; IRAW;
5770    FOR I = 1 TO NPRT
5780       PRINT #2, LAB$(I); LAG(I); cal(I); xoff(I); ISTAT(I);
5790    NEXT I
5800    PRINT #2, " "
5810    CLOSE #1
5820    CLOSE #2
5830    IF IPRT = 1 THEN LPRINT CHR$(12);
5840    RETURN
6100  'error.exit
6110  SCREEN 0
6120  LOCATE 10, 1
6130  COLOR 15
6140  PRINT err.msg$
```

```
6810  GOSUB 1900                                              'kz: check error
6820  value = cdioout: GOSUB 1640                             'kz: send dio cmd
6830  value = dioport: GOSUB 1740                             'kz: send dio port #
6840  value = instmode(idscale) + jmrun: GOSUB 1740           'kz: send instruction
6850  PRINT "stabilize NOx Molly": aidlet = xmolag: GOSUB 6540
7070  RETURN
7080  '             *********** PRINT SUBROUTINE ************
8000    PRINT #1, TITO$; "  "; dsname1$
8010    FOR I = 1 TO NINST
8020     IF ISTAT(I) = 1 THEN GOTO 8050
8030     PRINT #1, XA1(I); WXX(I, 1); X2(I); DEPVEL(I); WXX2(I); cal(I); xoff(I)
8040    ' Pr.next.i
8050    NEXT I
8060    PRINT #1, R; U; U2; C8; C9; WNDDIR; theta; eta;beta;
8070    PRINT #1, fsd(8, 0); fsd(8, 1); fsd(8, 2); to3; qo3 'kz
8080    PRINT #1, " "
8090    RETURN
8100  '--------Massman's cosine correction --- for u,v,w -- 2nd algo:28May87 --
8140  R2 = dat(2, xptr) * dat(2, xptr) + dat(3, xptr) * dat(3, xptr)
8141  IF R2 < .0000001# THEN RETURN
8142  SR2 = SQR(R2)
8144  sr2i = 1! / SR2
8150  ZMU0 = ABS(dat(2, xptr)) * sr2i
8160  ZSG0 = ABS(dat(3, xptr)) * sr2i
8164  R3 = R2 + dat(1, xptr) * dat(1, xptr)
8165  sr3i = 1! / SQR(R3)
8170  ZMU1 = SR2 * sr3i
8180  zsg1 = ABS(dat(1, xptr)) * sr3i
8190  f1 = -.484 * ZMU1 + 1.484
8200  dat(2, xptr) = dat(2, xptr) * f1 * (-.484 * ZMU0 + 1.484)
8210  dat(3, xptr) = dat(3, xptr) * f1 * (-.484 * ZSG0 + 1.484)
8220  dat(1, xptr) = dat(1, xptr) * (-.484 * zsg1 + 1.484)
8230  RETURN
8300  '****** BUTTERWORTH DIGITAL FILTER ******   Massman 13APR88
8310  xptr4 = xptr3: xptr3 = xptr2: xptr2 = xptr1: xptr1 = xptr0'kz: save last 4
      pointers
8320  xptr0 = xptr
8330  FOR p1 = 1 TO ninst
8340   FOR p2 = 4 TO 1 STEP -1                          ' kz: save last 4 origional
8350     datx(p1, p2) = datx(p1, p2 - 1)                '     data points
8360   NEXT p2
8370   datx(p1, 0) = dat(p1, xptr)                      'kz: current data input
8380   datintr = .0857864# * datx(p1, 0) + .3431456# * datx(p1, 1) + .5147184# *
       datx(p1, 2) +.3431456*datx(p1,3)
8385   dat(p1,xptr) = datintr + .0857864# * datx(p1, 4) - .3431456# * dat(p1,
       xptr2) - .0294372# * dat(p1, xptr4)
8390  NEXT p1      'kz: above eqn is digital filter
8400  RETURN
```

```
6435  PRINT "determine nox range:"; "testvolt8 ="; testvolt8; ", idscale= ";
      idscale
6450  IF testvolt8 > .7 THEN 6470
6460  IF instmode(idscale) > 0 THEN instmode(idscale) = instmode(idscale) - 1:
      GOTO 6480
6470  IF testvolt8 < 9.5 THEN RETURN
6471  IF instmode(idscale) < 6 THEN instmode(idscale) = instmode(idscale) + 1:
      GOTO 6480
6480  GOSUB 1900:
6490  value = cdioout:                          : GOSUB 1640
6500  value = dioport:                          : GOSUB 1740
6510  value = mode + instmode(idscale)+jmrun    : GOSUB 1740
6520  GOTO 6380
6530  '********************* waiting time ******************** :kz
6540    CALL GETTIME(H%, M%, s%, T%)                    ' Read time via asm.
6550    amin1 = M% + s% / 60
6560    CALL GETTIME(H%, M%, s%, T%)                    ' Read time via asm.
6570    amin2 = M% + s% / 60
6580    IF ABS(amin1 - amin2) < aidlet THEN GOTO 6560
6590    RETURN
6600  '********************* START RUN ********************** :kz
6610  GOSUB 1900                                        'check error
6620  value = cdioout:            GOSUB 1640             'send.cmd
6630  value = dioport:            GOSUB 1740             'send.byte
6640  value = instmode(2)+jmrun: GOSUB 1740             'kz: set to run mode
6650  PRINT "ambient air flush": aidlet = rlag: GOSUB 6540'ambient air in lines
6660  idscale = 2: ntl = 0: ical = 1
6670  'mode=0:gosub 6380 'nox set scale
6680  'inst=8:gosub 6700
6681  'xoff(8)=xoff(8)*fsd(8,0)/fsd(8,2)    'xoff(8) 1st set at zero read scale
6682  xoff(7) = 0              'xoff(6)=0 xoff(6)=0 for Teco 03 slow response
6683  xal4=xal(4)              'xal4=last 1/2 hour temp
6684  if xal4>55 then xal4=25  'set limits for sonic cal if Temp malfunctions
6685  if xal4<-25 then xal4=25
6686  for it=1 to 3
6687   cal(it) = .00660275# * (XA14 + 273)  'sonic cal from last period avg temp
6688  next it
6690  'cal(8)=cal(8)*fsd(8,2)/fsd(8,1)     'use when cal operating
6695  'cal(8)=cal8*fsd(8,2)/fsd(8,1)        'used when cal not operating
6696  GOSUB 5670                           'write adjusted setup
6697  RETURN
6700  '********************* RANGE SELECT ***************** :kz
6710  IF instmode(idscale) = 0 THEN fsd(inst, idscale) = 1E-12: GOTO 6790
6720  IF instmode(idscale) = 1 THEN fsd(inst, idscale) = 1E-11: GOTO 6790
6730  IF instmode(idscale) = 2 THEN fsd(inst, idscale) = 1E-10: GOTO 6790
6740  IF instmode(idscale) = 3 THEN fsd(inst, idscale) = 1E-09: GOTO 6790
6750  IF instmode(idscale) = 4 THEN fsd(inst, idscale) = 1E-08: GOTO 6790
6760  IF instmode(idscale) = 5 THEN fsd(inst, idscale) = 1E-07: GOTO 6790
6770  IF instmode(idscale) = 6 THEN fsd(inst, idscale) = 1E-06: GOTO 6790
6780  IF instmode(idscale) = 7 THEN fsd(inst, idscale) = 1E-05: GOTO 6790
6790  PRINT "fsd="; fsd(inst, idscale); "idscale = "; idscale
6795  RETURN
6800  '********************* NOx MOLLY ON/OFF ********************:kz
6805  if (mctr mod 2)=0 then jmrun=64 else jmrun=0   'kz: switch molly
```

Appendix C

Quality Control Data Sheets

The following are examples of the check sheets to be completed on every visit to the field site. They form an integral part of the quality control.

```
**************************************************************************
*                                                                        *
*                                SETUP                                   *
*                                                                        *
*                        DATA INPUT FOR FLUX,                            *
*              GENERAL PURPOSE EDDY CORRELATION PROGRAME                 *
*                                                                        *
**************************************************************************

Avg. time      Scan rate     # of channels    # of inst.     nprt     Boom dir
   30             80               8              8            8          23
Print? (0/1)     Disc for Output     Raw Data? (0/1)    Zlag     Clag     Rlag
  1                   "c"                 0              0.5      0.0      0.5
Scrn. Scale Instrument name       Lag time   Calib. Coeff.  Offset  Status
29          "W-son "              0          1.935597       0       0
15          "U-son "              0          1.935597       0       0
15          "V-son "              0          1.935597       0       0
100         "T"                   0          10             0       0
100         "1CAAM     "          2.3        1              0       0
50          "TEC01     "          2.3        200            0       0
150         "Vapour    "          0          -6.43079       0       0
100         "2CAAM     "          2.3        1              0       0
```

Data Acquisition System

Month_____ Year_____ Site_____

Day	Operator	Display On	Printer											Accoustic Sounder		Clean Hygrometer		
			Time	Paper	Channel 3 Temp	Channel 4		Channel 5		Channel 6		Channel 7		Time Hack	Paper	Readings		Time
						Inst	Value	Inst	Value	Inst	Value	Inst	Value			Bfre	Aftr	

Zero-Air System, Intake System and Calibration System

Month_____ Year_____ Site_____

Day	Time MST	Operator	Visual Inspection	Shelter Temp.	Intake System				Zero-Air			Comments, Weather
					Flowrate lpm	Residence Time O_3 s	Residence Time NOx s	Residence Time NO_2 s	Flowrate lpm	Pressure Tank psi	Pressure Outlet psi	

LEVEL 1 ZERO AND SPAN CHECK DATA FORM

Site identification _____ Pollutant _____

Location _____ Analyzer _____

Address _____ Serial number _____

Adjusted zero _____ Adjusted span _____

Date	Operator	Unadjusted zero, ppm	Span concentration, ppm	Unadjusted analyzer response		Difference, ppm
				VDC	ppm	

Chemical Instruments

Month_____ Year_____ Site_____

Day	CAAM 1				CAAM 2				TECO 1			TECO 2			Comments, Log Book Reference
	Flowrate	Output	Fluid Level		Flowrate	Output	Fluid Level		Flowrate		Output	Flowrate		Output	
	lpm	V	Lvl in.	Changed (MST)	lpm	V	Lvl in.	Changed (MST)	L. lpm	R. lpm	ppb	L. lpm	R. lpm	ppb	

O_3 Audit Data Sheet

Station (Name/Number)_____ Date_____

Address_____ Start Time_____

T_a_____°C; P_a_____ mm Hg; Auditor_____

Analyzer Make_____ Model_____ Serial #_____
Calibration Std._____ Span source_____
Last Cal. Date_____ Freq.(A)_____ Freq.(B)_____
Temp.(A)&(B)_____ Pressure (A)&(B)_____
Zero setting_____ Data acquisition system_____
Span setting_____ Recorder range_____

Audit system TECO 49PS Serial #_____ Cert.Date_____
Gain setting_____
Freq.(A)_____ Freq.(B)_____ Noise(A/B)_____
Cell Temp.(A/B)_____°C Sample flow (A/B)_____
Clean, dry air source_____

	0% FS		70-90% FS		40-60% FS		10-30% FS	
	Audit	Site	Audit	Site	Audit	Site	Audit	Site
1 Cell A								
Cell B								
2 Cell A								
Cell B								
3 Cell A								
Cell B								
4 Cell A								
Cell B								
5 Cell A								
Cell B								
Average								
Concentration Ave.-Zero	_____							
Difference (ppm/ppb)								
% Difference	_____							

site = _____ (slope) X actual + _____ (intercept)

correlation coefficient squared (r^2) = _____

Verified by _____ Date _____

PRECISION CHECK FORM

Site ID _____ Pollutant _____

Location _____ Analyzer _____

Address _____ Serial number _____

Date	Operator	Precision test gas concentration, ppm	Analyzer response,		Difference, ppm
			VOC	ppm	

Revision 1
27 October 1988

Appendix D

Front Range Ozone Monitoring Network Protocol

The following is the Research Protocol Methodology implemented at the other ozone monitoring sites operated by the U.S. Forest Service in the Front Range.

ANALYZER MAINTENANCE LOG

Site identification _____ Pollutant _____

Location _____ Instrument _____

Address _____ Serial number _____

Date	Initials of technician	Event initiating maintenance	Maintenance activity	Comments

3.2 *Calibrations* - The relationship of a measuring device or method to recognized standards. A calibration should consist of comparisons using at least three concentrations and a zero.

3.3 *Fortnight* - Two weeks.

3.4 *Part per Billion* (ppb) - One part per thousand million, i.e. 1 part in 10^9 by volume.

3.5 *Performance Audits* - Independent accuracy checks of the data collection instruments and recording devices using standards and personnel different from those who normally operate the equipment. This is not a calibration

3.6 *Precision* - A calculation upon a population of related data points for the purpose of quantifying the degree of variability in the accuracy of the data. Precision is calculated for each analyser on a quarterly basis.

3.7 *Precision Check* - Performed by generating an NBS-traceable test atmosphere containing 80 to 100 ppb of the pollutant being monitored. The test atmosphere is delivered to the analyser through as much of the ambient air sample delivery system as possible

3.8 *Primary Standards* - A method, device or material to which all similar measurements are referenced. Typically a material maintained by the National Bureau of Standards (NBS) and referenced to as a Standard Reference Material (SRM). However, no SRM exists for ozone. Primary standards for ozone must be generated locally using a U.V. photometer (Thermo Electron 49 PS).

3.9 *Quality Control* - The body of knowledge and techniques orientated to the correction of defects through process control. A system of activities performed by line personnel to provide quality data and products.

MONITORING AND CALIBRATION PROTOCOL FOR THE ROCKY MOUNTAIN RANGE AND FOREST EXPERIMENT STATION FOR OZONE MONITORING AND DATA COLLECTION

1.0 PURPOSE

This document will serve as a protocol for the collection of ambient ozone data. This procedures described within this document will be implemented at the Pawnee Grasslands, Manitou Springs and Brooklyn monitoring stations. The techniques described within are particular to the Thermo Electron 49 ambient ozone analyser and to the Thermo Electron 49 PS U.V. Photometer.

2.0 OBJECTIVES

The Thermo Electron 49 ambient ozone monitor measures the attenuation of light at ca. 254 nm due to ozone. The transmittance of light through ambient air in a cell is compared with that through a cell containing ambient air from which ozone has been removed. The ambient concentration is then calculated from Beer's law. Ozone concentrations will be measured with a precision of 20% and an accuracy of;

Ozone Concentration	Accuracy
0 ppb	± 2 ppb
40-80 ppb	25%
>80 ppb	15%

3.0 DEFINITIONS

3.1 *Accuracy* - The extent to which a measurement or the average of several measurements recorded by a single analyser agree with the true value. The difference between the true and the measured values is defined as the error. An analyser is considered accurate if the error is less than the tolerance or control limit.

5.0 SAMPLING PROCEDURES

5.1 Installation of Equipment

Analysers will be installed in a temperature controlled shelter (25 ± 5)°C, consistent with the manufacturer's recommendations. Pumps and other auxiliary equipment will be of appropriate size and securely mounted. Electrical and pneumatic connections will be of the minimum length and secured from abrasion and vibration. Signal wires will be shielded from spurious noise. Hazardous exhaust gases will be properly vented.

Calibration equipment will be maintained as required. Transfer standards will be certified and recertified as required. Primary standards will be periodically subjected to an inter-comparison with the Region VIII ozone standard in Denver, Colorado.

5.2 Calibrations

Calibrations will be performed;

- Upon installation of equipment.
- When ever Span Checks indicate an "out-of-tolerance" condition.
- Any time an audit indicates a discrepancy.
- After maintenance that may affect calibration.
- At least quarterly.

Calibrations are typically performed *in situ*, without disturbing the analysers normal sampling configuration.

5.2.1 Calibration Technique

Use the Thermo Electron 49 PS U.V. Photometer Primary Standard. At least three concentrations and a zero are required to determine an initial unadjusted calibration curve of the analyser.

Adjustment of the analyser response shall be made with an input concentration at 80-90% of full scale. The remaining concentrations will be used to establish the linearity of

3.10 *Span Check* (Level 1 Span Check) - Input generated by a calibrator to verify analyser performance. Usually a single point between 400 and 450 ppb. The results indicate change in system performance.

3.11 *Systems Audit* - The regular systematic review of procedures, documents and personnel that effects the collection, reduction and quality control of the data. The audits are typically performed annually by knowledgeable individuals independent of the routine operations.

3.12 *Traceability* - Refers to the written documentation supporting the accuracy, relative to a primary standard, of a method, device or material.

3.13 *Transfer Standard* (Secondary Standard) - A method, device or material which is calibrated against a primary standard for comparison with a third method, device or material.

4.0 RESPONSIBILITIES

4.1 Field Technician

- Instal and maintain monitoring and recording equipment.
- Maintain calibration equipment and conduct field calibrations as required.
- Retrieve data from storage modules and return data to the data processing centre.
- Conduct and track fortnightly Span Checks.
- Conduct and track fortnightly Precision Checks.
- Maintain records of site operation.

4.2 *Principle Investigator*

- Oversee operations at monitoring site.
- Review calibration documents.
- Calculate precision statistics.
- Validate, interpret and report the data.
- Update and review operational procedures and documentation.

6.0 DATA REDUCTION AND VALIDATION

The value and standard deviation of the ozone concentration will be recorded on an automatic data logger (either a Campbell CR 21X or computer with Data Translations A/D board) as half hourly averages. The data logger will initiate daily span and zero checks where available. Data will be returned to the central data handling station at least once per fortnight. Data validation routines will include range testing, consistency checks, relationship tests and screening. All data meeting or exceeding the validation criteria will be flagged for further consideration and examination.

Data will be flagged for further consideration if the following criteria are met or exceeded;

- Ozone concentration is less than zero.
- Ozone concentration is greater than 150 ppb.
- Constant ozone concentration for more than 8 hours.
- Ozone concentration greater than 100 ppb for 8 hours.
- Ozone concentration less than 10 ppb for 8 hours.
- The ozone concentrations stored on the data logger disagree with those recorded from the front panel meter during routine site visits ($\Delta \geq 10$ ppb).

7.0 INTERNAL QUALITY CONTROL CHECKS

Where possible automated daily zero and span checks will be conducted. In addition a manual zero and span check will be conducted fortnightly. If the span check shows that the instrument response is not within 7% of the nominal span value, or the zero value exceeds the previous value then corrective actions will be taken. The sites will be visited at least once per week when preventative maintenance tasks will be performed. All actions will be recorded on the appropriate data sheets.

response. Start and finish with zero. Record all values on "O_3-U.V. Photometer" calibration form.Calculate accuracy from the percent differences between the calibrator output and instrument response.

5.3 Span Checks

Perform Level 1 span and zero checks fortnightly to augment the automated daily span checks (if available). The zero and span settings should not be altered during this procedure.

5.3.1 Span Check Technique

Use the Thermo Electron 49 internal span "B" set at 80-90% of instrument full scale (400-450 ppb)

Record all values on "Level 1 Zero and Span Check Data Form"

Span check results beyond ± 7% of the nominal value requires investigation, repair and recalibration.

5.4 Precision Checks

Perform precision checks once a fortnight. Make no adjustments to the analyser during this procedure.

5.4.1 Precision Check Technique

Use Thermo Electron 49 internal span check "A" set at 80-100 ppb.

Record all values on "Precision Check Form"

Calculate precision statistics on a quarterly basis. At least six separate measurements will be made, and these values will be averaged. The precision will be calculated according to the formula;

$$\text{Precision} = \frac{\text{Calibrator Value - Instrument Average}}{\text{Calibrator Value}} \times 100$$

8.0 PREVENTATIVE MAINTENANCE

Routine maintenance will be carried out as suggested by the manufacturer, including weekly inlet filter changes. During the routine site visits the instrument installation will be inspected, i.e: the electrical and pneumatic fittings, data recording devices and the operation of the instrument. Record will be made of the flows through the instrument, front panel meter reading and current print-out (if available). All actions will be recorded on the relevant data sheet.

9.0 SYSTEMS AUDITS

The operation of the field sites will audited annually by a group independent of the monitoring programme. The auditors will have complete access to the field sites, data sheets, log books and data records.

10.0 CORRECTIVE ACTIONS

When ever questionable data values appear in the database, the operation of the instrument will be checked using the data sheets and site log. If the system was not functioning correctly then the datum in error will be eliminated from the database.

Appendix C:

Leaf Area Development in Four Communities of the Colorado Steppe

Colorado State University

Central Plains Experimental Range
Long Term Ecological Research
Department of Range Science
Fort Collins, Colorado 80523
(303) 491-4996

November 28, 1988

Karl Zeller
US Forest Service
Ft. Collins, CO

Dear Karl:

With this letter is a manuscript entitlied "Leaf Area Development in the Shortgrass Steppe of Colorado". This text should be considered as the final report, a product of the contract between the forest service and our LTER project. The contract was to measure the seasonal development of leaf area at the CPER at six times and at two sites. I expanded this to measure leaf area eight times and at four sites. If you require further details of this research, let me know.

Sincerely,

Donald L. Hazlett

Donald L. Hazlett
LTER Site Manager

cc. William Lauenroth
cc. Douglas Fox

Leaf Area Development in

Four Plant Communities of the Colorado Steppe

Donald L. Hazlett

Range Science Department and Natural Resource Ecology Laboratory, Colorado State University, Ft. Collins, CO 80523, USA

ABSTRACT. In the shortgrass steppe of Colorado seasonal patterns of leaf area development and soil water amounts were compared with net primary production in four plant communities that differed in soil texture and grazing histories. At each site the leaf area indices of old standing dead, live green, C-3 graminoids, C-4 grasses, cacti, forbs, shrubs and recent dead material were determined. Soil water was measured by a neutron probe for 30-75 cm depths. Maximum leaf area indicies of total green material ranged from 0.35-0.42, with the C-4 grasses constituting 58-74% and C-3 grasses 9-36% of these amounts. The importance of water to leaf area development of both C-3 and C-4 species was emphasized, since at all sites C-3 and C-4 species developed more than 55% of maximum leaf area during May, the time of

greatest soil water loss. Seasonal displacement of leaf area development between C-3 and C-4 species occurred: 1) early in the season, when C-3 leaf area was greater, and 2) during mid-summer, when C-4 grasses had higher leaf area amounts. However, leaf area development after summer precipitation events occurred for both C-4 (Bouteloua gracilis) and C-3 species (Carex eleocharis). Variations in the patterns and amounts of leaf area in regard to soil texture, soil water, grazing histories and nutrient availability are also discussed.

Key words: biomass, Colorado, leaf area index, photosynthetic pathways, shortgrass steppe

INTRODUCTION

Leaf area index (LAI) is an attribute of plant communities that indicates cover, influences water use via transpiration, enables comparisons of light utilization among communities and, if measured throughout the growing season, can indicate seasonal growth patterns. A main constraint on the amount of leaf area produced are high ratios of precipitation to evapotranspiration. In semiarid grasslands this ratio is high and leaf area indices are usually less than one (Woodward, 1987).

Since growth patterns among plant species can differ,

adaptations to climatic fluctuations and to resource availability patterns, a comparison of seasonal leaf area development among species or groups of species should reflect these differences. Of special interest in this regard are evolutionary adaptations reflected by growth patterns of plants with C-3 and C-4 photosynthetic pathways. Habitat characteristics of C-3 and C-4 plants have most often been examined at a broad spacial scale, regional or global focus, or for individual plants rather than at the plant community level. Terri and Stowe (1976) related climatic patterns to the abundance of C-4 grass species in North America. They reported a decrease in abundance of C-4 grasses from low to progressively higher latitudes and that few or no C-4 grasses occurred where July minimum temperatures were below 8 C. Ehleringer (1978) used differences in quantum yields between C-4 and C-3 plants in simulation models to predict that at a latitude of 45 N, CO_2 uptake by C-3 and C-4 canopies should be similar. He speculated that at 45 N the segregation of C-3 and C-4 plants should occur along minor topographical and environmental gradients. A summary of descriptive data for the microhabitats of 564 C-4 and 627 C-3 grass species indicated no clear habitat preference for either pathway type, but greater proportion of C-4 than C-3 grasses occurred in microsites characterized by low levels of shade and drier soils (Hitchcock and Chase, 1971)

Numerous laboratory studies on individual plants have

reported that C-4 grasses, relative to C-3 grasses, have higher maximum rates of photosynthesis, exhibit photosaturation at higher light intensities and have higher temperature optima for photosynthesis (Bjorkman 1975, Williams and Markley 1973, Williams 1974, Kemp and Williams 1980, Monson et al 1983). Other laboratory studies have shown that C-4 plants have high use efficiencies for water (Downes 1969) and nitrogen (Brown 1978). A general suggestion has been that under field conditions grass species with a C-3 pathway would grow primarily during the cool, early portion of the growing season and that C-4 grasses would grow primarily during the warmer, midsummer portion of the season. A shift to greater growth by C-4 plants was anticipated not only because of higher temperatures, but also because water availability is also less by midsummer.

Growth chamber results are useful to make predictions about what will happen under field conditions, but few field studies have tested these predictions by examining seasonal growth displacement of C-3 and C-4 grasses at the plant community level. Boutton et al (1980) measured more C-4 biomass in August than in June (only two harvest dates) and a relative increase in C-4 biomass as temperature increased and as precipitation and elevation decreased for seven sites in southeastern Wyoming. A 1^3C separation of C-3 and C-4 biomass in South Datoka also supported the hypothesis that productive periods of C-3 and C-4 grasses were displaced in

time (Ode et al 1980). Of interest in this and in more recent field studies (Barnes et al 1983, Liang et al 1988) is that plant communities with a greater number of C-4 species or with a greater C-4 biomass component do not necessarily represent the most productive communities. This contention does not fit with laboratory results of higher CO_2 uptake by C-4 plants and the anticipated higher productivity of C-4 dominated communities. Another example of field information that does not fit the predictions from laboratory studies was provided by Monson et al (1986). They compared growth of Agropyron smithii (C-3) and Bouteloua gracilis (C-4) in the shortgrass steppe and observed that maximum growth was not displaced in time as had been predicted by laboratory studies. Rather, the time of maximum leaf area increase was similar for both species, occurring during June. They attributed these similar growth patterns for C-3 and C-4 plants under field conditions to: 1) the importance of precipitation patterns on plant water stress and 2) to microclimatic differences between standard air temperature values and leaf surface temperature values.

Regional data compilations and laboratory research have identified environmental variables that correlate in a general way with geographical distributions and physiological characteristics of C-3 and C-4 plants. However, field studies that periodically sample biomass amounts as an indication of growth patterns for C-3 or C-4 plants have not

always fit anticipated patterns. Clearly, more field studies in areas of co-occurrence are needed to better understand the *in situ* characteristics of species with different photosynthetic pathways. In this study soil water, precipitation and leaf area were measured to examine relationships between the amounts and growth patterns of C-3 and C-4 plants. The following research questions were asked: What are the leaf area amounts and development patterns among life-forms and between C-4 grasses and C-3 graminoids (grasses and sedges) in four steppe communities? Do water availability patterns influence patterns of leaf area development of C-3 and C-4 plant species?

Site Description

This research was conducted during 1988 at the Central Plains Experimental Range (CPER) near Nunn, Colorado (42 42'N 104 46'W). Mean annual precipitation at the CPER from 1969-1987 was 321mm (s.d. 76 mm) with 80% of precipitation for this interval occurring from April to September. Although the three study sites were within 5 km of each other, during 1988 the range of April to September rainfall was 164 to 260 mm. The frost free period averages 135 days, during which time the mean maximum temperature is near 26 C (31 C during July and August) and the mean minimum temperature is near 9 C 14 during August). Evaporative demand during 1988 had a pattern similar to temperature (Figure 1) but was most

variable during May.

Leaf area index was determined for four plant communities that were on level terrain, but that varied in soil texture (Table 1) and grazing histories. The grazed clay-loam site was located at the swale position of a north facing catena, was co-dominated by Bouteloua gracilis (H.B.K.) Lag and Buchloe dactyloides (Nutt.) Englem. This site has been grazed for over 20 yr at the rate of 1.4 ha per yearling month with 1988 grazing beginning in July. The ungrazed sandy-loam site, located on an old stream terrace near Owl Creek, was dominated by B. gracilis, but was also characterized by the presence of Atriplex canescens Pursh (Nutt.) shrubs. This area has been protected from grazing since 1985. The final two study sites were on loam soil, soil representative of large areas of the CPER. Of these, the ungrazed loam site was within an exclosure protected from grazing since 1968 and the grazed loam site was just outside the exclosure in a pasture grazed at the rate similar to the clay loam site with 1988 grazing beginning May 27. Both loam sites were dominated by B. gracilis.

The C-3 graminoids encountered during the study were Argropyron smithii Rydb., Carex eleocharis Bailey, Festuca octoflora Walt, Oryzopsis hymenoides (R. & S.) Ricker, Sitanion hystrix and Stipa comata Trin. & Rupr.. The C-4 grasses encountered were Aristida purpurea Nutt., Bouteloua gracilis, Buchloe dactyloides (at clay-loam site only), and

Table 1. Soil properties of the four plant communities monitored for LAI develpment. Characteristics for the loam sites are from Schimel *et al* (1985).

	Site		
	Grazed Clay-Loam	Grazed and Ungrazed Loam	Ungrazed Sandy-Loam
Sand Content (%)			
0 - 30 cm	42	66-73	81
30 - 75 cm	27	64-72	79
Clay Content (%)			
0 - 30 cm	37	15-24	9
30 - 75 cm	53	20-24	11
Nitrogen (%)			
0 - 30 cm	.106	.103	.061

Sporobolus cryptandrus (Torr.) A. Gray. Shrubs encountered were Artemisia frigida Willd, Atriplex canescens, Chrysothamnus nauseosus (Pall.) Britt., Eriogonum effusum Nutt., and Gutierrezia sarothrae (Pursh) Britt. & Rusby. Forbs included Allium textile A. Nels. & Macbr., Cryptantha minima Rydb., Cymopterus montanus T. & G., Lepidium densiflorum Schrad., Leucocrinum montanum Nutt., Sphaeralcea coccinea (Pursh) Rydb., Thelesperma filifolium (Hook.) A. Gray, and Tradescantia occidentalis (Britt.) Smyth. All the above listed shrubs and forbs have C-3 photosynthetic pathways. The cactus species at all sites was Opuntia polyacantha Haw., the only species in this study with a CAM photosynthetic pathway.

MATERIALS AND METHODS

Leaf area index (LAI), a ratio between the amount of leaf area and the amount of ground surface area, was measured eight times at each of four sites during the 1988 growing season. Except for two determinations in June, LAI was measured once a month from April 13 to October 1. Each LAI determination was made by the non-destructive point-quadrat technique of Warren Willson (1963) using a frame with 5 cm intervals between pins. The number of contacts per pin when the rod is passed through the canopy at different angles from the horizontal are recorded. The average number of contacts per pin are then multiplied by coefficients to obtain LAI.

Although Wilson recommended using 3 pin angles, Knight (1972) compared LAI results from only the 32.5 angle and found a maximum error of only 0.05. Knight's equation was used in this study:

$$LAI = 0.87 f_{n\,32.5} \qquad (1)$$

The term f_n is the average number of contacts per pin for the 32.5 angle.

Pin contacts with canopy plant material were identified as dead or live plant tissue. Dead tissue contacts were further categorized as either "old dead", from previous growing seasons, or "current year dead". Live tissue contacts were hits with green plant tissue whether the plant part was leaf, stem, or reproductive. Live hits were categorized by species for grasses and to life-form for cacti, forbs and shrubs. Each category of canopy contact was entered into equation 1 for LAI determinations.

Pin contacts with the ground surface were identified as bare soil, litter, lichen, or crown. The crown category, including live or dead crowns, was recorded only for the last two measurements. All others were recorded separately for each determination. Since ground contacts are independent of angle of pin entry, ground contact data are presented on a percentage basis.

An advantage of LAI determinations by the point-quadrat technique over biomass harvesting, especially when growth patterns of C-3 and C-4 plants are of interest, is that the

same plants can be sampled each date and thereby reduce error associated with spatial variation in the proportion of C-3 and C-4 plants. To assure sampling the same areas, four transect were permanently marked at each study site. Transect end-points were established by randomly selecting two locations at each site. From one end-point a 15 m line was run north for 15 m and from the other location a line was run west for 15 m. Along each line two parallel transects were read by placing the point-quadrat frame in both directions from the line. For each transect 150 pins were run (125 in April), or 600 pins (500 in April) per LAI determination. Data from each transect was kept separate for statistical comparisons.

Soil water content measurements, using the neutron scattering method (Troxler model 1257), were taken at 30, 45, 60, and 75 cm depths for 2 access tubes (4 at sandy-loam site) per study area. This method estimates soil water content in a spherical area within a radius of approximately 22 cm from the measurement point. Therefore, in this study the soil water content was not estimated for the top 8 cm of soil nor at depths greater than 82 cm. From probe counts the volumetric soil water amounts were determined by a calibration equation developed by comparing probe counts with gravimetric soil water contents (n= 210) for CPER soils of all textures (r= 0.87). The neutron probe access tubes at the loam soil location were inside a 3 m diameter by 1.5 m

deep lysimeter core. Soil water contents were measured 11 times (2-4 week intervals) from February 29 to September 26.

Soil water loss was calculated for each site for two intervals using the water balance method. First, from the spring maximum value until 8 July, the measurement date nearest maximum LAI of all sites, and for the principal growing season from the spring maximum value until 24 August (Table 3). Volumetric soil water values were converted to cm of soil water for a 15 cm, shallow soil layer, based on probe values at the 30 depth and for a 45 cm, deep soil layer, based on the mean soil water contents at the 45, 60 and 75 cm depths.

Aboveground net primary production was estimated by standing crop of current year's biomass at the end of the growing season (Lauenroth et. al. 198). Standing crop biomass was determined at all four sites by clipping ten 0.25 m^2 quadrats at each site on August 11. Clipped biomass was sorted into old standing dead and to current year production of cacti, grass, forbs, and shrubs. All samples were oven dried at 70 C for 48 hours (288 hrs for cacti) and weighed. Duncan's multiple range test was used to assess statistical significance for cover, water loss, and biomass data.

Water use efficiencies were calculated to further compare LAI and biomass production among sites (Table 3). Ratios of graminoid and total NPP production per mm ET and of graminoid and total leaf area production per dm ET were

calculated. Evapotranspiration (ET) was estimated by summing total rainfall and soil water loss (water balance method) until 8 July, for leaf production ratios, and until 24 August for NPP ratios.

RESULTS

Maximum green LAI at the four steppe sites ranged from 0.35-0.42 (Table 2). Maximum green leaf area occurred during early June at the clay loam site, during late June at the sandy loam site and during July at grazed and ungrazed loam sites (Figs. 2-4). With one exception, 32-36% of maximum leaf area was produced by 5 May and 62-65% of maximum LAI was produced from 5 May to 1 June. The exception was a slightly different pattern at the grazed loam site where 41% of total leaf area was produced by 5 May and 57% from 5 May to 1 June.

There were differences among sites in ground cover. The area of bare soil was significantly less and basal crown cover was greater (33%) at the ungrazed sandy-loam site (Table 2). The lowest basal crown cover (18%) occurred at the grazed-loam site (Table 2). At the grazed clay-loam site surface litter was significantly less ($P < .05$), while surface cover of Parmelia chlorochroa Tuck., a crustose lichen, was significantly higher than at all other sites. Parmelia was most abundant at the grazed clay-loam site, more abundant at the grazed loam than at the ungrazed loam site and was completely absent from the sandy-loam site.

Table 2. Maximum LAI values for C-3 graminoid, C-4 graminoid, and total LAI in contrast to: 1) the seasonal range in LAI for cacti, forbs, and shrubs and 2) the seasonal range of cover percentages for bare soil, crown, litter, and lichens. For each row, mean values followed by the same letter are not significantly different (P< .05).

	Site			
	Grazed		Ungrazed	
	Clay-Loam	Loam	Loam	Sandy-Loam
Maximum LAI (mo/d)				
Total	.36 (6/1)a	.35 (7/13)	.40 (7/13)	.42 (6/23)
C-4	.21 (6/23)	.26 (7/13)	.26 (7/13)	.25 (6/23)
C-3	.13 (6/1)	.03 (6/23)	.08 (6/1)	.07 (6/1)
Old Dead	.19 (4/7)	.18 (4/7)	.41 (4/7)	.48 (4/7)
Range in LAI				
Cacti	<.02	.04 -.08	.02 -.06	.02 -.06
Forbs	<.02	<.02	.01 -.04	0 -.04
Shrubs	0	<.02	<.02	.01 -.04
Ground Cover (%)				
Bare soil	54 a	58 a	55 a	45 b
*Crown	26-27 ab	18 b	25-27 ab	32-34 a
Litter	10 a	23 b	21 b	22 b
Lichen	9 a	3 b	<1 b	0 b

* Mean of last 2 sample dates only.

Soil water content and seasonal loss of soil water at 22-38 cm and 38-83 cm depths varied with soil texture (Figs. 2-4). For both depths and for the entire season, the clay-loam site had a significantly higher volumetric soil water contents than the sandy-loam site ($P < .05$). With the exception of similar soil water contents in late April, this was also true for the clay-loam site in contrast to the loam site. Although volumetric soil water content was high, the loss of soil water from the maximum spring amount until 8 July was only 9 cm at the clay-loam site. This compared to a 25 cm loss at the loam sites, and a 47 cm loss at the sandy-loam site. Until 8 July, near the time of maximum leaf area, there was relatively greater soil water depletion at the loam and sandy-loam sites than at the clay-loam site. If soil water depletion from the spring maximum until 24 August is considered as 100%, the soil water depletion until 8 July was 56%, 42% and 96% for the clay-loam, loam, and sandy-loam sites, respectively. The loam and clay-loam soils supplied relatively more water to evapotranspiration during the hottest, driest portion of the growing season. The main reason for this difference appeared to be soil texture.

Net primary production (NPP), like soil water loss, was generally greater at the coarse-textured than at the fine-textured site (Table 3). Both total NPP and graminoid NPP were significantly greater at the ungrazed-loam site than at the grazed clay-loam site ($P < .05$). There was also

Table 3. Standing crop biomass on 11 August, evapotranspiration (rainfall plus soil water loss), and water use efficiency (WUE) ratios for NPP and leaf area production at each study site. For each row, means followed by the same letter are not significantly different ($P < .05$). Rainfall, ET, and soil water loss are from 1 April to 24 August.

	Site			
	Grazed		Ungrazed	
	Clay-Loam	Loam	Loam	Sandy-Loam
Standing Crop Biomass (g/m2)				
Cacti	11 a	18 a	19 a	14 a
Forbs	<2 a	<2 a	8 b	<2 a
Grass	59 a	81 ab	114 b	85 ab
Total NPP	71 a	113 ab	143 b	113 ab
Old Dead	2 a	5 a	102 b	13 ab
Rainfall (mm)	180	233	233	139
Soil Water Loss				
22-38 cm	15 a	17 a	17 a	12 a
38-83 cm	<1 a	42 b	42 b	37 b
Total ET	196	292	292	188
WUE Ratio to August: NPP (g/m^2) / Evapotranspiration (mm)				
Graminoid	.30	.28	.39	.60
Total	.36	.39	.49	.45
WUE Ratio to 8 July: Leaf Area (LAI) / Evapotranspiration (dm)				
Graminoid	.17	.10	.12	.17
Total	.18	.12	.14	.22

significantly more leaf area of old standing dead and of forbs ($P < .05$) at the ungrazed-loam than at other sites. There were no shrubs and less cacti at the clay-loam site. The amount of cacti, similar at all sites, ranged in biomass from 13-16% of total NPP. The amount of cactus leaf area relative to maximum total leaf area was a similar proportion, 14-23% at all but the clay-loam site. At the clay-loam site cactus production was 15% of total NPP and cactus LAI was only 6% of maximum.

Although leaf area is essential for plant production, there were no significant correlations between total or graminoid LAI and aboveground total or graminoid NPP. A meaningful relationship between LAI and production may be possible only if one species were considered, B. gracilis, and if leaf area date were combined with data on radiation and water utilization.

The water use ratios among sites were different, depending on whether ratios of total NPP to ET or ratios of maximum LAI to ET were examined (Table 3). Water use efficiencies (WUE) in terms of graminoid or total NPP per unit of evapotranspiration were highest at the ungrazed sites and lowest at the grazed sites. By this measure, the WUE of the sandy-loam site was twice a great as the clay-loam site, an example of higher productivity on sandy than on clay soils (Noy-Meir 1973). In contrast, when water use until the time of maximum leaf area was calculated, the clay-loam and the

sandy-loam sites had similar ratios; ratios that were greater than at either loam site (Table 3).

The abundance of C-3 and C-4 graminoids among sites was compared on the basis of actual LAI amounts (Figs 2-4, Table 2) and in terms of development relative to the time of maximum LAI (Fig 4). The LAI of C-4 grasses was very similar (0.21-0.26) at all study sites. In contrast, the highest LAI for C-3 graminoids was 0.13 at the clay-loam site and the lowest was 0.03 at the grazed-loam site. Within sites, the maximum leaf area of C-4 graminoids always occurred earlier, by 10-21 days, than the maximum leaf area of C-4 grasses. The time when the LAI of C-4 graminoids exceeded that of C-3 graminoids was during May at the clay-loam and ungrazed-loam sites, during early April at the sandy-loam site and, and most likely due to such a low amount of C-3 leaf area, did not occur at the grazed-loam site.

The time of maximum leaf area development was most similar for C-3 and C-4 plants at the clay-loam site, occurring during the last part of May. At the other sites, maximum leaf area occurred earlier for C-3 graminoids, during late May or June, than for C-4 graminoids, during late June or July (Fig. 5).

Main differences in C-3 and C-4 leaf area development patterns occurred either early in the season or in the summer, not during May. Before 1 May, all sites had produced 40-50% of maximum C-3 leaf area amounts, compared to less

than 20% of maxima amounts by C-4 plants (Fig. 5). However, early season amounts of C-3 and C-4 leaf area were significantly different only at the clay-loam site during April ($P < .05$), a difference attributed to the abundance of F. octofolia at this site. At maximum leaf area the leaf area of F. octofolia was 0.07 (54%) and C. eleocharis was 0.06 (46%).

The summer increases in total, C-3 and C-4 leaf area development occurred in response to rainfall (Figs. 2-4). Following a 40 mm precipitation event on 7 July both loam sites had a large resurgence in soil water content. Following this event, senescence of green leaf area accelerated, but there was only a slight increase in green leaf area (Fig. 3). A mid-July increase in soil water did not occur at the sandy loam site, where only 6 mm of rain fell on July 7, and was evident only to the 30 cm depth at the clay loam site where 24 mm of rain fell during this event.

Increases in the amount of total green LAI occurred at all sites in late summer, when a month of essentially no precipitation was ended by 24 mm of precipitation on September 11-14. This precipitation was uniform at all sites, but resulted in variable leaf area increases among sites of 6-19% of maximum LAI. After this event there was a significantly greater increase in leaf area only at the sandy-loam site in contrast to the clay-

loam site ($P < .05$). However, after the September rainfall the leaf area of C-4 graminoids was significantly greater than that of C-3 graminoids at all sites ($P < .05$).

Growth patterns of individual species and groups of species with C-3 or C-4 photosynthetic pathways were also compared (Fig 6). The time of maximum LAI and regrowth of B. gracilis varied among sites, with maximum LAI occurring from late June to mid July. At both loam sites large precipitation events on July 7 were followed by renewed production of B. gracilis leaf area. Renewed production did not occur at the sandy-loam site, much less precipitation there, and only a slight increase occurred for B. gracilis / B. dactyloides at the clay-loam site. The other C-4 species, A. purpurea and S. cryptandrus, also had maximum LAI during July or August, but unlike B. gracilis , these species did not renew leaf area production in response to the large July 7 event.

In general, C-3 species attained maximum LAI before C-4 species, usually during the last part of May (Fig. 5b). Exceptions to this timing were a late June leaf area maxima for: 1) C. eleocharis at the grazed-loam site and 2) cool season grasses at both loam sites (S. hystrix, S. cometa, and A. smithii). Carex eleocharis did not occur at the sandy-loam site, but for each of

the other sites C. eleocharis, like B. gracilis, was capable of renewing leaf area production whenever adequate moisture was available.

Discussion

The LAI development patterns among four steppe communities and between C-4 grasses and C-4 graminoids differed in the time of initial leaf area production, time of maximum LAI, and in late-season responses to moisture availability. Nevertheless, at all sites at lease two-thirds of the seasonal maximum total leaf area was produced during May (Fig. 5). This degree of synchrony in LAI development for communities on different soil types and with large differences in rainfall amounts expands to the community or even larger scale the suggestion by Monson (1986) that the time of maximum growth and photosynthesis can be similar for C-3 and C-4 species. Part of the explanation for this (Pearcy et. al. 1984) is that the higher photosynthetic rates for C-4 plants reported from growth chamber studies have been rates measured at light saturation. In field conditions, however, light availability can very greatly from saturation amounts. For example, daily cloud cover estimates for 17 years at the CPER indicate May as the month with the greatest cloud cover percentage (62%). High rainfall amounts and frequent

cloud cover apparently contribute to wide fluctuations in evapotranspiration during May (Fig. 1). Furthermore, the amount of old standing dead material, at a seasonal maximum at all sites during April, shade new leaf blades and can further influence canopy temperature and light levels. A consequence of wide May fluctuations in evaporative demand and variable amounts of canopy shading is probably a wide range in daily and hourly microclimatic conditions at level of the developing leaf. If microclimatic conditions at leaf surfaces alternate from conditions that favor photosynthetic activity of C-3 plants to conditions that favor C-4 plants, this variation can help explain how C-3 and C-4 species can coocur in the same plant community.

Early in the season it is temperature, perhaps also photoperiod, that strongly influences the initiation and rate of leaf area development. As the season progresses, temperatures also seems to mediate an earlier attainment of maximum leaf area for C-3 graminoids than for C-4 grasses. During June and July, however, water and nutrient availability, seem to be most influential than temperatures in determining the time and maximum amount of leaf area for any given year. For example, maximum leaf area occurred earlier at the clay-loam site, where water was quickly becoming unavailable to plants, and maximum leaf area occurred as

late as July for both loam sites where a large rain event made moisture available until mid-July. In years when a large early July events did not occur (1970 and 1971) leaf area measurements at the CPER by Knight (1973) reported maximum leaf area during late June for both a wet and a dry year, but the maximum leaf area amount was 25% less during the dry year. The point in the growing season when water becomes more unavailable to leaf area development, near the first of June, is also the time when soil water stores from the previous spring and winter are nearly depleted (Figs. 2-4; Liang, et. al. 1988).

Until mid-July there appeared to be adequate light, temperature, and moisture a both loam sites, but from 23 June to 13 July there were only small increases, 7-10% of maximum LAI, in leaf area development. This rain induced increase in leaf area was much less than the over 60% increase in leaf area of irrigated plots over controls reported by Knight (1973). Knight also reported that plots that were both irrigated and fertilized with nitrogen had 10 times more leaf area than controls. This information helps interpret the plateau of green leaf area that occurred at both loam sites. Although green leaf area at both loam sites maintained a plateau until mid-July, the current year production of leaf area (green plus current year's dead)

continued to increase until mid-August, especially at the grazed-loam site (Fig. 2). What was occurring was senescence of older and sprouting of new blades of grass, a sequence that may be related to nutrient, especially nitrogen, deficiencies. An adequate soil water, but low nitrogen status at the loam sites could have prompted senescence and translocation of nitrogen from senescing grass blades to younger, actively growing plant tissues. Whether translocation was occurring or not, the result was an increase in current year production while sustaining similar total leaf area amounts. This situation helps explain why correlations between total NPP and maximum leaf area amounts were not significant.

To account for high variability in precipitation amounts, intersite comparisons were made by calculating ratios of water use to NPP and water use per unit of leaf area (Table 3). At the sandy-loam and clay-loam sites the ratios of water use per unit of leaf area production (only to the time of maximum leaf area, not beyond) were similar for total NPP and identical for graminoid NPP. Since B. gracilis was a dominant species at both these sites, similar ratios of water use to leaf production of graminoids indicated in large part a similar water use efficiency for blue grama at sites with different soil textures. In contrast to these

ratios, the water use/NPP ratios were greater at the sandy-loam than at the clay-site, twice as great for graminoid water use efficiencies. The high C-4 leaf area at the sandy-loam site during May could be explained as water utilization from depth greater than those measured. However, since the sandy-loam site also produced significantly more C-4 leaf area following a uniform precipitation event in September, this response and the high water use ratio both indicated that water use efficiency for production was indeed greater at the sandy-loam site.

After attaining maximum LAI, when water availability became more unpredictable, both a C-4 species (B. gracilis) and a C-3 species (C. eleocharis) were capable or renewed leaf area development in response to precipitation events. A rapid growth response of B. gracilis is considered an important adaptive trait that enables this dominant species to better utilize the water from sporadic summer rainfall events (Sala and Lauenroth, 1982). The midsummer growth of C. eleocharis was also apparently in response to summer rainfall events. This result supported the suggestion of Monson et. al. (1983) that identified this sedge as capable photsynthetic acclimation. Like B. gracilis, the ability of C. eleocharis to photosynthesize at high temperatures was realized only

when water was available.

Although one C-3 species did respond, it was the C-4 grasses, especially B. gracilis, that showed the greatest total and relative amounts of leaf area development in response to summer and September precipitation. The failure of C-3 species to outrespond C-4 grasses during September, when temperatures are more amiable to C-3 photosynthesis, is of interest since this pattern differed from those reported for C-3 and C-4 grasses in mixed grass prairies in South Dakota (Ode, et. al. 1980 and Coppock et. al. 1983). In the mixed grass prairie there was a resurgence in C-3 grass production during September and October. One reason this did not occur in the shortgrass steppe may be that the suite of C-3 species in the communities sampled include only small amounts of Agropyron smithii. If dense stands of A. smithii were sampled, a late season response to water availability may well occur.

The influence of grazing on leaf area amounts were evident both in the amount of standing dead and in the relative abundance of different species guilds. The amount of leaf area of C-4 grasses was similar at grazed and ungrazed sites, but the proportion of C-4 leaf area that was B. gracilis was only 60% at the ungrazed loam site, compared to over 88% at the other sites. Furthermore, the leaf area of B. gracilis at the

ungrazed loam site relative to total maximum leaf area was only 38% , compared to a leaf area dominance of 58% or greater for B. gracilis at the other sites. Knight also indicated a reduction of B. gracilis leaf area in an exclosure relative to a grazed pasture and suggested that B. gracilis was more tolerant of grazing. In this study while the leaf area of B. gracilis was less at the ungrazed than at the grazed loam site, the leaf area of other C-4 grasses (S. cryptandrus and A. purpurea), of C-3 graminoids, and of forbs were all greater at the ungrazed loam site. Both protection from grazing and standing dead influences on microclimatic conditions seemed responsible for the shift in species abundances that occurred at the loam grazing exclosure.

In summary, the leaf area development patterns of four steppe communities indicated that when C-3 and C-4 species cooccur in a steppe communities they can also have similar times of maximum leaf development. Similar times of leaf area development indicated the important role of water in leaf development. The variable evapotranspiration amounts during May suggested that May temperature variations enabled growth of species with C-3 and C-4 photosynthetic pathways. In addition to temperature, grazing, soil texture and variable microclimates also seemed to influence the development patterns and relative amounts of C-3 and C-4 leaf area.

With so many factors interacting, it is difficult to predict what type of change could occur, for example, due to annual changes in rainfall or temperatures. However, tracking proportional leaf area amounts of forbs, shrubs, C-3 and C-4 species at the same locations at periodic intervals is an effective method of monitoring changes in vegetation structure.

Acknowledgments

This research was funded by the Shortgrass-Steppe Long-Term Ecological Research Program (National Science Foundation grant BSR-8114822) and by the USDA Forest Service Rocky Mountain Station, Ft. Collins, CO.

Literature Cited

Barnes, P. W., Tieszen, L. L., and Ode, D. J. 1983. Distribution, production, and diversity of C-3 and C-4 dominated communities in a mixed prairie. Can. J. Bot. 61:741-751.

Bjorkman, O., and J. Berry. 1973. High efficiency photosynthesis. Sci. Amer. 229:80-91.

Boutton, T. W., Harrison, A. T., and Smith, B. N. 1980. Distribution of biomass of species differing in photosynthetic pathway along an altitudinal transect in southeastern Wyoming grassland. Oecologia (Berlin) 45:287-298.

Brown, R. H. 1978. A difference in N use efficiency in C-3 and C-4 plants and its implications in adaptation and evolution. Crop Sci. 18:93-98.

Coppock, D. L., Detling J. K., Ellis, J. E., and Dyer, M. I. 1983. Plant-herbivore interactions in a north american mixed-grass prairie I. Effects of black-tailed prairie dogs on intraseasonal aboveground plant biomass and nutrient dynamics and plant species diversity. Oecologia (Berlin) 56:1-9.

Downes, T. W. 1969. Differences in transpiration rates between tropical and temperate grasses under controlled conditions. Planta, 88:261-273.

Ehleringer, J. 1978. Implications of quantum yield differences on the distribution of C-3 and C-4 grasses. Oecologia 31:255-267.

Hitchcock, A. S., and Chase, A. 1971. Manual of the grasses of the United States. 2nd ed, pp. 1-1051. New York: Dover.

Kemp, P. R., and Williams, G. J. III. 1980. A physiological basis for niche separation between Agropyron smithii (C-3) and Bouteloua gracilis (C-4). Ecology, 61:846-858.

Knight, D. H. 1973. Leaf area dynamics of a shortgrass prairie in Colorado. Ecology 54:891-896.

Liang, Y., D. L. Hazlett, and W. K. Lauenroth. Water-use efficiency of five plant communities in the shortgrass steppe. Oecologia (in revision).

Monson, R. K., Littlejohn, R. O., and Williams, G. J. III. 1983. Photosynthetic adaptation to temperature in four species from the Colorado shortgrass steppe. Oecologia 58:43-51.

Monson, R. K. 1984. A field study of photosynthetic temperature acclimation in Carex eleocharis Bailey. Plant, Cell and Environ. 7:301-308.

Monson, R. K., Sackschewsky, M. R., and Williams, G. J. III. 1986. Field measurements of photosynthesis, water-use efficiency, and growth in Agropyron smithii (C-3) and Bouteloua gracilis (C-4) in the Colorado shortgrass steppe. Oecologia 68:400-409.

Noy-Meir, I. 1973. Desert ecosystems: Environment and producers. Annual Rev. of Ecol. and Syst. 4:25-51.

Ode, D. J., Tieszen L.L., and Lerman J. C. 1980. The seasonal contribution of C-3 and C-4 plant species to primary production in a mixed prairie. Ecology 61: 1304-1311.

Pearcy R. W. and Ehlelringer, J. 1984. Comparative ecophysiology of C-3 and C-4 plants. Plant, Cell and Environ. 7:1-13.

Sala, O. E., W. K. Lauenroth and W. J. Parton. 1982. Plant recovery following prolonged drought in a shortgrass steppe. Agric. Meteor. 27:49-58.

Schimel D, Stillwell, M. A., and Woodmansee, R. G. 1985. Biogeochemistry of C, N, and P in a soil catena of the shortgrass steppe. Ecology 66(1): 267-282.

Terri J. A. and Stowe, L. G. 1976. Climatic patterns and the distribution of C-4 grasses in North America. Oecologia (Berlin) 23:1-12.

Warren-Wilson, J. 1963. Estimation of foliage denseness and foliage angle by inclined point quadrats. Aust. J. Bot. 11:95-105.

Williams G. J. III. 1974. Photosynthetic adaptation to temperature in C-3 and C-4 grasses. A possible ecological role in the shortgrass prairie. Plant Physiol 54:709-711.

Williams, G. J. III, Markley J. L. 1973. The photosynthetic pathway type of North American shortgrass prairies species and some ecological implications. Photosynthetica 7: 262-270.

Woodward, F. I. 1987. Climate and plant distribution. Cambridge University Press, 174 pages.

Fig. 1. Mean daily minimum temperatures (— — —), mean daily maximum temperatures (————) and mean daily pan evaporation amounts (--------) for weekly intervals during 1988 at the Central Plains Experimental Range.

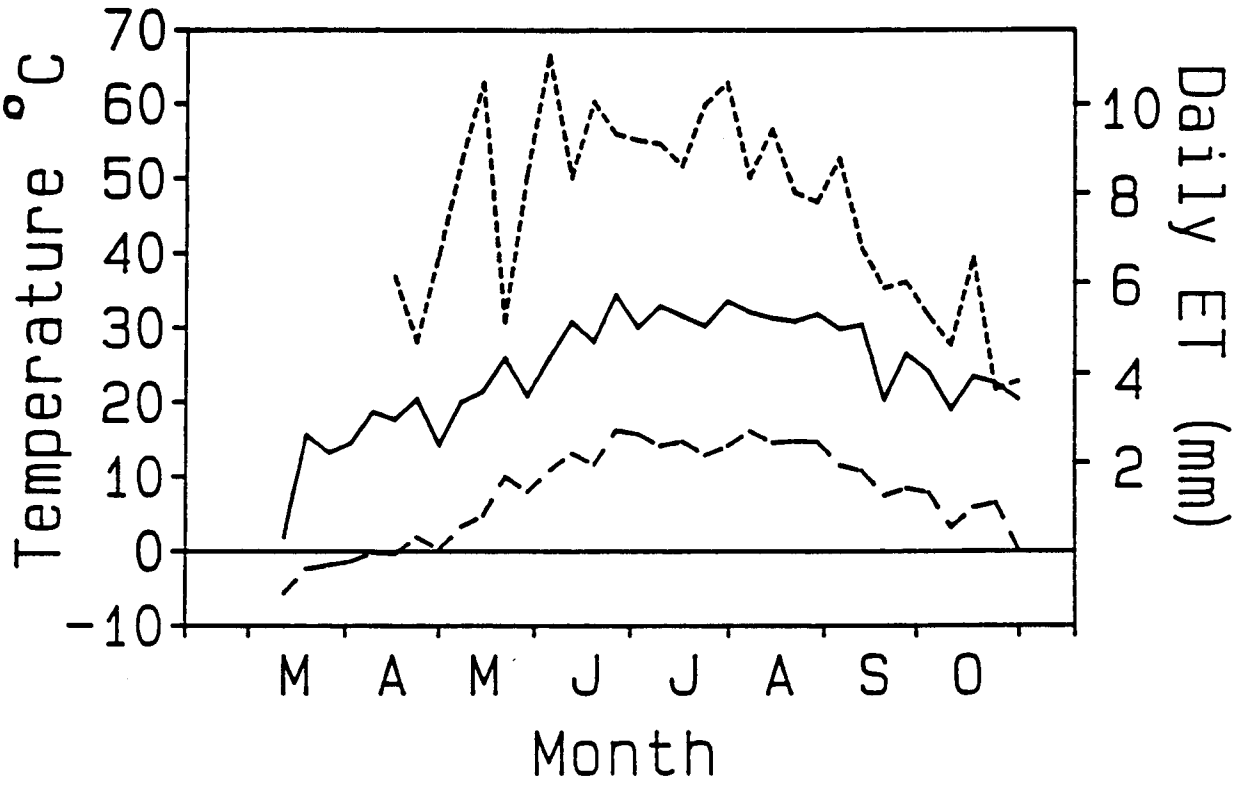
Temperature °C
70
60
50
40
30
20
10
0
-10
Daily ET (mm)
10
8
6
4
2
M
A
M
J
J
A
S
O
Month

Fig. 2. Seasonal patterns at the grazed clay-loam site for: a. total LAI (----------), green LAI (——————), LAI of current year dead (shaded); b. LAI of C-3 and C-4 graminoids; c.) soil water content; and d.) precipitation events. Vertical lines are one s.e. above and below the mean.

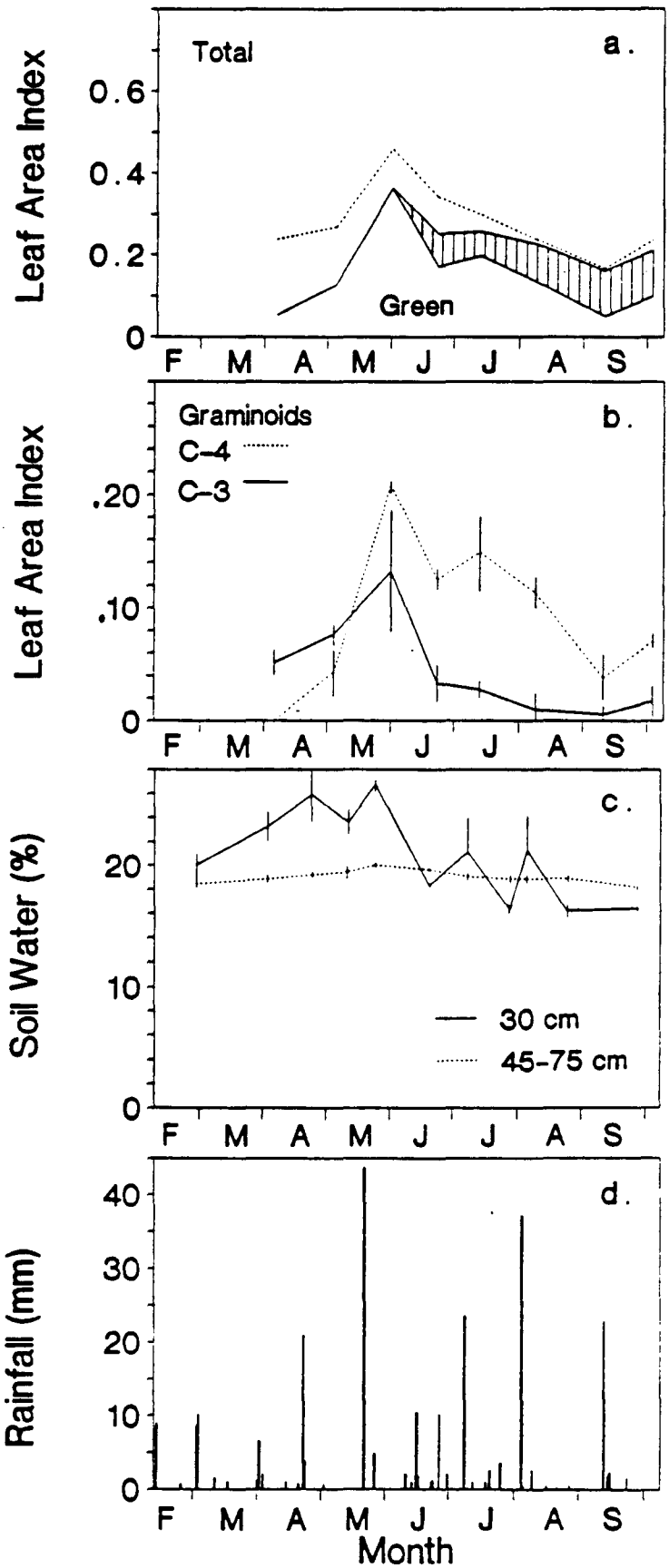
Leaf Area Index
Total
a.
0.6
0.4
0.2
0
Green
F M A M J J A S
Leaf Area Index
Graminoids
C-4
C-3
b.
.20
.10
0
F M A M J J A S
Soil Water (%)
c.
20
10
0
30 cm
45-75 cm
F M A M J J A S
Rainfall (mm)
d.
40
30
20
10
0
F M A M J J A S
Month

Fig. 3. Seasonal patterns at the loam sites: a. ungrazed and b. grazed for total LAI (----------), green LAI (——————), LAI of current year's dead (shaded); c. ungrazed site and d. grazed site for C-3 and C-4 graminoids; e. soil water content; and f. precipitation events. Vertical lines are one s.e. above and below the mean.

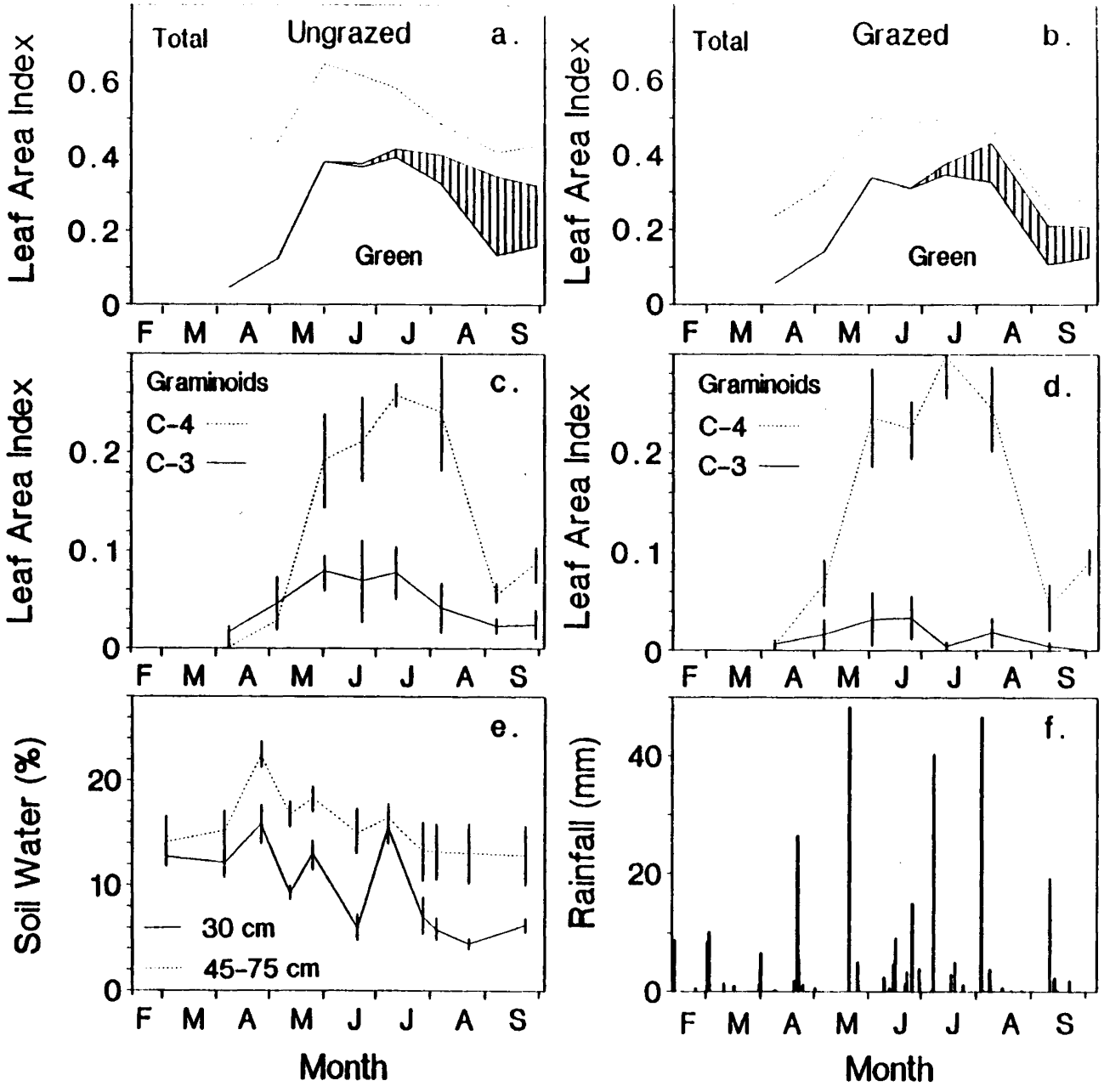
Total
Ungrazed
a.
Leaf Area Index
0.6
0.4
0.2
0
Green
F M A M J J A S
Total
Grazed
b.
Leaf Area Index
0.6
0.4
0.2
0
Green
F M A M J J A S
Graminoids
C-4
C-3
c.
Leaf Area Index
0.2
0.1
0
F M A M J J A S
Graminoids
C-4
C-3
d.
Leaf Area Index
0.2
0.1
0
F M A M J J A S
e.
Soil Water (%)
20
10
0
30 cm
45-75 cm
F M A M J J A S
Month
f.
Rainfall (mm)
40
20
0
F M A M J J A S
Month

Fig. 4. Seasonal patterns at the sandy-loam site for: a. total LAI (.....), green LAI (———), LAI of current year's dead (shaded), b. LAI of C-3 and C-4 graminoids; c. soil water content; and d. precipitation events. Vertical lines are one s.e. above and below the mean.

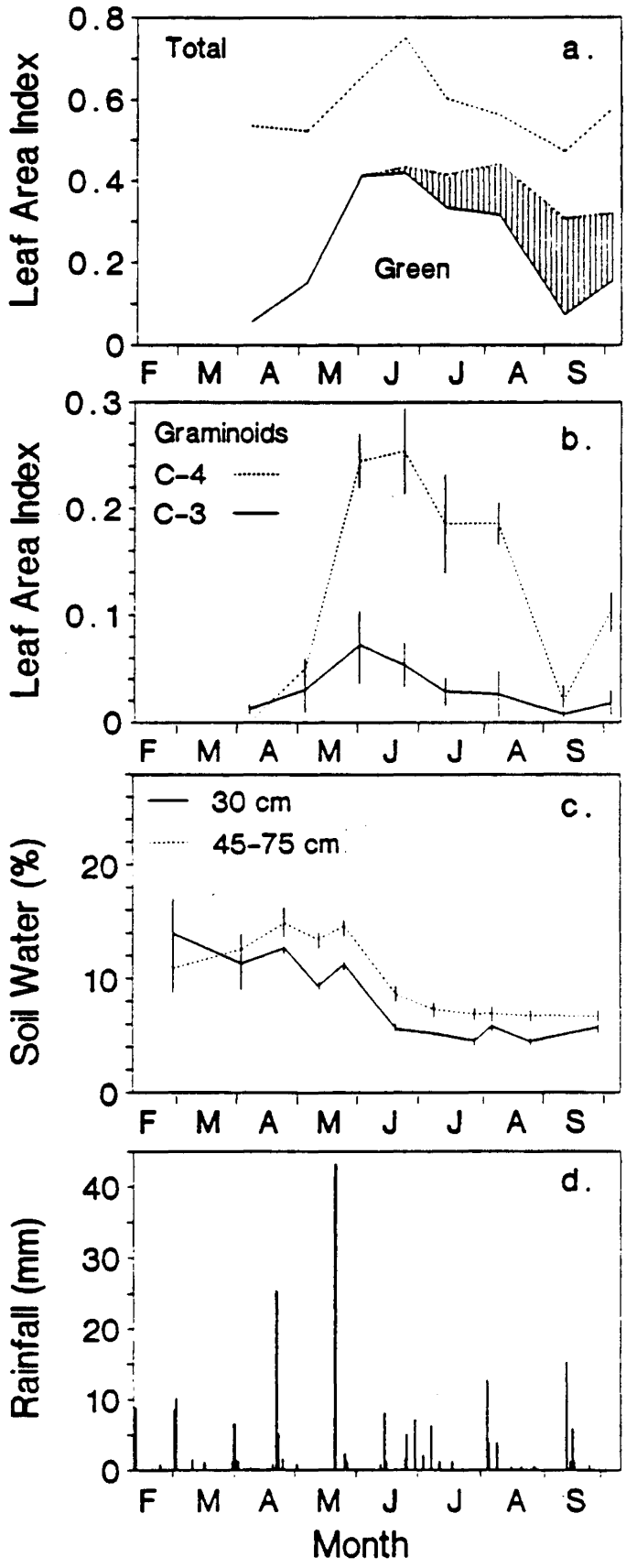
Leaf Area Index
0.8
0.6
0.4
0.2
0
Total
a.
Green
F M A M J J A S
Leaf Area Index
0.3
0.2
0.1
0
Graminoids
C-4
C-3
b.
F M A M J J A S
Soil Water (%)
20
10
0
30 cm
45-75 cm
c.
F M A M J J A S
Rainfall (mm)
40
30
20
10
0
d.
F M A M J J A S
Month

Fig. 5. Seasonal growth patterns relative to maximum LAI amounts for C-3 (————) and C-4 graminoids (----------) at the four study sites (a-d).

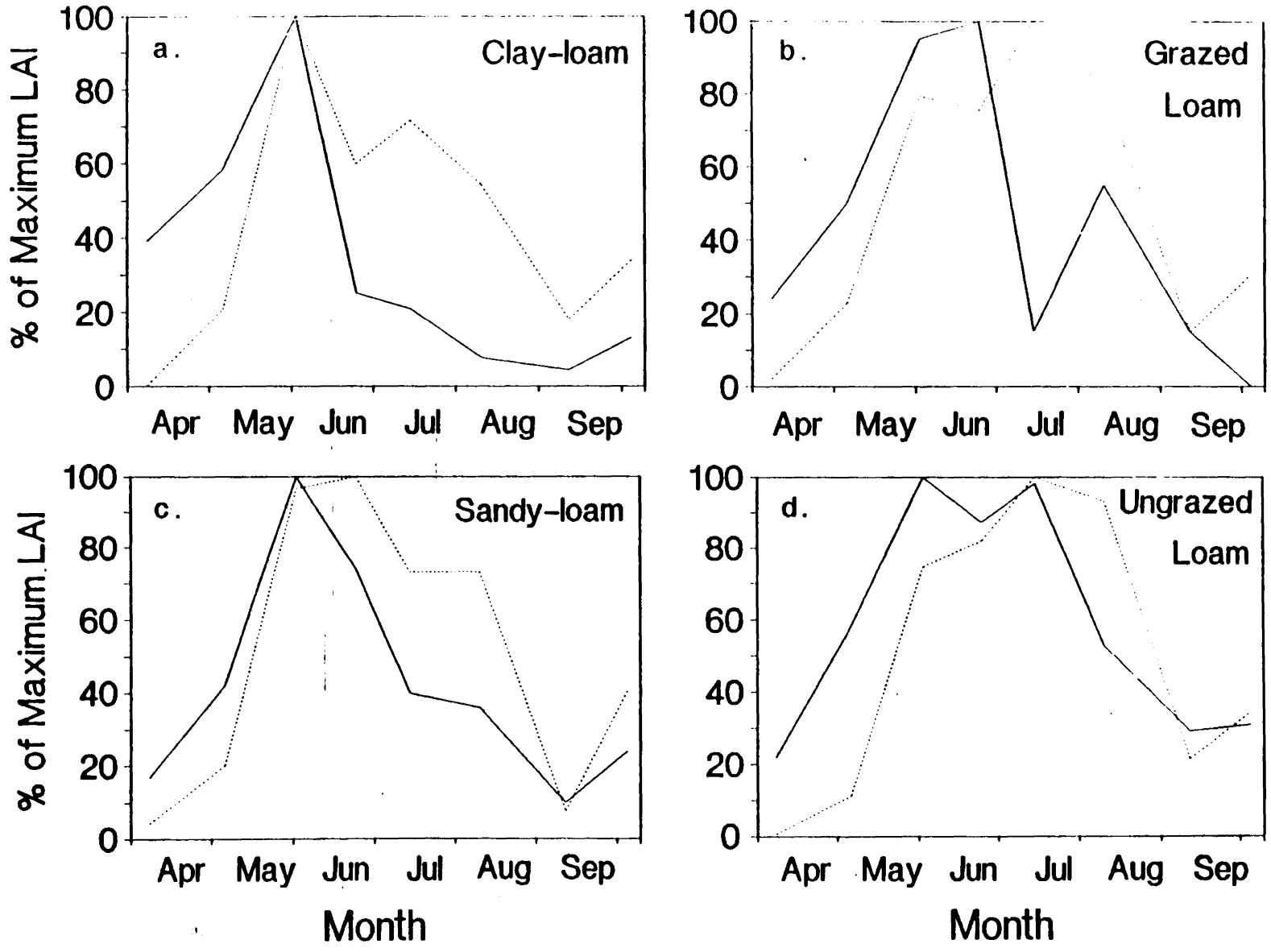
a.
Clay-loam
b.
Grazed
Loam
c.
Sandy-loam
d.
Ungrazed
Loam
% of Maximum LAI
% of Maximum LAI
100
80
60
40
20
0
Apr
May
Jun
Jul
Aug
Sep
Month
Month

Fig. 6. Seasonal patterns of LAI development for a. C-4 and b. C-3 species or groups of species. The C-4 taxa are: B. gracilis at the sandy-loam (.....), grazed loam (.....), and ungrazed-loam (———) sites; B. gracilis/B. dactyloides at the clay-loam site (--------); and composite LAI of A. purpurea (—·—·—·—) and S. cryptandrus (—··—··—) for both loam sites. The C-3 taxa are: C. eleocharis at the clay-loam (.....), grazed loam (.....) and ungrazed loam (———) sites; F. octoflora at the clay-loam site (—·—·—·); the combined LAI of S. comata and O. hymenoides (- - -) at the sandy-loam site: and the combined LAI of S. comata and A. smithii (*——*——*) for both loam sites.

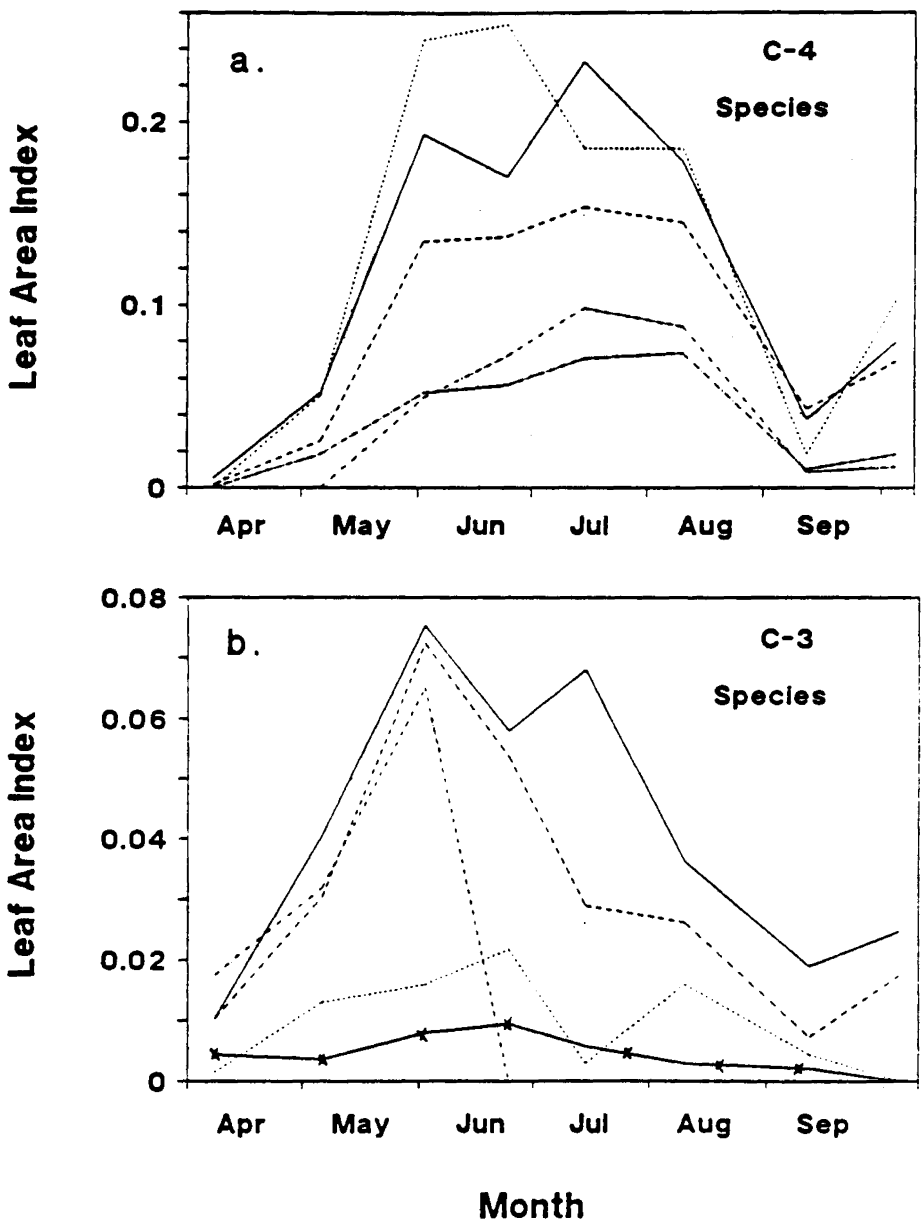
a.
C-4
Species
Leaf Area Index
0.2
0.1
0
Apr
May
Jun
Jul
Aug
Sep
b.
C-3
Species
Leaf Area Index
0.08
0.06
0.04
0.02
0
Apr
May
Jun
Jul
Aug
Sep
Month

Appendix D:

Report on the Fire at the Pawnee Grasslands Field Site on August 13, 1988

Report on the Fire at the Pawnee Grasslands Field Site on August 13, 1988

September 22, 1988

Introduction

At around midday Saturday, August 13, 1988, a fire occurred in the USFS instrument shelter located at the Pawnee grasslands field site. The fire was discovered by Dr. Donald Stedman midday Sunday, August 14, 1988. There was extensive damage to the contents of the shelter from the smoke and heat. The shelter and most of the instruments have since been refurbished, and data is being collected on a reduced scale as of September 22, 1988.

Damage and Current Status of Instruments

There was extensive smoke damage to the shelter and its contents. The ozone generator, Tylan flow controller, and relay switches in the total NO_x analyzer (NO_x Box) were destroyed. The other parts of the NO_x Box which were outside the instrument racks appear to have escaped serious damage. The chemiluminescent ambient air monitors (CAAMS) which were situated directly above the NO_x Box suffered superficial heat and smoke damage, as did the TECO 49 UV photometric ozone analyzers in the adjacent rack. These instruments were cleaned, serviced, and returned to operation. The data acquisition hardware required professional repair and service. The data stored on the Bernoulli cartridge was recovered by Technomics with approximately 70% success. The power supply in one of the sonic anemometer signal processing boxes was replaced and is now operating, and the other

has been sent to Applied Technologies, Inc., for repair. Much of the wiring and plumbing for the instruments were destroyed and have since been replaced. The Campbell CR21x data logger continued to operate during the fire and from the record of the "panel temperature" (i.e., the temperature inside the shelter), the time of the fire can be pinpointed (see Figure 1). The bottom of a small can of Freon was blown off and the release of Freon probably extinguished the fire.

The contents of the shelter were removed for cleaning and inspection. A new floor was laid in the shelter, and the instrument racks were painted before the instruments were returned. Some slight modifications have been effected to eliminate signal noise and provide more AC outlets near the instrument racks. Currently, two CAAM instruments are running at the site, both collecting ozone concentration and flux data. One UV photometric ozone analyzer is running; the other is waiting to be plumbed to the intake system and to be turned on. Only one anemometer is working, so only the upper intake system is in operation. Ozone, heat, and water vapor fluxes are being collected at the moment. The zero-air system is almost ready to be put into operation. Soil heat flux and net radiation data are being collected with the Campbell CR21x data logger.

Possible Causes

The hottest part of the fire was in the ozone generator of the NO_x box. This is probably where the fire started. Ozone is produced by flowing oxygen through high-voltage discharge tubes and arcing across

these tubes under vacuum can cause fire. In theory, a vacuum could have been created because there was no pressure relief valve present to prevent the tubes from being evacuated. However, the day before the fire the oxygen cylinder contained 1350 psi, sufficient to last approximately two weeks. To have lost so much oxygen overnight would require a sizeable leak such that it would be unlikely to result in a vacuum in the ozone generator. Downstream of the ozone generator is a water bubbler, which functions both to add water vapor to the analysis chamber and to scrub any oxides of nitrogen which may be produced in the discharge tubes (see Figure 2). Under normal operating conditions the ozone generator and water bubbler operate under 10-20 psi, regulated by the cylinder head and a frit downstream of the water bubbler. If there were a sudden loss of pressure at the discharge tubes, water would be pushed back into the discharge tubes, which could cause an electrical short circuit.

The temperature inside the shelter was constant (ca. 22°C) for three days preceding the fire. The diurnal variation seen previously had been eliminated by removing a heat load from the shelter. During the morning of the fire the temperature rose steadily to reach ca. 48°C. This phenomenon has been observed before as the air conditioning unit gathers a coating of ice and no longer cools. The increased temperature may have been a contributory cause of the fire, either by softening the pneumatic connections on the discharge tubes or by melting the tar inside the high-voltage transformer, leading to the short circuit.

Actions to Prevent a Future Fire

Any of the above possible causes are plausible explanations for the start of the fire. A pressure switch added in the oxygen lines to the discharge tubes could turn off the high-voltage supply whenever the pressure in the lines became dangerously low. A bleed valve could also be used to prevent the discharge tubes from being evacuated. The design of the discharge tubes could be improved to reduce the number of pneumatic fittings and relieve strain on the arms of the tubes. A glass water bubbler and trap would prevent water being blown back into the discharge tubes.

Daily inspections of the operation of the instruments and their environment would detect potential disasters before they happen. Ideally, this should be accomplished remotely by using computers and modems to report the status of each instrument to a Fort Collins base. Error checking routines could be included in the computer software which would shut the site down if a potentially dangerous situation arose.

Because the fire was apparently extinguished by the exploding Freon can, it would be prudent to store either such a can or other fire protection device in the shelter. Such a device should be nearer the instruments, but not placed in such a way as to damage the instruments should it be needed.

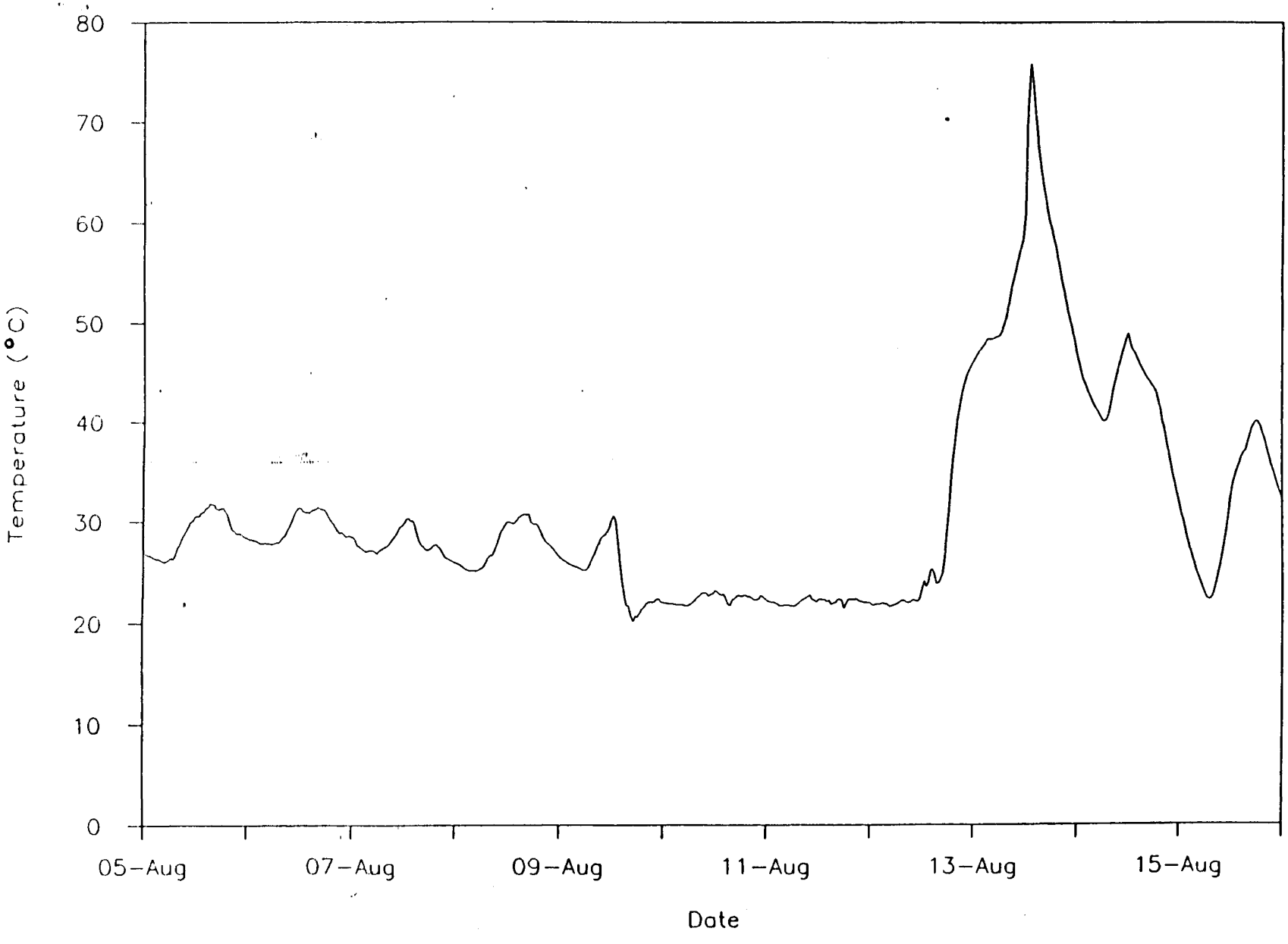

Figure 1. Temperature inside the shelter at the Pawnee grasslands field site from August 5 to August 15, 1988.

The data appear in two or three page tables in the following order:

	Page:
1. Heat Flux	E-2
2. Reynolds Stress	E-4
3. Ozone Average Concentration	E-7
4. Ozone Flux	E-9
5. NO2 Average Concentration	E-12
6. NO2 Flux	E-14
7. Average Temperature	E-17
8. Wind Direction	E-19
9. Wind Speed	E-21

USFS PAWNEE SITE

June, 1988

Heat Flux (meters/sec * deg. centigrade); Half Hour Averages * 100

Day	Hour	1:00		2:00		3:00		4:00		5:00		6:00		7:00		8:00		9:00		10:00		11:00		12:00		13:00	
1		-0.1	0.1	-1.9	-4.5	-4.9	-3.5	-3.2	-3.1	-2.8	-2.9	-3.7	-1.3	2.0	6.2	8.8	10.9	14.4	16.3	20.7	17.9	27.5	18.9	13.9	29.7	23.5	26.3	24.5
2		-0.8	-1.2	-1.1	-1.5	-1.2	-1.8	-4.0	-3.5	-3.5	-2.9	-2.4	-2.9	1.2	3.4	6.7	9.8	13.4	15.2	16.8	23.1	17.4	22.9	26.0	23.9	15.4		14.1
3		-0.5	-0.2	-0.3	-0.2	-0.0	-0.2	-0.1	-0.4	-0.3	-0.2	-0.1	-0.1	0.9		4.2	6.2	8.2	8.6	12.5	17.5	13.6	15.1	20.7	17.7	19.5	20.4	19.1
4		-1.4	-1.9	-1.6	-1.6	-1.5	-0.7	-1.4	-1.5	-0.7	0.1	-0.1	1.4	2.6	6.1	8.8	10.7	11.7	12.9	13.5	15.3	16.5	18.4	19.5	20.5	22.0	19.2	19.8
5		-1.5	-1.4	-1.3	-1.1	-1.0	-1.2	-1.5	-1.3	-0.9	-0.7	-0.4	0.7	2.9	5.9	8.5	10.5	14.9	14.1	15.9	18.8	21.4	0.0	0.0	29.6	20.8	20.2	17.9
6		-1.2	-0.5	-0.1	-0.3	-0.3	-0.4	-0.5	-0.4	0.1	-0.0	-0.2	0.4	2.2	4.1	6.2			10.7	11.4	12.7	14.2	17.7	18.3	18.2	16.8	18.7	15.2
7																		6.9	9.8	10.1	11.2	9.5	10.8		12.4	11.6	16.3	15.8
8		-0.6	-0.3	-0.1	-0.0	-0.5	-0.4	-0.7	-0.9	-2.4	-1.2	-1.8	-1.6	0.1	1.5	3.1	5.0	6.4	8.9	11.5	10.2	11.4	14.4	17.0	16.1	7.8	13.7	5.7
9		0.0	-0.8	-0.9	-0.1	-0.4	-0.4	0.0	-0.2	0.1	-0.4	-0.7	-0.4	-0.1	1.4	6.6	4.5	4.2		17.2	9.3	11.2	9.4	22.9	20.0	23.8	22.0	15.1
10		0.2	-0.2	-0.0	-0.1	0.1	0.1	-0.5	-0.1	-0.3	-0.2	-0.1	0.4	1.0	4.2		8.7	9.5	11.7	12.1	13.5	15.9	14.3	15.5	21.1	17.7	20.3	22.0
11		-0.5	-0.6	-0.9	-1.0	-0.8	0.6	-0.0	0.1	-0.6	-0.1	-0.2	-0.1	0.1	1.7	2.9	2.5	5.9	5.6	8.0	6.9	5.5	13.5	20.7	16.3	14.2	8.3	
12		-1.0	-0.6	-0.6	-0.3	-0.4	-0.4	-0.5	-0.2	0.0	-0.1	0.1	-0.4	1.5	0.4	0.9	1.1	2.0	3.3	2.8	8.3	13.9	18.8	18.6	19.0	25.5	30.1	27.9
13		-3.2	-2.9	-2.7	-1.8	-1.2	-1.4	-0.9	-0.5	-0.5	-0.5	-0.3	-0.3	2.3	4.4		10.9	9.7	11.6	11.6	14.0	21.2	27.9	25.7	25.3	14.2	12.1	7.2
14		-1.4	-1.8	-2.2	-2.1	-1.9	-1.7	-1.6	-2.0	-2.0	-1.9	-1.3	0.1	1.5	2.3	5.6		10.2	14.3	16.1	14.4	17.8	18.0	24.0	20.7			17.0
15		-0.3	-1.0	-2.1	-0.9	-0.2	-0.2	-0.1	0.1	0.4	-0.2	0.5		1.4	4.3	5.6	8.2	11.3	13.1	18.7	18.8	18.2	21.4	25.7	26.3	25.7	25.4	16.6
16																					11.1	12.6	14.0	12.8	16.6	12.8		
17																												
18		-0.3	-0.7	-0.5	-1.1	-1.7	-1.1	-1.7	-0.6	-1.0	-1.6	-0.8	-0.2	-0.8	-0.7	-0.5	0.6	3.5	3.4	9.1	5.7	5.1	12.2	19.3	11.6	11.2	13.8	
19		-0.0	0.1	0.1	-0.5	-0.9	-1.1	-1.0	-1.4	-0.9	-0.7	-2.2	-1.4	-2.2	-2.1	-1.2	1.5	3.2	6.8	9.9	10.9	13.4	17.7	16.8	18.8	21.0	17.4	28.3
20		-1.4	-1.5	-0.5	0.6	0.1	-1.8	-1.9	-0.8	0.1	0.2	-0.7	-0.1	-0.5	0.2	1.3	2.9	5.8	5.0	7.2	8.6	13.4	10.9	13.5	15.8	16.8	16.0	15.4
21		-0.6	-1.2	-2.3	-2.8	-2.6	-3.3	-3.8	-2.7	-3.8	-4.8	-3.1	-2.0	-1.8	-0.6	1.6	2.1	5.4	5.1	12.2	15.8	21.7		23.9	25.7	20.1	14.1	16.9
22		-3.7	-4.9	-4.0	-3.7	-3.5	-3.8	-3.5	-3.3	-3.2	-2.0	-2.9	-1.3	-2.0	-1.7	-1.2	4.0	4.7	8.3	10.4	14.0	15.7	15.3	11.0	11.5	14.8	9.4	10.7
23		-1.8	-0.8	-0.2	0.1	0.2	-0.8	-0.5	-0.4	-0.6	-0.0	-0.1	-0.1	-0.1		0.8	2.4	3.9	6.0	9.1	7.2	12.3	4.3	14.2	14.5	15.3	16.5	18.1
24																												
25		-3.4	-1.4	-1.6	-0.7	-0.8	-2.3	-2.6	-3.0	-5.6	-4.3	-3.2	-4.0	-3.1	-5.7	-4.1	-5.6	-1.3	-0.2	0.0	0.8	-0.6	-1.0	-0.7	-0.7	-0.7	0.2	0.8
26																												
27																					9.1	13.7	12.5	13.6	15.1	16.6	15.3	17.3
28		-1.1	-0.9	-1.0	-0.1	-0.4	0.2	-0.7	-0.4	0.2	-0.4	-0.3	0.2	2.1	5.1	6.4	9.6	11.1	11.8	14.2	17.6	17.2	20.5					
29		-1.7	-2.3	-2.2	-1.7	-2.1	-1.3	-1.1	-1.4	-1.4	-1.7	-1.2	-0.7	1.8	0.9	1.3		2.7	4.0	1.9	1.6	8.3	6.8	4.3	2.3			
30		-2.3	-2.5	-0.7	-0.1	-0.7	-1.6	-1.7	-6.7	-4.0	-1.8	-1.0	-0.4	1.3	2.5	4.6	9.3	11.4	9.4	10.0	20.1	21.9	25.0	21.2	21.2	17.4	15.6	
Min:		-3.7	-4.9	-4.0	-4.5	-4.9	-3.8	-4.0	-6.7	-5.6	-4.8	-3.7	-4.0	-3.1	-5.7	-4.1	-5.6	-1.3	-0.2	0.0	0.8	-0.6	-1.0	-0.7	-0.7	-0.7	0.2	0.8
Ave:		-1.2	-1.2	-1.2	-1.1	-1.1	-1.2	-1.4	-1.4	-1.4	-1.2	-1.1	-0.6	0.6	2.0	3.5	5.5	7.5	9.0	11.3	12.4	14.4	14.6	16.7	18.0	16.8	16.9	16.4
Max:		0.2	0.1	0.1	0.6	0.2	0.6	0.0	0.1	0.4	0.2	0.5	1.4	2.9	6.2	8.8	10.9	14.9	16.3	20.7	23.1	27.5	27.9	26.0	29.7	25.7	30.1	28.3
%Data:		80	77	77	77	77	77	77	77	77	77	77	74	77	71	71	68	77	77	81	87	87	84	81	84	77	71	68

(continued)
Heat Flux

Day	Hour 14:00		15:00		16:00		17:00		18:00		19:00		20:00		21:00		22:00		23:00		24:00		DAILY Min	Ave	Max	% Data
1	20.4	10.3	10.7	15.9		15.3	8.3	6.7	2.2	0.7	-3.3	-2.1	0.5	-0.4	-0.3	-0.1	-0.7	-0.2	-0.2	-0.1	-0.3		-4.9	6.7	29.7	98
2	14.3	17.0	14.1	13.1	10.0	9.7	5.4	3.5	2.6	0.1	-1.6	-1.7	-0.8	-0.1	-0.1	0.2	0.1	-0.2	-0.2	-0.2	-0.2		-4.0	5.7	26.0	98
3	14.2	18.4	14.6	12.7	11.5	11.3			2.4	0.2	-1.9	-0.9	-1.7	-2.1	-2.4	-2.3	-2.2	-2.1	-1.8	-1.7	-1.6		-2.4	5.5	20.7	94
4	20.1	20.1	17.5	13.5	11.5	9.8	7.8	3.6	1.1	-1.0	-2.5	-3.6	-3.5	-2.7	-3.5	-3.3	-3.0	-2.5	-1.7	-1.7	-1.7		-3.6	5.9	22.0	100
5	10.3	11.2	11.4	9.3	2.4	-0.4	-1.0	-1.1	-1.5	-2.0	-2.3	-3.0	-2.7	-2.2	-2.4	-2.3	-1.9	-0.9	-0.7	-0.4	-0.4		-3.0	4.4	29.6	100
6	15.6	13.4	13.8		9.3	6.7	5.2	2.1	-0.0	-1.4	-1.7	-1.4	-1.9	-0.8	-0.1	-0.1							-1.9	5.5	18.7	83
7	15.7	13.3		11.0	7.8	1.4	-0.1	-1.0	-0.7	-0.7	-0.9	-0.4	-1.3	-3.8	-2.8	-2.6	-1.7	-0.1	-1.2	-1.7	-0.5				16.3	63
8	4.2	15.6	3.9	12.1	9.6	6.9	6.1	1.7	-1.7	-2.0	-2.6	-2.1	-2.6	-0.9	-1.2	-0.6	-0.9	-0.8	-0.5	-0.1	-0.1		-2.6	3.5	17.0	100
9	17.1	4.8	-7.4	-4.2	-5.5	-3.9	-1.4	-5.6	-3.7	-1.8		-0.8	-1.1	-1.7	-1.1	-0.9	-1.8	-1.6	-1.2	-0.9	-0.3		-7.4	3.1	23.8	96
10	12.8	14.9	10.3	6.4	5.0	5.4	2.0	2.1	0.4	-0.5	-2.9	-1.0	-0.1	-0.5	-0.5	-2.4	-1.3	-0.2	-0.2	-1.1	0.3		-2.9	5.0	22.0	98
11	6.6	4.7	1.7	2.8	6.0	5.0	5.0	2.5	0.2	-1.2	-0.9	-0.9	-6.0	-3.5	-2.2	-1.4	-0.9	-1.6	-0.5	-1.5	-0.9		-6.0	2.6	20.7	98
12	22.9	20.5	17.7	18.2	12.7	4.4	0.2	0.0	-0.5	-0.2	-1.1	-1.4	-1.1	-2.3	-4.3	-0.9	-4.5	-0.4	-1.0	0.4	-0.8		-4.5	5.2	30.1	100
13	2.9	0.4	0.1	1.5	5.6	3.0	1.2	1.1	2.4	0.4	-0.3	-0.8	-0.6	-0.0	-0.1	-0.4	-0.6	-1.5	-0.6	-1.0	-0.6		-3.2	4.1	27.9	98
14	22.9	20.5	19.5	12.1	17.6	10.0	5.0	3.4	2.9	2.2	-0.2	-0.5	-0.7	-1.6	-0.9	-0.8	-0.9	-0.8	-0.5	-0.4	-0.2		-2.2	5.6	24.0	94
15	5.3	-2.5																					-2.5	8.6	26.3	58
16																										13
17											-0.3	-1.5	-1.7	-2.8	-3.1	-3.2	-0.9	-0.3	-0.6	-0.1	-0.9					23
18	4.9	0.4	0.2	-0.3	-1.2	-1.1	0.7	0.1	0.6	1.3	0.1	0.0	-0.0	-0.5	-1.7	-1.6	-1.9	-1.9	-2.6	-1.5			-2.6	1.7	19.3	96
19	22.6	16.9	3.2	2.6	2.6	3.2		5.4	4.3	1.7	0.7	-1.0	-0.4	-0.1	-1.8	-1.0	-1.7	-2.0	-1.1	-0.3	-1.0		-2.2	4.3	28.3	98
20	17.7	18.7	19.3	14.8	11.1	5.4	2.7	0.5	0.1	-0.1	-0.6	-0.5	-0.6	-0.2	-0.2	-5.1	-0.2	-0.1	-0.1	-0.6	-0.6		-5.1	4.3	19.3	100
21	14.2	1.4				0.5	3.0	1.6	1.9	0.4	-1.6	-1.0	-0.3	-0.0	-0.2	-0.0	0.7	0.2	0.2	-0.1	-0.8		-4.8	3.4	25.7	92
22	17.8	26.4	12.7	5.4	-0.8	-3.3	-0.1		0.5	-0.9	0.5	-0.4	-0.6	-0.1	-0.1	-0.1	-1.1	-0.1	0.0	-0.2	-0.3		-4.9	3.0	26.4	98
23	20.3	12.5	1.3	0.2		3.1	2.5	3.6	1.4	0.8	2.6	0.5	-0.1	0.1	-0.0	0.2	0.1						-1.8	4.0	20.3	88
24					16.2	16.3	12.3	11.0	9.9	4.7	2.8	0.5	-0.8	-0.4	-1.3	-0.3	-0.1	-3.5	-4.0	-3.5	-4.5					35
25	7.6	13.9	9.1	-0.4	0.5	-2.6																	-5.7		13.9	69
26																										0
27	17.6	19.6	16.7	14.3	15.0	13.4	7.5	6.0	4.8	7.1		-1.8	-2.0	-2.0	-1.6	-1.4	-1.8	-1.6	-1.5	-0.7	-1.2					58
28	14.1	15.2	15.1	16.1	7.7	3.9	3.3	1.9	3.2	-0.4	-0.9	-1.2	-0.1	-0.9	-0.5	-0.4	-0.3	-1.4	-1.2	-2.2	-2.2		-2.2	4.2	20.5	90
29						3.4	3.4	1.8	-0.5	0.8	0.6		-0.5	-1.1	-3.0	-0.8	-2.7	-4.7	0.1	0.3	-5.3		-5.3	0.2	8.3	79
30			18.3		16.5	10.4	7.9	0.3	-0.6	0.5	-0.3	-1.0	-0.3	-0.5									-6.7	5.9	25.0	77

																						MONTHLY Min	Ave	Max	ZData
Min:	2.9	-2.5	-7.4	-4.2	-5.5	-3.9	-1.4	-5.6	-3.7	-2.0	-3.3	-3.6	-6.0	-3.8	-4.3	-5.1	-4.5	-4.7	-4.0	-3.5	-5.3	-7.4			
Ave:	14.3	12.8	10.2	8.4	7.8	5.3	3.8	2.2	1.3	0.3	-0.8	-1.1	-1.2	-1.2	-1.4	-1.3	-1.3	-1.2	-0.9	-0.8	-1.1		4.3		
Max:	22.9	26.4	19.5	18.2	17.6	16.3	12.3	11.0	9.9	7.1	2.8	0.5	0.5	0.1	-0.0	0.2	0.7	0.2	0.2	0.4	0.3			30.1	
ZData:	77	77	71	68	71	84	74	74	81	81	77	81	84	84	81	81	77	74	74	74	71				80

USFS PAWNEE SITE

June, 1988

Reynold's Stress (m2/sec2); Half Hour Averages * 10

Day	1:00		2:00		3:00		4:00		5:00		6:00		7:00		8:00		9:00	
1	-0.08	-0.12	-0.23	-1.51	-1.60	-0.89	-0.74	-0.77	-0.56	-0.96	-3.00	-3.15	-5.12	-6.05	-5.26	-4.61	-3.68	-3.27
2	-0.11	-0.15	-0.22	-0.29	-0.19	-0.19	-0.62	-0.78	-1.17	-1.06	-1.25	-1.55	-1.85	-2.68	-3.40	-3.12	-3.17	-2.19
3	-0.03	-0.02	-0.02	-0.02	-0.04	-0.05	-0.01	-0.03	-0.05	-0.08	-0.07	-0.10	-0.10	-0.13	-0.20	-0.38	-0.33	-0.10
4	-0.14	-0.23	-0.22	-0.17	-0.14	-0.04	-0.15	-0.18	-0.12	-0.04	-0.05	-0.06	-0.28	-0.27	-0.25	-0.47	-0.31	-0.67
5	-0.21	-0.20	-0.16	-0.09	-0.12	-0.17	-0.26	-0.22	-0.13	-0.13	-0.23	-0.39	-0.92	-0.92	-1.07	-0.70	-0.56	-1.01
6	-0.03	-0.02	-0.04	-0.01	-0.02	-0.07	-0.10	-0.04	0.01	-0.00	-0.09	-0.23	-0.36	-0.24	-0.13	0.00	0.00	-0.14
7																	-1.22	-1.06
8	-0.05	-0.03	-0.03	-0.02	-0.03	-0.01	-0.05	-0.08	-0.35	-0.21	-0.42	-0.78	-1.08	-1.14	-1.00	-0.81	-0.83	-0.80
9	0.02	-0.14	-0.19	-0.02	-0.08	-0.06	-0.08	-0.00	-0.02	-0.01	-0.03	-0.06	-0.07	-0.02	0.06	-0.29	-0.06	0.00
10	-0.01	-0.00	0.01	-0.03	0.02	0.01	-0.04	-0.06	-0.02	-0.01	-0.04	-0.13	-0.28	-0.29		-0.68	-0.26	0.10
11	-0.03	-0.06	-0.07	-0.11	-0.07	0.02	-0.01	0.00	-0.03	-0.01	-0.04	-0.06	-0.02	-0.22	-0.21	-0.33	-0.61	-0.49
12	-0.13	-0.17	-0.09	-0.05	-0.07	-0.04	-0.13	-0.00	-0.02	-0.03	-0.01	-0.05	-0.11	-0.16	-0.15	-0.09	-0.21	-0.06
13	-1.44	-0.90	-0.92	-0.28	-0.29	-0.30	-0.20	-0.09	-0.07	-0.10	-0.05	-0.25	-0.42	-0.35		-0.40	-0.47	-1.00
14	-1.13	-1.37	-2.23	-2.52	-1.84	-1.46	-1.38	-2.27	-1.41	-1.24	-0.98	-0.85	-1.20	-0.74	-0.61	0.00	-0.45	-0.30
15	-0.02	-0.09	-0.32	-0.06	-0.12	-0.04	-0.00	-0.00	-0.00	0.00	-0.01	0.00	-0.41	-0.50	-0.30	-0.71	-1.35	-1.01
16	0.00	-0.00	-0.02	-0.07	-0.05	-0.06	-0.02	0.00	-0.03	0.01	-0.02	-0.05	-0.06	-0.08	-0.21	-0.15	-0.14	-0.22
17																		
18	-0.05	-0.07	-0.07	-0.08	-0.18	-0.09	-0.12	-0.07	-0.14	-0.17	-0.05	-0.03	-0.07	-0.10	-0.10	-0.24	-0.51	-0.25
19	-0.00	-0.02	-0.02	-0.03	-0.08	-0.12	-0.26	-0.15	-0.18	-0.08	-0.23	-0.30	-0.50	-0.73	-1.04	-1.46	-2.14	-2.80
20	-0.20	-0.20	-0.05	0.01	0.00	-0.20	-0.18	-0.05	-0.04	0.01	-0.11	-0.00	-0.04	-0.06	-0.26	-0.19	-0.22	-0.05
21	-0.07	-0.18	-0.47	-0.46	-0.43	-0.53	-0.69	-0.31	-0.75	-1.23	-0.66	-0.45	-0.42	-0.82	-1.19	-0.78	-0.91	-0.54
22	-1.41	-3.89	-2.76	-1.62	-1.18	-1.42	-1.07	-0.90	-0.83	-0.35	-0.69	-0.39	-0.54	-1.54	-2.05	-1.77	-1.76	-2.04
23	-0.21	-0.15	-0.06	0.00	-0.01	-0.13	-0.09	-0.08	-0.15	-0.01	-0.02	-0.02	-0.06	0.00	-0.29	-0.30	-0.22	0.03
24																		
25	-1.70	-0.30	-0.27	-0.18	-0.02	-0.23	-1.06	-1.09	-2.45	-0.48	-0.21	-0.65	-2.75	-2.46	-0.52	-1.15	-0.36	-0.33
26																		
27																		
28	-0.08	-0.03	-0.04	-0.05	-0.02	-0.02	-0.07	-0.06	0.02	-0.04	-0.11	-0.13	-0.27	-0.35	-0.15	-0.23	-0.31	-0.44
29	-1.25	-1.48	-2.00	-1.41	-1.10	-0.37	-0.38	-0.48	-0.36	-0.45	-0.68	-1.00	-0.94	-1.03	-1.08	0.00	-0.84	-0.58
30	-0.42	-0.35	-0.13	-0.02	-0.03	-0.44	-0.34	-2.60	-5.36	-4.58	-2.95	-2.87	-3.47	-3.30	-4.84	-5.55	-5.52	-5.72
Min:	-1.7	-3.9	-2.8	-2.5	-1.8	-1.5	-1.4	-2.6	-5.4	-4.6	-3.0	-3.2	-5.1	-6.0	-5.3	-5.5	-5.5	-5.7
Ave:	-0.4	-0.4	-0.4	-0.4	-0.3	-0.3	-0.3	-0.4	-0.6	-0.4	-0.5	-0.5	-0.9	-1.0	-1.1	-1.0	-1.0	-1.0
Max:	0.0	-0.0	0.0	0.0	0.0	0.0	-0.0	0.0	0.0	0.0	-0.0	0.0	-0.0	0.0	0.1	0.0	0.0	0.1
%Data:	83	81	81	81	81	81	81	81	81	81	81	81	81	81	74	81	84	84

(Continued)
Reynolds Stress

Hour	10:00			11:00		12:00		13:00		14:00		15:00		16:00		17:00		18:00
Day																		
1	-3.36	-2.67	-3.08	-2.64	-2.79	-3.80	-3.18	-3.88	-2.71	-3.38	-2.61	-2.25	-2.37		-2.40	-3.77	-3.28	-2.62
2	-2.63	-3.29	-2.25	-2.84	-2.22	-2.47	-2.42	0.00	-2.88	-3.00	-2.53	-2.59	-2.27	-1.91	-2.01	-1.74	-2.35	-1.63
3	-0.10	-0.56	-0.24	-0.13	-0.50	-0.59	-1.31	-0.60	-0.38	-0.68	-0.26	-0.82	-0.64	-0.71	-1.14	0.00	0.00	-0.94
4	-0.54	-0.80	-0.94	-1.76	-0.97	-1.32	-1.75	-1.64	-2.16	-1.76	-2.17	-1.87	-1.17	-1.55	-2.12	-2.64	-2.54	-2.14
5	-0.99	-1.38	-1.66			-1.24	-1.64	-2.40	-2.01	-1.79	-3.20	-2.70	-3.53	-3.05	-1.83	-1.80	-1.51	-1.90
6	0.06	-0.09	-0.42	-0.00	0.04	-0.59	-0.33	-0.67	-0.36	0.03	-0.24	-0.09		-0.58	-0.68	-0.73	-0.48	-0.57
7	-0.74	-0.36	-0.43	-0.52		-0.45	-0.41	-1.01	-0.90	-0.73	-0.97		-0.60	-0.48	-0.16	-0.48	-0.42	0.00
8	-0.63	-0.83	-0.89	-0.61	-0.78	-0.79	-0.93	-1.23	-1.39	-0.43	-2.00	-1.31	-2.16	-1.30	-0.89	-1.03	-1.03	-0.32
9	-0.56	-0.11	-0.42	-1.06	-1.34	-0.85	-0.92	-1.64	-1.40	-1.68	-1.85	-1.06	-0.60	-0.80	-0.96	-1.53	-1.61	-0.72
10	-0.11	-0.19	-0.24	-0.36	-0.35	-1.14	-0.49	-0.72	-1.23	-0.65	-0.79	-0.62	-0.62	-0.47	-0.72	-0.57	-1.01	-0.51
11	-0.38	-0.59	-0.59	-0.43	-0.50	-0.26	-0.86	-0.61		-0.98	-3.17	-1.86	-1.62	-1.27	-1.71	-2.08	-2.88	-2.78
12	-0.02	-0.40	-0.09	-0.37	-0.05	-0.38	-0.86	-0.99	-1.05	-1.42	-0.05	-0.76	-0.76	-0.78	-0.78	-1.03	-2.87	-0.57
13	-0.55	-0.24	-0.26	-0.78	-0.37	-0.39	0.10	-0.44	-1.76	-0.67	-0.53	-0.48	-0.07	-1.06	-0.95	-0.41	-0.22	-0.09
14	-0.55	-0.73	-0.32	-0.95	-0.33	-0.27			-0.59	-0.02	-0.33	-0.69	-0.59	-0.79	-0.79	-0.05	-1.03	-0.87
15	-1.40	-1.26	-0.85	-1.19	-1.71	-1.13	-0.71	-1.28	-0.66	-0.47	-0.16	-1.03	0.01	-0.18	-0.60	-1.25	-0.95	-1.28
16	-0.22	-0.40	-0.32	-0.49	0.05	-0.51	-0.35											
17																		
18	-0.73	-0.69	-0.26	-0.14	-1.09	-2.08	-0.84	-0.45		-0.04	-0.24	-2.21	-1.95	-1.25	-1.88	-2.10	-1.42	-0.97
19	-2.17	-1.75	-1.29	-0.99	-0.55	-0.30	-0.84	-0.48	-1.09	-1.93	-0.12	-0.62	-0.52	-0.29	0.01		-0.60	-0.43
20	-0.04	-0.25	-0.67	-0.31	-0.46	-0.60	-0.26	-0.68	-0.51	-0.23	0.03	-0.47	-0.30	-0.74	-0.82	-0.43	-0.37	-0.19
21	-1.91	-2.61	-2.43		-1.86	-1.89	-1.50	-1.02	-0.66	-1.07	-0.88				-0.63	-1.37	-1.00	-1.61
22	-1.57	-1.49	-0.91	-1.11	-0.46	-0.23	-0.07	-0.34	-0.01	-0.32	0.02	-0.27	-1.78	-0.62	-0.53	-0.11		0.03
23	-0.24	-0.09	-0.50	-0.18	-0.39	-0.69	-0.36	-0.50	-0.56	-1.12	-0.32	-0.46	-0.48		-1.06	-0.79	-0.89	-0.65
24														-0.58	-0.94	-1.09	-0.67	-0.37
25	-0.60	-1.21	-1.12	-0.88	-0.97	-1.00	-0.62	-0.08	-0.90	-0.93	-0.31	-1.88	-2.29	-4.76	-0.74			
26																		
27		-0.28	-0.65	-0.66	-1.25	-0.64	-0.94	-0.71	-1.09	-1.06	-0.64	-1.54	-1.34	-1.26	-1.28	-1.12	-1.37	-1.03
28	-0.51	-0.78	-0.89	-1.19						-0.41	-0.48	-0.54	-0.55	-0.71	-0.50	-0.54	-0.44	-0.93
29	-0.13	0.08	-0.24	0.02	-0.26	-0.27									-0.45	-0.53	-0.45	-0.40
30	-4.76	-5.79	-4.65	-5.53	-4.22	-3.74	-3.12	-2.47				-1.49		-1.48	-0.45	-0.92	-0.65	-0.51
Min:	-4.8	-5.8	-4.7	-5.5	-4.2	-3.8	-3.2	-3.9	-2.9	-3.4	-3.2	-2.7	-3.5	-4.8	-2.4	-3.8	-3.3	-2.8
Ave:	-1.0	-1.1	-1.0	-1.0	-1.0	-1.1	-1.0	-1.0	-1.2	-1.0	-1.0	-1.2	-1.2	-1.2	-1.0	-1.1	-1.2	-0.9
Max:	0.1	0.1	-0.1	0.0	0.0	-0.2	0.1	0.0	-0.0	0.0	0.0	-0.1	0.0	-0.2	0.0	0.0	0.0	0.0
XData:	84	87	87	81	77	84	77	74	68	77	77	74	71	74	87	81	81	84

(continued)
Reynolds Stress

Day	19:00	20:00	21:00	22:00	23:00	24:00	DAILY Min	DAILY Ave	DAILY Max	% Data
1	-2.32 -1.75	-0.36 -0.04	-0.78 -0.07	-0.01 -0.11	-0.06 -0.04	-0.01 -0.01	-6.0	-2.1	-0.0	98
2	-1.82 -1.29	-0.56 -0.10	0.00 -0.00	-0.00 -0.01	-0.00 -0.01	-0.03 -0.01	-3.4	-1.4	0.0	100
3	-1.05 -0.61	-0.11 -0.15	-0.25 -0.31	-0.28 -0.26	-0.33 -0.26	-0.27 -0.18	-1.3	-0.3	0.0	100
4	-2.22 -1.45	-1.09 -1.09	-0.63 -1.10	-1.21 -0.93	-0.52 -0.34	-0.34 -0.25	-2.6	-0.9	-0.0	100
5	-1.70 -0.98	-1.28 -1.87	-1.18 -0.67	-0.63 -0.49	-0.13 -0.04	-0.04 -0.02	-3.5	-1.1	-0.0	96
6	-0.69 -0.33	-0.15 -0.20	-0.08 -0.03				-0.7	-0.2	0.1	85
7	-0.06 -0.10	0.06 -0.06	-1.22 -0.76	-0.34 -0.01	0.00 -0.26	-0.31 -0.07	-1.2	-0.5	0.1	63
8	-0.39 -0.55	-0.40 -0.34	-0.10 -0.16	-0.07 -0.16	-0.08 -0.09	-0.06 -0.02	-2.2	-0.6	-0.0	100
9	-1.31	-0.10 -0.72	-1.47 -1.17	-0.55 -0.69	-0.68 -0.45	-0.21 -0.03	-1.8	-0.6	0.1	98
10	-0.25 -1.82	-0.49 -0.04	-0.05 -0.18	-0.77 -0.09	0.01 0.00	-0.04 0.01	-1.8	-0.3	0.1	98
11	-3.17 -1.66	-0.69 -0.70	-0.65 -0.84	-0.33 -0.22	-0.16 -0.05	-0.35 -0.12	-3.2	-0.7	0.0	98
12	-0.04 -0.41	-0.55 -3.05	-2.28 -2.24	-0.54 -0.19	-0.29 -0.44	-0.71 -0.76	-3.1	-0.5	-0.0	100
13	-0.28 -0.27	-0.35 -0.09	-0.01 -0.00	-0.12 -0.58	-1.21 -1.25	-1.16 -0.53	-1.8	-0.5	0.1	98
14	-1.06 -0.76	-0.77 -0.33	-0.36 -0.24	-0.37 -0.48	-0.36 -0.16	-0.07 -0.00	-2.5	-0.8	0.0	96
15	-0.62 -0.79	-0.37 -0.28	-0.44 -0.25	-0.17 -0.32	-0.03 -0.02	-0.00 0.02	-1.7	-0.5	0.0	100
16							-0.5	-0.1	0.0	52
17	-0.96	-0.33 -0.83	-1.73 -1.36	-0.35 -0.14	-0.02 -0.04	-0.00 -0.03	-1.7	-0.5	-0.0	23
18	-0.67 -0.36	-0.03 0.00	0.01 -0.25	-0.71 -0.52	-0.48 -0.60	-0.21 0.00	-2.2	-0.5	0.0	98
19	0.04 -0.22	-0.27 -0.02	-0.00 0.01	-0.02 -0.13	-0.14 -0.09	0.00 -0.07	-2.8	-0.5	0.0	98
20	-0.05 -0.28	-0.10 -0.15	-0.01 -0.05	-0.13 -0.03	-0.01 0.01	-0.08 -0.09	-0.8	-0.2	0.0	100
21	-1.41 -1.75	-0.70 -0.28	-0.13 -0.00	-0.01 -0.02	0.00 0.00	-0.01 -0.11	-2.6	-0.8	0.0	92
22	-0.77 -1.03	-0.98 -0.38	-0.03 -0.00	0.00 -0.13	-0.03 0.01	-0.05 -0.07	-3.9	-0.8	0.0	98
23	-0.23 -0.30	-0.10 -0.03	-0.00 0.01	0.01 -0.00			-1.1	-0.3	0.0	90
24	-0.24 -0.71	-0.30 -0.10	-0.02 0.01	0.00 0.03	-1.45 -1.45	-1.46 -2.19	-2.2	-0.7	0.0	35
25							-4.8	-1.0	-0.0	69
26							ERR	ERR	ERR	0
27	-1.47	-0.58 -0.50	-0.42 -0.27	-0.23 -0.27	-0.29 -0.25	-0.11 -0.18	-1.5	-0.8	-0.1	58
28	-0.60 -0.43	-0.35 -0.01	-0.04 -0.01	-0.00 -0.01	-0.26 -1.24	-1.51 -1.23	-1.5	-0.4	0.0	90
29	-0.82 -0.20	0.00 -0.08	-0.55 -2.17	0.02 -1.10	-2.41 0.01	-0.03 -0.57	-2.4	-0.6	0.1	83
30	-0.65 -0.84	-0.43 -0.03	-0.04				-5.8	-2.4	-0.0	77

	19:00	20:00	21:00	22:00	23:00	24:00	MONTHLY Min	MONTHLY Ave	MONTHLY Max	MONTHLY %Data
Min:	-3.2 -1.8	-1.3 -3.1	-2.3 -2.2	-1.2 -1.1	-2.4 -1.5	-1.5 -2.2	-6.0			
Ave:	-0.9 -0.8	-0.4 -0.4	-0.5 -0.5	-0.3 -0.3	-0.4 -0.3	-0.3 -0.3		-0.7		
Max:	0.0 -0.1	0.1 0.0	0.0 0.0	0.0 0.0	0.0 0.0	0.0 0.0			0.1	
%Data:	84 81	87 87	87 84	81 81	77 77	77 77				83

USFS PAWNEE SITE

June, 1988
Ozone Average Concentration (ppb); Half Hour Averages.

Day	1:00		2:00		3:00		4:00		5:00		6:00		7:00		8:00		9:00		10:00		11:00		12:00		13:00	
1	23.1	31.1	34.9	36.2	37.5	36.8	36.9	39.2	39.3	41.8	48.7	49.1	48.9	49.1	49.3	49.3	49.3	50.3	52.2	53.6	55.6	55.8				
2	38.5	30.1	21.0	19.6	20.5	22.3	28.5	28.8	28.2	27.0	27.4	28.1	28.2	28.6	28.8	30.6	31.9	38.4	45.8	44.6	43.7	42.8	44.5	44.1	43.1	44.9
3	21.6	21.4	24.5	24.4	23.0	23.9	22.8	23.8	23.4	20.0	19.6	22.7	36.8	47.8	48.2	51.0	53.0	53.7	55.0	56.3	58.0	59.7	61.6	64.0	63.5	63.5	64.0
4	37.0	36.9	38.3	39.3	39.6	38.0	35.8	36.9	36.6	37.1	38.5	36.5	44.7	47.5	49.5	51.6	54.1	56.7	59.5	60.4	60.4	59.9	60.3	61.1	60.2	59.6	58.8
5	44.8	42.9	42.0	37.6	36.4	37.7	38.7	35.8	34.9	33.0	33.2	36.1	40.1	42.5	44.0	46.2	47.8	48.9	49.4	50.3	51.3				53.7	54.1	53.8
6	37.5	37.4	38.5	37.1	32.6	28.8	28.1	28.7	24.6	29.0	26.4	30.7	33.5	36.2	37.4	38.7	41.7	45.1	47.2	50.4	54.1	57.5	58.6	58.7	59.3	59.6	60.2
7																	48.0	49.4	50.4	51.4		40.2	40.2	61.9	64.7	61.9	62.4
8	30.3	22.2	26.8	30.2	30.4	30.2	32.9	33.0	34.5	33.0	27.7	25.6	25.7	29.3	32.9	37.4	43.9	47.3	48.5	49.6	51.1	52.5	54.0	55.7	54.8	56.1	56.0
9	25.6	29.7	38.5	35.1	35.6	31.1	28.9	30.3	32.4	29.6	29.8	29.2	32.1	33.3	39.8	46.1	50.7	55.1	57.7	59.5	59.9	60.0	59.3	58.3	60.5	59.5	59.0
10	20.4	16.0	23.8	22.4	24.4	24.9	17.7	27.2	24.4	20.4	17.4	22.2	27.7	29.3	30.8	34.5	36.6	38.7	41.4	44.3	46.4	49.7	51.2	54.0	58.2	61.3	64.3
11	25.3	24.1	25.2	23.7	25.6	28.0	31.1	32.3	25.7	28.1	26.5	28.3	26.3	32.2	29.5	32.9	42.2	45.8	47.8	50.9	54.3	57.1	58.0	57.6	58.2	56.3	60.1
12	26.3	22.8	20.5	21.4	24.8	22.3	21.4	19.2	19.0	21.8	18.4	18.5	25.6	33.2	35.7	40.9	44.8	46.4	50.6	51.0	51.1	52.2	53.5	55.2	56.7	58.0	58.3
13	41.3	38.4	38.6	33.1	26.5	29.2	27.1	26.2	27.0	25.1	26.2	26.3	30.2	46.1	49.2	49.4	48.4	46.1	46.7	47.5	48.6	49.7	50.8	51.3	53.0	53.5	54.0
14	36.7	42.4	49.1	50.7	42.0	42.6	45.8	47.4	47.3	43.5	39.1	41.8	41.2	40.7	42.9	41.6	43.4	44.1	45.9	47.6	48.9	50.2	51.0	51.7	53.3	54.3	54.8
15	39.1	37.5	37.9	34.0	30.6	29.3	25.2	21.8	19.4	20.9	16.7	22.0	33.3	37.7	42.0	47.5	51.7	54.5	57.3	57.8	58.6	59.8	59.9	59.8	60.5	61.1	61.6
16	33.5	29.1	24.3	21.9	25.3	24.2	25.9	22.2	18.9	22.7	18.5	17.5	19.5	32.6	36.4	43.8	47.9	53.2	58.9	49.7	48.1	49.7	52.9	55.7		41.9	
17	26.7	24.8	31.0	20.8	33.3	31.4	32.4	28.2	29.5	28.9	32.9	30.3	29.7	37.8	41.0	44.3	50.8	53.2	55.0	57.9	56.1	54.5	58.4				
18	34.1	32.0	32.1	32.7	31.9	30.0	29.7	27.2	26.6	26.6	24.9	26.6	27.4	30.0	35.9	39.5	45.4	49.0	51.9	54.4	54.6	54.3	59.3	59.0	64.3	66.6	65.6
19	42.0	36.3	35.9	31.1	31.3	30.4	29.5	30.5	30.5	31.7	31.6	32.2	33.2	34.7	39.0	43.0	46.1	49.1	50.9	52.1	53.5	54.3	54.7	54.4	54.9	54.8	55.3
20	36.5	36.3	32.4	33.0	29.7	30.5	28.9	25.4	23.5	22.1	18.8	21.7	23.8	29.0	34.8	42.3	47.6	51.9	55.5	57.7	59.2	60.7	63.5	65.1	66.7	67.9	68.4
21	30.2	31.8	32.4	31.3	35.2	32.7	36.8	35.8	37.2	36.4	35.5	36.3	36.8	38.1	40.2	42.4	45.0	48.7	52.6	54.8	53.7	58.0	54.7	59.0			
22																											
23	38.0	37.9	37.6	37.4	37.5	37.7	37.6	37.7	38.1	37.5	37.6	37.8	39.5	40.6	42.5	45.4	48.6	51.3	53.8	55.5	55.1	56.5	59.5	61.5	62.5	62.9	63.0
24	37.9	37.7	37.9	37.8	37.6	37.4	37.1	37.0	37.0	37.0	37.5	37.8	38.5	40.2	41.9	44.6	47.9	51.3	54.2	57.1	58.2	58.3	59.6	61.2	62.3	61.5	61.2
25	40.5	36.6	32.8	31.4	36.4	45.6	49.6	41.9	43.6	42.6	42.7	41.3	40.2	40.3	34.3	34.7	36.1	36.6	38.3	37.0	38.1	39.3	44.9	46.3	54.3	59.0	63.4
26	23.2	22.9	17.4	19.8	23.1	25.5	24.3	26.6	31.6	28.1	28.6	25.8	31.9	40.1	43.0	45.4	52.4	54.4	60.3	63.8	65.9	67.7	69.8	72.6	75.2	76.0	78.4
27	37.8	33.3	38.6	38.4	31.6	32.9	27.2	24.2	16.3	12.5	14.7	17.8	31.8	35.7	39.9	41.7	43.0	49.7	53.2	57.3	58.5	57.7	53.2	53.2	53.9	54.7	57.9
28	34.3	35.5	35.4	36.7	31.1	26.3	24.7	24.1	25.7	21.3	24.2	26.2	32.2	35.8	39.4	42.7											
29	50.3	56.2	63.8	61.1	61.6	58.9	56.0	43.6	45.8	44.3	45.5	45.5	48.3	44.0	49.2		47.2	51.8	53.8	53.6	55.9	57.8	56.3	58.8			
30	29.2	29.5	24.7	21.4	24.2	21.9	21.8	24.9	30.5	32.6	32.7	31.6	30.8	32.0	37.1	42.9	48.9	48.7	49.0	48.1	42.0	45.2	54.0	53.5	53.5	53.9	55.9
Min:	20.4	16.0	17.4	19.6	20.5	21.9	17.7	19.2	16.3	12.5	14.7	17.5	19.5	28.6	28.8	30.6	31.9	36.6	38.3	37.0	38.1	39.3	40.2	44.1	43.1	41.9	44.9
Ave:	33.6	32.6	33.4	32.4	32.1	31.8	31.5	30.7	30.4	29.8	29.3	30.2	33.5	37.3	39.8	42.6	46.2	48.9	51.5	52.6	53.4	54.1	55.5	57.4	58.6	59.0	60.1
Max:	50.3	56.2	63.8	61.1	61.6	58.9	56.0	47.4	47.3	44.3	48.7	49.1	48.9	49.1	49.5	51.6	54.1	56.7	60.3	63.8	65.9	67.7	69.8	72.6	75.2	76.0	78.4
%Data:	93	90	90	90	90	90	90	90	90	90	90	90	90	90	90	87	90	90	90	90	87	87	84	81	74	74	74

(continued)
Ozone Concentration

Day	Hour 14:00	15:00	16:00	17:00	18:00	19:00	20:00	21:00	22:00	23:00	24:00	DAILY Min	Ave	Max	% Data
1						38.5 35.4	35.8 39.9	39.9 37.2	37.7 36.6	32.2 30.9	34.3	23.1	41.4	55.8	69
2	46.3 44.4	45.2 44.3	43.1 42.7	42.2 41.1	40.3 39.3	46.4 46.5	42.4 40.3	38.7 38.6	35.5 28.2	26.2 25.4	23.8	19.6	35.8	46.5	98
3	64.3 65.0	66.4 68.2	69.5 73.1		65.9 63.3	60.3 55.2	50.5 48.0	45.8 44.4	42.8 40.8	40.6 39.7	37.6	19.6	46.7	73.1	96
4	58.8 58.8	58.7 58.3	58.1 58.8	59.1 59.3	59.0 58.7	58.1 56.3	56.3 52.8	52.0 52.4	50.7 49.5	48.0 46.4	46.3	35.8	51.1	61.1	100
5	52.5 53.2	55.2 56.8	56.9 55.7	55.4 56.0	56.9 56.7	56.1 54.7	51.8 53.5	54.4 51.7	49.3 45.4	43.9 39.6	38.8	33.0	47.3	56.9	94
6	60.4 59.5	58.3 58.1	56.6 56.1	56.9 57.0	58.3 58.3	55.3 52.0	49.7 46.8	46.6				24.6	46.4	60.4	88
7	60.1 59.7	59.2	60.8 61.8	58.7 61.3	56.3 52.3	48.3 45.5	47.4 50.7	49.3 49.2	51.0 51.1	48.5 39.9	32.8	32.8	52.5	64.7	63
8	56.2 56.9	55.9 54.5	54.9 55.9	55.2 52.6	45.9 41.7	40.2 38.9	35.1 33.1	39.9 39.4	31.6 38.1	30.5 26.9	28.5	22.2	40.9	56.9	100
9	58.3 57.8	47.2 41.5	40.8 39.9	43.1 43.8	42.8 41.5	37.1	35.0 32.5	34.2 34.9	30.2 25.3	23.7 24.6	24.3	23.7	41.0	60.5	98
10	62.8 64.9	66.5 64.4	71.5 81.5	78.2 80.4	84.8 79.2	51.7 43.5	36.6 36.0	31.4 35.9	38.4 35.8	35.7 33.7	31.5	16.0	43.4	88.4	100
11	57.3 53.7	54.3 53.2	55.9 57.3	50.8 45.3	48.5 46.4	42.9 41.9	40.1 42.2	39.4 40.8	38.4 35.4	32.3 28.3	25.7	23.7	40.9	60.1	100
12	59.8 59.9	61.2 60.9	62.6 66.9	64.3 52.9	52.1 47.4	42.1 36.7	49.7 52.3	58.4 54.2	54.1 51.5	49.2 43.5	39.8	18.4	43.5	66.9	100
13	57.7 58.8	52.6 53.8	58.4 56.8	54.9 55.5	56.3 55.7	54.5 47.9	42.4 37.6	36.2 32.2	33.5 37.1	40.2 43.7	39.2	25.1	43.6	58.8	100
14	55.9 56.6	57.1 58.1	58.8 57.4	56.1 55.4	55.3 55.2	54.4 52.6	50.7 48.2	45.0 42.2	44.2 45.7	43.1 39.7	40.7	36.7	48.2	58.8	100
15	62.2 61.7	53.2 55.4	49.6	54.8 56.8	51.6 49.6	45.7 42.8	40.6 40.6	36.7 35.6	34.5 34.4	36.3 38.2	34.7	16.7	43.7	62.2	98
16		80.2 81.5	73.6 65.1	64.0 65.5	61.7 66.5	58.7 48.2	43.4 39.1	44.1 40.9	42.3 43.4	35.4 24.0	28.3	17.5	42.7	81.5	92
17						49.7	48.9 54.0	52.3 51.2	47.6 46.6	43.0 39.2	35.0	24.8	41.3	58.4	69
18	60.6 56.9	50.4 47.5	47.6 48.9	50.5 50.8	52.8 53.3	53.0 52.1	45.5 45.5	42.8 44.0	47.1 45.9	44.4 43.9	41.6	24.9	44.5	66.6	100
19	56.1 56.0	56.4 55.8	56.0 55.5	55.5 55.3	54.9 54.0	52.0 48.7	45.0 46.9	46.0 48.0	48.2 44.7	42.8 40.1	38.8	29.5	45.4	56.4	100
20	67.8 68.0	65.9	69.4 68.4	73.3 69.4	66.4 59.4	54.2 49.0	46.1 49.1	47.4 51.6	48.3 43.9	39.3 33.3	32.5	18.8	47.6	73.3	98
21												30.2	41.5	59.0	50
22				49.8 49.7	48.4 46.9	45.5 44.2	43.2 42.3	41.3 40.5	39.8 39.2	38.7 38.4	38.2	38.2	43.1	49.8	31
23	62.0 58.9	55.4 53.3	52.3 51.7	51.2 50.3	49.8 49.2	48.1 47.0	45.6 44.2	43.0 41.8	40.9 40.3	39.6 39.0	38.4	37.4	46.9	63.0	100
24	61.2 59.5	58.8 60.0	58.6 56.9	53.0 52.6	52.2 51.6	49.7 51.7	47.9 47.3	44.2 46.9	50.6 42.0	45.9 48.6	43.2	37.0	48.5	62.3	100
25	60.2 55.3	57.2 56.3	56.7 50.5	44.4	45.5 51.2	49.8 49.8	45.7 42.8	39.0 36.2	29.1 30.8	35.5 36.5	27.4	27.4	43.1	63.4	98
26	80.5 82.9	86.0 87.9	87.7 87.9	80.2 73.4	67.5 62.0	56.4 51.9	44.3 39.7	35.6 35.9	35.5 34.8	45.3 52.8	44.7	17.4	51.4	87.9	100
27	60.7 60.7	61.4 61.4	61.4 62.1		64.2 30.4	44.4 57.3	53.3 51.4	49.4 44.2	44.3 42.7	39.6 37.2	34.7	12.5	44.1	64.2	96
28	74.1 73.0	71.6 70.8	68.3 69.3	68.9 68.8	67.3 66.2	61.2 57.7	54.3 49.9	44.4 41.7	38.0 34.7	51.4 52.9	50.3	21.3	46.8	74.1	77
29			71.5 78.2	82.7 80.8	73.6 73.6	70.9 63.5	52.4 44.7	45.2 40.6	42.9 39.7	39.3 34.2	34.8	34.2	54.4	82.7	83
30	55.7 56.4	49.4 46.4	57.3 58.2	57.7 54.8	51.5 50.1	51.8 49.2	45.3 40.9	40.3 36.6	33.2 30.5	31.7 26.8	25.0	21.4	40.6	58.2	100

												MONTHLY Min	Ave	Max	%Data
Min:	46.3 36.4	45.2 41.5	40.8 39.9	42.2 41.1	40.3 30.4	38.5 35.4	35.0 32.5	31.4 32.2	29.1 25.3	23.7 24.0	23.8	12.5			
Ave:	60.5 59.1	59.1 58.9	60.3 60.2	59.0 57.7	56.7 54.1	51.5 48.5	45.7 44.6	43.5 42.5	41.4 39.8	39.4 37.4	35.4		45.0		
Max:	80.5 82.9	86.0 87.9	87.7 87.9	82.7 80.4	84.8 79.2	70.9 63.5	56.3 54.0	58.4 54.2	54.1 51.5	51.4 52.9	50.3			88.4	
%Data:	77 77	74 81	81 84	77 81	87 87	87 94	94 94	94 90	90 90	90 90	90				90

USFS PAWNEE SITE

June, 1988

Ozone Flux (ppb * meters/second); Half Hour Averages * 10.

Hour	1:00		2:00		3:00		4:00		5:00		6:00		7:00		8:00		9:00	
Day																		
1	0.23	0.43	-0.32	-0.27	-0.58	-0.31	-0.35	-0.41	-0.24	-0.09	-0.62	-0.71	-0.96	-1.38	-1.16	-0.92	-1.09	-1.09
2	-0.53	-0.17	-0.04	-0.21	-0.20	-0.20	-0.32	-0.30	-0.33	-0.34	-0.38	-0.45	-0.55	-0.59	-0.66	-0.82	-1.13	-1.74
3	-0.22	-0.11	-0.12	-0.07	0.01	-0.01	-0.03	-0.10	-0.09	-0.12	-0.18	-0.39	-0.94	0.00	-1.10	-1.34	-1.28	-1.10
4	-0.25	-0.38	-0.26	-0.25	-0.36	-0.10	-0.30	-0.31	-0.24	-0.10	-0.33	-1.23	-1.32	-1.33	-1.37	-1.60		
5																		
6																		
7																		-1.13
8	0.12	0.29	-0.17	0.00	-0.09	-0.09	-0.12	-0.13	-0.38	-0.12	-0.22	-0.35	-0.51	-0.65	-1.00	-0.71	-1.11	-1.65
9	0.02	0.31	-0.13	-0.05	-0.10	-0.16	-0.12	-0.07	-0.06	-0.04	-0.17	-0.28	-0.46	-0.61	-1.63	-1.08	-1.07	
10	0.09	-0.20	-0.10	-0.11	0.10	0.01	-0.33	-0.05	-0.18	-0.21	-0.15	-0.63	-0.92	-1.26		-1.21	-1.42	-1.60
11	-0.17	-0.18	-0.07	-0.11	-0.14	0.08	-0.02	0.04	-0.24	-0.06	-0.10	-0.44	-0.36	-0.96	-0.56	-0.22	-1.71	-1.32
12	-0.28	-0.09	-0.17	-0.13	-0.16	-0.21	-0.09	-0.03	-0.01	-0.07	0.01	-0.56	-0.38	-0.54	-0.71	-1.41	-0.95	-1.36
13	-1.02	-0.71	-0.87	-0.86	-0.57	-0.66	-0.39	-0.26	-0.27	-0.18	-0.22	-0.56	-0.82	-1.86		-0.09	-1.32	-1.41
14	-0.97	-0.91	-1.29	-0.81		-0.42	-0.63	-0.79	-0.92	-0.46	-0.75	-0.96	-1.56	-1.75	-1.46		-0.47	-2.33
15	-0.24	-0.32	-0.65	-0.17	-0.00	-0.10	0.06	0.09	0.23	-0.16	-0.12		-1.03	-0.72	-1.10	-1.40	-1.45	-0.78
16	-0.39		-0.19	-0.18	-0.01	-0.09	-0.21	-0.03	-0.01	-0.01	-0.31	-0.42	-0.63	-0.95	-1.90	-1.41	-1.45	-1.42
17																		
18	-0.09	-0.10	-0.29	-0.16	-0.22	-0.44	-0.19	-0.19	0.19	-0.32	-0.15	-0.02	-0.27	-0.21	-0.33	-0.68	-1.61	-1.46
19	0.06	-0.14	0.05	-0.04	-0.09	-0.16	0.10	-0.35	-0.09	-0.02	-0.15	-0.10	-0.49	-0.70	-0.75	-0.62	-1.49	-1.60
20	-0.24	-0.24	-0.17	0.05	0.04	-0.37	-0.21	-0.13	0.27	0.09	-0.05	0.03	-0.13	-0.18	-0.35	-0.68	-1.40	-1.18
21	-0.09	-0.13	-0.26	-0.41	-0.16	-0.31	-0.39	-0.34	-0.35	-0.59	-0.36	-0.17	-0.36	-0.60	-0.75	-0.80	-1.41	-1.18
22	-0.48	-0.52	-0.87	-0.82	-0.66	-0.81	-0.56	-0.73	-0.39	-0.73	-0.37	-0.17	-0.55	-0.50	-0.66	-0.94	-1.20	-0.69
23	-0.44	-0.37	-0.38	0.17		-0.36	-0.15	-0.35	-0.43	-0.07	-0.05	-0.08	-0.22	0.00	-1.14	-1.46	-1.03	-1.41
24																		
25	-0.64	-0.39	-0.33	-0.07	-0.19	-0.66	-0.59	-0.83	-0.70	-0.63	-0.64	-0.86	-1.23	-1.29	-0.83	-2.66	-0.88	-0.73
26																		
27																		
28	-0.23	-0.11	-0.30	-0.08	-0.28	0.07	-0.43	-0.20	0.11	-0.25	-0.43	-0.75	-1.18	-0.99		-1.74		
29	-1.09	-0.48	-1.02	-0.69	-0.82	-0.48	-0.39	-0.62	-0.55	-0.46	-1.26	-1.39	-1.31	-1.64	-0.63		-1.01	-1.25
30	-0.30	-0.46	-0.20	-0.11	-0.18	-0.09	-0.36	-0.96	-1.24	-1.29	-0.86	-0.89	-0.86	-1.27	-1.21	-2.50	-1.82	
Min:	-1.09	-0.91	-1.29	-0.86	-0.82	-0.81	-0.63	-0.96	-1.24	-1.29	-1.26	-1.39	-1.56	-1.86	-1.90	-2.66	-1.82	-2.33
Ave:	-0.31	-0.23	-0.36	-0.23	-0.22	-0.25	-0.26	-0.31	-0.26	-0.27	-0.34	-0.52	-0.74	-0.87	-0.96	-1.16	-1.25	-1.32
Max:	0.23	0.43	0.05	0.17	0.10	0.08	0.10	0.09	0.27	0.09	0.01	0.03	-0.13	0.00	-0.33	-0.09	-0.47	-0.69
ZData:	77	71	74	74	68	74	74	74	74	74	74	71	74	74	65	68	68	65

(continued)
Ozone Flux

Hour	10:00			11:00			12:00			13:00			14:00			15:00			16:00			17:00			18:00
Day																									
1	-1.42	-1.16	-1.80	-1.61	-1.54	-2.30	-1.26	-1.49	-1.45	-1.52	-1.61	-1.38	-1.57									-0.56	-0.86	-0.69	
2	-1.13	-1.78	-1.25	-1.72	-1.90	-1.78	-1.32		-1.57	-1.26	-1.64	-1.64	-1.39	-1.17	-1.18	-1.06	-1.12	-1.05							
3	-1.65	-2.11	-1.45	-1.73	-2.31	-2.21	-1.78	-2.54	-2.46	-3.36	-1.41	-1.57	-1.84	-1.88	-1.31			-1.64							
4																									
5																									
6																									
7	-1.59	-1.05				-1.01	-1.01	-2.01	-1.08	-1.92	-1.52		-2.11	-1.85	-0.65	-1.08	-0.82	-0.34							
8	-0.99	-1.51	-1.49	-1.63	-2.06	-2.30	-1.47	-1.43	-1.43	-1.83	-2.18	-1.31	-1.22	-1.40	-1.47	-1.93	-0.90	-0.38							
9	-1.65	-1.34	-1.60	-1.58	-2.26	-1.57	-1.74	-1.73	-1.54	-2.30	-1.14	-0.70	-0.83	-1.54	-2.00	-0.94	-1.42	-1.43							
10	-1.61	-2.00	-2.22	-2.07	-2.36	-3.03	-2.67	-2.88	-3.21	-2.08	-2.73	-2.26	-2.02	-1.44	-1.66	-1.62	-2.08	-1.62							
11	-0.71	-1.15	-1.05	-1.96	-2.64	-1.93	-1.94	-1.51		-1.53	-1.15	-1.20	-1.26	-1.47	-1.17	-1.19	-0.88	-0.28							
12	-1.08	-0.52	-2.33	-2.08	-1.90	-1.74	-2.10	-3.33	-2.22	-0.76	-3.50	-1.76	-1.83	-1.97	-1.12	-1.00	-1.04	-0.58							
13	-1.31	-1.43	-1.66	-1.83	-1.76	-1.78	-1.22	-1.45	-1.28	-1.27	-0.90	-0.80	-1.36	-2.05	-1.25	-0.69	-0.89	-0.96							
14	-2.21	-1.69	-2.03	-2.09	-2.58	-2.03			-2.84	-3.09	-1.44	-3.40	-2.30	-2.07	-1.87	-1.40	-1.30	-1.31							
15	-1.55	-1.72	-0.23	-1.81	-1.77	-1.67	-1.96	-2.49	-2.20	-1.11	-1.01	-0.13	-0.19		-1.73	-2.48	-1.96	-1.53							
16	-1.64																								
17																									
18	-2.96	-1.16	-1.14	-1.47	-1.32	-1.60	-1.77	-1.39		-2.56	-0.76	-0.40	-0.79	-0.71	-1.54	-0.96	-1.05	-1.66							
19	-1.34	-1.19	-1.38	-1.61	-1.49	-1.52	-1.58	-1.47	-2.19	-1.82	-1.39	-1.24	-0.99	-1.26	-1.56		-0.99	-1.26							
20	-1.76	-0.89	-0.73	-0.84	-1.12	-1.89	-1.25	-1.37	-1.92	-1.45	-1.69	-1.60	-1.39	-2.06		-1.52	-0.77	-0.83							
21	-1.62	-1.83	-2.46												-1.68	-1.33	-0.98	-1.19							
22	-1.44	-1.86	-1.53	-1.50	-1.43	-1.69	-1.62	-1.49	-1.57	-2.20	-2.11	-1.38	-1.31	-1.04	-0.54	-1.46		-1.07							
23	-1.61	-1.54	-2.03	-1.61	-2.18	-2.18	-2.26	-2.34	-2.49	-2.51	-2.00	-1.13	-1.46		-1.38	-0.73	-1.45	-0.97							
24														-1.03	-2.06	-1.84	-1.41	-1.95							
25	-1.06	-1.33	-1.23	-1.02	-1.06	-1.38	-1.42	-1.19	-2.24	-1.93	-2.30	-2.03	-1.44	-1.51	-0.94										
26																									
27		-0.77	-2.16	-1.97	-1.47	-1.90	-1.75	-1.75	-1.71	-2.14	-2.25	-1.89	-1.72	-1.82	-1.72	-1.44	-1.52	-1.83							
28										-2.85	-2.62	-2.28	-3.01	-1.76	-1.77	-1.65	-1.65	-1.72							
29	-1.05	-1.26	-1.23	-1.30	-2.00	-0.98									-0.63	-2.20	-1.55	-0.87							
30														-2.23	-1.65	-1.93	-0.99	-0.98							
Min:	-2.96	-2.11	-2.46	-2.09	-2.64	-3.03	-2.67	-3.33	-3.21	-3.36	-3.50	-3.40	-3.01	-2.23	-2.06	-2.48	-2.08	-1.95							
Ave:	-1.49	-1.39	-1.55	-1.65	-1.85	-1.83	-1.67	-1.88	-1.96	-1.97	-1.77	-1.48	-1.50	-1.59	-1.40	-1.38	-1.22	-1.14							
Max:	-0.71	-0.52	-0.23	-0.84	-1.06	-0.98	-1.01	-1.19	-1.08	-0.76	-0.76	-0.13	-0.19	-0.71	-0.54	-0.56	-0.77	-0.28							
ZData:	68	68	65	61	61	65	58	55	55	65	65	61	65	61	71	68	68	74							

(continued)
Ozone Flux

Day	Hour 19:00	20:00	21:00	22:00	23:00	24:00	DAILY Min	Ave	Max	% Data
1	-0.74 -0.50	-0.12 -0.31	-0.16 -0.30	-0.06 -0.31	-0.09 -0.11	-0.14 -0.30	-2.30	-0.77	0.43	96
2	-0.72 -0.87	-0.40 -0.15	-0.13	0.10 0.08	-0.05 -0.07	-0.02 -0.06	-1.90	-0.77	0.10	96
3	-1.71 -0.85	-0.03 -0.29	-0.36 -0.47	-0.36 -0.39	-0.45 -0.23	-0.28 -0.33	-3.36	-0.96	0.01	96
4										33
5										0
6										0
7	-0.37 -0.43	-0.34 -0.28	-1.05 -0.58	-0.44 -0.36	-0.06 0.16	-0.15 -0.14				56
8	-0.48 -0.61	-0.41 -0.36	-0.11 -0.14	-0.10 -0.46	-0.45 -0.20	-0.06 -0.05	-2.30	-0.78	0.29	100
9	-0.68	-0.23 -0.67	-0.77 -0.72	-0.50 -0.72	-0.64 -0.61	-0.45 -0.19	-2.30	-0.85	0.31	96
10	-0.83 -0.25	-0.11	-0.16 -0.16	-0.31 -0.12		-0.26 0.12	-3.21	-1.13	0.12	92
11	-0.77 -0.72	-0.45 -0.45	-0.56 -0.70	-0.29 -0.29	-0.82 -0.19	-0.52 -0.28	-2.64	-0.76	0.08	98
12	-0.20 -0.41	-0.70 -0.70	-0.98 -0.84	-0.54 -0.78	-0.53 -0.52	-0.43 -0.32	-3.50	-0.94	0.01	100
13	-0.67 -0.73	-0.28 -0.22	-0.01 -0.05	-0.26 -0.59	-0.56 -0.99	-0.95 -0.77	-2.05	-0.89	-0.01	98
14	-1.43 -0.82	-0.86 -0.33	-0.65 -0.35	-0.63 -0.84	-0.62 -0.44	-0.25 -0.10	-3.40	-1.31	-0.10	92
15	-0.92 -1.08	-0.49 -0.52	-0.71 -0.72	-0.41 -0.68	-0.09 -0.01	-0.25	-2.49	-0.87	0.23	94
16										38
17		0.49	-0.49 -1.21	-0.89 -0.42	-0.12 -0.06	-0.09 -0.18				19
18	-0.78 -0.75	-0.28 -0.12	-0.25 -0.57	-0.27 -0.35	-0.45 -0.93	-0.23	-2.96	-0.76	0.19	96
19	-0.91 -1.07	-0.54 -0.12	-0.09 -0.86	-0.33 -0.53	-0.49 -0.22	-0.07 -0.21	-2.19	-0.77	0.10	98
20	-0.21 -0.80	-0.50 -0.41	-0.12 0.11	-2.20 -0.07	-0.06 -0.03	-0.11 -0.08	-2.20	-0.69	0.27	98
21	-0.65 -0.46	-0.64 -0.51	0.05 -0.05	-0.04 0.18	-0.04 0.12	-0.07 -0.05	-2.46	-0.59	0.18	77
22	-1.82 -1.46	-1.21 -0.84	-0.10 -0.21	-0.04	-0.07	-0.31 -0.42	-2.20	-0.96	-0.04	94
23	-0.27 -0.87	-0.64 -0.13	-0.03 0.01	0.18 0.04			-2.51	-0.94	0.18	88
24	-0.98 -1.45	-0.75 -0.61	-0.08 -0.27	-0.03 0.16	-1.29 -1.13	-0.78 -0.81				35
25							-2.66	-1.10	-0.07	69
26										0
27	-2.04	-0.70 -0.66	-0.60 -0.37	-0.12 -0.39	-0.38 -0.38	-0.26 -0.42				58
28	-1.24 -0.67	-0.72 -0.04	-0.44 -0.06	-0.02 -0.05	-0.53 -0.67	-0.84 -0.66	-3.01	-0.89	0.11	75
29	-1.35 -1.01		-0.41 -1.38	-0.64 -0.71	-0.80 0.10	-1.49	-2.20	-1.00	0.10	75
30	-1.21 -1.01	-0.60 -0.09	-0.18							56
							MONTHLY Min	Ave	Max	%Data
Min:	-2.04 -1.46	-1.21 -0.84	-1.05 -1.38	-2.20 -0.84	-1.29 -1.13	-0.95 -1.49	-3.50			
Ave:	-0.91 -0.80	-0.50 -0.33	-0.36 -0.44	-0.36 -0.35	-0.41 -0.32	-0.31 -0.34		-0.88		
Max:	-0.20 -0.25	-0.03 0.49	0.05 0.11	0.18 0.18	-0.04 0.16	-0.02 0.12			0.49	
%Data:	74 68	71 71	74 74	74 71	68 65	68 65				71

USFS PAWNEE SITE

June, 1988
NO2 Average Concentration (ppb); Half Hour Averages.

Day	1:00		2:00		3:00		4:00		5:00		6:00		7:00		8:00		9:00		10:00		11:00		12:00		13:00			
1	9.0	5.7	3.4	2.2	1.7	1.7	1.7	1.6	1.6	1.6	1.6	1.5	1.4	1.4	1.3	1.3	1.3	1.3	1.3	1.3	1.3	1.4	1.3			
2	2.0	3.2	5.6	6.0	4.9	4.7	3.3	2.1	1.9	2.5	1.8	1.6	1.5	1.4	1.5	1.1	1.1	1.2	1.3	1.1	1.1	1.1	1.1	1.1	1.1	1.2
3	9.3	7.7	6.8	6.3	5.8	5.4	5.5	5.0	4.4	4.7	5.1	4.6	3.3	2.3	2.0	1.9	1.6	1.5	1.4	1.5	1.5	1.5	1.5	1.5	1.3	1.3	1.3
4	3.1	3.3	3.1	2.9	2.9	3.2	3.3	2.9	2.8	3.0	2.8	2.9	2.3	2.2	2.3	2.5										
5																										
6																										
7																										
8	11.3	19.0	11.2	5.7	7.8	7.8	5.6	4.0	3.8	3.8	3.2	3.6	6.9	5.8	3.6	2.2	1.5	1.4	1.3	1.3	1.2	1.2	1.4	1.3	1.3	1.2	1.2
9	3.8	4.5	4.0	4.7	5.3	9.9	12.4	9.5	5.8	7.3	6.4	5.9	5.5	5.3	4.9	4.2	3.6	3.1	2.7	2.5	2.5	2.4	2.1	1.9	1.9	1.8	1.6
10	12.4	15.0	7.8	7.0	5.8	5.7	8.5	4.6	5.2	6.4	7.1	4.6	2.8	2.5		2.6	2.7	2.5	2.5	2.5	2.6	2.7	2.7	3.0	2.9	3.2	3.4
11	7.1	6.3	6.1	7.5	9.7	8.6	9.2	9.1	10.9	11.2	8.2	5.2	4.4	4.5	4.1	3.3	2.6	2.3	2.4	2.3	2.7	2.7	2.4	2.2	2.1	1.9	2.1
12	5.2	5.3	6.4	5.9	5.2	5.9	6.3	7.2	6.2	5.4	5.5	4.8	3.7	3.3	3.1	2.8	2.8	3.4	3.4	3.1	2.8	2.8	2.6	2.6	2.6	2.7	2.6
13	2.8	3.3	3.3	4.8	7.8	4.7	4.8	4.4	4.0	6.4	4.3	3.6	3.3	2.6		2.5	2.5	2.6	2.6	2.4	2.4	2.4	2.5	2.6	2.8	2.5	2.8
14	13.1	6.9	4.1	3.7	15.8	13.7	6.2	4.4	4.0	5.4	6.9	4.3	4.5	4.7	3.6	2.6	2.6	2.8	2.9	2.9	2.8	2.7	2.8	2.9	2.8	3.0	3.2
15	4.3	4.0	3.5	3.9	4.6	4.8	5.0	4.9	5.3	4.8	4.7	4.1	4.2	4.8	5.9	5.4	5.7	7.3	4.8	3.5	3.0	2.9	2.6	2.6	2.7	2.6	2.7
16	6.5	7.4	8.3	8.3	6.5	7.7	8.0	8.9	9.8	10.7	11.8	9.4	8.8	8.2	4.8												
17																											
18	5.6	5.1	6.2	6.5	6.3	5.3	4.6	6.4	8.8	7.9	8.3	8.3	7.2	5.3	4.2	3.6	3.7	5.0	3.5	2.1	2.0	1.7	1.5	1.5	2.2	2.0	2.0
19	4.2	4.7	5.4	7.5	6.1	7.6	5.4	3.8	2.9	2.3	2.2	2.4	2.4	2.5	1.8	1.5	1.8	1.4	1.3	1.5	1.5	1.7	1.8	1.4	1.3	1.1	1.1
20	1.5	1.5	1.7	1.9	2.4	2.2	2.7	2.9	2.9	3.2	3.8	3.5	4.1	3.7	3.7	3.4	3.1	2.5	1.6	1.4	1.1	1.2	1.2	1.2	1.3	1.3	1.2
21	8.1	8.3	9.1	8.4	7.6	7.7	4.2	4.7	3.9	4.0	3.7	3.6	3.3	3.5	3.3	4.5	4.1	2.8									
22	4.6	5.8	3.6	3.5	3.8	3.8	4.0	6.6	10.0	3.7	2.7	4.2	5.7	9.1	3.0	2.5	2.7	2.4	2.1	2.3	2.1	1.8	1.9	1.9	1.9	1.9	1.9
23	5.4	6.0	6.1	8.4	9.1	7.8	6.5	8.1	6.1	8.6	9.8	9.2	8.0	8.2	6.2	5.3	5.0	5.0	4.7	4.8	4.6	4.3	4.1	3.9	4.0	4.4	4.8
24																											
25	5.9	5.8	6.5	7.5	10.6	10.2	5.5	3.5	3.0	3.7	3.9	4.8	3.7	3.3	3.7	3.8	4.9	5.2	5.6	6.7	6.8	7.5	5.9	4.4	4.2	4.5	3.3
26																											
27																				6.8	5.1	4.3	4.1	3.8	3.3	3.3	3.3
28	6.4	6.2	6.3	6.3	7.7	8.7	7.0	5.9	5.7	5.7	5.2	4.6	4.9														
29	4.8	4.8	4.2	5.3	4.8	5.0	5.1	10.2	6.0	5.7	5.7	8.6	4.9	17.6	6.6		6.3	7.6	7.8	4.8	3.5	3.1	3.6	3.3			
30	7.1	5.1	6.0	7.6	5.9	7.7	6.8	4.1	6.1	5.1	3.6	3.1	3.3	4.1	3.1	3.6											
Min:	1.5	1.5	1.7	1.9	1.7	1.7	1.7	1.6	1.6	1.6	1.6	1.5	1.4	1.4	1.3	1.1	1.1	1.2	1.3	1.1	1.1	1.1	1.1	1.1	1.1	1.1	1.1
Ave:	6.2	6.3	5.6	5.7	6.4	6.5	5.7	5.4	5.3	5.4	5.1	4.7	4.4	4.8	3.6	3.0	3.1	3.2	3.0	2.9	2.7	2.6	2.5	2.3	2.3	2.3	2.3
Max:	13.1	19.0	11.2	8.4	15.8	13.7	12.4	10.2	10.9	11.2	11.8	9.4	8.8	17.6	6.6	5.4	6.3	7.6	7.8	6.8	6.8	7.5	5.9	4.4	4.2	4.5	4.8
ZData:	77	74	74	74	74	74	74	74	74	74	74	74	74	71	65	65	61	61	58	61	61	61	61	61	55	55	55

USFS PAWNEE SITE
June, 1988
NO2 Average Concentration (ppb); Half Hour Averages

Day	14:00		15:00		16:00		17:00		18:00		19:00		20:00		21:00		22:00		23:00		24:00		DAILY Min	Ave	Max	% Data
1													1.3	1.4	1.5	1.7	1.8	2.1	2.5	2.5	2.3		1.3	2.0	9.0	69
2	1.3	1.2	1.2	1.1	1.1	1.0	1.0	1.0	1.0	1.0	1.2	1.4	1.7	1.8	2.0	2.0	3.4	5.0	4.6	7.2	8.9		1.0	2.2	8.9	100
3	1.2	1.3	1.2	1.3	1.3	1.4		1.3	1.3	1.3	1.3	1.5	1.5	1.6	1.8	2.0	2.4	2.9	2.9	2.8	3.0		1.2	2.8	9.3	98
4																										33
5																										0
6																										0
7				1.1	1.1	1.2	1.2	1.4	1.5	1.5	1.5	1.8	2.7	1.8	1.3	1.5	1.5	1.5	1.3	2.6	4.7					38
8	1.2	1.1	1.3	2.0	2.0	1.8	2.0	2.2	3.8	4.0	3.9	3.4	4.4	4.4	3.4	3.0	2.9	3.3	4.1	3.4	2.9		1.1	3.8	19.0	100
9	1.6	1.8	2.6	3.9	4.3	5.3	3.8	2.4	2.6	3.6		5.5	7.1	11.2	10.7	9.5	12.4	16.9	16.4	13.4	11.4		1.6	5.8	16.9	98
10	3.1	3.1	3.2	2.8	3.4	4.3	4.1	5.3	5.7	7.0	3.6	4.4	5.8	5.5	6.4	5.3	5.1	4.5	3.7	3.4	4.5		2.5	4.7	15.0	98
11	2.5	2.5	2.2	2.4	2.3	2.3	2.4	4.2	2.7	2.4	2.6	3.3	5.6	2.7	3.2	3.2	4.3	4.3	4.8	4.7	5.3		1.9	4.4	11.2	100
12	2.6	2.5	2.5	2.4	2.5	2.9	3.1	2.2	1.8	2.3	3.7	9.3	2.2	2.3	2.0	2.2	2.0	1.9	2.1	2.8	2.7		1.8	3.6	9.3	100
13	2.8	2.7	3.1	3.5	3.4	3.3	3.3	3.4	3.2	3.5	3.1	3.6	4.0	5.0	6.0	4.7	4.5	3.7	4.3	4.0	5.5		2.4	3.6	7.8	98
14	3.2	3.1	2.9	2.7	2.6	2.4	2.6	3.0	3.0	2.9	3.1	3.3	3.6	4.0	4.3	4.3	4.2	3.9	4.1	4.6	4.0		2.4	4.3	15.8	100
15	2.9	3.2	3.5	3.7	4.5	4.2	3.5	3.0	2.9	3.0	3.1	3.3	3.8	3.9	4.5	4.7	4.9	5.5	5.3	5.2	6.2		2.6	4.2	7.3	100
16																										31
17													3.8	2.9	2.7	3.5	3.3	3.6	4.1	4.7	6.2					19
18	2.0	2.0	2.3	2.7	2.5	2.2	3.1	2.2	1.9	1.9	2.0	2.0	2.3	3.0	3.3	4.9	2.9	2.4	3.1	3.6	4.3		1.5	3.8	8.8	100
19	1.1	1.1	1.2	1.2	1.2	1.1	1.1	1.1	1.1	1.1	1.1	1.2	1.3	1.6	1.7	1.8	1.7	1.4	1.5	1.5	1.5		1.1	2.2	7.6	100
20	1.2	1.2		1.2	1.2	7.8	3.4	3.8	4.1	3.4	7.2	6.6	5.4	6.1	6.0	5.0	4.8	4.9	5.5	6.1	6.4		1.1	3.3	7.8	98
21						3.6	2.7	2.9	2.6	3.3	3.9	3.6	3.7	4.2	4.0	6.6	7.2	6.1	4.8	5.4	7.6		2.6	4.9	9.1	71
22	1.9	1.9	1.9	2.0	2.1	2.7	4.9	4.1	5.3	4.7	3.5	3.4	3.9	6.9	6.6	6.2	10.6	4.9	7.5	7.8	7.2		1.8	4.2	10.6	100
23	4.1	3.7	4.2	4.8	6.0	5.2	4.2	4.4	4.4	5.4	3.7	3.9	5.6	8.2	8.4	11.1	13.6						3.7	6.1	13.6	92
24					2.7	2.8	2.7	2.5	2.4	2.3	2.4	2.6	2.8	3.1	3.7	4.1	4.3	4.7	4.2	6.6	7.2					35
25	3.3	3.8	4.1	3.9	3.5	3.7																	3.0	5.0	10.6	69
26																										0
27	3.3	3.5	3.7	3.8	3.9	3.7	3.7	3.8	3.7	3.4	4.1	4.8	5.7	5.9	6.2	7.2	5.8	5.4	6.2	6.4	6.7					60
28			2.6	2.6	2.7	2.7	2.7	2.8	2.8	2.8	3.4	3.8	4.2	5.2	6.2	7.0	8.1	7.9	6.7	5.0	4.2					67
29						6.7	5.7	5.8	6.7	6.8	8.8		19.3	17.8	4.8	5.5	4.4	3.2	3.8	5.1	5.2		3.1	6.6	19.3	79
30							0.6	0.5	0.4	0.5	0.4	0.4	0.5	0.5												50
																							MONTHLY Min	Ave	Max	% Data
Min:	1.1	1.1	1.2	1.1	1.1	1.0	0.6	0.5	0.4	0.5	0.4	0.4	0.5	0.5	1.3	1.5	1.5	1.4	1.3	1.5	1.5		0.4			
Ave:	2.3	2.3	2.6	2.6	2.7	3.3	2.9	2.9	2.9	3.1	3.2	3.5	4.3	4.6	4.4	4.7	5.1	4.5	4.7	5.0	5.4			4.1		
Max:	4.1	3.8	4.2	4.8	6.0	7.8	5.7	5.8	6.7	7.0	8.8	9.3	19.3	17.8	10.7	11.1	13.6	16.9	16.4	13.4	11.4				19.3	
%Data:	55	55	55	61	65	71	68	71	71	71	68	68	77	77	74	74	74	71	71	71	71					70

USFS PAWNEE SITE

June, 1988

Nitrogen Dioxide Flux (Covariance); Half Hour Averages.

Day	1:00		2:00		3:00		4:00		5:00		6:00		7:00		8:00		9:00	
1	-3.46	-2.25	0.28	-2.37	1.02	0.55	0.33	0.38	0.08	0.55	-0.52	-0.80	0.50	1.57	0.71	0.23	0.13	0.22
2	0.85	0.55	-1.22	-0.13	0.51	0.40	-1.53	-0.85	0.52	0.15	0.94	0.05	-0.07	0.14	-1.07	-0.06	0.53	0.17
3	0.43	1.15	0.63	0.27	-0.15	-0.31	0.02	0.01	-0.03	0.12	-0.17	-0.00	0.35	0.61	1.02	0.00	0.68	0.68
4	0.38	0.87	0.36	0.41	0.61	-0.02	0.41	0.30	0.07	-0.23	0.22	0.13	0.88	1.00	1.26	0.83		
5																		
6																		
7																		
8	-3.30	-6.00	4.66	0.19	0.00	0.08	0.24	0.25	-1.06	-1.74	-1.34	-0.54	-0.46	-0.75	1.18	-0.04	0.26	0.66
9		-0.16		0.16			1.62	0.42	0.29	-0.22	0.60	0.42	0.82	-0.03		1.24	0.36	
10	-0.37			0.32			1.59	-0.67	1.11	0.78	0.19	0.31	0.22	0.77		1.39	2.16	
11	1.23	0.56	-0.33	0.59	-1.83		0.42		0.42	-0.00	0.33	0.34	-0.24	-0.53	-0.07		1.80	
12	0.51	-0.51	-0.42	-0.00	-0.11	-0.01	-0.54	-0.00	-0.04	0.22	-0.09	0.15	-0.77	-0.40	-0.40	-0.17	-0.15	0.17
13	0.50	-0.07	-0.17	1.63	-2.63	-0.50	-0.59	-0.40	-0.18	-4.59	0.07	-1.01	-0.75	-0.29	0.00	0.22	-0.12	-0.29
14	4.01	-1.18	2.49	-1.29			-3.99	-1.58	0.89	-4.77	1.01	-0.19	-0.75	0.18	1.06	-0.39	1.78	2.82
15	-0.02	0.43	0.34	-0.32	-0.47	0.06					-0.03	-1.02	-0.39	-0.35	-0.96	-0.18	-1.11	-1.48
16		0.13	1.39	-0.99		-0.58			-0.37		0.67	-0.27	-0.45	1.62	0.72			
17																		
18	-0.22	0.45	-0.56	-0.07	0.23	0.12	0.36	-0.29	-3.23	0.83	-0.31	0.09	0.01	-0.02	0.38	-0.24	-0.73	1.31
19	-0.01	-0.09	-0.01	-0.32	0.34	-0.34	-3.00	0.03	-0.18	-0.26	0.15	-0.10	-0.31	0.09	1.43	0.05	-0.31	0.40
20	0.14	0.02	0.16			0.52	0.15	0.14	-0.05		0.83		0.18	-0.23	0.03	0.21	0.61	0.81
21	-0.54	-0.37	-1.09	2.53	-0.02	-0.05	0.16	-1.04	0.14	0.58	0.31	1.53	0.84	0.07	0.14	0.40	1.81	1.29
22	0.09	-9.67	-0.39	-0.50	-0.11	1.08	0.48	2.61	-5.51	7.19	-0.56	-1.02	-0.58	6.36	-1.01	0.26	0.56	0.64
23	1.39	1.25	3.00		-1.13	1.86	0.02	1.74	1.59	0.43	-0.04	0.56	0.56	-0.68	0.44	0.86	1.08	
24																		
25	-7.86	0.78	0.66	0.05	-0.27	2.78	4.70	2.03	0.49	2.09	2.39	1.91	1.78	2.39	2.37	4.46	1.90	1.62
26																		
27																		
28	0.88	0.56	0.28	0.16	1.94	-0.17	0.45	0.13		-0.10	-0.66	-0.71	-1.37					
29	6.39	1.92	1.37	0.94	2.14	0.40	-0.07	4.21	0.27	-1.14	4.73		1.06				-1.04	0.00
30	-1.93	2.10	0.31	0.39	0.16	-2.96	0.43		-11.0	6.87	-1.27	-1.66	0.07	3.77	-0.06	4.19		
Min:	-7.86	-9.67	-1.22	-2.37	-3	-3.0	-3.99	-1.58	-11.0	-4.77	-1.34	-1.66	-1.37	-0.75	-1.07	-0.39	-1.11	-1.48
Ave:	-0.04	-0.43	0.56	0.08	0.01	0.15	0.08	0.39	-0.75	0.34	0.32	-0.09	0.05	0.73	0.38	0.70	0.54	0.60
Max:	6.39	2.10	4.66	2.53	2.14	2.78	4.70	4.21	1.59	7.19	4.73	1.91	1.78	6.36	2.37	4.46	2.16	2.82
XData:	70	71	68	68	58	61	68	61	68	65	74	68	74	68	61	61	61	48

(continued)

Nitrogen Dioxide Flux

Hour	10:00			11:00			12:00			13:00			14:00			15:00			16:00			17:00			18:00	
Day																										
1	0.24	0.12	0.16	0.07	0.29	0.50																				
2	0.23	0.17	0.35	0.37	0.32	0.89	0.11	1.53	0.11	0.11	-0.04	0.20	0.34	0.12	0.29	0.10	0.12	0.06								
3	0.86	1.03	0.55	0.35	0.84	1.02	0.68	0.60	0.66	0.37	0.74	0.37	0.32	0.41	0.38		0.04	0.10								
4																										
5																										
6																										
7													0.20	0.21	0.19	0.12	-0.10									
8	0.62	0.49	0.18	0.53	0.50	0.53	0.39	0.25	0.30	0.20	0.40	0.49	1.07	0.41	1.07	0.94	-0.11	-0.08								
9	1.13	0.90	0.62	0.85	1.60	1.06	1.02	0.69	0.33	-0.02	0.27	0.00	6.97	12.19	12.76	7.23	6.51	4.82								
10	4.07	4.28	5.60	4.77	7.63	10.10	8.12	10.01	11.47	7.01	6.45	4.72	4.32	3.70	2.46	2.71										
11	0.75	0.69	0.39	0.79	1.16	1.44	1.23	1.34		0.93	0.20	0.12	0.08	0.07	0.74	0.27	-1.91	-2.64								
12	-0.27	0.16	0.22	0.38	0.08	0.31	0.30	0.87	0.51	0.55	0.04	0.16	0.35	0.12	0.10		0.24	0.11								
13	-0.11	0.00	-0.11	0.18	0.10	0.19		-0.12	-0.57	-0.27	-0.18	-0.29	-0.42	-0.62	-0.39	-0.35	-0.29	-0.20								
14	3.27	2.83	3.96	3.94	5.57	4.99			5.57	5.91	5.78	4.25	4.36	3.91	2.66	1.80	1.22	1.29								
15	-1.97	1.22	0.47	0.26	0.36	1.20	1.13	1.31	1.04	0.91		-0.37			0.51	2.51	1.81	0.42								
16																										
17																										
18	1.28	-1.38	-0.29	0.38	0.53	0.35	0.21			0.78	0.32	0.33	1.18	-0.73	0.79	-1.00	0.09	-0.11								
19	0.26	0.12	0.18	0.77	0.43	0.36	0.67	0.38	0.80	0.59	0.72	0.15	0.29	0.35		0.36	0.32	0.28								
20	0.88	0.30	0.55	0.23	0.26	0.25	0.44	0.43	0.39	0.35			0.31	0.08		0.31	0.22	0.19								
21																										
22	1.06	0.34	1.13	0.76	1.13	0.72	1.97	1.04	1.11	0.99		0.73	0.07	2.24	3.46	5.52										
23	2.21	3.12	5.00	4.77	5.71	6.79	7.62	7.84	10.21	9.58	6.98	5.45	3.07													
24														2.42	1.66	1.20	1.34	1.12								
25	2.07	2.72	4.03	2.80	3.16	3.82	4.87	1.60	2.86	3.56	6.56	8.08	5.98													
26																										
27		1.47	3.15	1.87	2.55	2.40	2.91	2.53	2.55	2.69	3.04	2.34	2.04	2.33	1.99	0.85	1.37	1.45								
28												1.31	1.56	0.80	0.88	0.60	0.63	0.94								
29	0.35		0.70		2.72	0.04									3.17	3.62	2.82	-0.07								
30																0.45	0.34	0.56								
Min:	-1.97	-1.38	-0.29	0.07	0.08	0.04	0.11	-0.12	-0.57	-0.27	-0.18	-0.37	-0.42	-0.73	-0.4	-1.00	-1.91	-2.64								
Ave:	0.94	1.03	1.41	1.34	1.84	1.95	2.11	2.02	2.49	2.01	2.23	1.65	1.78	1.65	1.92	1.51	0.81	0.48								
Max:	4.07	4.28	5.60	4.77	7.63	10.10	8.12	10.01	11.47	9.58	6.98	8.08	6.97	12.19	12.76	7.23	6.51	4.82								
ZData:	58	58	61	58	61	61	48	48	48	55	45	55	58	55	55	58	58	55								

(continued)

Nitrogen Dioxide Flux

Day	Hour 19:00			20:00		21:00		22:00		23:00		24:00	DAILY Min	Ave	Max	% Data
1				-0.46	-0.30	0.20	0.08	0.23	0.03	0.14	0.03	0.56	-3.46	-0.03	1.57	69
2	0.06	-0.12	0.14	0.07		0.16		-0.38	0.23	-0.30	-0.11	0.30	-1.53	0.12	1.53	96
3	0.15	0.03	-0.05	0.04	0.08	0.36	0.36	0.47	0.97	0.53	0.53	0.66	-0.31	0.40	1.15	98
4													-0.23	0.47	1.26	33
5													ERR	ERR	ERR	0
6													ERR	ERR	ERR	0
7	0.10	0.33		1.36	1.49	-0.04	-0.02			-0.13	-1.05	1.24	-1.05	0.28	1.49	29
8	0.49	1.23	0.10	0.78	-0.15	-0.42		-0.01	0.18	0.11	-0.01	0.13	-6.00	0.06	4.66	98
9	2.61		-0.81				1.16	0.90	-1.67	3.55	0.35	0.73	-1.67	1.88	12.76	79
10	2.44	13.88	0.77	-0.20	0.66		1.37	-1.06			0.89		-1.06	3.44	13.88	75
11	-4.21	-1.47	3.35	-4.27	1.69	0.69	0.04	-0.49	3.31	0.10	0.69	0.28	-4.27	0.19	3.35	90
12		-1.38		-1.15	0.02	-0.30	-0.23	0.40	-0.50		0.05	-0.20	-1.38	-0.04	0.87	92
13	-0.22	-0.31	-0.70	-0.11	-0.12		0.26	0.27	-1.67	-1.10	0.69	-0.03	-4.59	-0.34	1.63	96
14	0.84	1.05	1.45	0.52	0.99	0.29	1.35	1.97	1.52	0.83	0.43		-4.77	1.69	5.91	90
15	0.35		-0.03		-0.25				-0.14	-0.25			-1.97	0.15	2.51	71
16													-0.99	0.19	1.62	21
17				-2.86	-1.91	-1.21	1.49	0.60	0.21	0.64	0.00	-1.34	-2.86	-0.49	1.49	19
18	0.42	-0.05	0.07			1.38					0.20	-0.03	-3.23	0.07	1.38	83
19		0.26	0.12				0.70	0.37	0.15	0.09		0.02	-3.00	0.15	1.43	88
20	0.28	0.90	4.37	-0.01	0.58	-0.20	0.18	-0.16	-0.14	0.00	-0.06	-0.36	-0.36	0.34	4.37	85
21				1.71	0.14		0.46	0.10			0.80	-0.21	-1.09	0.40	2.53	50
22	11.74	2.58	4.82	3.84	0.48			-0.67	0.42	0.00	2.88	1.71	-9.67	1.16	11.74	90
23		1.01	1.35										-1.13	3.02	10.21	65
24	0.82	0.77	0.50	0.51	0.17				2.86	-3.03	-0.70	-2.85	-3.03	0.49	2.86	29
25													-7.86	2.46	8.08	65
26													ERR	ERR	ERR	0
27	1.61	1.54	1.84	1.88	1.90	1.75	-0.64	1.03	1.26	1.07	0.66	1.24	-0.64	1.82	3.15	60
28	1.15	0.74	1.15	-0.11	2.13	0.80		0.53	3.55	2.03	5.60	1.93	-1.37	0.92	5.60	63
29	1.25	1.35			1.23			3.65	3.73		-2.08	3.38	-2.08	1.62	6.39	60
30	0.16	0.45	0.34	0.08	0.07								xxxxxx	0.08	6.87	48

													MONTHLY Min	Ave	Max	%Data
Min:	-4.21	-1.47	-0.81	-4.27	-1.91	-1.21	-0.64	-1.06	-1.67	-3.03	-2.08	-2.85	-11			
Ave:	1.11	1.20	1.04	0.09	0.47	0.27	0.47	0.43	0.79	0.25	0.49	0.38		0.78		
Max:	11.74	13.88	4.82	3.84	2.13	1.75	1.49	3.65	3.73	3.55	5.60	3.38			13.88	
%Data:	58	61	58	58	61	42	45	58	58	55	65	61				61

USFS PAWNEE SITE

June, 1988

Average Temperature (Degrees Centigrade); Half Hour Averages.

Day	1:00		2:00		3:00		4:00		5:00		6:00		7:00		8:00		9:00		10:00		11:00		12:00		13:00	
1	5	6	7	9	9	9	8	8	8	8	10	11	12	12	13	14	15	16	17	17	18	18	18	19	19	19	19
2	13	13	13	13	13	13	13	13	13	13	13	14	16	17	18	18	19	19	20	20	20	21	21	21	21		22
3	10	10	10	10	10	10	9	9	9	8	9	12	15	17	18	19	19	19	19	20	20	20	21	22	22	22	23
4	13	13	12	12	12	11	11	11	10	10	11	12	13	14	15	16	18	19	20	21	22	23	24	25	25	26	26
5	15	14	14	13	13	13	13	13	12	12	13	14	15	16	16	17	17	18	19	20	21			19	25	25	26
6	13	13	12	12	11	10	10	10	9	10	10	12	13	14	16	18	19	20	21	22	23	24	25	25	26	27	28
7																	27	28	29	30	30	30		30	30	30	30
8	19	18	17	16	17	16	17	16	17	16	17	19	20	22	24	26	28	28	29	29	30	30	30	30	30	30	30
9	18	18	19	18	18	17	17	17	16	16	16	17	18	19	21	21	22	23	24	24	24	25	26	26	26	27	27
10	13	12	13	12	12	12	10	12	11	10	10	12	13	14		17	17	19	20	21	22	23	24	25	26	26	27
11	15	15	15	14	15	15	16	17	14	15	15	17	19	22	22	23	24	25	26	26	26	27	28	29	29	29	29
12	13	13	12	12	13	13	13	12	11	12	11	12	15	17	18	18	19	20	20	21	22	22	23	23	24	25	25
13	16	16	16	15	13	13	12	12	12	12	12	12	14	16		16	17	16	16	17	18	19	19	20	21	21	21
14	12	12	12	11	11	11	11	11	11	11	11	12	12	13	14		15	15	16	16	17	17	18	18	19	19	19
15	15	14	14	13	12	12	11	11	10	11	11	13	15	16	17	18	19	19	19	20	21	21	22	23	23	24	24
16																			20	21	22	22	23	23	23		
17																											
18	18	17	16	16	15	15	15	13	15	14	14	14	14	16	18	20	23	24	25	26	26	27	28	28	28	29	28
19	18	17	17	16	15	15	15	15	15	16	16	17	17	18	21	23	25	26	27	28	28	29	29	29	30	30	30
20	20	19	18	18	16	17	17	17	16	14	14	15	15	17	20	22	23	25	26	26	27	27	28	28	29	29	30
21	17	18	18	19	20	19	20	19	20	20	20	20	19	22	24	25	25	26	28	29	29		30	30	30	30	30
22	20	22	21	21	21	20	20	20	20	22	23	20	21	22	21	23	24	25	26	26	27	28	28	28	29	29	29
23	17	16	16	15	15	15	15	14	15	14	14	14	14	16	17	19	20	21	22	23	23	23	25	26	27	28	28
24																											
25	24	22	22	21	21	20	21	23	23	20	21	22	19	18	19	20	20	21	22	22	21	20	20	20	20	20	22
26																											
27																				19	20	21	22	23	24	24	24
28	16	16	16	16	15	14	13	13	13	12	14	15	16	17	19	19	20	21	22	22	23	24					
29	19	19	18	17	18	18	17	16	16	16	17	18	19	20	20		21	21	21	22	23	23	22	20			
30	20	19	19	18	19	19	20	20	19	17	16	16	15	15	15	16	17	17	17	19	20	21	21	22	22	22	
31																											
Min:	5	6	7	9	9	9	8	8	8	8	9	11	12	12	13	14	15	15	16	16	17	17	18	18	19	19	19
Ave:	16	16	15	15	15	14	14	14	14	14	14	15	16	17	18	19	20	21	22	23	23	23	24	24	25	26	26
Max:	24	22	22	21	21	20	21	23	23	22	23	22	21	22	24	26	28	28	29	30	30	30	30	30	30	30	30
%Data:	80	80	80	80	80	80	80	80	80	80	80	80	80	80	73	73	83	83	87	90	90	83	80	87	83	77	77

(continued)
Average Temperature

Day	Hour 14:00	15:00	16:00	17:00	18:00	19:00	20:00	21:00	22:00	23:00	24:00	DAILY Min	Ave	Max	% Data
1	20 19 20 20			20 21 20	20 20 20	19 18	17 16	15 14	14 14	13 13	13	5	15	21	98
2	22 22 22 22	22	22	22 21	21 20	19 17	16 15	14 14	13 12	11 11	11	11	17	22	98
3	22 23 23 23	23	23	23	22 22	21 19	18 17	17 16	16 15	15 14	13	8	17	23	96
4	26 27 27 27	27	27	26 26	26 25	24 22	21 20	20 19	18 18	17 16	16	10	19	27	100
5	26 26 26 26	25	25	24 24	24 23	22 22	21 20	18 18	17 16	15 14	14	12	19	26	96
6	28 29 29 29	29	29	29 29	28 28	26 24	23 21	21 19				9	20	29	90
7	30 31	31	31	30 30	29 28	27 26	26 25	25 25	25 25	26 25	25 21	19	19	28	31	63
8	29 30 29 27	28	28	29 28	26 25	24 23	22 21	21 21	21 21	19 18	18	16	24	30	100
9	27 26 21 22	23	21	19 19	19 18		18 17	17 17	16 15	15 15	14 14	14	20	27	98
10	28 28 29 29	29	29	29 28	27 27	26 24	22 21	20 21	22 20	19 18	17	10	20	29	98
11	28 25 25 25	25	25	24 23	22 21	20 19	18 17	15 16	16 16	15 14	14	14	21	29	100
12	26 26 26 27	27	27	26 24	25 24	23 22	20 19	20 19	20 22	22 17	16	11	20	27	100
13	20 20 20 20	20	17	17 17	18 18	18 16	15 14	14 13	14 14	12 12	12	12	16	21	98
14	20 21 21 21	21	21	21 21	21 21	20 19	18 18	17 17	17 17	16 16	15	11	16	21	98
15	24 22											10	17	24	60
16												20	22	23	15
17						26	25 24	23 22	22 21	21 20	19 19	19	22	26	23
18	29 28 25 24	23	23	23 24	24 26	26 26	26 25	22 22	21 20	19 19	18	13	22	29	100
19	30 30 30 30	30	30	31 30	30 30	30 29	27 26	25 26	25 24	24 22	21	15	24	31	100
20	30 30 31 31	31	30	30 30	29 29	28 27	26 25	24 25	24 24	22 20	19	14	24	31	100
21	30 28		28	28 28	28 27	25 25	25 23	23 21	20 19	19 19	18	17	24	30	92
22	30 30 30 28	23	21	23 26	26 25	24 23	23 21	21 20	19 19	17 16	15	15	23	30	100
23	29 29 29 28		28	29 28	28 28	29 29	27 25	25 23	20			14	22	29	90
24		33	33	33 33	33 33	32 32	31 30	28 27	26 26	26 22	23	22	29	33	35
25	23 25 25 22	16	17									16	21	25	69
26															0
27	25 25 25 25	26	26	25 25	25 26		23 21	21 20	19 19	19 18	17 17	17	22	26	58
28	26 26 27 27	26	26	26 26	26 26	25	23 22	22 21	20 20	19 20	19 19	12	20	27	90
29			23	23 23	22 23	24	21	21 21	21 22	23 24	23 22	16	20	24	79
30	23	24	24	24 23	22 22	22 21	19 18					15	19	24	77
31															

	MONTHLY Min	Ave	Max	ZData
Min:	5			
Ave:		20		
Max:			33	
ZData:				81

USFS PAWNEE SITE

June, 1988
Wind Direction

Day	1:00		2:00		3:00		4:00		5:00		6:00		7:00		8:00		9:00		10:00		11:00		12:00		13:00	
1	355	321	296	278	293	297	293	300	318	317	293	297	295	294	292	288	295	301	315	312	318	323	328	333	333	331	327
2	144	273	317	321	329	333	322	310	300	301	303	303	309	322	341	354	1	348	357	359	1	353	354	355	5		353
3	354	336	338	336	335	340	338	339	340	14	339	28	14	181	193	196	161	164	157	148	150	132	127	143	129	127	141
4	110	111	113	112	107	102	100	107	109	17	74	46	126	131	121	117	117	113	121	122	130	132	138	144	131	130	132
5	110	104	99	86	91	104	110	106	103	99	104	109	123	131	134	140	132	118	126	125	127	68	68	129	124	129	135
6	81	70	54	10	14	21	25	7	18	15	15	39	39	52	46	41	67	95	120	110	117	102	123	111	104	109	110
7																	262	247	239	217	175	181		181	170	152	146
8	322	334	32	25	357	339	337	341	340	341	341	335	335	327	337	343	316	331	2	22	12	359	38	60	46	359	2
9	345	237	212	193	210	224	274	98	112	89	100	85	75	29	356	9	40	58	80	90	61	59	88	84	99	108	124
10	98	59	35	55	46	36	21	48		356	14	19	43	63		97	102	98	110	91	96	112	128	128	137	131	135
11	341	345	339	344	10	52	55	35	3	15	19	353	353	300	175	196	229	207	183	179	179	172	155	155	172	45	246
12	319	328	340	347	336	334	306	337	358	337	3	6	350	329	331	335	10	86	135	123	124	113	103	111	74	93	97
13	67	91	9	329	338	342	354	1	356	11	15	18	21	66		95	85	96	96	83	67	87	81	98	191	232	259
14	345	355	348	336	351	359	4	356	4	2	6	358		5	27		85	73	60	84	62	75	71	92	95	99	89
15	83	71	93	91	84	63	77	57	59	56	32	345	176	173	180	173	174	158	165	160	165	151	146	156	134	145	140
16	16	339	330	349	331	9	6	348	17	35	26	338	71	92	103	103	112	119	132	142	133	139	130	129	145		
17																											
18	307	341	345	344	339	351	335		336	348	8	16	13	357	355	345	357	5	355	1	10	8	328	331	232	216	246
19	39	16	340	344	342	341	346	351	351	338	322	321	308	290	306	315	326	329	335	343	342	337	340	338	344	349	351
20	35	47	56	30	23	43	90	82	329	342	342	348	348	4	348	345	317	177	151	151	155	153	150	154	148	163	161
21	355	315	304	305	313	309	302	315	308	307	313	320	328	320	310	312	318	292	295	301	306		309	311	330	319	332
22	335	340	344	349	349	350	346	332	328	354	313	350	353	7	11	354		10	21	13	26	40	62	94	86	75	98
23	115	110	14	342	322	336	345	40	29	34	13	40	39	235	106	157	155	149	149	153	150	136	149	157	149	163	156
24																											
25	333	346	294	332	345	44	76	60	90	75	96	70	41	38	85	157	342	352	85	71	86	75	40	29	61	5	31
26																											
27																				159	159	164	169	162	159	161	154
28	106	105	94	103	28	23	45	57	47	9	35	9	2	352	51	86	80	82	94	119	121	136					
29	289	293	303	317	332	347	358	1	13	336	333	343	1	356	1		346	351	333	20	18	8	143	147			
30	314	308	334	6	343	34	18	346	354	356	352	353	357	348	343	343	352	351	351	355	359	4	9	3	356		
ZData:	83	83	83	83	83	83	83	80	80	83	83	83	80	83	77	77	83	87	87	90	90	87	83	87	83	73	77

(continued)
Wind Direction

Day \ Hour	14:00		15:00		16:00		17:00		18:00		19:00		20:00		21:00		22:00		23:00		24:00		% Data
1	335	329	318	309		295	293	301	296	289	291	304	324	14	16	61	106	112	32	21	344		98
2	4	355	4	5	19	16	27	25	34	43	60	65	78	104	141	342	329	335	336	336	342		98
3	109	125	119	127	132	136			132	131	127	119	115	114	113	110	111	114	116	114	111		96
4	126	124	124	126	126	128	127	130	130	133	133	129	129	122	125	126	124	125	124	118	117		100
5	141	136	141	136	137	137	134	133	132	131	129	128	132	127	123	116	104	66	74	68	69		100
6	100	115	108	99	108	101	130	151	144	145	145	137	146	157	165								88
7	138	133		162	147	159	143	131	95	63	66	96	189	165	149	127	122	166	104	308	345		63
8	54	21	90	85	71	64	72	74	70	66	72	71	76	77	98	221	250	190	53	32	344		100
9	127	131	161	142	138	182	191	177	192	281		165	208	215	207	176	148	158	141	147	124		98
10	152	144	165	170	176	192	193	216	221	252	160	174	172	188	224	56	95	82	76	42	332		96
11	5	8	21	17	10	318	332	324	313	313	346	5	22	80	101	69	44	317	339	309	331		100
12	117	118	123	123	130	192	218	250	260	212	254	224	166	137	105	73	317	194	209	88	54		100
13	264	271	291	116	100	84	68	43	75	71	75	99	98	112	52	353	348	1	13	21	345		98
14	121	123	93	125	109	117	135	167	165	156	141	133	121	114	106	93	100	97	123	137	123		96
15	154	208	251	95	31	30	39	85	124	133	131	121	118	118	110	128	121	132	122	73	24		100
16																							52
17											315	305	281	283	293	31	23	29	28	341	336		23
18	154	227	294	326	315	321	331	325	331	313	309	313	346	133	176	200	220	218	225	241	256		98
19	326	6	357	42	57	35	111	145	138	127	109	125	123	123	61	293	6	61	41	77	61		100
20	141	153	137	147	171	172	161	186	193	244	292	319	340	333	339	37	345	357	343	338	346		100
21	337	331				224	221	219	218	206	215	201	191	180	160	172	5	23	357	351	347		92
22	11	59	46	113	173	142	59	65	77	140	151	142	133	140	325	334	46	64	50	50	63		98
23	155	154	172	176		216	218	223	212	195	233	192	197	150	317	341	29						90
24					131	148	170	166	128	123	95	95	87	94	112	112	84	358	11	328	335		35
25	9	29	31	358	210	225																	69
26																							0
27	156	157	165	164	164	161	164	170	162	149		157	147	141	135	126	134	133	133	143	126		58
28	100	119	143	134	133	130	141	138	137	143	159	173	133	115	102	96	76	344	350	338	322		90
29						175	161	159	167	159	171		198	322	349	52	331	356	45	228	266		79
30			9		6	3	359	13	14	12	12	25	64	80									75
																						Month	
%Data:	80	80	77	77	77	90	83	83	87	87	83	87	90	90	87	83	83	80	80	80	80		83

USFS PAWNEE SITE

June, 1988
Wind Speed (meters/sec); Half Hour Averages.

Day	1:00		2:00		3:00		4:00		5:00		6:00		7:00		8:00		9:00		10:00		11:00		12:00		13:00	
1	1.8	1.2	2.2	6.6	5.6	4.9	4.8	4.6	4.3	5.1	8.4	8.7	10.6	11.1	10.9	10.9	9.5	8.4	8.1	7.7	6.9	7.4	7.5	8.1	8.3	8.7	7.6
2	0.1	2.0	2.9	2.9	2.6	2.8	4.1	4.7	5.3	4.8	5.2	5.9	6.5	7.7	8.5	8.4	8.0	7.4	7.8	7.3	7.1	7.3	7.1	7.3	7.6		7.1
3	1.7	2.3	2.4	2.7	2.6	2.5	2.2	2.4	2.3	1.5	1.5	1.9	1.5	0.2	1.0	0.9	1.3	1.6	2.0	2.2	2.5	2.7	3.6	2.9	3.9	3.6	3.3
4	3.7	4.1	3.9	3.8	3.3	3.0	3.3	3.2	1.8	0.5	0.8	1.0	1.8	2.2	2.4	2.7	3.2	4.3	4.4	4.9	5.3	5.7	5.4	5.5	6.1	6.2	7.3
5	4.2	4.0	3.6	3.6	3.5	3.7	4.0	3.5	3.6	3.4	3.6	4.3	5.2	5.2	5.0	4.1	3.7	4.3	5.1	5.2	6.0			5.4	7.3	7.3	7.1
6	3.2	3.0	2.3	2.1	3.0	3.3	3.4	2.4	2.0	2.3	2.0	2.5	2.8	2.7	2.1	1.8	1.5	1.7	1.8	2.1	2.3	2.4	2.5	2.8	3.1	3.3	3.0
7																	4.7	3.8	2.6	1.7	1.9	2.2		2.9	3.5	4.3	4.6
8	1.5	2.4	2.4	2.2	2.9	2.6	3.0	3.2	3.7	3.0	3.3	3.9	4.7	4.8	4.6	4.0	4.0	3.1	2.6	4.2	3.9	3.6	4.9	3.2	4.3	2.7	3.5
9	1.8	1.2	1.9	0.8	1.4	0.9	0.3	1.3	0.7	2.3	2.8	2.0	2.0	0.9	1.1	2.0	1.2	1.3	1.6	2.2	3.1	4.4	4.0	4.8	5.6	6.4	6.9
10	1.0	1.1	1.6	1.7	1.7	1.9	1.8	2.4	1.8	2.2	2.2	2.2	3.2	2.8		2.8	2.8	2.3	2.0	1.6	2.8	2.2	2.9	3.5	3.9	3.7	4.3
11	2.8	3.5	3.0	3.2	2.8	2.4	2.1	2.2	1.0	1.6	2.2	1.4	0.7	0.5	1.5	1.6	1.5	1.9	1.7	2.4	2.4	2.5	1.9	0.8	1.4	0.9	1.4
12	2.3	2.4	2.4	1.5	3.0	1.6	1.2	2.2	1.4	1.0	0.8	1.2	1.6	1.7	1.7	1.6	1.2	0.5	1.2	1.9	2.0	2.3	2.5	2.9	3.9	4.4	3.9
13	5.5	6.1	3.8	3.1	2.8	3.0	2.8	2.5	2.6	2.6	2.7	3.0	2.9	2.8		3.1	3.6	4.4	3.1	2.5	2.4	3.1	3.6	3.2	1.2	2.6	5.3
14	4.9	5.6	6.9	5.5	6.6	5.9	5.3	7.1	5.9	5.4	4.7	4.4	4.6	3.8	3.8		2.5	2.7	2.5	2.8	2.7	2.5	2.9	2.6	2.4	2.3	2.5
15	1.8	3.4	3.7	3.0	1.0	1.6	2.4	1.7	1.6	1.7	0.6	0.2	1.2	1.8	1.3	2.3	4.0	5.4	5.4	5.0	5.1	5.3	5.6	5.0	5.2	5.2	4.3
16	2.4	2.3	2.1	2.1	2.5	2.3	1.6	1.6	2.2	1.8	1.5	1.1	1.3	2.7	2.4	1.7	1.7	2.0	1.9	2.2	2.3	2.2	2.7	3.4	2.7		
17																											
18	1.0	2.3	3.3	3.4	3.4	3.2	2.5	1.5	3.1	2.4	2.9	2.2	2.1	2.6	2.5	2.2	2.8	2.4	2.8	3.6	3.3	2.5	4.7	6.3	2.1	1.2	0.9
19	0.7	2.1	2.5	2.8	3.6	3.2	3.5	2.8	3.0	3.0	3.0	3.6	3.5	3.1	4.3	5.1	6.5	6.9	6.4	5.7	4.5	3.8	4.0	3.9	3.7	3.4	3.9
20	4.4	4.2	2.7	2.8	2.4	3.5	3.6	0.9	1.2	2.4	1.9	2.4	1.8	1.5	2.1	1.7	0.9	0.6	2.0	2.4	3.4	3.3	3.1	3.6	3.4	3.3	2.9
21	1.8	2.3	2.9	3.9	4.1	4.2	4.6	3.2	4.1	5.3	4.5	4.1	3.8	4.3	5.1	4.4	4.0	3.1	5.2	6.8	6.1		5.3	4.8	4.9	4.6	4.7
22	5.5	8.8	7.5	6.1	5.5	5.5	4.9	4.3	4.4	3.6	4.1	3.7	4.0	6.6	7.1	5.6	6.3	6.7	6.1	5.4	4.1	3.2	2.1	1.1	2.3	1.6	1.8
23	3.2	2.0	1.6	1.7	1.6	1.8	2.5	2.4	2.5	1.9	1.3	1.8	1.2	0.1	0.4	0.6	0.8	0.9	1.0	1.2	2.9	2.5	2.7	2.2	2.7	3.7	4.0
24																											
25	5.8	3.3	2.7	2.5	2.8	3.1	5.8	5.4	8.6	4.5	3.9	5.2	8.9	8.0	4.1	0.3	3.4	3.4	2.9	6.2	5.3	5.4	5.9	5.1	3.9	1.6	4.6
26																											
27																				2.8	3.6	4.1	4.2	3.7	4.5	4.4	5.1
28	3.2	3.1	1.6	0.9	1.6	1.9	2.4	2.9	2.5	2.2	2.8	2.0	2.4	2.6	2.1	2.7	3.2	3.1	3.5	4.5	4.7	5.3					
29	5.1	6.1	6.5	5.9	4.8	3.1	3.7	3.5	3.1	3.4	3.7	4.5	4.3	4.8	4.7		4.3	3.9	2.2	1.6	3.2	1.6	1.4	1.4			
30	3.4	3.4	1.9	1.2	1.9	4.5	3.2	6.1	10.0	9.6	8.3	7.8	8.5	8.2	10.0	9.6	10.7	10.7	10.9	11.0	10.2	10.9	10.0	9.1	8.5	7.7	
Min:	0.1	1.1	1.6	0.8	1.0	0.9	0.3	0.9	0.7	0.5	0.6	0.2	0.7	0.1	0.4	0.3	0.8	0.5	1.0	1.2	1.9	1.6	1.4	0.8	1.2	0.9	0.9
Ave:	2.9	3.3	3.1	3.0	3.1	3.1	3.2	3.1	3.3	3.1	3.1	3.2	3.7	3.7	3.9	3.5	3.7	3.7	3.7	4.0	4.1	3.9	4.2	4.1	4.3	4.1	4.3
Max:	5.8	8.8	7.5	6.6	6.6	5.9	5.8	7.1	10.0	9.6	8.4	8.7	10.6	11.1	10.9	10.9	10.7	10.7	10.9	11.0	10.2	10.9	10.0	9.1	8.5	8.7	7.6
%Data:	83	83	83	83	83	83	83	83	83	83	83	83	83	83	77	77	87	87	87	90	90	83	80	87	83	77	77

(continued)
Wind Speed

Day	Hour 14:00		15:00		16:00		17:00		18:00		19:00		20:00		21:00		22:00		23:00		24:00		DAILY Min	Ave	Max	% Data
1	8.1	7.3	6.9	7.0		7.7	9.0	8.6	7.3	7.6	5.9	3.5	2.2	1.4	2.2	2.4	2.0	1.2	2.1	1.7	0.9		0.9	6.1	11.1	98
2	7.6	6.9	7.1	6.7	7.0	6.7	7.3	7.3	7.3	7.7	6.3	4.7	2.9	1.4	0.6	1.3	1.8	2.2	2.1	2.1	2.1		0.1	5.3	8.5	98
3	4.3	4.4	4.8	4.3	5.2	5.7			5.7	5.3	4.8	3.7	3.7	3.9	4.3	4.4	4.5	4.6	4.3	4.2	3.7		0.2	3.2	5.7	96
4	7.6	7.5	7.5	7.3	7.6	8.1	8.4	8.4	8.2	7.7	7.1	6.2	6.2	5.6	6.5	6.6	5.8	5.1	4.6	4.3	4.5		0.5	5.0	8.4	100
5	6.7	8.4	9.1	9.6	9.6	8.2	8.0	7.8	7.7	7.2	6.3	7.4	7.6	6.7	5.1	4.9	4.6	2.5	2.7	2.8	2.5		2.5	5.5	9.6	96
6	2.8	2.9	3.3	2.0	3.7	4.6	4.4	4.0	4.3	4.3	3.6	3.5	3.1	2.2	1.2								1.2	2.8	4.6	88
7	4.2	4.3		3.8	3.1	2.4	3.8	3.6	2.3	2.8	2.6	1.0	1.6	5.0	5.0	4.4	2.9	1.0	2.3	2.6	0.9		0.9	3.1	5.0	63
8	3.9	2.8	5.8	8.4	6.6	5.6	5.0	5.3	4.1	4.0	4.5	4.3	4.0	3.0	2.7	0.7	1.4	0.7	2.8	1.6	0.9		0.7	3.6	8.4	100
9	6.5	7.1	5.8	4.5	5.1	3.9	3.9	5.2	3.1	5.7		2.1	3.3	4.3	3.5	3.2	4.2	4.3	3.4	2.8	2.0		0.3	3.2	7.1	98
10	4.1	3.7	3.2	3.1	2.4	2.8	2.6	3.5	2.3	1.5	6.0	2.9	0.9	0.7	0.5	4.7	2.6	3.0	3.2	2.3	2.6		0.5	2.6	6.0	98
11	4.6	8.5	7.3	6.2	5.2	6.0	6.6	7.4	7.5	8.2	5.4	4.7	4.4	5.9	6.2	3.7	2.4	2.7	2.6	3.0	2.6		0.5	3.4	8.5	100
12	4.0	4.4	4.1	4.3	3.7	3.0	4.1	7.8	2.8	0.9	3.0	2.6	10.0	9.0	7.8	3.2	0.8	2.1	2.4	4.9	4.9		0.5	3.0	10.0	100
13	3.5	2.9	2.3	1.4	6.1	5.6	4.0	2.6	1.4	3.0	3.6	4.0	2.8	1.2	0.7	2.7	4.0	5.2	6.0	5.4	3.3		0.7	3.3	6.1	98
14	2.1	2.7	3.4	2.9	3.3	2.8	3.2	4.4	4.6	5.0	4.9	4.7	4.3	3.9	3.4	3.8	4.1	3.9	2.5	1.8	1.8		1.8	3.9	7.1	98
15	3.7	2.0	4.1	1.4	2.8	4.2	6.0	5.1	6.4	5.0	4.9	4.4	4.2	4.9	3.7	2.7	3.2	1.3	0.9	1.3	2.0		0.2	3.3	6.4	100
16																							1.1	2.1	3.4	52
17											4.2	2.8	4.5	7.0	5.3	3.0	2.4	3.0	2.2	1.2	2.2		1.2	3.4	7.0	23
18	0.6	1.6	6.6	6.6	4.7	6.0	6.5	5.5	4.4	3.2	3.0	0.9	0.7	1.1	2.6	3.0	2.9	2.7	3.4	2.1	0.2		0.2	2.9	6.6	100
19	2.3	2.6	2.6	2.2	0.8	2.5	0.3	3.4	3.0	2.1	2.3	3.7	2.7	1.9	1.7	2.4	2.5	3.1	4.1	3.1	3.3		0.3	3.2	6.9	100
20	2.6	3.1	2.9	3.3	3.3	3.8	3.4	1.9	1.2	1.2	2.7	2.0	2.4	1.8	2.5	1.5	1.1	2.0	2.7	2.9	3.0		0.6	2.5	4.4	100
21	4.4	2.6				3.3	4.3	3.6	4.7	4.1	4.7	2.8	1.8	1.3	1.8	1.0	0.8	2.2	2.6	2.9	3.3		0.8	3.7	6.8	92
22	2.6	2.1	1.6	7.1	4.2	3.8	1.5	1.0	1.5	4.3	5.5	4.9	3.5	1.4	0.5	1.4	2.2	1.4	1.3	2.4	1.4		0.5	3.8	8.8	100
23	4.8	3.8	2.8	2.7		3.4	3.1	3.7	2.5	1.4	1.8	0.6	0.9	0.4	0.5	1.5	1.8						0.1	2.0	4.8	90
24					3.4	4.0	4.3	2.4	2.9	1.6	3.7	3.4	2.6	2.5	3.0	2.5	1.4	5.8	5.4	5.7	6.7		1.4	3.6	6.7	35
25	4.3	2.9	6.1	7.5	9.1	3.7																	0.3	4.7	9.1	69
26																										0
27	5.2	5.2	5.5	5.8	5.7	5.6	5.7	5.6	5.6	6.2		4.3	3.9	3.8	3.5	3.6	3.8	3.5	3.1	2.3	2.0		2.0	4.4	6.2	58
28	3.4	3.1	3.3	3.0	4.5	4.0	4.4	3.6	3.8	4.4	3.1	2.7	1.2	2.1	2.5	2.6	2.4	3.0	5.5	5.3	4.9		0.9	3.1	5.5	90
29						2.6	3.7	3.8	3.2	4.6	2.8		0.9	1.9	6.4	2.0	3.2	6.9	1.4	0.8	2.1		0.8	3.5	6.9	79
30			4.5		3.9	4.0	4.3	4.2	3.9	4.3	4.9	4.0	2.8	2.9									1.2	6.5	11.0	77

	Min	Ave	Max	XData
Min:	0.6	1.6	1.6	1.4	0.8	2.4	0.3	1.0	1.2	0.9	1.8	0.6	0.7	0.4	0.5	0.7	0.8	0.7	0.9	0.8	0.2		0.1			
Ave:	4.3	4.3	4.8	4.8	4.8	4.6	4.7	4.8	4.3	4.4	4.3	3.5	3.3	3.2	3.2	2.9	2.8	3.1	3.1	2.9	2.6			3.7		
Max:	8.1	8.5	9.1	9.6	9.6	8.2	9.0	8.6	8.2	8.2	7.1	7.4	10.0	9.0	7.8	6.6	5.8	6.9	6.0	5.7	6.7				11.1	
XData:	80	80	77	77	77	90	83	83	87	87	83	87	90	90	87	83	83	80	80	80	80					83